STUDY ON OPEN AND CLOSED CHEMICAL THERMAL ENERGY STORAGE TECHNOLOGY WITH LOW-REGENERATION TEMPERATURE

Presented by: Hongzhi Liu

Supervisor: Prof. Katsunori Nagano

2014

Division of Human Environmental Systems

Graduate School of Engineering

Hokkaido University

TABLE OF CONTENTS

NOMENCLATURE

Abbreviation

CHP	Chemical heat pump;
CFCs	Chlorofluorocarbons;
COP	Coefficient of performance;
EG	Expanded graphite;
HCFCs	Hydrochlorofluorocarbons;
LDF	Linear driving force model;
PCMs	Phase change materials;
SWEAT	Salt Water Energy Accumulation and Transformation;
SWSs	Selective water sorbents;
WSS	Wakkanai siliceous shale;

Symbols

a	Extent of conversion (–).
A	Pre-exponential factor of Arrhenius equation;
$A(\omega)$	Constant changing with sorption amount;
$B(\omega)$	Constant changing with sorption amount;
B_{ih}	Heat transfer Biot number (−);
B_{im}	Mass transfer Biot number (−);
C_p	Specific heat (J/ (kg·K));
d_a	Hydraulic diameter of the air channel (m);
d_p	Pore diameter (m);

D_m Molecular diffusion coefficient (m^2/s);

D_K Knudsen diffusion coefficient (m^2/s);

D_P Overall pore diffusivity (m^2/s);

D_s Coefficient of surface diffusion (m^2/s);

$D_{s,0}$ Constant for surface diffusivity calculation (m^2/s);

D_{eff} Apparent pore diffusion coefficient based on gas side (m^2/s);

E Activation energy of desorption (J/mol);

E_{total} Total electricity consumption (J);

E_{re} Necessary electricity consumption for material regeneration (J);

f Air flow rate, Q_a /3600 (m^3/s);

h Heat transfer coefficient ($W/(m^2 \cdot K)$);

h_m Convective mass transfer coefficient (m/s);

H_L Latent heat (J/g);

$k(\boldsymbol{T})$ Rate constant;

k_a Air side mass transfer coefficient based on solid side (m/s);

k_s Solid side mass transfer coefficient (m/s);

K Overall mass transfer coefficient (m/s);

L Length of the unit (m);

Le Lewis number (−);

M Molecular weight (g/mol);

m Weight (g);

$m_{H2O}(T)$ Mass of water sorbed at temperature T (g);

m_{salt} Total salt mass in the composite material (g);

m_{CaCl2} Total $CaCl_2$ mass in the composite material (g);

$m_{s,dry}$	Mass of the dry composite material (kg);
n	Molecules of water with respect to one molecule of salt (mol_{H2O}/mol_{salt});
Nu	Nusselt number (−);
P	Pressure (Pa);
P_e	Electricity power (W);
P_v	Pressure in atmospheres (Pa);
q	Power (W);
q_S	Specific power (W/kg);
q_V	Volumetric power (W/L);
Q_a	Air flow rate (m^3/h or m^3/s);
Q_V	Volumetric heat storage density (J/m^3);
Q	Heat amount (J);
r_a	Condensation heat of water vapor (kJ/kg);
r_p	Pore's radius (m);
R	Universal gas constant (8.314 J/(mol·K));
RH	Relative humidity of air (%);
t	Time (s);
T	Temperature (ºC);
$\boldsymbol{T}$	Temperature (K);
u	Velocity (m/s);
V	Volume of the honeycomb heat storage unit (m^3);
$\boldsymbol{V}$	Volume of the reactor (m^3);
W_V	Volumetric heat transfer rate of the heat storage unit (W/m^3);
x	Mixing weight ratio of hygroscopic salt LiCl and WSS (%);

x_a Absolute humidity (g/kg$_{DA}$);

X_a Mass flow of water vapor in the air (g/s);

X_V Volumetric heat storage density percentage (%);

z Direction of length (m);

Greek letters

α Sorption equilibrium constant (g/g);

β Heating rate (K/min);

ΔH Sorption heat (J/kg);

ΔT Inlet and outlet temperature difference (ºC);

Δt Time interval (s);

$\Delta\omega$ Change of the sorption amount (g$_{H2O}$/g$_{sample}$);

δ_a The thickness of air, equals to d_a/4 (m);

δ_s Thickness (m);

ε Coefficient of heat extraction performance during the heat release process (−);

ε_s Porosity of the composite porous material (−);

η Heat recovery rate (−);

λ Effective thermal conductivity (W/(m·K));

ρ Bulk density (kg/m^3);

τ_p Tortuosity of real pores (−);

τ_s Tortuosity factor for surface diffusion (−);

ω Sorption amount (g$_{H2O}$/g$_{sample}$);

ω_s Sorption amount on the gas and solid surface (g$_{H2O}$/g$_{sample}$);

$\omega_{WSS}(T)$ Sorption amount of WSS at temperature T (g_{H2O}/g_{sample});

Subscripts

a	air;
con	Condensation or condenser;
$CaCl_2$	Calcium chloride;
C	Cooling;
desor	Desorption process;
dry	Dry state of composite material;
e	Equilibrium state;
eff	Effective;
ev	Evaporation;
evap	Evaporator;
H	Heating;
H_2O	Water or water vapor;
l	Liquid;
LiCl	Lithium chloride;
max	Maximum;
in	Inlet;
out	Outlet;
p	Peak;
re	Regeneration;
reac	Reactor;
s	Solid material;

salt	Hygroscopic salt;
sor	Sorption process;
total	Total;
WSS	Wakkanai siliceous shale;
0	Initial condition;

LIST OF FIGURES

LIST OF TABLES

1 INTRODUCTION

1.1 NECESSARITIES OF DEVELOPING THERMAL ENERGY STORAGE TECHNOLOGY

Energy is inevitable for humankind, and a safe and accessible supply of energy is crucial for the sustainability of modern societies [1]. In recent years, the energy consumption has been continuously increasing resulting in increase of greenhouse gases emissions. Therefore, in order to realize an energy sustainable society, cycle use of fossil fuel energy and development of renewable energy is hoped to be able to solve the problems exhibited in the current energy society.

1.1.1 Cyclic utilization of fossil fuel in industrial sector

The demand of fossil fuel has been increasing in recent years. Continuous usage of fossil fuels faces several challenges: depletion of fossil fuel reserves, global warming and other environmental concerns caused by emission of greenhouse gases, geopolitical and military conflicts and increasing of fossil fuel price [1].

World ultimate conventional oil reserves are estimated at 2,000 billion barrels, while the global daily consumption of oil is 71.7 million barrels [1]. Of course different countries are at different stages of their reserve depletion, but the fossil fuel's reserves are limited, which means that it is not possible to use the fossil fuel forever.

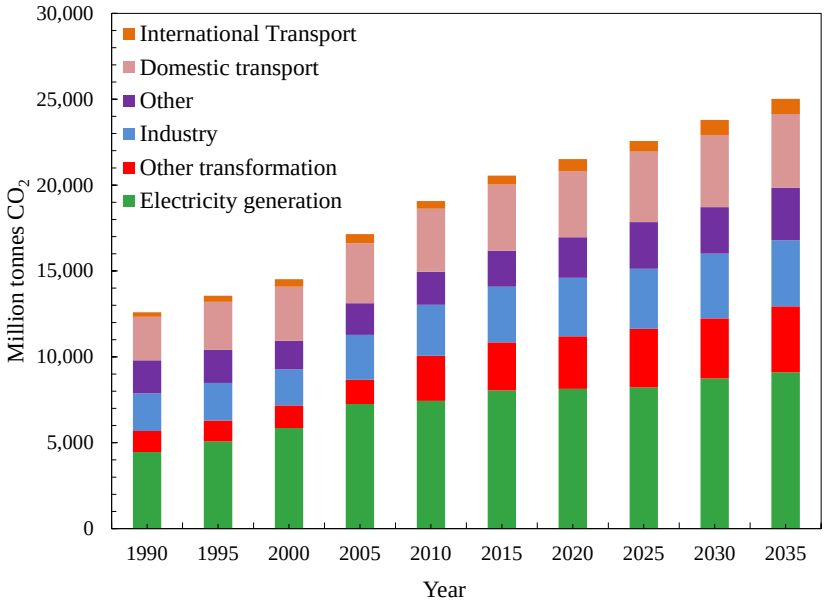

Fig. 1-1 CO_2 emissions from fuel consumptions [2]

The second problem to use fossil fuel like coal or petroleum is emission of greenhouse gases. Global greenhouse gas emissions are dominated by energy production, and the emission of main greenhouse gas CO_2 in future is shown in Fig. 1-1.

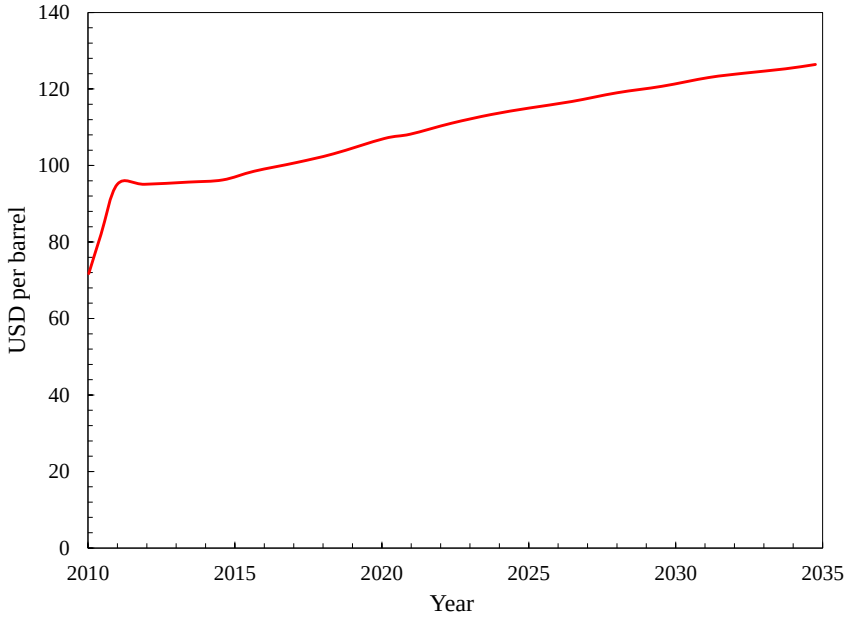

Fig. 1-2 Assumed oil prices [2]

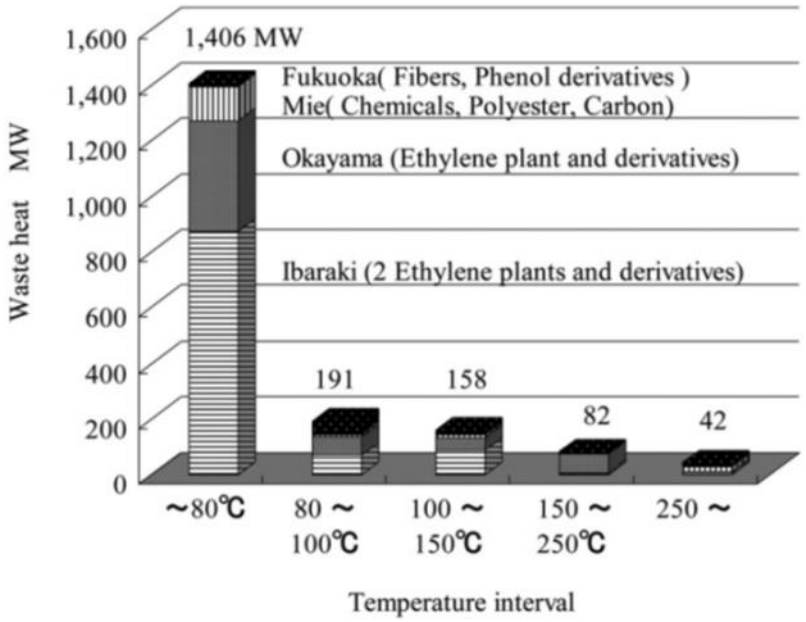

Fig. 1-3 Total waste heat for one of the chemical industries [3]

Another problem caused by continuous consumption of fossil fuel energy is the increase of fuel price. Oil prices have been volatile since the first oil shock in 1970s,

and the Asia-Pacific Economic Cooperation (APEC) gave their oil price assumptions in Fig. 1-2.

The above mentioned problems indicate that solution for sustainable energy usage situation is needed to be developed, and one is to cyclic use of energy, especially utilization large amount of waste heat. In Japan, about 12.5% imported oil [3] is discharged, and Fig. 1-3 illustrates the total waste heat released from one of the chemical industrials with four plant site located in each listed prefecture. From Fig. 1-3 we can see that large amount of low temperature heat (< 100ºC) is discharged to the atmosphere. Therefore, low temperature (< 100ºC) advanced heat recovery technology needs to be prompted to reduce fossil fuel consumption and the impact of utilizing fossil fuel energy on environment.

1.1.2 Utilization of renewable energy such as solar energy

Renewable energy resources such as solar energy are abundant, inexhaustible and environmentally friendly. The development of renewable energy can contribute to securing long-term sustainable energy society, and reduce the impact to environment. In fact, among all the types of renewable energy, solar energy is closely related with the low-temperature heat supply for industrial, residential and transport sectors. Although solar energy is abundant, clean and safe, the supply of solar energy is periodic following yearly and diurnal cycles with lower energy density compared with the energy flux densities found in conventional fossil fuel devices like coal or oil-fired furnaces. On the other hand, the energy demand is also unsteady following yearly and diurnal cycles for both industrial and residential needs. Therefore, the development of the solar energy storage is necessary and the storage of solar energy is assumed to solve the current problems of using solar energy with low efficiency, because the main role of thermal energy storage is to reduce the time or rate mismatch between supply and demand side [4]. Energy storage is also an important key technology to realize efficient energy utilization especially for the energy hard to be stored effectively. Fig. 1-4 illustrates trend shift of energy supply and demand chain in future, which needs not only high efficient renewable energy produce and utilization system, but also efficient thermal energy storage system.

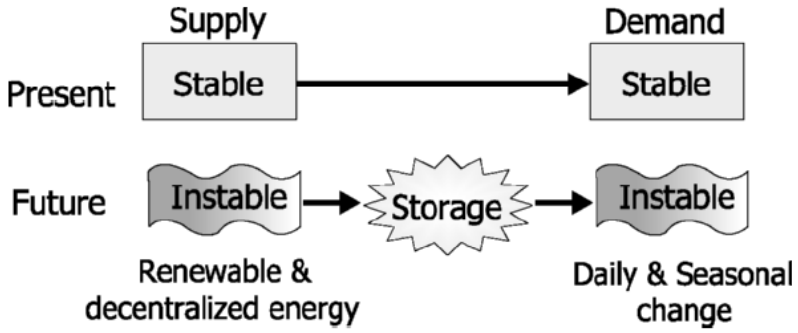

Fig. 1-4 Trend shift of energy chain between energy supply and demand sides [5]

Therefore, based on the increased demand for energy, rise of the consumption of fossil fuel associated with the depletion of fossil fuels and the increased emission of greenhouse gases, and the high potential of utilization of renewable energy (e.g. solar energy) all require the development of more efficient process to save energy and to utilize renewable energy efficiently.

1.2 OVERVIEW OF THERMO ENERGY STORAGE TECHNOLOGIES

Thermal energy storage is defined as the temporary holding of thermal energy in the form of hot or cold substances for later utilization [6]. Thermal energy storage is one of the key technologies for energy conservation, which caused increasing attention to study this essential technique. Dincer et al. [7] pointed out that thermal energy storage technology has been successfully applied to many existing applications all over the world, particularly in developed countries, and he also emphasized that this technology is an extraordinary technology that can reduce energy cost, energy consumption, improve indoor air quality, increase flexibility of operation and reduce initial and maintenance costs [8]. Developing efficient and inexpensive energy storage devices is as important as developing new sources of energy [9]. The importance of thermal energy storage has motivated many researchers to study various aspects of this technology. There are three main types of thermal energy storage technology: sensible heat storage, latent heat storage and chemical thermal energy storage (sorption and thermochemical) [10-12]. If one tries to get an overview of thermal energy storage systems one would be overwhelmed by the large number of possible technical solutions and the variety of storage systems. Table 1-1 gives an overview of thermal energy storage methods:

Table 1-1 An overview of thermal energy storage methods [9]

Type of Thermal Energy Storage	Functional Principle	Phases	Examples
Sensible Heat	Temperature change of the medium with highest possible heat capacity	Liquid	Hot water, organic liquids, molten salts, liquid metals
		Solid	Metals, minerals, ceramics
Latent Heat	Essentially heat of phase change	Liquid-Solid	Nitrides, Chlorides, Hydroxides, Carbonates, Fluorides, Eutectics
		Solid-Solid	Hydroxides
Chemical Heat	Large amount of chemical energy is absorbed and released due to shifting of equilibrium by changing pressure and temperature	Solid-Gas	CaO/H_2O, MgO/H_2O. $FeCl_2/NH_3$
		Gas-Gas	CH_4/H_2O
		Liquid-Gas	$LiBr/H_2O$, $NaOH/ H_2O$, H_2SO_4/ H_2O

1.2.1 Sensible heat storage

In sensible thermal energy storage system, heat is stored/extracted by heating/cooling a liquid or a solid material without phase change through a heat transfer interaction [6]. The amount of heat stored in a sensible heat storage system depends on the temperature change of the material and the weight of the storage material, which can be expressed as follows:

$$Q = mC_p\Delta T \qquad 1\text{-}1$$

In the above equation, m and C_p denote the weight and specific heat of the heat storage material, and ΔT is the temperature difference of the material before and after the heat storage process. From the aspect of the heat storage density, high specific heat capacity is valuable for a sensible heat storage system. Typical sensible heat storage materials include liquids like water, heat transfer oils and some inorganic molten salts, and solid like rocks, pebbles and refractory [13].

1.2.1.1 Liquid heat storage material

(1) Water

Water is the most commonly used material in a sensible heat storage system with the highest specific heat and low price. Water is non-toxic, non-combustible and widely available. Heat exchangers may be avoided if water is used as the heat carrier in the collector. Nowadays, with reasonable cost and simple implementation, most solar water heating and space-heating systems use hot water storage tanks located either inside or outside of the buildings (cf. Fig. 1-5).

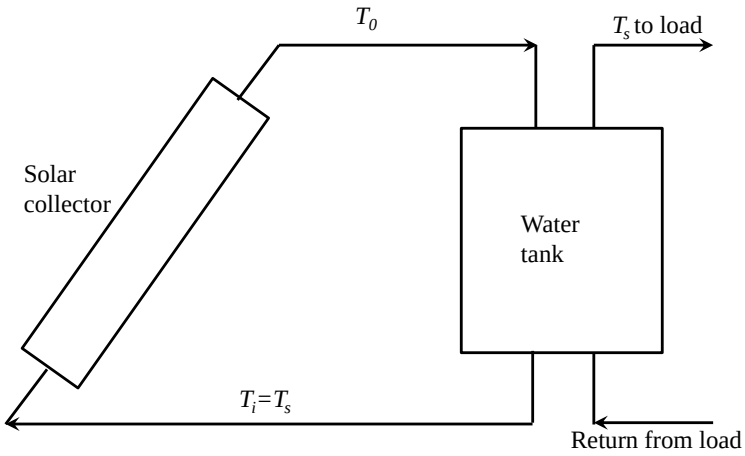

Fig. 1-5 A typical system using water tank storage, with water circulation through collector to add energy and through the load to remove energy [14]

However, there are two main disadvantages of water thermal energy storage system: the first one is that the water storage tanks are made from a variety of materials such as steel, concrete and fiberglass and tanks are suitably insulated with glass wool, mineral wool or polyurethane. The cost of the insulation represents a significant part of the total cost because of the thick insulation from 10 to 20 cm. The other disadvantage is that the working temperatures are limited to less than 100ºC and often have to be far below this boiling temperature.

(2) Heat transfer oils

Heat transfer oils are used in sensible heat storage systems for intermediate temperatures ranging from 100ºC to 300ºC [9]. The problem of using heat transfer oils is its degradation with time, especially when they are used above their recommended temperature limit. Safety problems are also presented since there is a possibility of ignition above their flash point. A further limitation to the use of heat transfer oils is their cost limiting their usage in small systems.

(3) Molten inorganic salts

A few molten inorganic salts have been considered for high temperatures (300ºC and above). Sodium hydroxide is a kind of high temperature storage material, which has a melting point of 320ºC and could be used for temperature up to 800ºC. However, it is highly corrosive and it is difficult to contain it at higher temperatures [9].

1.2.1.2 Solid heat storage media

(1) Rock and pebbles

Energy can be stored in rocks or pebbles packed in insulated vessels and it is often used in conjunction with solar air heaters for temperatures up to 100ºC with simple design and relative low price. Schematic of a packed bed system is shown in Fig. 1-6. Direct contact between the solid storage media and a heat transfer fluid is necessary to minimize the cost of heat exchange in a solid system.

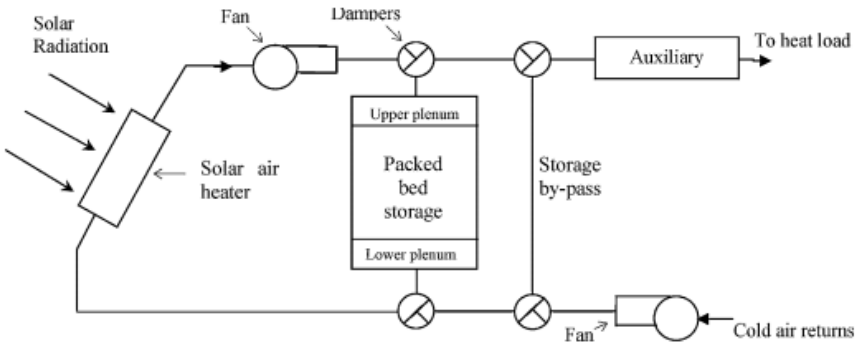

Fig. 1-6 A typical packed bed thermal energy storage system [15]

The use of rocks for thermal storage provides the following advantages [15]: (a) Rocks are not toxic and non-flammable; (b) Rocks are inexpensive; (c) Rocks act both as heat transfer surface and storage medium in the above system. The heat transfer between air and a rock bed is good, due to the very large heat transfer area, and the effective heat conductance of the rock pile is low, due to the small area of contact between the rocks. In this case the heat loss will be low. Compared to the water heat storage system, larger amounts of solid are needed due to the exhibiting lower storing capacity. The cost of the storage media per unit energy stored is, however, still acceptable for rocks.

(2) Building fabric thermal energy storage

For this kind of thermal energy storage system, the building structure itself can also be used as the medium to store thermal energy. In this way, both overall cost in construction and electricity cost for later residential heating and cooling can be reduced [13].

(3) Seasonal solid thermal energy storage

Borehole thermal energy storage and Gravel-water thermal energy storage are two types of seasonal sensible storage methods [13]. In general, the choice of the substance used depends largely on the temperature level of the application, water being used for temperature below 100ºC and refractory bricks being used for temperatures around 1000ºC [9].

In general, sensible heat storage systems suffer from the disadvantage of being bigger in size. A second disadvantage is that they cannot store or deliver energy at a constant temperature.

1.2.2 Latent heat storage

Heating a material undergoing a phase change (usually melting) is called latent heat storage [9]. The stored thermal energy during a latent storage process depends upon the mass *m* and latent heat of fusion *L* of the material.

$$Q = mH_L \qquad 1\text{-}2$$

The equation 1-2 shows the heat stored when the storage operates isothermally at the melting point of the material. If the system operates over temperatures range from T_1 to T_2 that includes the melting point, the amount of energy stored is given by:

$$Q = m\left[\left(\int_{T_1}^{T^*} C_{ps}\,dT\right) + \left(\int_{T^*}^{T_2} C_{pl}\,dT\right)\right] \qquad 1\text{-}3$$

Where C_{ps} and C_{pl} represents the specific heats of the solid and liquid phases and T^* is the melting point.

Based on the phase change during the storage process, the latent heat storage can be classified into solid-liquid, liquid-gas and solid-solid phase change materials (PCM) [12, 16]. During these three types of PCMs, solid-solid PCM is rarely suitable for the thermal energy storage in buildings. Liquid-gas PCMs have large amounts of heat of transformation, but large changes in volume make the system complex and impractical [13]. Heat storage through phase change from solid to liquid has the advantage of compactness by exhibiting relatively high thermal energy storage density since the latent heat of fusion of most materials is much larger than the enthalpy change for

temperature increase. Moreover, the solid-liquid PCMs involve relatively small changes in volume.

The comparison between the solid-liquid PCMs and typical sensible heat storage materials were shown in Table 1-2, from which the exhibited advantages of the solid-liquid PCMs can be clearly seen. By using latent heat storage systems, large volumes required by the other two typical sensible heat storage systems are eliminated. PCMs are the most compact thermal energy storage system during the three compared systems (water, rock, solid-liquid PCMs). The initial costs are small because of PCM system's compactness.

There are mainly three solid-liquid types of PCMs: organic-PCM, inorganic-PCM and eutectic-PCM, and each of them can be further categorized into more detailed groups as shown in Fig. 1-7 [17]. In general, low phase-change point PCMs include paraffins, fatty acids, and hydrates. Many PCMs have been applied in building materials and solar heaters with detailed thermophysical properties studied. Sugar alcohols such as erythritol and mannitol have a high phase-change point over 100ºC. Molten salts were the most popular PCMs with a high phase-change point.

Though there are so many advantages of solid-liquid PCMs, they do have some problems: they have to undergo solidification and therefore cannot generally be used as heat transfer media in a solar collector or the load. Thermal conductivity of many PCMs is so poor resulting in large heat exchange area of the utilization area. Moreover, some of them are corrosive and special containers are needed. Finally, the price of latent heat storage materials is much higher than the sensible heat storage media generally employed, like water and rocks.

Table 1-2 Comparison of different storage techniques for solar space heating and hot water production applications [9]

	Sensible Heat Storage		Latent Heat Storage (PCM)
	Water	Rock	(Solid-Liquid)
A) Comparison between different heat storage media			
Operating temperature range choice	Limited	Large	Large, depending on the material
Specific heat	High	Low	Medium
Thermal conductivity properties	Low, convection effects improve heat transfer rate	Low	Very low, insulating
Thermal storage capacity per unit mass and volume for small temperature differences	Low	Low	High
Stability to thermal cycling	Good	Good	Insufficient data
Availability	Overall	Almost overall	Dependent on the choice of material
Cost	inexpensive	Inexpensive	Expensive
Comparison of heat transfer properties and life of different types of thermal stores			
Required heat exchanger geometry	Simple	Simple	Complex
Temperature gradients during charging and discharging	Large	Large	Small
Thermal stratification with effect	Existent, works positively	Existent, works positively	Generally non-existent, Proper choice of material
Simultaneous charging appropriate discharging exchanger	Possible	Not possible	Possible with selection of heat
Integration with solar heating/cooling systems	Direct integration with water systems	Direct integration with air systems	Indirect integration
Cost of pumps, fan, etc.	Low	High	Low
Corrosion with conventional materials of construction	Corrosion eliminated through corrosion inhibitors	Non-corrosive	Presently only limited information avalable
Life	Long	Long	Short

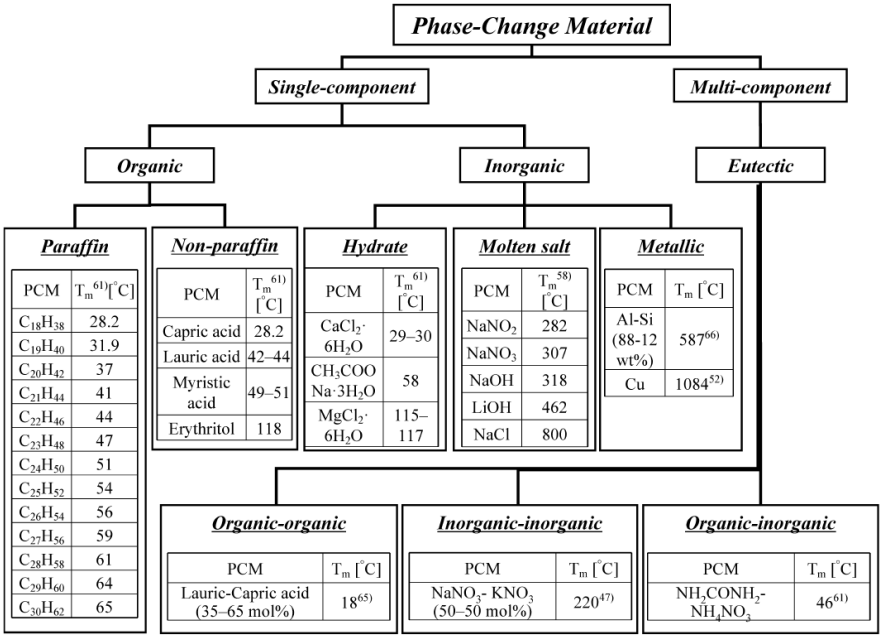

Fig. 1-7 Classification of PCMs, with examples of PCM candidates and their melting points [17]

1.2.3 Chemical thermal energy storage

Chemical thermal energy storage is an indirect way to store heat, in which heat is used to produce a certain physic-chemical reaction (sorption and thermochemical reaction) and then the products can be stored. The heat is released when the reverse reaction occurs [9].

Usually, it is difficult to make clear boundary distinctions between terms as “chemical thermal energy storage”, “thermochemical storage” and “sorption storage” [18]. Fig. 1-8 shows the chemical and sorption storage classification, in which the definition of thermochemical storage overlaps the definition of sorption storage as well as chemical storage. Sorption phenomena can involve both thermo-physical and thermo-chemical aspects [4], which is a general term including both absorption and adsorption. In thermochemical energy storage system, heat is stored after a dissociation reaction and then recovered in a chemically reverse reaction [11]. In this research, we consider that the chemical thermal energy storage includes sorption and thermochemical reactions [11].

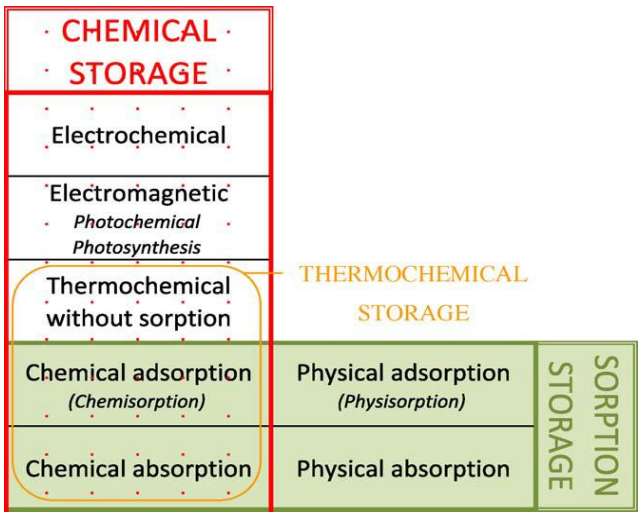

Fig. 1-8 Classification of chemical storage and sorption storage [4]

1.2.3.1 Principle of chemical thermal energy storage

Sorption and thermochemical storage systems are based on performing a reversible chemical reaction (or desorption), which allows absorption of heat in the decomposition (desorption) process, an endothermic process. A reverse synthesis reaction is exothermic process to release the stored heat in endothermic process [12].

Sorption and thermochemical storage systems use a reverse physic-chemical reaction to store energy, and C is the compound. With heat supply, C can be dissociated into products A and B, which can be stored separately. C will be formed with a heat release when A and B bound together [5] (cf. Eq. 1-4).

$$C + \text{heat} \Leftrightarrow A + B \qquad 1\text{-}4$$

In general, the following three main processes are included in a thermal energy storage system: charging, storing and discharging. The three processes are illustrated for thermochemical energy storage in Fig. 1-9 [6].

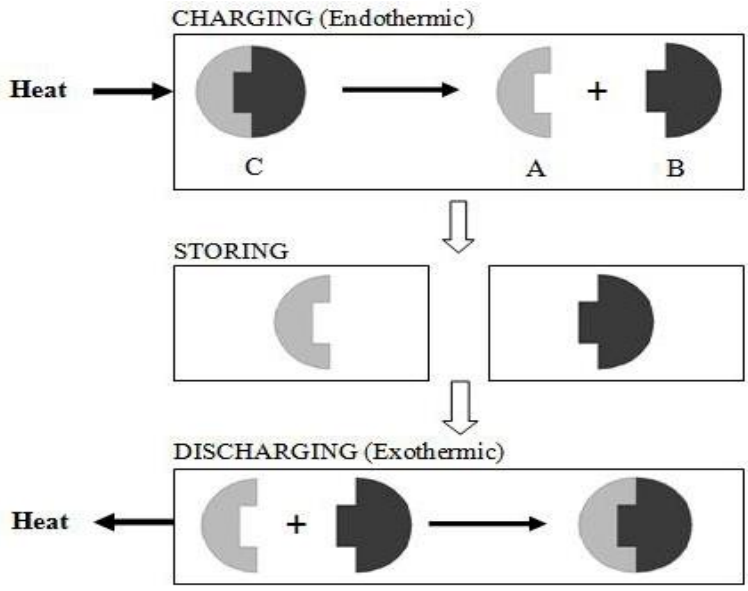

Fig. 1-9 Processes involved in a chemical energy storage cycle: charging, storing and discharging [6, 11]

1.2.3.2 Advantages and disadvantages of chemical thermal energy storage technology

Of the above described main thermal energy storage methods, sensible and latent heat storage systems are in use, while chemical thermal energy storage systems are being proposed for use in the future. The different types of the thermal energy storage systems are compared in Table 1-3, which considers some relevant performance parameters. The main advantages of chemical thermal energy storage are listed as follows [19]:

(1) High thermal energy density resulting in small volume of material (cf. Fig. 1-10);

(2) Many chemical heat pumps are able to make cooling and heating at the same time.

The main disadvantages [19]:

(1) Complexity of the closed system;

(2) High price of the material;

(3) Relatively high regeneration temperature are required;

(4) Degradation of the material (after a certain cycles use).

Table 1-3 Comparison of different types of thermal energy storage based on various performance factors [11]

Performance parameter	Type of thermal energy storage		
	Sensible heat storage	Latent heat storage	Chemical heat storage (Sorption and Thermochemical)
Temperature range	Up to: 110ºC (water tanks) 50ºC (aquifers and ground storage) 400ºC (concrete)	20-40ºC (paraffins) 30-80ºC (salt hydrates)	20-200ºC
Storage density	Low (with high temperature interval); 0.2 GJ/m^3 (for typical water tanks)	Moderate (with low temperature interval): 0.3-0.5 GJ/m^3	Normally high: 0.5-3 GJ/m^3
Lifetime	Long	Often limited due to storage material cycling	Depends on reactant degradation and side reactions
Technology status	Available commercially	Often commercially for some temperatures and materials	Generally not available, but undergoing research and pilot project tests
Advantages	Low cost Reliable Simple application with available materials	Medium storage density Small volumes Short distance transport possibility	High storage density Low heat losses (storage at ambient temperatures) Long storage period Long distance transport possibility High compact energy storage
Disadvantages	Significant heat loss over time (depending on level of insulation) Large volume needed	Low heat conductivity Corrosivity of materials Significant heat losses (depending on level of insulation)	High capital costs Technically complex

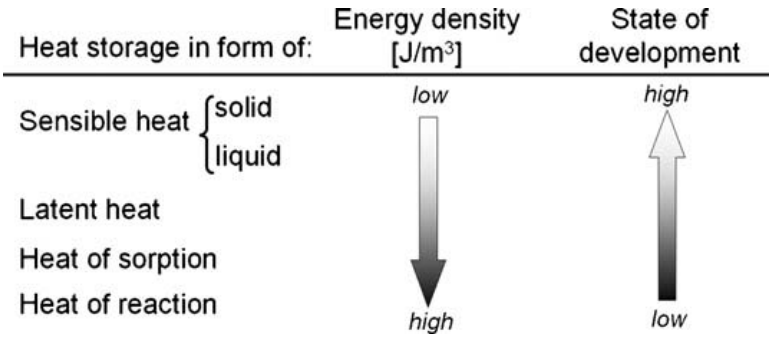

Fig. 1-10 Energy storage density of physical and chemical changes [4]

1.2.3.3 Main challenges and selection criteria for chemical thermal energy storage

The research related to chemical thermal energy storage is confronting the following challenges [4]:

(1) The choice of the best system (open or closed);

(2) The storage density optimization linked to the choice of materials;

(3) The vessels/tanks design;

(4) The heat exchangers design and the reactors configuration;

(5) Pressure drop;

(6) The low-regeneration temperature;

(7) Efficiency;

(8) Cost;

1.3 REVIEW ON CURRENT RESEARCH ON THERMOCHEMICAL ENERGY STORAGE TECHNOLOGY

In this section, the researches related to the chemical thermal energy storage will be reviewed. The methods to stored heat with temperature lower than 100ºC will be mainly concentrated. Thermochemical storage systems can be divided into open and closed systems [12]. The open system is based on the sorption processes to release heat and desorption process to store heat. Closed systems work with a closed working fluid circuit isolated from the atmosphere [19].

1.3.1 Open chemical thermal energy storage technology

In an open sorption thermal energy storage system, air is working as the heat and mass transfer medium flowing into the solid thermal energy storage materials, where the air can contact directly with the material (cf. Fig. 1-11) [20]. Gaseous working fluid of open system is directly discharged to the environment and operated at atmospheric pressure [21]. Normally, only water is possible to be used as the candidate of the working fluid. The working solid materials are required to be non-toxic and non-flammable in open systems. In open thermal energy storage systems, the heat charging process and heat discharging process are separated to maintain low heat loss [12]. In view of the environmental impact and low-temperature heat sources (< 100ºC), water vapor sorption on solid materials is promising as a kind of thermal energy storage method [22-24].

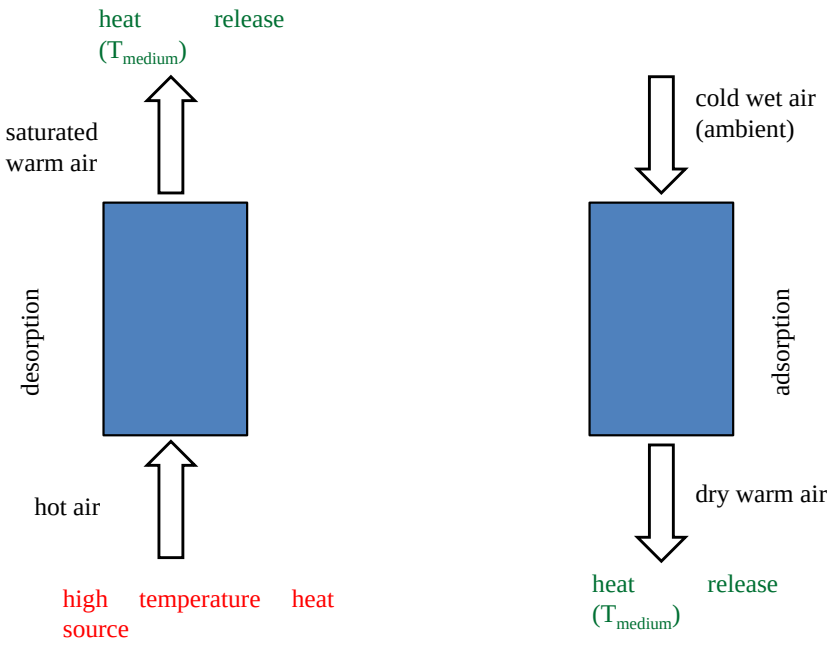

Fig. 1-11 Open principle of open thermochemical energy storage [4, 12]

So far, there are few research studies about open sorption thermal energy storage system. Abedin et al. [25] investigated a closed and an open thermochemical energy storage systems based on energy and exergy methods. The adopted exergy method enhances assessments of energy method. For their open heat storage system, Zeolite 13X was used as thermal energy storage material. The overall energy and exergy efficiencies are 69% and 23%, respectively. Moreover, there is a significant margin for heat loss reduction and efficiency improvement for open thermal energy storage system [6, 25]. Wu et al. [26, 27] developed an open-type thermal energy storage setup with 40 kg composite sorbent pellets (silica gel filled with $CaCl_2$). Moreover, they also reported a three-dimensional numerical model [28] to determine the dynamic characteristics of composite sorbents and to calculate the specific capacity and coefficient of performance (COP) of the open system. According to their results, the developed system showed high thermal energy storage density and can be regenerated at low temperature (<100ºC). However, the computational results were validated with the experimental results on open system, and the specific thermal energy storage capacity increased while the COP decreased. Ostrovskii et al. [29, 30] have proposed a non-stationary model to describe water sorption in a flow adsorber with a fixed bed of selective water sorbents (SWSs) (calcium chloride in a porous matrix) at pressures of 7 atm and 1 atm, respectively. And analytical expression for the sorption rate constant as

a function of the moisture content of the sorbent is proposed that takes into account the monotonic decrease in this constant with an increase in the amount of water sorbed. Unfortunately, both of the two open systems described above [26, 27, 29, 30] keep the functional fluid flowing through the inter particles of their composite materials without an individual flow passage for fluid, which would cause a high pressure drop. Moreover, a heat exchanger is needed to improve the heat exchange between the air and the composite material [26].

For seasonal solar energy storage, the choice was focused on a techno-economical study carried out at Energy Research Centre of the Netherlands (ECN) [31] with a large reactor. The $MgCl_2 \cdot 6H_2O$ was adopted as the thermal energy storage material. In order to avoid the problems related to overhydration of pure material, the magnesium chloride hydrated was impregnated into a carried material. $MgCl_2 \cdot 6H_2O$ has shown its potential as a thermochemical material for seasonal heat storage due to its high thermal energy storage density and suitable temperature release [32]. However, this compound has several limitations for long-term storage because of its instability and decomposition at temperatures higher over 135ºC.

Composite materials have been developed recently as novel thermal energy storage materials by impregnating hygroscopic salt inside the matrix of a porous adsorbent for multiple applications [23, 33]. An open system utilizing the sorption and desorption of their developed composite material by impregnating $CaCl_2$ or LiBr into the pores of KSKG silica gel, γ-alumina and porous carbon. A solar driven water production lab-scale unit was demonstrated. Their results showed that per 10 tonnes of the dry sorbent can produce 3-5 tonnes of water per day.

1.3.2 Closed chemical thermal energy storage technology

In closed thermal energy storage system, the components cannot be exposed to the atmosphere. As can be seen in Fig. 1-12, in heat release process, water vapor can be used to combine with the working material and the operation pressure of the working fluid can be adjusted. The thermal energy transferred to or from the closed system needs to use heat exchanger. Compared to the open thermal energy storage system, the heat storage density is lower for the closed system due to the water vapor has to be

stored at the same time as the working adsorbent [20]. However, closed systems are able to supply higher output temperatures for heating applications than open system, but usually requires higher temperatures during the heat charging process than the open system [12]. Meanwhile, closed systems can be used to supply low temperatures for space cooling [34].

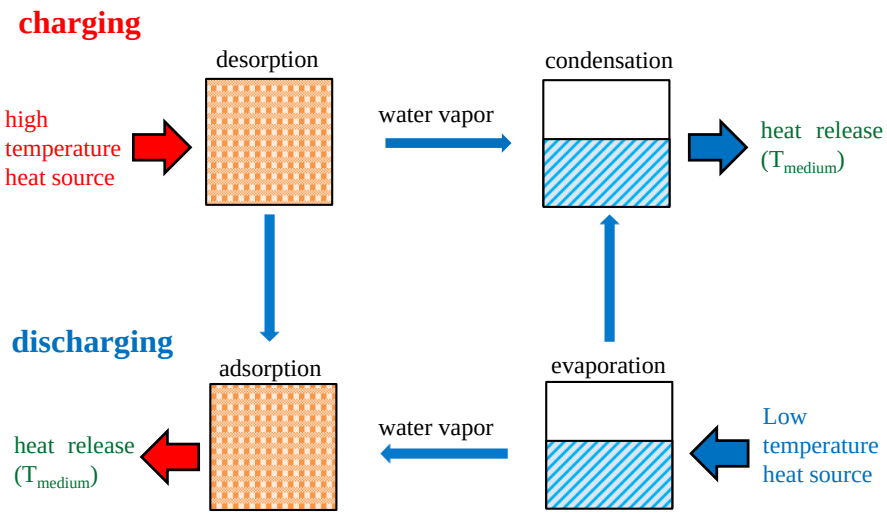

Fig. 1-12 Operation principle of closed thermochemical energy storage [4, 12]

Today there are many publications on various closed thermal energy storage systems and their applications.

1.3.2.1 Low temperature (< 100ºC) chemical thermal energy storage materials

In view of the environmental impact and low-temperature heat sources (< 100ºC), water vapor sorption on solid materials is promising as a kind of thermal energy storage method [23, 24]. Tahat [35] investigated silica gel theoretically and experimentally during both heating and cooling modes of a thermochemical heat pump/energy store system. Saha et al. [36, 37]developed a new silica gel adsorption chiller driven by low-temperature waste heat from 60ºC to 95ºC. However, the specific energy storage capacity is not so high because of low adsorption amount and low adsorption heat [23], consequently incurring large and heavy thermal energy storage apparatus.

Zeolite is also tested by Cuypers et al. [38] from the Netherlands. Initial experiments for themochemical storage took place on a glass/desorption and evaporation/condensation. Although it shows adequate loading and unloading cycles

with a maximum specific unloading power of 164 W/kg, it suffered from thermal losses and low heat exchange rate.

Recently, significant progresses have been achieved in development of novel adsorbent materials for low temperature heating and cooling applications. Well known superior commercial adsorbents are the Mitsubishi AQSOA [3].

There are also some pure chemical substances being researched as potential low-temperature energy storage materials. Boer et al. [39] developed a Sodium sulfide (Na_2S) cooling system with a copper wire-fin heat exchanger. Na_2S-H_2O has a eutectic melting point of 83ºC [40], which imposes the upper limits for the regeneration temperature in its system. The storage capacity of Na_2S in the form of $Na_2S \cdot 5H_2O$ is approximately 3.84 MJ/kg for heat and 2.54 MJ/kg (1,300 kWh/m^3) for cooling with a coefficient of performance (COP) of 0.84 and 0.57, respectively. The conclusion that the monohydrate or pentahydrate of sodium sulphide gives a high thermal energy storage density and a high thermal power density was given by Iammak et al. [41]. However, Boer et al. [39] revealed that it is very corrosive and has to be operated under high vacuum condition.

Abedin et al. [25, 42] investigated a closed thermochemical energy storage systems using energy and exergy methods. Exergy analysis can be used to identify the locations and reasons of themodynamic losses and evaluate the efficiencies of the developed closed thermal energy storage system. In their closed system, $SrBr_2 \cdot 6H_2O$ was used as thermal energy storage material. The overall energy and exergy efficiencies are 50% and 9%, respectively. Lahmidi et al. [43] simulated a sorption process based on a system using strontium bromide incorporated into a solar energy storage system, and an experimental tests were conducted corresponding to the temperature ranges used in solar heating and cooling system [44]. They concluded that the adopted simple model will be valuable for optimization of the solid-gas reactor design. The developed prototype is still insufficient to supply the required heating and cooling powers in summer or mid-season because of a low heat transfer at the interface between the material and heat exchanger [44].

Several potential materials for seasonal storage of solar energy have been tested by ECN [45-48]. The magnesium sulphate heptahydrate ($MgSO_4 \cdot 7H_2O$) was concluded to

be promising for the development of an autonomous thermochemical storage system [46, 48] as presenting theoretically a very good potential in terms of solar energy storage with high density of almost 780 kWh/m^3 [49] at temperature level of 122ºC. $MgSO_4 \cdot 7H_2O$ is non-toxic and non-corrosive but expensive. It is essential that salt hydrates can incorporate large amounts of water into the crystal lattice. When the hydrated salt is heated, the water is driven off. In solar energy storage system, the heat collected by solar collectors can be employed to dehydrate the salt. The anhydrous salt is stored until needed. Recently, van Essen et al. [50] assessed the capability of $MgSO_4 \cdot 7H_2O$ as a suitable thermochemical energy storage material by experiments, as well as Balasubramanian et al. [51], who used a mathematical model. The simulated method can help identify optimal materials for thermochemical storage within practical constraints. However, $MgSO_4 \cdot 7H_2O$ cannot release all the stored heat in practical condition [50].

For investigation of $CaCl_2$ as thermal energy storage material, Fujii et al. [52] developed a chemical heat pump using calcium chloride to store solar energy. Plate type heat exchanger with 24 plates was used in the reactor, and 50 g $CaCl_2$ was put on each plate. A regeneration temperature of 90ºC was adopted to regenerate the calcium chloride hydrates. They concluded that their developed system is promising as space heat device. Sasaki et al. [53] also tested $CaCl_2$ as a thermal energy storage material to recover waste heat. The developed system cannot run within a large temperature and pressure range In order to avoid the deliquescence of $CaCl_2$.

The $CaSO_4$ was tested by Ogura et al [54-57]. In the heat storing step, it was found possible to store exhaust in the temperature range around 120ºC and the effects of heat storing temperature on heat storing rates were clarified. In the heat releasing step, it was found that cold-heat of less than 5ºC was recovered in an evaporator, while hot-heat was generated in the reactor. By adding ethylene glycol into the water, a cold heat lower than -15ºC can be even obtained. However, only 297 kJ of heat [54] can be stored in a reactor filled with 2,400 g of $CaSO_4$ (i.e., its heat storage density is 123.75 kJ/kg) because of its small theoretical reaction heat (16.8 kJ/mol).

Indeed, a pure salt can hardly be directly used, because of corrosive properties, strong swelling and expansion when reacting with water, very slow kinetics and hysteresis of the reaction with water [58]. Composite materials have been developed recently as

novel thermal energy storage materials by impregnating hygroscopic salt inside the matrix of a porous adsorbent for multiple applications.

Aristov et al. [23, 59-68] presented sorption properties and kinetics of the selective water sorbents (SWSs), and evaluated their thermodynamic performance in heat pump and refrigeration systems. In 2002, Freni et al. [67] tested the thermal conductivity of SWS-1L ($CaCl_2/SiO_2$), SWS-2L (LiBr/ SiO_2) under the working conditions of a sorption chiller using "hot wire method". The sorbent thermal conductivity increases considerably as sorption amount rises. The influence of grain size and temperature on Kinetics of water sorption on SWS-1L was performed by a microbalance under isothermal external conditions by Aristov et al. [69]. A remarkable enhancement of the sorption rate and apparent diffusion constant can be obtained with the decrease in the particle size.

Effect of the adsorbent nature, grain size, residual non-adsorbable gas, heating rate, local shape of adsorption isobar on the adsorption dynamics and specific cooling power was studied [70-73] for SWS-1L. Their results showed that near-exponential kinetic curves were found for a majority of sorption and desorption runs. A specific cooling power of 0.5-2 kW/kg can be easily obtained with a simple configuration of loose adsorbent grains. Large deviations from the equilibrium the heat and mass transfer can be more efficient than under quasi-equilibrium conditions.

Restuccia et al. [74] developed a lab-scale chilling module working with the composite sorbent SWS-1L packed outside of a heat exchanger. The interesting sorption properties of SWS-1L yield a high COP=0.6 that gives a promising alternative to the common zeolite or silica gel for application in solid sorption units driven by low temperature heat (90-95ºC). The measured low specific power of the device is a result of not optimized geometry of the adsorber and of the pelletised shape of the adsorbent. Heat transfer optimization is going to be solved to increase the specific power.

Freni et al. [75] conducted an experimental testing on an advanced solid sorption chiller based on a finned tubes heat exchanger coated with a compact layer of SWS-1L. The experimental results showed a specific power of 150-200 W/kg of adsorbent and a cycle time of 10-20 min. The heat exchanger was assembled using special aluminum alloy finned tubes, in which the fins and the tube are a single body. The other

components were also made of an aluminum alloy to reduce the inert weigh. It is considered that the increased heat transfer through the adsorbent bed is the reason of high specific power of the chiller.

Other SWSs adopted into a sorption chiller were also tested by Aristov et al. [76-78].

1.3.2.2 Medium temperature (100-300ºC) chemical thermal energy storage materials

For the medium temperature chemical thermal energy storage materials, Magnesium oxide is a typical material being researched by Kato et al. The kinetic dynamics, durability and feasibility of the MgO/H_2O were studied in [79-83]. The magnesium was considered to be able to combine with the decentralized cogeneration [81]. This medium temperature chemical heat pump can enhance the energy utilization efficiency of the cogeneration system by soring surplus exhausted heat from the cogeneration system.

However, the pure MgO/H_2O chemical heat pumps need a heat source higher than 350ºC. In order to utilize heat below 300ºC, composite magnesium hydroxides contained with other metal ion (Ni, Co) were made [84, 85]. The mixed hydroxides was dehydrated at 200-300ºC, which means that it has the potential to store medium temperature heat discharged from internal combustion engines and high temperature systems. Kim et al. [86, 87] evaluated a chemical heat pump with reactivity enhancement of chemical materials EMCs, which is a mixture comprising expanded graphite, $Mg(OH)_2$ and $CaCl_2$. The EMCs was proved to have higher dehydration rate and hydration reactivity of up to 200ºC compared to the pure $Mg(OH)_2$.

1.3.2.3 High temperature (> 300ºC) chemical thermal energy storage materials

There are several groups doing a research on high temperature chemical thermal energy storage material: $CaO-H_2O$, which needs to be dehydrated at around 500ºC. Nagoya University's Matsuda et al. [88] studied the $Ca(OH)_2/CaO$ reversible thermochemical reaction involving both heat storage and heat-release characteristics experimentally. In 1988, a high-temperature chemical heat pump on laboratory scale by combining a $Ca(OH)_2/CaO$ reversible thermochemical reaction with the evaporation of water in two hermetic cylindrical vessels were constructed [89].

Ogura et al. [90, 91] investigated a $CaO-H_2O$ chemical heat pump by improving the heat transfer rate in the reactor by inserting copper fins experimentally and numerically. In 1993, the cooling and refrigeration by the $CaO-H_2O$ chemical heat pump were investigated experimentally. Low temperature level heat around 0ºC is possible to be generated, but the mass transfer at low pressure should be enhanced in order to improve heat generation [92].

Fujimoto et al. [93, 94] did research on dynamic simulation of an experimental prototype $CaO/Ca(OH)_2$ high temperature chemical heat pump. Optimum operation conditions of the system were also confirmed as improvement of condensation condition in condenser. With the developed system, 80ºC hot water and 5ºC cold heat can be obtained, although the heat exchangers need to be improved [95].

Several different designs of high temperature chemical heat pumps system were proposed and tested by Ogura et al. [96-98]. They were supposed to supply hot air, store heat, and supply heating and cooling.

Table 1-4 Summary of studies on closed chemical thermal energy storage systems

Author	Working pairs	Heat source temperature	Nature	Applications and solution/validation/results
Abedin and Rosen [25, 42]	$SrBr_2 \cdot H_2O$	80ºC	Analytical	Energy and exergy methods, both for open and closed thermochemical energy storage systems.
Lahmidi et al. [43, 44]	$SrBr_2 \cdot H_2O$-expanded natural graphite	80ºC	Experimental and numerical	Solid/gas sorption process combined with solar heat system was simulated. The adopted simple model will be valuable for optimization of the solid-gas reactor design. The prototype of the closed system is still insufficient to supply the heating and cooling in summer or mid-season because of a low heat transfer at the interface between the material and heat exchanger.
Boer et al. [39]	Na_2S-Cellulose	83ºC	Experimental	A shell-and-tube design sodium sulfide cooling system with a copper wire-fin heat exchanger was developed, which can achieve a maximum value of SCP of 500 W/kg Na_2S.
Iammak et al. [41]	Na_2S-EG	80-95ºC	Experimental	A modular chemical heat pump with tube-and-tube design reactor was operated at 80-95ºC, and the overall heat transfer coefficient and COP were improved.
Fujii et al. [52]	$CaCl_2/H_2O$	90ºC	Experimental	A plate heat exchanger reactor was designed to improve heat transfer of the heat exchanger and material. A total COP of 0.256 was achieved.
Sasaki et al. [53]	$CaCl_2/H_2O$	130ºC	Experimental	A chemical heat storage tank using $CaCl_2/CaCl_2 \cdot {}_2H_2O$ was developed, with which the reaction rate can reach 80% with a hydration/dehydration time 5 to 6 hours.
Sharonov et al [99]	$MgCl_2 \cdot 2H_2O$, etc	120.3ºC	Analytical	Chemical and adsorption heat pumps, the second law efficiency, and degradation of the efficiency due to the thermal entropy production.
Essen et al. [50]	$MgSO_4 \cdot 7H_2O$	122ºC	Experimental	The properties of the material during charing and discharging were studied showing that $MgSO_4 \cdot 7H_2O$ can be dehydrated at temperature below 150ºC. But the stored heat is difficult to release in discharging process in practical condition.
Balasubramanian et al. [51]	$MgSO_4 \cdot 7H_2O$	200ºC	Numerical	Mathematical model to investigate the capability of salt hydrates to store thermochemical energy, employing a finite difference scheme.

Table 1-4 Continued

Author	Working pairs	Heat source temperature	Nature	Applications and solution/validation/results
Ghommen et al. [100]	$MgSO_4 \cdot 7H_2O$	200ºC	Numerical	Modelling the heat release during a thermochemical hydration reaction, dimensionless parameters have influence on the heat release process.
Posern et al. [101]	$MgSO_4$-$MgCl_2$	130ºC	Experimental	Isothermal heat of sorption and thermogravimetry, reduce the deliquescence relative humidity and increased the capacity of condensation.
Ogura et al. [54]	$CaSO4 \cdot 2H_2O$	100ºC	Experimental	In the heat storing step, it was found possible to store exhaust in the temperature range around 120ºC and the effects of heat storing temperature on heat storing rates were clarified. In the heat releasing step, it was found that cold-heat of less than 5ºC was recovered in an evaporator, while hot-heat was generated in the reactor.
Aristov et al. [59, 60]	$CaCl_2$mesoporous KSK/microporous KSM silica gel (SWS-1L/SWS-1S)	150ºC/120ºC	Experimental	Sorption isobars, isotherms, isosteric sorption heat of SWS-1L/SWS-1S were identified.
Freni et al. [67]	$CaCl_2$-mesoporous KSK silica gel, LiBr mesoporous KSK silica gel (SWS-1L/SWS-2L)	130ºC	Experimental and Numerical	The thermal conductivity of SWS-1L (CaCl2/SiO2), SWS-2L (LiBr/ SiO2) under the working conditions of a sorption chiller was tested using “hot wire method”, which increases considerably as sorption amount rises. The effect of the thermal conductivity of composite material on the specific power of chiller was calculated, indicating that the enhancement of heat transfer properties of the adsorbent bed is necessary.
Aristov et al. [69]	$CaCl_2$-mesoporous KSK silica gel (SWS-1L)	130ºC	Experimental	The influence of grain size and temperature on kinetics of water sorption on SWS-1L was performed by a microbalance under isothermal external conditions indicating small particle size can enhance sorption rate and apparent diffusion constant. A dynamic model was proposed to study the influence of main operation parameters on the system performance.

Table 1-4 Continued

Author	Working pairs	Heat source temperature	Nature	Applications and solution/validation/results
Restuccia et al. [74]	$CaCl_2$ - mesoporous KSK silica gel (SWS-1L)	90-95ºC	Experimental and Numerical	A lab-scale chilling module working with the composite sorbent SWS-1L packed outside of a heat exchanger wad developed. A high COP but a low specific power was found due to the low heat transfer between the material and heat exchange.
Saha et al. [102]	$CaCl_2$ - mesoporous KSK silica gel (SWS-1L)	85ºC	Numerical	A single effect two-bed adsorption chiller utilizing SWS-1L was simulated. The new material provides better cooling capacity and performance compared to the conventional RD silica gel chiller.
Freni et al. [75]	$CaCl_2$ - mesoporous KSK silica gel (SWS-1L)	95-100ºC	Experimental	The experimental testing on an advanced solid sorption chiller based on the heat exchanger coated with working material was presented. The performance is better than the pelletized bed reactor in [74].
Freni et al. [103]	$Ca(NO_3)_2$ - mesoporous KSK silica gel (SWS-8L)	90-95ºC	Experimental	Influence of the cycle time on performance of the system was conducted; high COP can be obtained by prolonging the cycle time.
Sapienza et al. [77]	$LiNO_3$-Vermiculite (SWS-9V)	68ºC, 90ºC	Experimental	Low regeneration temperature (< 70ºC), the cycle performance dependents on cycle time and duration of the isobaric adsorption and desorption.
Aristov et al. [78]	$LiNO_3$-silica KSK (SWS-9L)	65-75ºC	Experimental	Intermittent cooling cycle with adsorption and desorption, the duration of desorption phase has efficient on the cycle COP and SCP.
Kim et al. [86]	$Mg(OH)_2$-Expanded graphit-$CaCl_2$	200-300ºC	Experimental and analytical	Reactivity enhancement of chemical materials, EMC (mixed material containing expanded graphite (EG), $Mg(OH)_2$, and $CaCl_2$) have potential in MgO/H_2O chemical heat pump.
Ogura et al. [98]	CaO	594ºC	Experimental	A heat enhancement mode chemical heat pump assisted convective hot air dryer was proposed and tested. Enlarging heat exchanger, use stainless mesh and increasing air flow rate can improve hot air production.

Thermochemical energy storage systems utilize renewable energy or waste heat over a wide temperature range. Table 1-4 provides a list of studies for different solution methods in investigating closed chemical thermal energy storage systems. Among all

the research methods, the analytical model are simple and quick to calculate the performance of the material [12]. The experimental methods are basic method to examine the performance of a material to act as a thermal energy storage material.

1.4 PROBLEMS IDENTIFICATION

An overall review on the chemical thermal energy storage has been carried out, from which the chemical thermal energy storage has shown some advantages as following [12]:

(1) Higher energy density compared to physical change thermal energy storage methods;

(2) Long-term storage can be achieved with low heat loss;

(3) Easily transmitted to generate heat at another location;

(4) Wide temperature range and characteristics;

Currently, the research of chemical thermal energy storage is still at an experimental stage and some challenges and barriers are still needed to be overcome. More research, development and demonstration projects are required to prove the viability and superiority of chemical thermal energy storage technology.

Although there are some promising thermochemical potential materials under research, there are some main problems for researchers to overcome to do further research about chemical thermal energy storage.

(1) Chose appropriate system (closed or open) according to different application targets.

(2) The low heat and mass transfer properties of the chemical materials should be improved. Some methods to deal with increasing high thermal conductivity were proposed or concluded by Fujioka et al. [104, 105] and Kim et al. [86, 87].

(3) A very important characteristic of a heat storage system is its volumetric energy capacity, or mass specific thermal energy storage density. The smaller and the lighter the heat storage unit, the better is the storage system. Therefore, a good system should have a long storage time and a small volume per unit of stored energy.

(4) The price of the material should be reasonable, as well as the cost of the storage unit: this includes the initial cost of the storage medium, the containers and insulation, and the operating cost.

(5) The regeneration temperature of the material should be suitable for the available heat source temperature. For example, in order to store large amount of low-temperature waste heat discharged from industrial sector and solar energy, the regeneration temperature of the material should be not so high.

(6) The stability of the chemical thermal energy storage material needs to be evaluated.

(7) In closed thermal energy storage systems operated in vacuum conditions, the presence of non-condensable gases can reduce strongly the performance of the system [39]. Therefore, how to avoid leakage in a closed system is vital for a successful negative pressure closed thermal energy storage system.

(8) The heat exchangers design and reactors configurations are so important for a mature chemical thermal energy storage system.

(9) High efficient heat storage system is expected to be developed.

The technology of chemical thermal energy storage has been developed to a point where it can have a significant effect on modern life. Therefore, the above mentioned challenges should be overcome as much as possible to develop a sustainable energy utilization society in future.

1.5 OBJECTIVES OF THIS RESEARCH

In this study, a comprehensive review of various types of thermal energy storage systems, especially chemical thermal energy storage technologies are presented. Principles of open and closed chemical thermal energy storage systems were given in section 1.3.1 and 1.3.2, respectively.

There are several objectives of this thesis, which are listed as follows:

(1) The first objective is to develop a suitable material for a chemical thermal energy storage system with high heat storage density by considering the above mentioned problems of the chemical thermal energy storage.

(2) The second objective is to develop an open sorption thermal energy storage system, which can be utilized to recover low temperature waste heat (< 100ºC) discharged from industrial sector (cf. Fig. 1-3) and solar energy.

(3) The third objective in this research is to design an optimizing closed chemical thermal energy storage system to supply both heat and cold heat.

1.6 OUTLINE OF THIS THESIS

Chapter 1 presents a general introduction of the thesis. This includes the background of the thermal energy storage, introduction of the three main categories of thermal energy storage technology, especially the chemical thermal energy storage technology, and a detail description of the current research situation of the chemical thermal energy storage technology.

In Chapter 2, a new composite mesoporous material impregnated with $CaCl_2$ was developed. The physical properties, sorption properties, stability and regeneration temperature et al. were investigated before being incorporated into an open chemical thermal energy storage system with a honeycomb shape. The regeneration temperature, flow rate of the air in heat release process, relative humidity of the inlet air, and content of the salt were discussed.

In Chapter 3, a numerical simulation model was created to investigate the capability of the above developed composite mesoporous thermal energy storage unit to store thermochemical energy. This program, based on the effect of coupled heat and mass transfer. The simulation results were validated by the experimental values. Using our simulation program, the effects of the inlet air temperature and relative humidity, humid air flow rate, and thermal energy storage unit length on the system's performance were studied. At last, a realistic application was proposed and simulated.

Chapter 4 examined a new composite material by impregnating LiCl, and the performance of this composite material was compared with the composite material impregnated with $CaCl_2$ with same sorption amount. The reasons caused the observed different performances of these two composite material were given.

In Chapter 5, a basic research of the composite material impregnated with LiCl was done by determining the isobaric and isosteric sorption chart of the composite material/water working pair in a closed thermal energy storage system. Then the operation cycle was determined. A small scale sorption air cooler by using the developed composite material was built, and the performance of the air cooler was tested.

In Chapter 6, a larger scale closed chemical thermal energy storage lab-scale prototype using the developed composite material in Chapter 5 is introduced. The performance of the coated type reactor was evaluated and tested.

Chapter 7 presents several application proposals for both the developed open and closed chemical thermal energy storage systems.

Chapter 8 presents a general conclusion of the study.

1.7 SUMMARY

Thermal energy storage can store both industrial waste heat and renewable energy to save fossil fuel and enlarge the energy market consumption percentage of the renewable energy. Within all the types of thermal energy storage, chemical heat storage technology no matter the open type or the closed type, they show their potential to store thermal energy with temperature less than 100ºC, which corresponds to the temperature of large emissions of industrial waste heat released to the atmosphere, and solar heat stored by solar collectors.

The objective of this thesis is to solve the above mentioned problems of the chemical thermal energy storage, develop a suitable material and design open and closed chemical thermal energy storage systems to store low-temperature waste heat discharged from industrial sector (cf. Fig. 1-3) and solar energy.

1.8 REFERENCE

[1] M. Asif, T. Muneer, Energy supply, its demand and security issues for developed and emerging economies, Renewable and Sustainable Energy Reviews, 11(7) (2007) 1388-1413.

[2] A.A.P.E.R. Centre, APEC energy demand and supply outlook, APEC Asia Pacific Energy Rearch Centre, 2013.

[3] K. Hirata, H. Kakiuchi, Energy saving for ethylene process by Adsorption Heat Pump, Applied Thermal Engineering, 31(13) (2011) 2115-2122.

[4] K.E. N'Tsoukpoe, H. Liu, N.L. Pierrès, L. Luo, A review on long-term sorption solar energy storage, Renewable and Sustainable Energy Review, 13 (2009) 2385-2396.

[5] K. Y., Chemical energy conversion technologies for efficient energy use, in: Thermal energy storage for sustainable energy consumption, Springer, Netherlands, 2007, pp. 377-391.

[6] A.H. Abedin, Themochemical energy storage systems: modeling, analysis and design, University of Ontario Institute of Technology, 2010.

[7] I. Dincer, S. Dost, X. Li, Performance analyses of sensible heat storage systems for thermal applications, International Journal of Energy Research, 21(12) (1997) 1157-1171.

[8] I. Dincer, M.A. Rosen, Energetic, environmental and economic aspects of thermal energy storage systems for cooling capacity, Applied Thermal Engineering, 21 (2001) 1105-1117.

[9] O.E. Ataer, Storage of thermal energy

[10] H. Kameyama, Y. Kato, Honebuto energy road map, Kagaku Kogyo Sya, Japan, 2005.

[11] A.H. Abedin, M.A. Rosen, A critical review of thermochemical energy storage systems, The Open Renewable Energy Journal, 4 (2011) 42-46.

[12] Y. Ding, S.B. Riffat, Thermochemical energy storage technologies for building applications: a state-of-the-art review, International Journal of Low-Carbon Technologies, 0(1-11) (2012).

[13] S. Gao, State of the art thermal energy storage solutions for high performance buildings, University of Jyväskylä, 2010.

[14] J.A. Duffie, W.A. Beckham, Solar Engineering of Thermal Processes, 2nd ed., John Wiely and Sons, 1991.

[15] H. Singh, R.P. Saini, J.S. Saini, A review on packed bed solar energy storage systems, Renewable and Sustainable Energy Reviews, 14(3) (2010) 1059-1069.

[16] S.M. Hasnain, Review on sustainable thermal energy storage technologies, Part I: heat storage materials and techniques, Energy Conversion and Management, 39(11) (1998) 1127-1138.

[17] T. Nomura, N. Okinaka, T. Akiyama, Technology of Latent Heat Storage for High Temperature Application : A Review, ISIJ International, 50(9) (2010) 1229-1239.

[18] J.C. Gores, A. Castell, L.F. Cabeza, Thermochemical energy storage and conversion: A-state-of-the-art review of the experimental research under practical conditions, Renewable and Sustainable Energy Review, 16 (2012) 5207-5224.

[19] P. Gantenbein, A. Hauer, H.M. Henning, D. Jaenig, H. Kerskes, T. Núñez, K. Visscher, Thermal properties of materials for thermo-chemical storage of solar heat, 2005.

[20] H.Ö. Paksoy, Thermal Energy Storage for Sustainable Energy Consumption-Fundamentals, Case studies and Design., Springer, 2007.

[21] H. Liu, K. Nagano, D. Sugiyama, J. Togawa, M. Nakamura, Honeycomb filters made from mesoporous composite material for an open sorption thermal energy storage system to store low-temperature industrial waste heat, International Journal of Heat and Mass Transfer, 65 (2013) 471-480.

[22] C.Y. Liu, K. Morofuji, K.Tamura, K. Aika, Water sorption of $CaCl_2$ containing materials as heat storage media, Chemistry Letters, 33(3) (2004) 292-293

[23] E.A. Levitskij, Y.I. Aristov, M.M. Tokarev, V.N. Parmon, "Chemical heat accumulators": A new approach to accumulating low potential heat, Solar Energy Materials and Solar Cells, 44 (1996) 219-235.

[24] W. Wongsuwan, S. Kumar, P. Neveu, F. Meunier, A review of chemical heat pump technology and applications, Applied Thermal Engineering, 21 (2001) 1489-1519.

[25] A.H. Abedin, M.A. Rosen, Closed and open thermochemical energy storage: Energy- and expegy-based comparisons, Energy, 41 (2012) 83-92.

[26] D. Zhu, H. Wu, S. Wang, Experimental study on composite silica gel supported $CaCl_2$ sorbent for low grade heat storage, International Journal of Thermal Sciences, 45 (2006) 804-813.

[27] H. Wu, S. Wang, D. Zhu, Effects of impregnating variables on dynamic sorption characteristics and storage properties of composite sorbent for solar heat storage, Solar Energy, (2007) 864-871.

[28] H. Wu, S. Wang, D. Zhu, Y. Ding, Numerical analysis and evaluation of an open-type thermal storage system using composite sorbents, International Journal of Heat and Mass Transfer, 52 (2009) 5262-5265.

[29] N.M. Ostrovskii, N.A. Chumakova, N.M. Bukhavtsova, N.V. Vernikovskaya, Y.I. Aristov, Effect of capillary condensation on water sorption by composite calcium chloride in a porous matrix sorbents, Theoretical Foundations of Chemical Engineering, 41(2) (2007) 200-204.

[30] N.M. Ostrovskii, N.A. Chumakova, N.M. Bukhavtsova, N.V. Vernikovskaya, Y.I. Aristov., Modeling of the limiting step of Water Sorption by Composite Sorbents of the "Calcium Chloride in Porous Matrix" Type, Theoretical Foundations of Chemical Engineering, 41(1) (2007) 83-90.

[31] H.A. Zondag, V.M.v. Essen, L.P.J. Bleijendaal, B.W.J. Kikkert, M. Bakker, Application of $MgCl_2 \cdot 6H_2O$ for thermochemical seasonal solar heat storage, in: the 5th International Renewable Storage Conference IRES 2010, Berlin, Germany, 2010.

[32] C. Ferchaud, H. Zondag, R.d. Boer, C. Rindt, Characterization of the sorption process in thermochemical material for seasonal solar heat storage application, in: The 12th International Conference on Energy Storage, 2012, pp. 1-10.

[33] Y.I. Aristov, M.M. Tokarev, L.G. Gordeeva, V.N. Snytnikov, V.N. Parmon, New composite sorbent for solar-driven technology of fresh water production from the atmosphere, Solar Energy, 66(2) (1999) 165-168.

[34] A. Hauer, E. avemann, Open absorption systems for air conditioning and thermal energy storage, in: H. Paksoy (Ed.) Thermal Energy Storage for Sustainable Energy Consumption, Springer Netherlands, 2007, pp. 429-444.

[35] M.A. Tahat, Heat-pump/energy-store using silica gel and water as a working pair, Applied Energy, 69 (2001) 19-27.

[36] B.B. Saha, S. Koyama, J.B. Lee, K. Kuwahara, K.C.A. Alam, Y. Hamamoto, A. Akisawa, T. Kashiwagi, Performance evaluation ofa low-temperature waste heat driven multi-bed adsorption chiller, International Journal of Multiphase Flow, 29 (2003) 1249-1263.

[37] B.B. Saha, S. Koyama, T. Kashiwagi, A. Akisawa, K.C. Ng, H.T. Chua, Waste heat driven dual-mode, multi-stage, multi-bed regenerative adsorption system, International Journal of Refrigeration, 26 (2003) 749-757.

[38] R. Cuypers, C. Finck, E. Henquet, H. Oversloot, A.d. Geus, MERITS: More effective use of renewables including compact seasonal thermal energy storage, in: The 12th International Conference on Energy Storage, 2012.

[39] R.d. Boer, W.G. Haije, J.B.J. Veldhuis, S.F. Smeding, Solid-sorption cooling with integrated thermal storage: the SWEAT prototype, in, The International Conference on Heat Powered Cycles, HPC, Larnaca, Cyprus, 2004.

[40] R.d. Boer, W.G. Haije, J.B.J. Veldhuis, Determination of structural, thermodynamic and phase properties in the Na_2S-H_2O system for application in a chemical heat pump, Thermochimica Acta, 395 (2003) 3-19.

[41] K. Lammak, W. Wongsuwan, T. Kiatsiriroj, Investigation of modular chemcial energy storage performance, in: The Joint Conference on Sustainable Energy and Environment (SEE), Hua Hin, Thailand, 2004, pp. 504-507.

[42] A.H. Abedin, M.A. Rosen, Assessment of a closed thermochemical energy storage using energy and exergy methods, Applied Energy, 93(0) (2012) 18-23.

[43] H. Lahmidi, S. Mauran, V. Goetz, Definition, test and simulation of a thermochemical storage process adapted to solar thermal systems, Solar Energy, 80(7) (2006) 883-893.

[44] S. Mauran, H. Lahmidi, V. Goetz, Solar heating and cooling by a thermochemical process. First experiments of a prototype storing 60 kWh by a solid/gas reaction, Solar Energy, 82 (2008) 623-636.

[45] V.M.v. Essen, J.C. Gores, L.P.J. Bleijendaal, H.A. Zondag, R. Schuitema, M. Bakker, W.G.J.v. Helden, Characterization of salt hydrates for compact seasonal thermochemical storage, in: The 3rd International Conference of Energy Sustainability ES 2009, San Francisco, California, USA, 2009.

[46] K. Visscher, J.B.J. Veldhuis, Comparison of candidate materials for seasonal storage of solar heat through danamic simulation of building and renewable energy system, in: The 9th International Building Performance Simulation Association, Montreal, Canada, 2005.

[47] K. Visscher, Simulation of thermo chemial seasonal storage of solar heat-material selection and optimum performance simulation, in: 2nd workshop Matlab/Simulink for building simulation, Paris, France, 2004.

[48] K. Visscher, J.B.J. Veldhuis, H.A.J. Oonk, P.J.v. Ekeren, J.G. Blok, Compact seasonal storage of solar heat, ECN, 2004.

[49] C. Bales, Laboratory tests of chemcial reactions and prototype sorption storage uints, 2008.

[50] V.M.v. Essen, H.A. Zondag, J.C. Gores, L.P.J. Bleijendaal, M. Bakker, R. Schuitema, W.G.J.v. Helden, Z. He, C.C.M.Rindt, Characterization of $MaSO_4$ hydrate

for thermochemical seasonal heat storage, Journal of Solar Energy Engineering, 131 (2009) 041014-041011-041017.

[51] G. Balasubramanian, M. Ghommem, M.R. Hajj, W.P. Wong, J.A. Tomlin, I.K. Puri, Modeling of thermochemical energy storage by salt hydrates, International Journal of Heat and Mass Transfer, 53 (2010) 5700-5706.

[52] I. Fujii, T. Arai, Y. Saitoh, Investigation on chemical heat pump using calcium chloride, in: Proceedings of Japan Solar Energy Society/Japan Wind Energy Association Joint Conference, 1997, pp. 289-292.

[53] M. Sasaki, S. Uemura, H. Ogura, Heat storage characteristics of chemical heat storage tank using $CaCl_2/CaCl_2 \cdot 2H_2O$ for heat transport system by vehicle, in: Conference of Heating, Air-Conditioning and Sanitary Engineers of Japan, Sapporo, Japan, 2012, pp. 2645-2648.

[54] H. Ogura, M. Kubota, H. Suzuki, T. Yamakawa, Fundamental Experimental Study on Chemical Heat Pump for Storing Low-Temperature Waste Heat and Releasing Cold-Heat, KAGAKU KOGAKU RONBUNSHU, 35(5) (2009) 506-510.

[55] H. Mikami, M. Kubota, H. Ogura, H. Suzuki, Studies on cold-heat production of chemical heat pump for refrigeration truck driven by waste heat, in: Conference of Refrigeration and Air-conditioning in Japan, Kanazawa, 2010, pp. 607-610.

[56] H. Ogura, Energy recycling system using chemical heat pump container, Energy Procedia, 14 (2012) 2048-2053.

[57] M. Haguro, Y. Shibata, Y. Otsubo, H. Ogura, Studies on reaction rates of $CaSO_4/CaSO_4 \bullet 1/2H_2O$ reversible reaction for chemical heat pump, KAGAKU KOGAKU RONBUNSHU, 35(4) (2009) 390-395.

[58] Y.I. Aristov, New composite adsorbents for conversion and storage of low temperature heat: Activity in the Boreskov Institute of Catalysis, Journal of Heat Transfer Society of Japan, 45(192) (2006) 12-19.

[59] Y.I. Aristov, M.M.Tokarev, G.Cacciola, G. Restuccia, Selective water sorbents for multiple applications, 1. $CaCl_2$ confined in mesopores of silica gel: sorption properties, Reaction Kinetics and Catalysis Letters, 59(2) (1996) 325-333.

[60] Y.I. Aristov, M.M. Tokarev, G. Restuccia, G. Cacciola, Selective water sorbents for multiple applications, 2. $CaCl_2$ confined in micropores of silica gel: sorption properties, Reaction Kinetics and Catalysis Letters, 59(2) (1996) 335-342.

[61] Y.I. Aristov, G.D. Marco, M.M. Tokarev, V.N. Parmon, Selective water sorbents for multiple applications, 3. $CaCl_2$ solution confined in micro- and mesoporous silica

gels: pore size effect on the “solidification-melting” diagram, Reaction Kinetics and Catalysis Letters, 61(1) (1997) 147-154.

[62] M.M. Tokarev, Y.I. Aristov, Selective water sorbents for multiple applications, 4. CaCl2 confined in silica gel pores: sorption/desorption kinetics, Reaction Kinetics and Catalysis Letters, 62(1) (1997) 143-150.

[63] Y.I. Aristov, G. Restuccia, G. Cacciola, M.M. Tokarev, Selective water sorbents for multiple applications, 7. Heat conductivity of $CaCl_2$–SiO_2 composites, Reaction Kinetics and Catalysis Letters, 65(2) (1998) 277-284.

[64] Y.Y. Tanashev, Y.I. Aristov, Thermal conductivity of a silica gel + calcium chloride system: the effect of adsorbed water, Journal of Engineering Physics and Thermophysics, 73(5) (2000) 876-883.

[65] Y.D. Pankratev, M.M.Tokarev, Y.I. Aristov, Calorimetric study of water sorption in the system "salt confined to porous matrix". Russian Journal of Physical Chemistry, 75 (2001) 910-914.

[66] Y.I. Aristov, G. Restuccia, G.Cacciola, V.N. Parmon, A family of new working materials for solid sorption air conditioning systems, Applied Thermal Engineering, 22 (2002) 191-204.

[67] A. Freni, M.M. Tokarev, G. Restuccia, A.G. Okunev, Y.I. Aristov, Thermal conductivity of selective water sorbents under the working conditions of a sorption chiller, Applied Thermal Engineering, 22 (2002) 1631-1642.

[68] B. Dawoud, Y.I. Aristov, Experimental study on the kinetics of water vapor sorption on selective water sorbents, silica gel and aluminia under typical operating conditions of sorption heat pumps, International Journal of Heat and Mass Transfer, 46 (2003) 273-281.

[69] Y.I. Aristov, I.S. Glaznev, A. Freni, G. Restuccia, Kinetics of water sorption on SWS-1L (calcium chloride confined to mesoporous silica gel): influence of grain size and temperature, Chemical Engineering Science, 61 (2006) 1453-1458.

[70] I.S. Glaznev, D.S. Ovoshchnikov, Y.I. Aristov, Kinetics of water adsorption/desorption under isobaric stages of adsorption heat transformers: The effect of isobar shape, International Journal of Heat and Mass Transfer, 52 (2009) 1774-1777.

[71] Y.I. Aristov, Optimal adsorbent for adsorptive heat transformers: Dynamic considerations, International Journal of Refrigeration, 32 (2009) 675-686.

[72] I.S. Glaznev, Y.I. Aristov, Kinetics of water adsorption on loose grains of SWS-1L under isobaric stages of adsorption heat pumps: the effects of residual air, International Journal of Heat and Mass Transfer, 51 (2008) 5823-5827.

[73] Y.I. Aristov, B. Dawoud, I.S. Glaznev, A. Elyas, A new methodology of studying the dynamics of water sorption/desorption under real operating conditions of adsorption heat pumps: Experiment, International Journal of Heat and Mass Transfer, 51 (2008) 4966-4972.

[74] G. Restuccia, A. Freni, S. Vasta, Y.I. Aristov, Selective water sorbent for solid sorption chiller: experimental results and modelling, International Journal of Refrigeration, 27 (2004) 284-293.

[75] A. Freni, F. Russo, S. Vasta, M. Tokarev, Y.I. Aristov, G. Restuccia, An advanced solid sorption chiller using SWS-1L, Applied Thermal Engineering, 27 (2007) 2200-2204.

[76] A. Freni, A. Sapienza, I.S. Glaznev, Y.I. Aristov, Experimental testing of a lab-scale adsorption chiller using a novel selective water sorbent "silica modified by calcium nitrate", International Journal of Refrigeration, 35 (2012) 518-524.

[77] A. Sapienza, I.S. Glaznev, S. Santamaria, A. Freni, Y.I. Aristov, Adsorption chilling driven by low temperature heat: New adsorbent and cycle optimization, Applied Thermal Engineering, 32(0) (2012) 141-146.

[78] Y.I. Aristov, A. Sapienza, D.S. Ovoshchnikov, A. Freni, G. Restuccia, Reallocation of adsorption and desorption times for optimisation of cooling cycles, International Journal of Refrigeration, 35(3) (2012) 525-531.

[79] Y. Kato, N. Yamashita, K. Kobayashi, Y. Yoshizawa, Kinetic study of the hydration of magnesium oxide for a chemical heat pump, Applied Thermal Engineering, 16(11) (1996) 853-862.

[80] Y. Kato, K. Kobayashi, Y. Yoshizawa, Durability to repetitive reaction of magnesium oxide/water reaction system for a heat pump, Applied Thermal Engineering, 18(3-4) (1998) 85-92.

[81] Y. Kato, F. Takahashi, A. Watanabe, Y. Yoshizawa, Thermal analysis of a magnesium oxide/water chemical heat pump for cogeneration, Applied Thermal Engineering, 21(10) (2001) 1067-1081.

[82] Y. Kato, Y. Yoshizawa, Application of a chemical heat pump to a generation system, International Journal of Energy Research, 25 (2001) 129-140.

[83] Y. Kato, Y. Sasaki, Y. Yoshizawa, Magnesium oxide/water chemical heat pump to enhance energy utilization of a cogeneration system, Energy, 30 (2005) 2144-2155.

[84] J. Ryu, R. Takahashi, N. Hirao, Y. Kato, Effect of transition metal mixing on reactivities of magnesium oxide for chemical heat pump, Journal of Chemical Engineering of Japan, 40(13) (2007) 1281-1286.

[85] Y. Kato, R. Takahashi, T. Sekiguchi, J. Ryu, Study on medium-temperature chemical heat storage using mixed hydroxides, International Journal of Refrigeration, 32 (2009) 661-666.

[86] S.T. Kim, J. Ryu, Y. Kato, Reactivity enhancement of chemical materials used in packed bed reactor of chemical heat pump, Progress in Nuclear Energy, 53 (2011) 1027-1033.

[87] S.T. Kim, J. Ryu, Y. Kato, Reactivity enhance of packed bed chemical material using expanded graphite for chemical heat pump, in: The 12th International Conference on Energy Storage, 2012.

[88] H. Matsuda, S.K. Lee, T. Ishizu, M. Hasatani, Heat-release characteristics of CaO packed bed accompanied by exothermic hydration, KAGAKU KOGAKU RONBUNSHU, 13(1) (1987) 20-28.

[89] H. Matsuda, M. Miyazaki, M. Hasatani, Temperature response of the solid particle bed in a high-temperature chemical heat pump using $Ca(OH)_2$/CaO reversible thermochemical reaction, KAGAKU KOGAKU RONBUNSHU, 14(6) (1988) 769-778.

[90] H. Ogura, M. Miyazaki, H. Matsuda, M. Hasatani, M. Yanadori, M. Hiramatsu, Experimental study on heat transfer enhancement of the solid reactant particle bed in a chemical heat pump using $Ca(OH)_2$/CaO reaction, KAGAKU KOGAKU RONBUNSHU, 17(5) (1991) 916-923.

[91] H. Ogura, M. Miyazaki, H. Matsuda, M. Hasatani, M. Yanadori, M. Hiramatsu, Numerical analysis of heat transfer in particle-bed reactor with fins in chemical heat pump using Ca $(OH)_2$/ CaO reaction, KAGAKU KOGAKU RONBUNSHU, 18(5) (1992) 669-676

[92] H. Ogura, M. Kanamori, H. Matsuda, M. Hasatani, Generation of low-temperature heat by use of $CaO/H_2O/Ca(OH)_2$ reaction, KAGAKU KOGAKU RONBUNSHU, 19(6) (1993) 941-946.

[93] S. Fujimoto, E. Bilgen, H. Ogura, $CaO/Ca(OH)_2$ chemical heat pump system, Energy Conversion and Management, 43 (2002) 947-960.

[94] S. Fujimoto, E. Bilgen, H. Ogura, Dynamic simulation of $CaO/Ca(OH)_2$ chemical heat pump systems, Exergy, An International Journal, 2 (2002) 6-14.

[95] S. Fujimoto, H. Ogura, H. Iwamoto, M. Abe, H. Kage, Y. Matsuno, S. Baba, S. Muta, Optimum operating conditions of a chemical heat pump using calcium oxide/water reaction for effective utilization of surplus electricity, KAGAKU KOGAKU RONBUNSHU, 29(1) (2003) 20-26.

[96] H. Ogura, T. Yamamoto, H. Kage, Efficiencies of $CaO/H_2O/Ca(OH)_2$ chemical heat pump for heat storing and heating/cooling, Energy, 28 (2003) 1479-1493.
[97] H. Ogura, S. Yasuda, Y. Otsubo, A.S. Mujumdar, Continuous operation of a chemical heat pump, Asia-Pacific Journal of Chemical Engineering, (2007) 118-123.
[98] H. Ogura, T. Yamamoto, H. Kage, Y. Matsuno, A.S. Mujumdar, Effects of heat exchange condition on hot air production by a chemical heat pump dryer using $CaO/H_2O/Ca(OH)_2$ reaction, Chemical Engineering Journal, 86 (2002) 3-10.
[99] V.E. Sharonov, Y.I. Aristov, Chemical and adsorption heat pumps: Comments on the second law efficiency, Chemical Engineering Journal, 136(2–3) (2008) 419-424.
[100] M. Ghommem, G. Balasubramanian, M.R. Hajj, W.P. Wong, J.A. Tomlin, I.K. Puri, Release of stored thermochemical energy from dehydrated salts, International Journal of Heat and Mass Transfer, 54(23–24) (2011) 4856-4863.
[101] K. Posern, C. Kaps, Calorimetric studies of thermochemical heat storage materials based on mixtures of $MgSO_4$ and $MgCl_2$, Thermochimica Acta, 502(1–2) (2010) 73-76.
[102] B.B. Saha, A. Chakraborty, S. Koyama, Y.I. Aristov, A new generation cooling device employing $CaCl_2$-in-silica gel-water system, International Journal of Heat and Mass Transfer, 52 (2009) 516-524.
[103] A. Freni, A. Frazzica, B. Dawoud, S. Chmielewski, L. Calabrese, L. Bonaccorsi, Adsorbent coatings for heat pumping applications: Verification of hydrothermal and mechanical stabilities, Applied Thermal Engineering, 50(2) (2013) 1658-1663.
[104] K. Fujioka, High thermal conductive reactant for chemical heat pump, Journal of Heat Transfer Society of Japan, 45(192) (2006) 40-45.
[105] K. Fujioka, K. Hatanaka, Y. Hirata, Composite reactants of calcium chloride combined with functional carbon materials for chemical heat pumps, Applied Thermal Engineering, 28 (2008) 304-310.

2 DEVELOPMENT OF COMPOSITE MATERIAL MADE FROM $CaCl_2$ FOR AN OPEN CHEMICAL THERMAL ENERGY STORAGE SYSTEM

Hokkaido University

2.1 INDTODUCTION

Today, a significant amount of low-temperature industrial waste heat (< 100ºC) is directly emitted to the ambient environment. Therefore, a storage method with low heat loss and high heat storage density to store this type of heat must be developed. By capturing low-temperature industrial heat, fossil energy demand and carbon dioxide emissions could be sufficiently reduced. The objective of this research is to develop an effective sorption thermal energy storage material and investigate the performance of an open sorption thermal energy storage system using the developed material to store low-temperature industrial waste heat. The material should have a regeneration temperature below 100ºC and exhibit good stability. For practical use, its thermal energy storage density should be as high as possible.

With a sorption thermal energy storage method, heat is stored by a reversible desorption/sorption process [1]. In view of the environmental impact and low-temperature heat sources, water vapor sorption on solid materials is promising as a kind of thermal energy storage method [2-4]. Silica gel is a common sorption heat pump material, and its potential as a thermal energy material for storing low-temperature heat was also examined. Tahat [5] investigated silica gel theoretically and experimentally during both heating and cooling modes of a thermochemical heat pump/energy store system. Saha et al. [6] developed a new silica gel adsorption chiller driven by low-temperature waste heat from 60ºC to 95ºC. However, the specific energy storage capacity is not so high because of low adsorption amount and low adsorption heat [3], consequently incurring large and heavy thermal energy storage apparatus.

There are also some pure chemical substances being researched as potential low-temperature energy storage materials. Boer et al. [7] developed a Sodium sulfide (Na_2S) cooling system with a copper wire-fin heat exchanger. Na_2S-H_2O has a eutectic melting point of 83ºC [8], which imposes the upper limits for the regeneration temperature in its system. The storage capacity of Na_2S in the form of $Na_2S \cdot 5H_2O$ is approximately 3.84 MJ/kg for heat and 2.54 MJ/kg (1,300 kWh/m3) for cooling with a coefficient of performance (COP) of 0.84 and 0.57, respectively. However, Na_2S is very corrosive and must be used in a vacuum system to prevent contact with metals. Magnesium chloride hexahydrate ($MgCl_2 \cdot 6H_2O$) has shown its potential as a thermochemical

material for seasonal heat storage due to its high thermal energy storage density and suitable temperature release [9, 10]. However, this compound has several limitations for long-term storage because of its instability and decomposition at temperatures higher over 135ºC. Ogura et al. [11, 12] found that $CaSO_4 \cdot 2H_2O$ can be used as a heat storage material to store exhaust gas and heat from refrigeration/freezing vehicles at temperatures near 120ºC and can recycle the energy to be used in the air conditioning system during an idling stop. However, only 297 kJ of heat can be stored in a reactor filled with 2,400 g of $CaSO_4$ (i.e., its heat storage density is 123.75 kJ/kg) because of its small theoretical reaction heat (16.8 kJ/mol).

Composite materials have been developed recently as novel thermal energy storage materials by impregnating hygroscopic salt inside the matrix of a porous adsorbent for multiple applications [3, 13-18]. Levitskij et al. [3] proposed the composite porous material for chemical heat accumulation in 1995. Aristov et al. [13] presented sorption properties of the selective water sorbents (SWSs), and calculated their thermodynamic performance in heat pump and refrigeration systems. Dawoud and Aristov [14] investigated the kinetics of water sorption on the composite mesoporous materials (based on silica gel and alumina) under three sorption heat pump operation conditions. All the tested materials were disposed as loose pellets in the small apparatus. Their results showed that the composite material exhibited lower kinetics of water sorption compared to the host matrices. Jänchen et al. [15] tested the storage density of granulated and impregnated mesoporous material in a lab-scaled closed storage system. Zhu et al. [16] investigated an open-type thermal energy storage setup equipped with 40 kg composite sorbent pellets. Unfortunately, there are few researches have been done on the experimental study of examining the thermal energy storage performance of the developed low-temperature sorption heat storage material. Moreover, little work has been done on the experimental study of improving heat and mass transfer in a system from the viewpoint of material's novel structure.

In this research, we used a natural mesoporous Wakkanai siliceous shale (WSS) as the matrix to create a ceramic honeycomb filter with cell wall's thickness of 0.28 mm. The mesoporous composite material was formed by impregnating $CaCl_2$ in the mesopores of this ceramic filter. After the material was formed, the physical properties, sorption

properties, regeneration temperature, and stability were measured. An open thermal energy storage experimental setup was constructed and used to test the suitability of the honeycomb composite filter for use as a sorption thermal energy storage material.

2.2 MATERIAL

2.2.1 Manufacturing procedure of the composite mesoporous material with $CaCl_2$

WSS is a type of siliceous mudstone that is widely distributed in the northern part of Hokkaido in Japan. WSS is a natural mesoporous material whose main composition is silicon dioxide (SiO_2) [19]. The material exhibits a relatively high sorption property, with main pore diameters of 4 to 20 nm. For use in practical conditions, the material was sintered in an oven at 800ºC for 2 hr to ensure the existence of mesopores and to significantly improve its strength characteristic. If the sinter temperature is greater than 800ºC or the sinter time is longer than 2 hr, the mesopores in the WSS will disappear. When the maximum sinter temperature is 800ºC and the sinter time is less than 2 hr, ceramics can be formed in locations where the mesopores remain.

It is well known that for a sorption thermal energy storage system, low heat and mass transfer rates are significant problems that limit the development of sorption thermal energy storage technology. To solve this problem, a honeycomb ceramic filter (10 cm (width) × 10 cm (length) × 20 cm (height)) with 36 cells/cm^2 was developed using sintered WSS. The filter was made of 80% WSS and 20% binder (clay), whose structure is presented in Fig. 2-1. The thickness of the wall of each cubic cell is 0.28 mm.

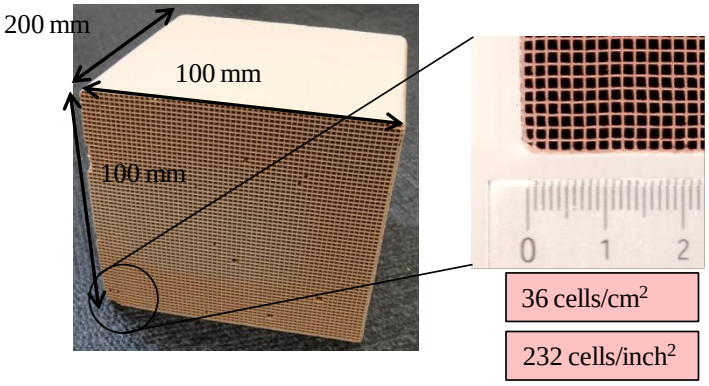

（Wakkanai siliceous shale (WSS) 80%, binder 20%）

Fig. 2-1 Image of a WSS filter

Stability of hygroscopic $CaCl_2$ was observed in our previous work. In our research, $CaCl_2$-supported ceramic composite mesoporous material was obtained by impregnating WSS with a $CaCl_2$ solution. First, the original filters were dried at 200ºC in an oven for 4 hr to obtain their dry weight. Then, three original filters were cooled to room temperature and immersed in aqueous solutions of $CaCl_2$ with concentrations of 4.0 wt%, 25.0 wt% and 40.0 wt%. These solutions were stirred for several minutes at room temperature. The three filters were vacuumed in a vacuum container to 3.14×10^3 Pa (the saturated water vapor pressure at 25ºC) for 15 min, 150 min, and 250 min, respectively. After being dried in an oven at 200ºC, weight percentages of 2.2 wt%, 13.0 wt%, and 22.4 wt% $CaCl_2$ composite mesoporous ceramic filters were finally obtained. The original ceramic material is denoted as WSS, and the other three $CaCl_2$-supported composite ceramic samples are denoted as WSS + 2.2 wt% $CaCl_2$, WSS + 13.0 wt% $CaCl_2$, and WSS + 22.4 wt% $CaCl_2$.

2.2.2 Physical properties of the composite material

The pore volume and specific surface area of the mesoporous material were measured by standard nitrogen gas sorption/desorption measurements. The pore volume distributions of the original ceramic material and the other composite samples are presented in Fig. 2-2. It can be observed that the pores of the original ceramic material were filled by $CaCl_2$, and the pore volume decreased with supporting content of $CaCl_2$. The composite material's specific surface area was calculated by the Brunauer-Emmett-Teller (BET) equation. The fine pore volume calculated by Barrett, Joyner, and Halenda (BJH) is presented in Table 2-1 along with the true density and porosity. The specific surface area of the WSS decreased from 111.7 m^2/g to 38.4 m^2/g after being impregnated with 22.4 wt% $CaCl_2$. The porosity of the WSS also decreased from 60% to 49% after filling with 22.4 wt% $CaCl_2$. From the physical characteristics (Table 2-1 and Fig. 2-2) of the WSS and the other three composite samples, it is readily understood that the $CaCl_2$ was generally located inside the pores [20, 21], which mainly caused the decrease of the specific surface area, pore volume and porosity.

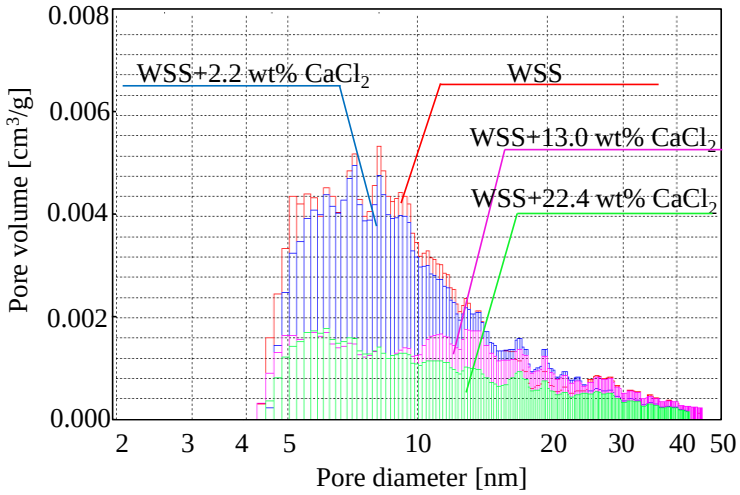

Fig. 2-2 Pore size distributions of the four composite samples

Table 2-1 Physical properties of the four samples

Properties \ Samples	WSS	WSS +2.2wt%$CaCl_2$	WSS +13.0wt%$CaCl_2$	WSS +22.4wt%$CaCl_2$
Specific surface area (m^2/g)	111.7	100.9	49.9	38.4
Pore volume (cm^3/g)	0.309	0.290	0.209	0.152
True density (kg/m^3)	2150	2150	2150	2150
Porosity (%)	60	59	54	49

2.2.3 Sorption properties of the composite material

Water vapor sorption isotherms of the WSS and composite material at 25ºC were tested at each relative humidity condition (see Fig. 2-3). The composite material developed in this research interacts with water vapor based on the following mechanisms [22]: a) Heterogeneous adsorption on the pore surface of ceramic material; b) Chemical reaction (chemical adsorption) between vapor and the salt; c) Liquid absorption by the hydrate $CaCl_2 \cdot nH_2O$. When the relative humidity was 95%, the water vapor sorption amount of the WSS + 2.2 wt% $CaCl_2$ was twice as large as that of the WSS. In contrast, for WSS + 13.0 wt% $CaCl_2$ and WSS + 22.4 wt% $CaCl_2$, the sorption amount was five times and eight times that of the WSS, respectively. Thus because of $CaCl_2$ the latter two mechanisms were the main sorption behavior of the composite

material [22]. In regard to the isotherm sorption line of WSS, the surface adsorbs water vapor, causing monolayer coverage at low pressures. Water molecules can also condense within pores that are sufficiently large to accommodate multi-molecular layers at pressures below the normal saturation pressure. This behavior, called capillary condensation, is characterized by hysteresis, which produces a type IV isotherm. However, the isotherm sorption line of WSS + 22.4 wt% $CaCl_2$ indicates that crystalline hydrates were formed at low relative humidity, and then salt solution was formed particularly at a high relative humidity, which filled the pores either completely or partially. It is this volume filling that leads to the high sorption capacity of composite materials [22]. The high sorption amount is considered to be effective in increasing the heat storage density. By adding $CaCl_2$, the driving force of the sorption becomes the interaction of the water vapor with the hygroscopic $CaCl_2$.

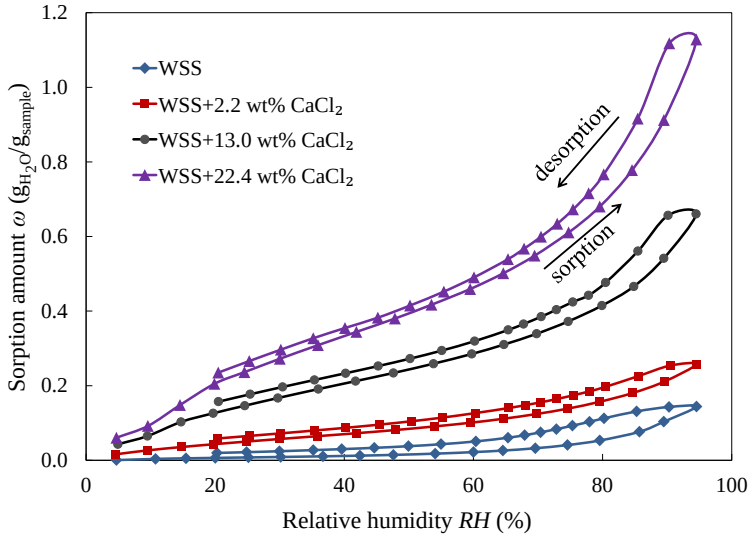

Fig. 2-3 Water vapor sorption amounts of the four composite samples

2.2.4 Regeneration temperature measurement

The sorption isobars of the composite material and pure $CaCl_2$ were measured in a temperature range of 25ºC to 230ºC at a partial water vapor pressure of 22.18 hPa by thermogravimetric (TG)/differential thermal analysis (DTA), the results of which are shown in Fig. 2-4 (a) (for pure $CaCl_2$: 25-45ºC is not shown). The water vapor content

was calculated as $\omega = m_{H_2O}(T)/m$ $\omega = \mathrm{m_{H_2O}(T)/m}$. The desorption isobar exhibited what is known as temperature hysteresis for a sorption isobar.

$$n = [\omega - (1 - m_{CaCl_2}/m_{s,dry})\omega_{WSS}(T)][(M_{CaCl_2}/M_{H_2O})/(m_{CaCl_2}/m_{s,dry})] \quad 2\text{-}1$$

The three plateaus of the desorption isobar of pure $CaCl_2$ represent three hydrates, $CaCl_2 \cdot H_2O$, $CaCl_2 \cdot 2H_2O$, and $CaCl_2 \cdot 4H_2O$ from high to low temperatures. The low-temperature hydrate, $CaCl_2 \cdot 6H_2O$, was not observed in our experimental conditions, both for the pure calcium chloride and composite material, as it is easily melted [23]. Two clear sorption water vapor plateaus can be detected in the isobar of the composite material supported with 22.4 wt% $CaCl_2$ and one plateau for the WSS + 13.0 wt% $CaCl_2$. However, the isobars of the WSS and WSS + 2.2 wt% $CaCl_2$ exhibited no plateaus. In our case, for the composite material supported with 13.0 wt% $CaCl_2$ and 22.4 wt% $CaCl_2$, the water content can also be presented as a number of water molecules with respect to one molecule of calcium chloride.

The water content plateaus of the composite material supported with 22.4 wt% $CaCl_2$ in Fig. 2-4 (b) were $n \approx 1$ and $n \approx 2$, which unambiguously indicate the formation of the crystalline hydrates $CaCl_2 \cdot H_2O$ and $CaCl_2 \cdot 2H_2O$, respectively. A clear sorption plateau was also reported in the sorption isobars by Aristov et al. [24] due to the formation of salt hydrate in their composite material supported by $CaCl_2$ in pores of silica gel. Their results also demonstrated that the solid crystalline hydrates $CaCl_2 \cdot H_2O$ and $CaCl_2 \cdot 2H_2O$ formed during desorption. In our case, the formation of calcium chloride tetrahydrate was not so clear compared to crystalline dihydrate. It can be seen from Fig. 2-4 (b) that calcium chloride monohydrate was obtained at 99.8ºC for WSS + 22.4 wt% $CaCl_2$. However, calcium chloride monohydrate cannot be heated into anhydrous calcium chloride completely by increasing the temperature to 150ºC. The mesopores (mainly 4 – 20 nm) existed in the Wakkanai siliceous shale will affect the formation of crystalline calcium chloride hydrate according to [22]. Their research illustrated that no hydrate formation was found when the matrix's pore diameter is 3.5 nm, which indicates that the hydrated salt continuously changed its structure. But the merit is that the composite material can be regenerated at temperature around 100ºC because of the small sorption amount at this temperature (Fig. 2-4 (a)).

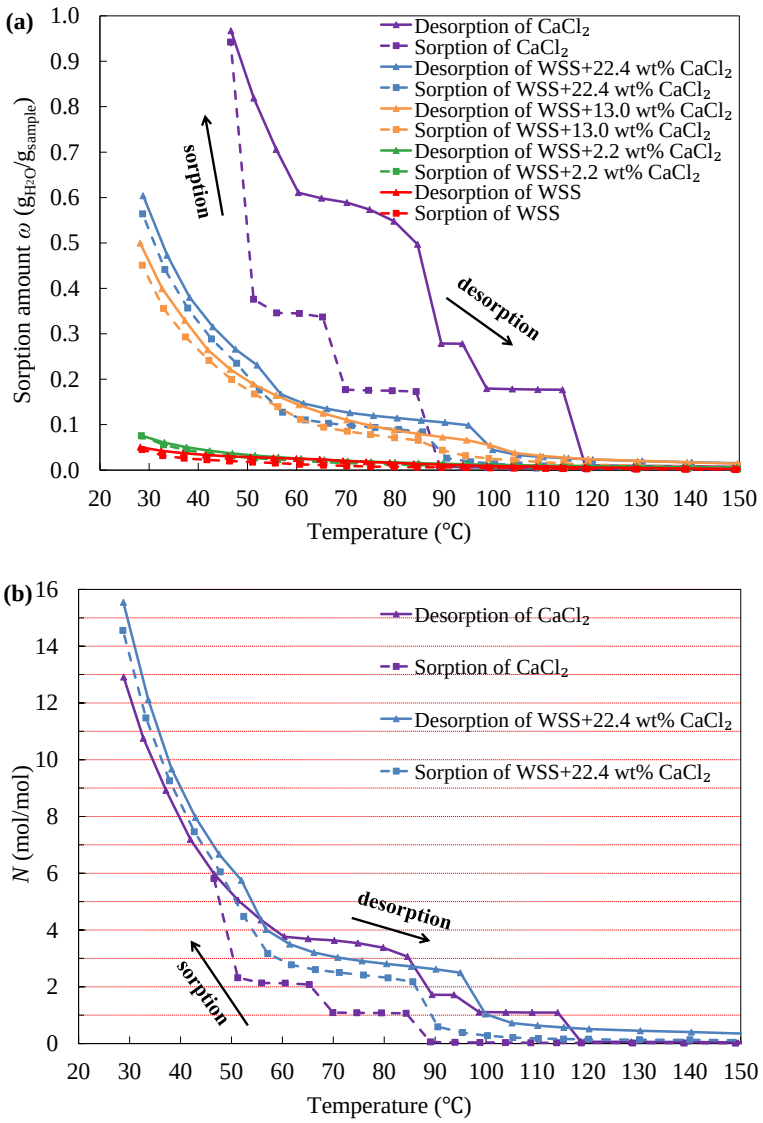

Fig. 2-4 (a) Isobars of the water vapor sorption of pure $CaCl_2$ and the composite materials and (b) isobars of the water vapor sorption of pure $CaCl_2$ and WSS+ 22.4 wt% $CaCl_2$ at a partial water vapor pressure of 22.18 hPa

2.2.5 Stability of the composite material

To obtain the stability properties of all of the composite samples, we repeated the desorption/sorption cycles 25 times according to [18, 25, 26].

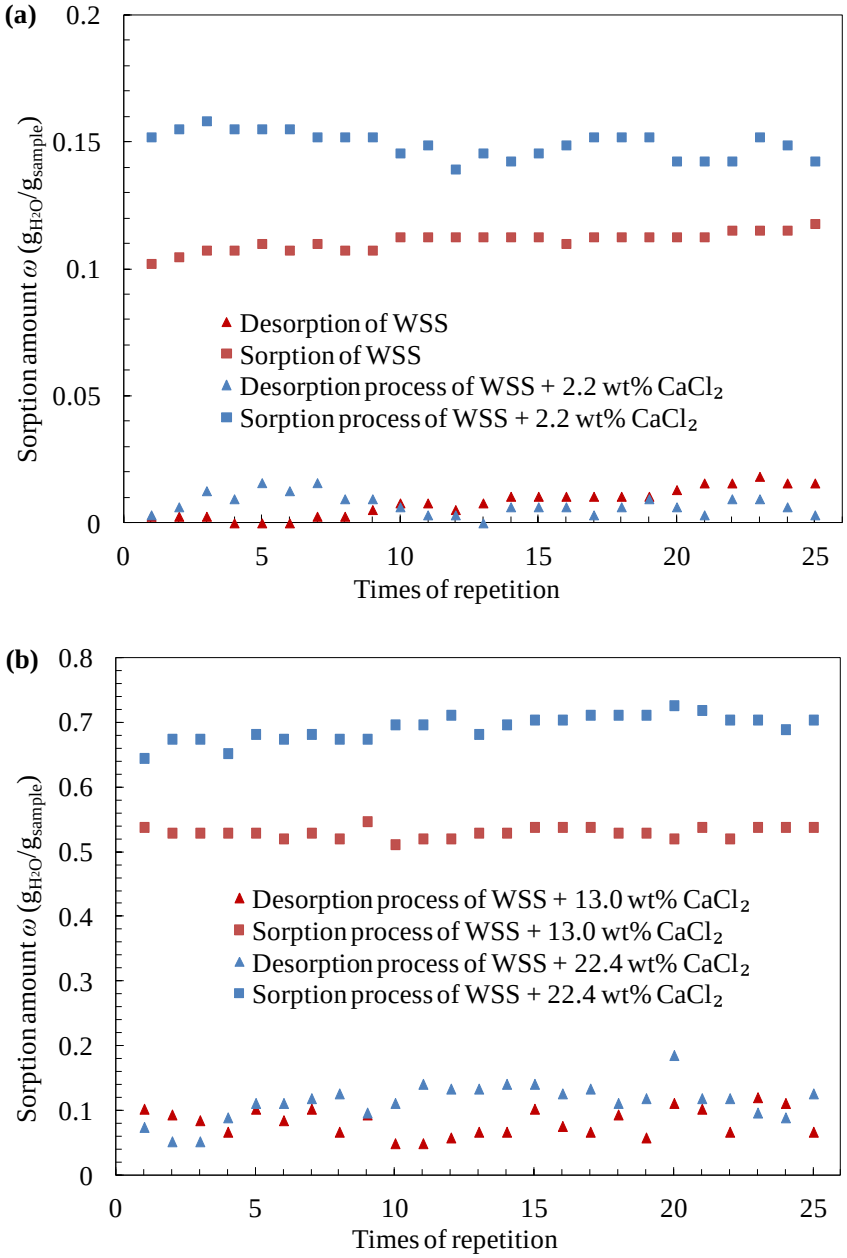

Fig. 2-5 (a) Stability of WSS and WSS + 2.2 wt% $CaCl_2$ and (b) stability of WSS + 13.0 wt% $CaCl_2$ and WSS + 22.4 wt% $CaCl_2$ (Desorption process: 120°C; sorption process: 25°C, *RH* 90%)

In this experiment, the temperature was increased to 120°C in the dehydration process and maintained at 25°C at a constant relative humidity of 90% during the sorption process. The stability results of the composite material are illustrated in Fig. 2-5 (a) and (b). Afterwards, the sorption amount at each relative humidity (5%-95%) at 25°C before the stability test and after 25 repetitions was measured for each sample (cf. Fig.

2-6). It can be observed that for all samples, for both a relative humidity of 90% and other relative humidity conditions, after 25 repetitions, the sorption amount remained unchanged compared to that before the stability test indicating that the composite material is stable.

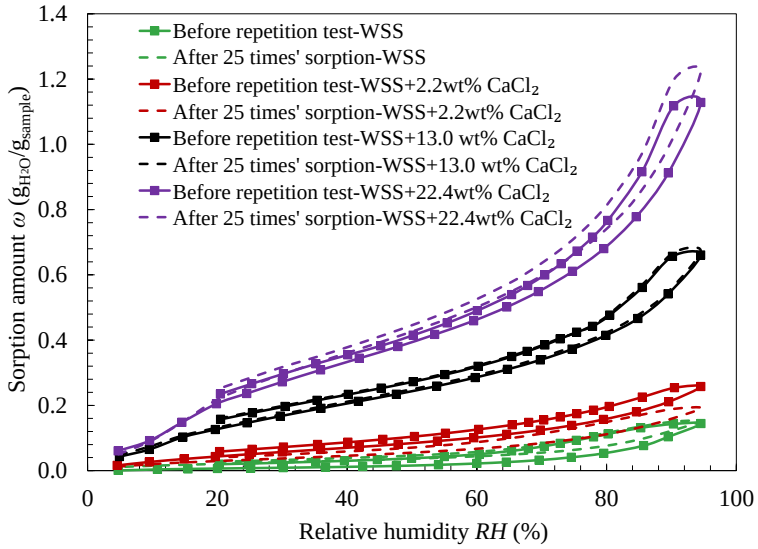

Fig. 2-6 Sorption amount of the four composite samples before and after the repetition tests

2.3 OPEN SROTPION TEHRMAL ENERGY STORAGE SYSTEM

2.3.1 Principle of the open sorption thermal energy storage system

A sorption thermal energy storage material can be used as either sorption heat pump operated under a vacuum or an open sorption thermal energy storage system operated at atmospheric pressure. An open sorption thermal energy storage experimental setup was constructed in this study to examine the performance of the composite material as a thermal energy storage material in the form of a honeycomb filter. An open system can use endothermic and exothermic processes to store heat and recover it at atmospheric pressure.

In the heat storage (heat charging or endothermic) mode, hot air is used to regenerate the material. During the regeneration process, the water vapor bonded to the material is discharged to the ambient environment and the heat is stored in the dry material. In the heat supply (heat discharging or exothermic) mode, high-humidity air is flowed through the system to recover the exothermic heat due to the sorption of the water vapor.

2.3.2 Description of the open sorption thermal energy storage experimental setup

Four filters were tested, as shown in Table 2-2. One filter was the original WSS ceramic honeycomb filter shown in Fig. 2-1, and the other three filters were filled with different amounts of $CaCl_2$. The dimensions of each filter were 10 cm × 10 cm × 20 cm. A schematic diagram of the experimental setup is provided in Fig. 2-7. The tested filter was placed inside a stainless steel casing that fit the size of the filter. High-temperature and low-relative-humidity air in the heat storage process was created by a hot-air producer. Humid air in the heat release mode was supplied by a highly stable temperature and humidity thermostat chamber.

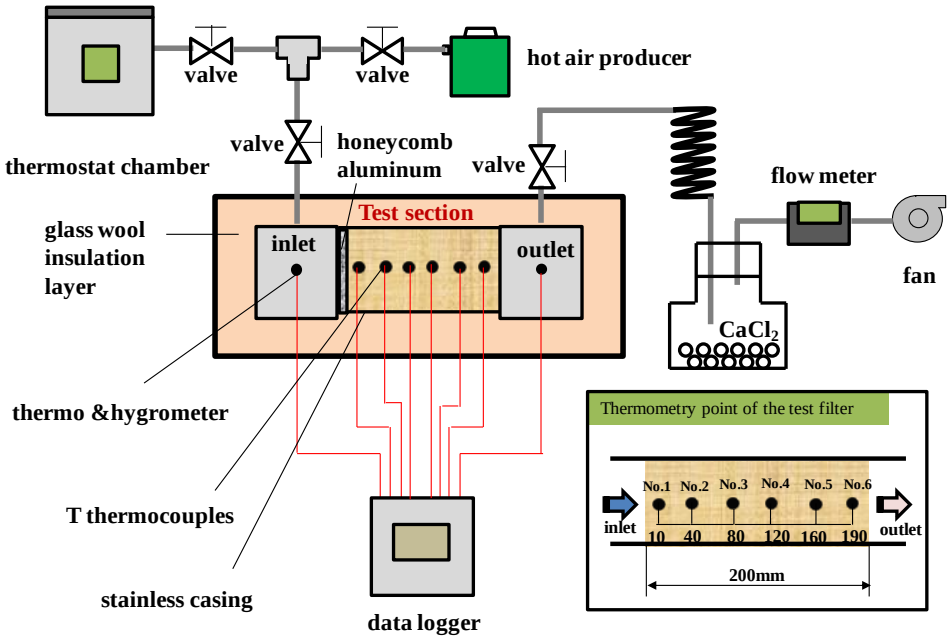

Fig. 2-7 Open sorption thermal energy storage experimental setup

Table 2-2 Experimental conditions for the different filters

	WSS	WSS +2.2wt% $CaCl_2$		WSS +13.0wt% $CaCl_2$			WSS +22.4wt% $CaCl_2$			
Regeneration temperature (ºC)	80	80	60	80	100	120	60	80	100	120
Moisture air flow rate (m^3/h)	1.0	1.0		1.0				1.0		
	1.5	1.5		1.5				1.5		
	2.0	2.0	2.0	2.0	2.0	2.0	2.0	2.0	2.0	2.0
				2.5				2.5		
	3.0	3.0		3.0[a]				3.0		

[a]: Three different relative humidity condition of *RH* 70% ± 3%, *RH* 80 ± 3% and *RH* 93% ± 3% at 25ºC were tested at the humid air's flow rate of 3 m^3/h.

The relative humidity and temperature of the inlet and outlet air were measured and recorded using two high-temperature Rotronic thermo hygrometers (Rotronic Instrument Corp., Hauppauge, NY, USA). The thermo hygrometer can be used in a temperature range of -100ºC-200ºC and a relative humidity of 0-100%. The accuracies can reach *RH* ± 0.8% and ± 0.1ºC at 23ºC. Six T-type Φ1.0 mm sheathed thermocouples were inserted into the test section, and their exact positions are provided

in Fig. 2-7. After the regeneration process, the material was cooled to the initial temperature of the filter during the heat release process. Humid air (25ºC, *RH* 93% ± 3% for all experiments except cases listed as superscript a in Table 2-2) was then flowed through the tested filter, which resulted in water vapor being sorbed while sorption heat being released and removed by the flowing air.

Such parameters as the impregnated $CaCl_2$ amount, regeneration temperature, and flow rate and relative humidity of the humid air, were examined with this proposed open sorption thermal energy storage system. The experimental air conditions are provided in Table 2-2. For the heat charging process, the regeneration air temperature was varied from 60 to 120ºC (60ºC, *RH* 3.9% ± 0.3%; 80ºC, *RH* 2.0% ± 0.3%; 100ºC, *RH* 1.7% ± 0.1% and 120ºC, *RH* 1.7% ± 0.1%.), and the flow rate changed from 1.0 to 3.0 m^3/h during the heat release process.

2.4 RESULTS AND DISCUSSION

2.4.1 Influence of the filling amount of $CaCl_2$

The outlet temperature of air flowing through the filters supported with different amounts of $CaCl_2$ is shown in Fig. 2-8. The conditions were a regeneration temperature of 80ºC and a humid air (25ºC, *RH* 93% ± 3%) flow rate of 2.0 m^3/h in the heat release process. The highest outlet air temperatures for the WSS, WSS + 2.2 wt% $CaCl_2$, WSS + 13.0 wt% $CaCl_2$, and WSS + 22.4 wt% $CaCl_2$ were 36.2ºC, 43.5ºC, 46.3ºC, and 45.8ºC, respectively. An outlet air temperature greater than 40ºC lasted approximately 58 min (with a range of 16-74 min) for the WSS + 2.2 wt% $CaCl_2$, 350 min (31-381 min) for the WSS + 13.0 wt% $CaCl_2$, and 525 min (30-555 min) for the WSS + 22.4 wt% $CaCl_2$. The surface adsorption is very quick compared to the salt absorption. For the WSS + 2.2 wt% $CaCl_2$, the effect of the salt absorption is smaller than that of the filter with large filling amount of $CaCl_2$. That's why the outlet air temperature was lower than 40ºC after 58 min. The absorption process gradually proceeded, so the long duration of supplying high-temperature air was observed in the composite filters with large amount of $CaCl_2$. We assume that for an actual system, an air temperature difference of greater than 15ºC is required for waste heat recovery with a long temperature duration of 5-8 hr for different applications. In this case, WSS is not suitable for use as a sorption thermal energy storage material because of its low outlet air temperature, and WSS + 2.2 wt% $CaCl_2$ is also inappropriate for short durations of maintaining a high outlet air temperature. In other words, a honeycomb filter supported by 13.0 wt% $CaCl_2$ can supply air at temperatures exceeding 40ºC for longer than 5 hr, and the WSS + 22.4 wt% $CaCl_2$ can provide a high temperature for almost 9 hr.

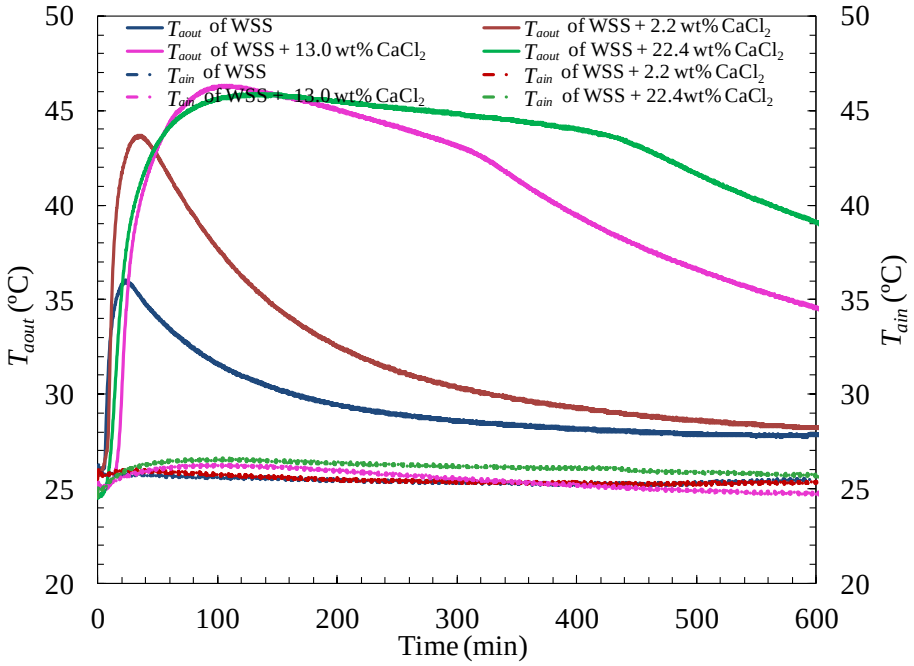

Fig. 2-8 Time change of the inlet and outlet air temperatures (Filters: four kind of filters; Regeneration temperature: 80°C; Humid air flow rate: 2.0 m^3/h)

2.4.2 Effect of regeneration temperature on heat recovery air

Filters supported with 13.0 wt% and 22.4 wt% $CaCl_2$ were used to determine the regeneration temperature for a real application. The results of this investigation are provided in Fig. 2-9 (a) and (b). Regeneration temperatures of 60°C, 80°C, 100°C, and 120°C were measured, and a humid air flow rate of 2.0 m^3/h was set in the heat release process (25°C, *RH* 93% ± 3%). For both filters, the highest outlet air temperature increased with greater regeneration temperatures. Using the same assumption of an actual system described in the last section, WSS + 13.0 wt% $CaCl_2$ must be regenerated at a temperature exceeding 80°C to assure a high-temperature air supply duration longer than 5 hr, whereas the same regeneration temperature for the WSS + 22.4 wt% $CaCl_2$ supplies high-temperature air for 8 hr. Next, we discussed the volumetric heat storage density, which is defined as follows:

$$Q_V = C_{p,a}\rho_a Q_a (T_{a,out} - T_{a,in})t / V \qquad 2\text{-}2$$

$$Q_V = C_{p,a}\rho_a Q_a / V \sum_{T_{aout} \geq 40°C} (T_{a,out} - T_{a,in})\Delta t \qquad 2\text{-}3$$

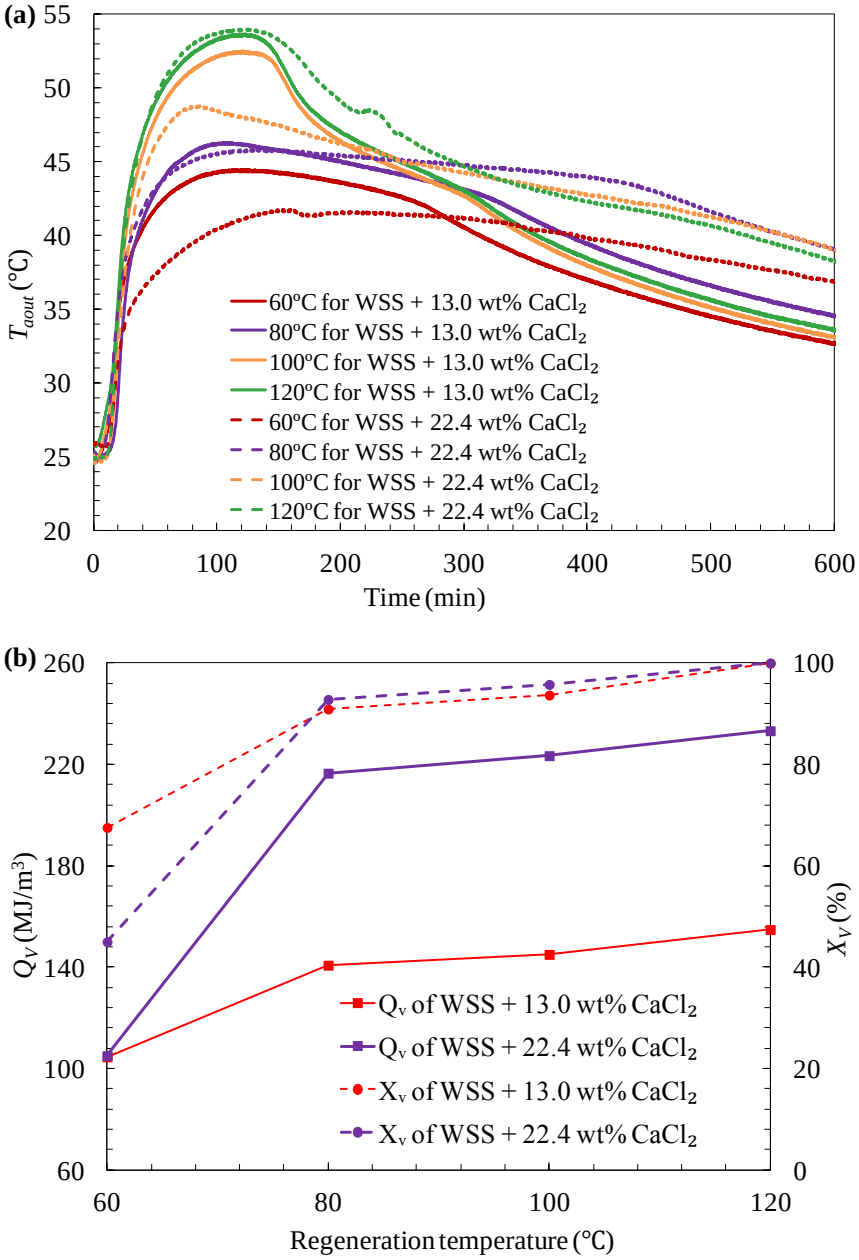

Fig. 2-9 (a) Time variation of the outlet air temperature and (b) variation of the volumetric heat storage density corresponding to different regeneration temperatures (Filters: WSS + 13.0 wt% $CaCl_2$ and WSS + 22.4 wt% $CaCl_2$; Humid air flow rate: 2.0 m^3/h)

In the previous section, we assumed that in a real application, the temperature difference should exceed 15ºC. In this case, the volumetric heat storage density is calculated only when the outlet air temperature is greater than 40ºC. The volumetric heat storage densities at different regeneration temperatures of WSS + 13.0 wt% $CaCl_2$

and WSS + 22.4 wt% $CaCl_2$ were compared (see Fig. 2-9 (b)). Assuming that the volumetric heat storage density at a regeneration temperature of 120ºC is the basic standard, then for WSS + 22.4 wt% $CaCl_2$, the volumetric heat storage density percentage at 100ºC was 95.8% and those at 80ºC and 60ºC were 93% and 45%, respectively; for WSS + 13.0 wt% $CaCl_2$, the volumetric heat storage density percentage at 100ºC was 93.7% and those at 80ºC and 60ºC were 90.9% and 67.5%, respectively. These results imply that this composite filter can be regenerated over a wide temperature range (80ºC-100ºC) with similar volumetric heat storage densities.

2.4.3 Influence of humid air flow rate in the heat release process

Time changes in the outlet air temperature after flowing through filters filled with 13.0 wt% and 22.4 wt% $CaCl_2$ at different air flow rates (1.0-3.0 m^3/h) were measured. Before the humid air flowed in, both filters were regenerated at 80ºC. Fig. 2-10(a) illustrates that for each filter, the duration of high-temperature air (> 40ºC) decreased with increasing air flow rate. However, the rising rate of outlet air temperature increased with the increasing of air flow rate. The outlet air temperature resulted from the balance between the released sorption heat and the heat transferred with the flowing air. When the air flow rate was increased, the thickness of the air film near each channel's surface thinned, so the water vapor diffusion rate would be increased due to lower gas film resistance. More water vapor could diffuse to the composite material and be sorbed by generating more heat at the same time. The generated heat was consumed to heat the flowing cold air. On the other hand, when the air flow rate was increased, the heat transfer rate could be increased. Therefore, the outlet air temperature rising rate accelerated with the higher air flow rate because of the larger generated sorption heat and the increased heat transfer rate.

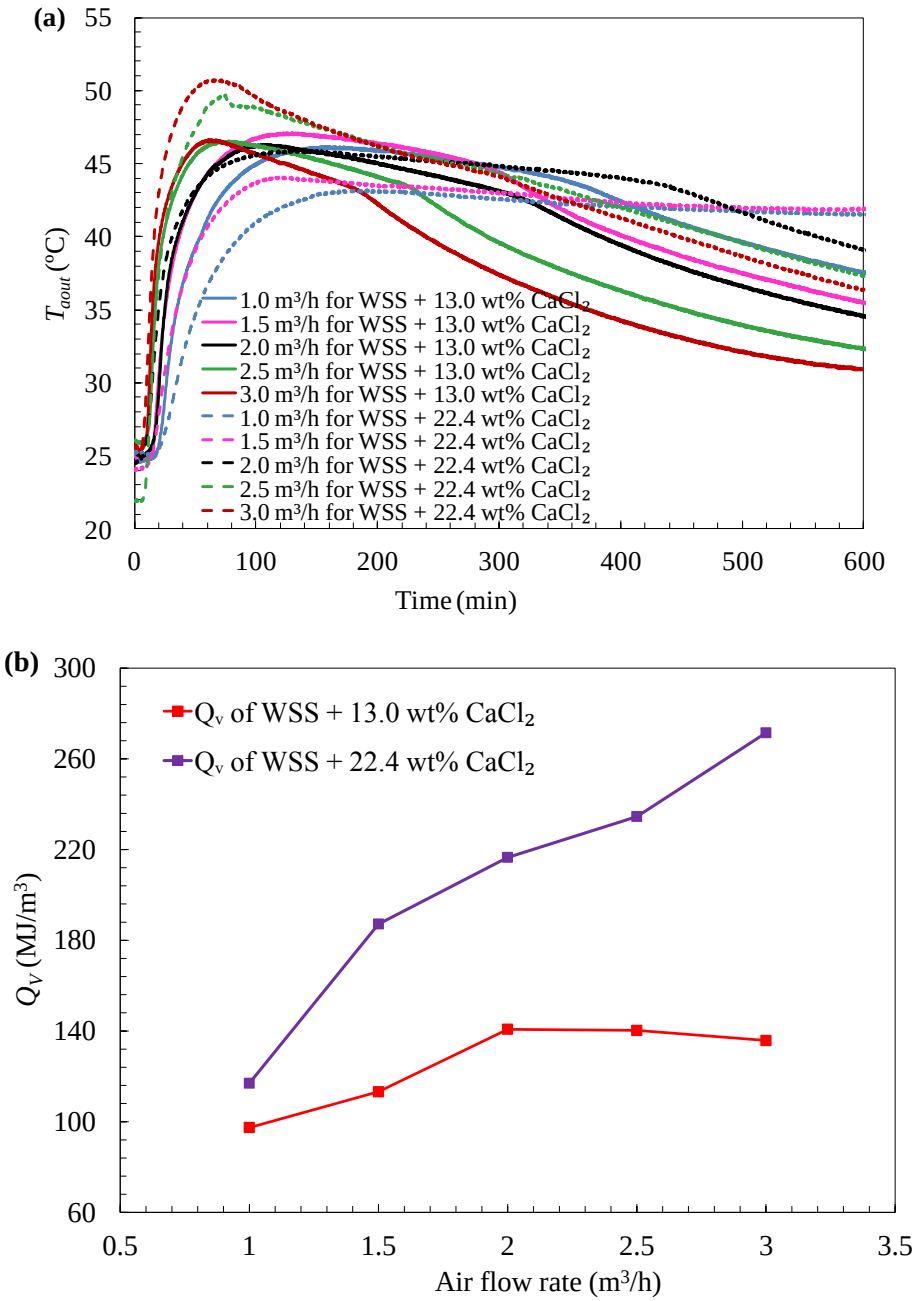

Fig. 2-10 (a) Time variation of the outlet air temperature and (b) variation of the volumetric heat storage density corresponding to different air flow rates (Filters: WSS + 13.0 wt% $CaCl_2$ and WSS + 22.4 wt% $CaCl_2$; Regeneration temperature: 80°C)

Using the same assumption for practical use, for the WSS + 13.0 wt% $CaCl_2$, high-temperature outlet air (> 40°C) can last 5 hr if the air flow rate is less than 2.0 m^3/h. In contrast, for the WSS + 22.4 wt% $CaCl_2$, when the air flow rate was 3.0 m^3/h, the outlet

air temperature reached 51ºC, and the time duration of the temperature exceeding 40ºC lasted longer than 7 hr, which almost fulfills the objective of supplying air for 8 hr.

It can be clearly seen from Fig. 2-10 (b) that for WSS + 22.4 wt% $CaCl_2$, the volumetric heat storage densities at flow rates of 1.0 and 1.5 m^3/h were lower than that at other three air flow rates. This is due to the following three reasons: (a) the outlet air temperature was still greater than 40ºC within the calculation time from 0 to 720 minutes; (b) with the relatively small air flow rate, the convective heat transfer rate was not so high resulting in the low outlet air temperature; (c) the low air flow rate resulted in low released sorption heat due to the small amount of water vapor that transferred to the composite material. For WSS + 22.4 wt% $CaCl_2$, the volumetric heat storage density increased linearly with air flow rate. In contrast, the volumetric heat storage density remained constant when the air flow rate exceeded 2.0 m^3/h for WSS + 13.0 wt% $CaCl_2$ because of the limited sorption capacity of the filter. The high-temperature air duration decreased with air flow rate. Limited by a certain amount of water vapor sorption, the volumetric heat storage density was balanced by the increasing air flow rate and decreasing high-temperature duration.

2.4.4 Effect of relative humidity of inlet air temperature in the heat release process

The effect of relative humidity of the inlet air on the outlet air temperature was illustrated in Fig. 2-11. The result was got by regenerating the WSS + 13.0 wt% $CaCl_2$ at 80ºC, and changing the relative humidity of the supplied air as 70% ± 3%, 80 ± 3% and 93% ± 3% at 25ºC, when the flow rate of humid air was 3 m^3/h.

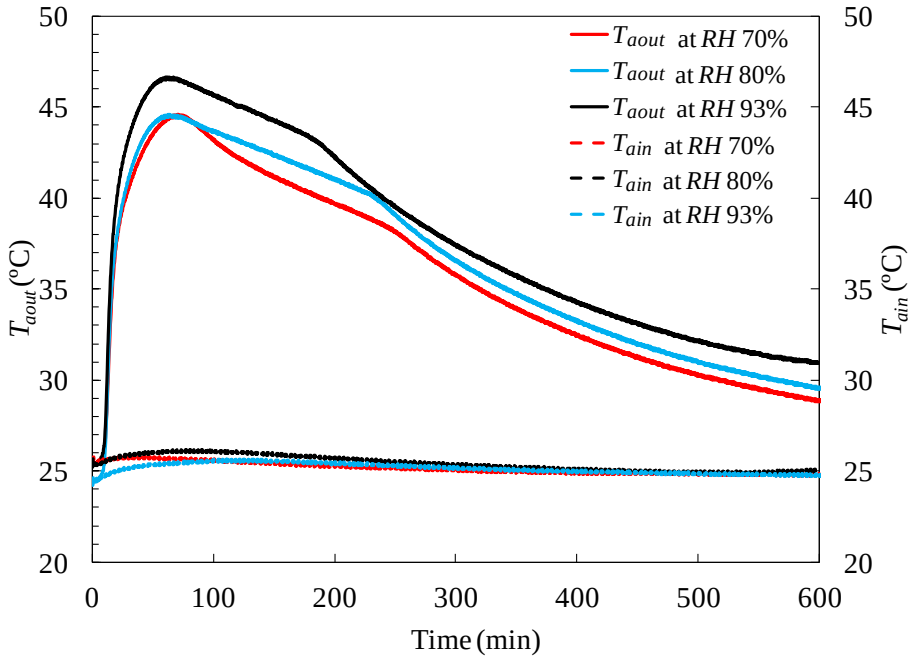

Fig. 2-11 Time variation of the inlet and outlet air temperature during the heat release process corresponding to different inlet air relative humidities (Filter: WSS + 13.0 wt% $CaCl_2$; Regeneration temperature: 80°C; Humid air flow rate: 3.0 m^3/h)

The result clearly showed that the outlet air temperature was increased and the high outlet air temperature (> 40°C) duration time was prolonged by increasing the inlet air humidity. It can be easily understood from Fig. 2-3, when the relative humidity is high, the sorption amount will increase accordingly, which means that the total sorption amount is higher compared to that under low relative humidity. Therefore, the high total sorption amount brought about long duration of supplied air with high outlet temperature. From the viewpoint of mass transfer, high humidity air means high driving force of the water vapor diffusion because of high concentration difference. It gave us a hint that the humidity of the supplied air should be as high as possible at a certain temperature.

2.4.5 Thermal performance of the composite filter

2.4.5.1 Regeneration process (heat charging process)

In order to activate the filter for use, the hot air was supplied to regenerate it. When there were no big differences of relative humidity and temperature between the inlet and outlet air, the process ended. Fig. 2-12 shows the results of regeneration process of the WSS + 22.4 wt% $CaCl_2$ when the hot air's flow rate was 3.7 m^3/h. The time variation of the inlet and outlet air temperature, the temperature of the WSS + 22.4 wt% $CaCl_2$ were illustrated in Fig. 2-12. It can be observed that the charging temperature of the flowing air increased from about 25ºC to 80ºC within 80 min as a result of the heat loss from the inlet and the cold radiation heat transfer from the filter. The temperatures at each testing position of the filter decreased in the first several minutes due to the higher desorption heat. At the end of the desorption process, the filter needed to be cooled down to the initial temperature of the heat release process. If only sensible heat was considered, the heating power (the charging heat) input in regeneration process was approximately 1250 kJ.

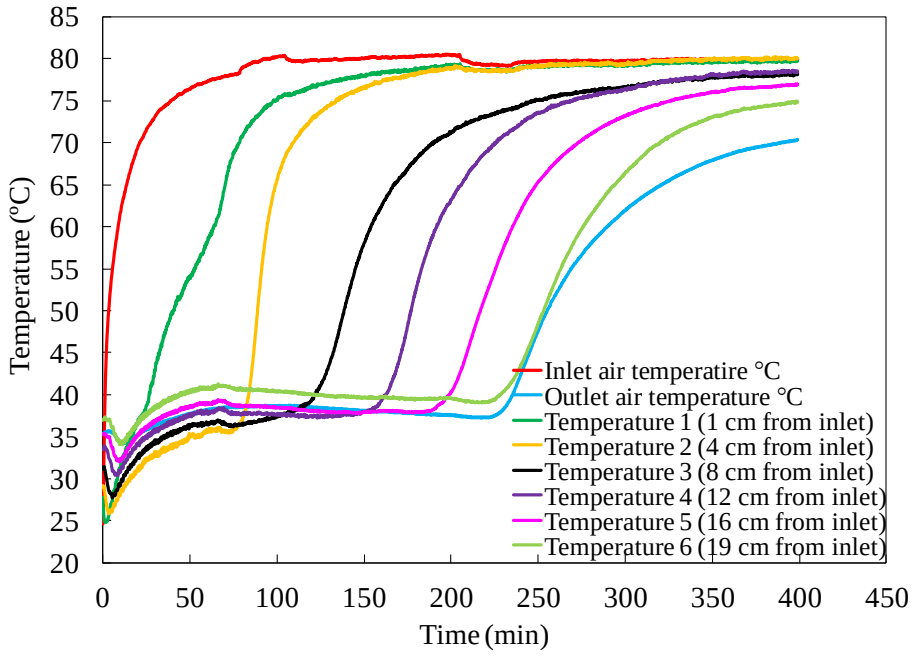

Fig. 2-12 Temperature of the filter and inlet and outlet air temperature change with time during the heat regeneration process (Filter: WSS + 22.4 wt% $CaCl_2$; Regeneration temperature: 80ºC; Hot air flow rate: 3.7 m^3/h)

2.4.5.2 Sorption process (heat release process)

For practical use, both the temperature and humidity of the air supplied by the open sorption thermal energy storage system should be considered (see Fig. 2-13). The WSS + 22.4 wt% $CaCl_2$ filter was regenerated at 80ºC, and humid air (25ºC, *RH* 93% ± 3%) was supplied at a flow rate of 3.0 m^3/h. As the sorption process progressed, the outlet water vapor content increased when stable inlet air was supplied simultaneously. The change of the water vapor sorption amount can be calculated according to air flow rate and absolute humidity of the inlet and outlet air (see Fig. 2-13):

$$\Delta\omega = \left\{ \int_0^t \rho_a Q_a (x_{ain} - x_{aout}) dt \right\} / m \qquad 2\text{-}4$$

The sorption heat was assumed to be the condensation heat of water vapor r_a = 2,260 kJ/kg. Under this condition, the sorption heat in the heat release process can be calculated as follows:

$$Q = (\Delta\omega) r_a m / 1{,}000 \qquad 2\text{-}5$$

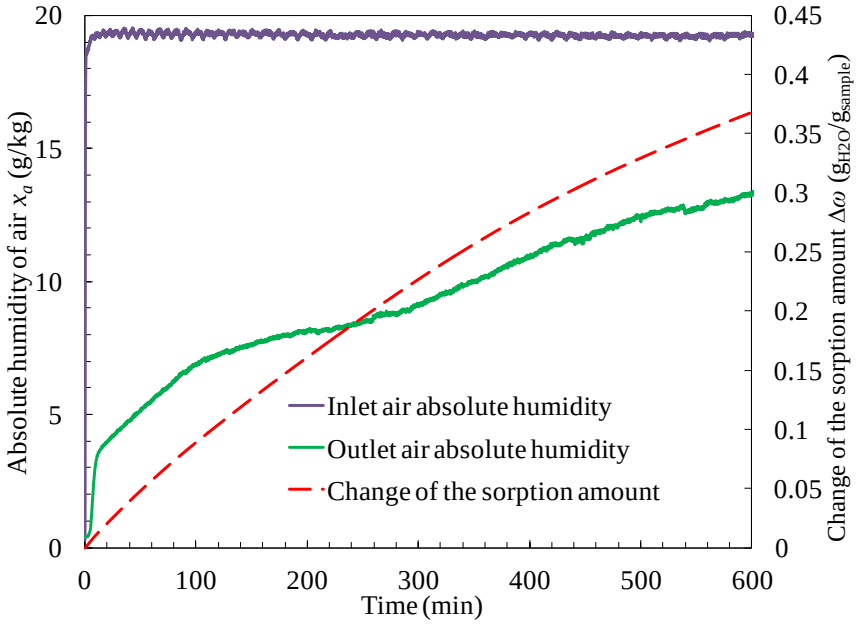

Fig. 2-13 Time change of the absolute humidity of air and change of the water vapor sorption amount during the heat release process (Filter: WSS + 22.4 wt% $CaCl_2$; Regeneration temperature: 80ºC; Humid air flow rate: 3.0 m^3/h)

The released sorption heat by the WSS + 22.4 wt% $CaCl_2$ filter in the heat discharging process within 600 min was about 841 kJ. According to Fig. 2-10 (b), the effective heat obtained by the same filter was 543 kJ. Therefore, the coefficient of heat extraction performance in the heat discharging process can be expressed as the following equation:

$$\varepsilon = (Q_V V) / Q \qquad 2\text{-}6$$

For the WSS + 22.4 wt% $CaCl_2$, ε = 65% with an air flow rate of 3.0 m^3/h.

The temperature of the filter and outlet air temperature increased due to the sorption heat release. The inlet and outlet air temperatures, each position's temperature change with time, and the temperature distributions along the length of the WSS + 22.4 wt% $CaCl_2$ filter are illustrated in Fig. 2-14 (a) and (b). The temperature of each test position reached their maximum within 40 min. The outlet air was applicable 16 min later after the heat release process started. The highest temperature during the heat release process, 61ºC, occurred at a position of 12 cm from the inlet (see Fig. 2-14 (a)). The first point of each temperature distribution line in Fig. 2-14 (b) is the inlet air temperature, and the last point is the outlet air temperature. It is clear that after supplying humid air for 30 min to 3 hr, the filter's highest temperature occurred at a position 16 cm from the inlet, and the temperature at 12 cm from the inlet was less than 2ºC lower than that at 16 cm. In other words, if the released heat duration is less than 3 hr in a real application, the length of the filter can be shorter, such as 12 cm or 16 cm. The constant temperature difference after 1 hr was caused by the limited convective heat transfer rate between the air and filter.

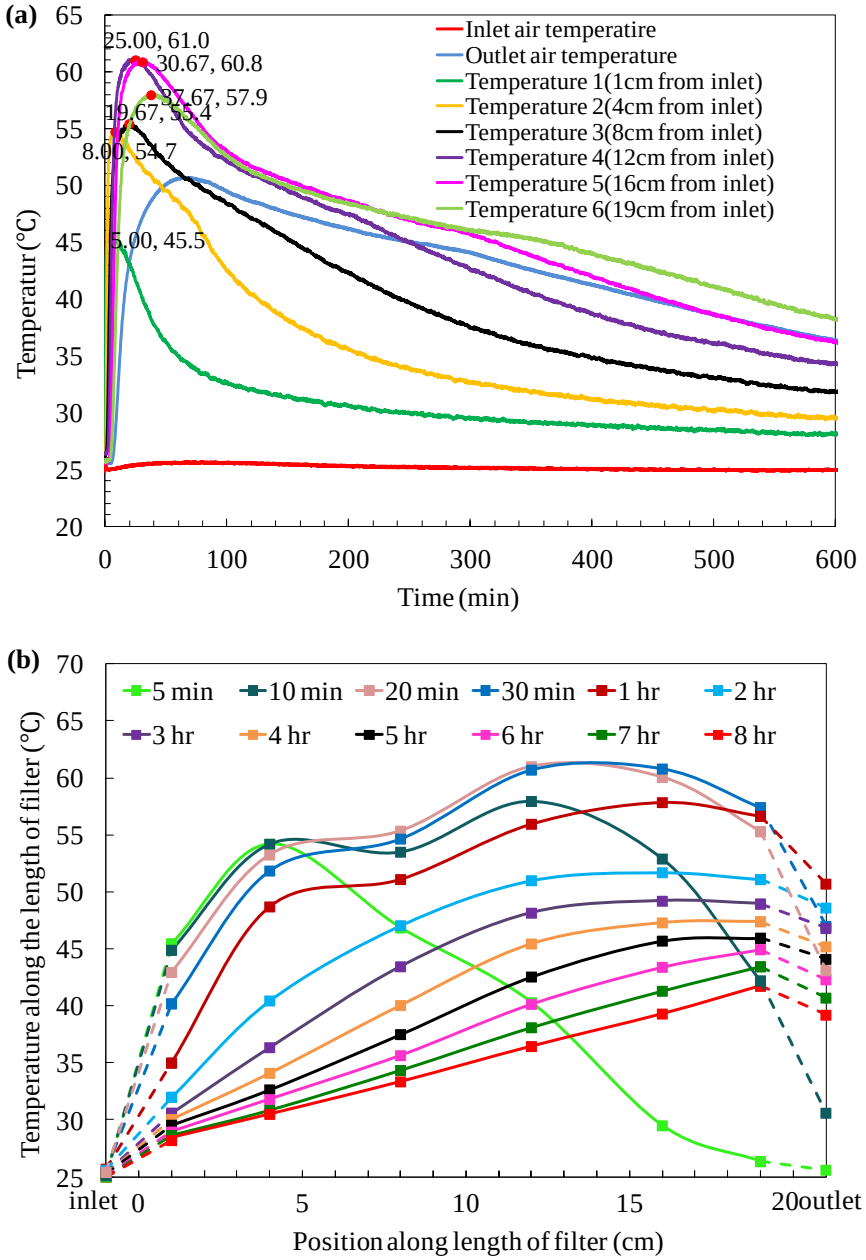

Fig. 2-14 (a) Temperature of the filter and inlet and outlet air temperature change with time and (b) temperature distributions along the length of the WSS + 22.4 wt% $CaCl_2$ filter in the heat release process (Filter: WSS + 22.4 wt% $CaCl_2$; Regeneration temperature: 80°C; Humid air flow rate: 3.0 m^3/h)

2.4.6 Volumetric heat transfer rate

Assuming that the outlet air in the heat release process is used for space heating, it is reasonable to consider that only sensible heat would be used if the indoor air were not overly dry. Therefore, the volumetric heat transfer rate is defined as follows:

$$W_V = C_{p,a}\rho_a Q_a (T_{aout} - T_{ain})/V \qquad 2\text{-}7$$

The average volumetric heat transfer rate is an effective parameter to design an actual open sorption thermal energy storage system. Fig. 2-15 shows the volumetric heat transfer rate of the four filters for a humid air flow rate of 3.0 m^3/h and a regeneration temperature of 80ºC. The volumetric heat transfer rate of the filter supported with a high content of $CaCl_2$ can be maintained at a high value over the entire testing time, which indicates that it can supply stable heat over a long period time for practical use. Humid air transferred a heat transfer rate peak of 13.3 kW/m^3 in the case of the WSS + 22.4 wt% $CaCl_2$ filter with a volume of 2 L (10 cm × 10 cm × 20 cm) and a weight of 926.2 g. Considering the assumption for practical use, the WSS + 22.4 wt% $CaCl_2$ filter maintained an average value of 10.5 kW/m^3 for 432 min (outlet air temperature > 40ºC).

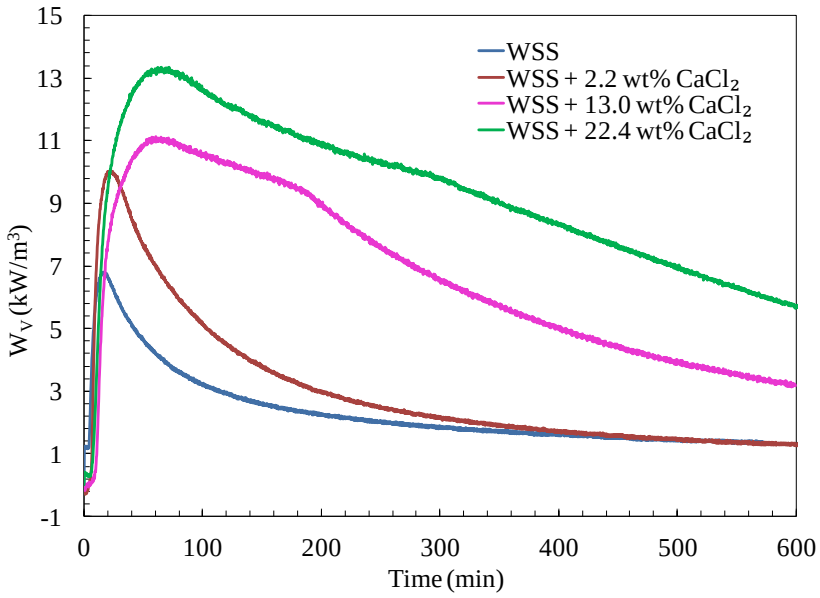

Fig. 2-15 Time variation of the volumetric heat transfer rate of the four filters (Filters: four kind of filters; Regeneration temperature: 80ºC; Humid air flow rate: 3.0 m^3/h)

A comparison between the specific thermal energy storage density and volumetric heat storage density of the composite material (WSS + 13.0 wt% $CaCl_2$ and WSS + 22.4 wt% $CaCl_2$) and other typical heat storage materials was illustrated in Fig. 2-16. A temperature difference of 15ºC was adopted to calculate the specific heat storage density for sensible thermal energy storage material. Both the specific heat storage density and the volumetric heat storage density of the composite material were calculated according to the sorption heat and the maximum sorption amount. The two developed composite filters show high storage density. It indicates theoretically that this kind of material can store much more energy without causing heavy weight and large volume of heat storage unit.

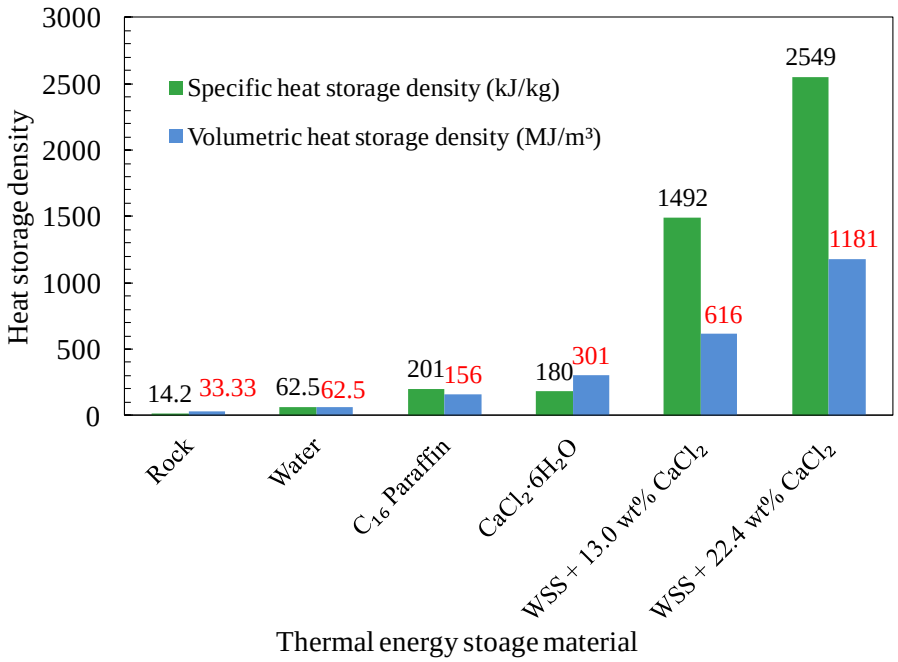

Fig. 2-16 A comparison of the heat storage densities of composite material WSS + 13.0 wt% $CaCl_2$ and WSS + 22.4 wt% $CaCl_2$ and other thermal energy storage materials

2.5 SUMMARY

A composite mesoporous material was formed by filling $CaCl_2$ into mesopores of a type of ceramic material (WSS) for sorption thermal energy storage. Before filling the mesopores with $CaCl_2$, the WSS was constructed into a honeycomb shape to ensure a large contact area and low pressure loss.

(1) The water vapor sorption capacity of the composite material increased significantly with the impregnation of hygroscopic $CaCl_2$.

(2) The composite material can be regenerated at approximately 100ºC indicating conditions that are suitable for storing low-temperature industrial waste heat or solar heat (< 100ºC).

(3) The composite material also exhibited good stability through 25 repetition tests.

An open sorption thermal energy storage experimental setup was constructed to examine the developed composite material. A 2-L composite honeycomb filter was placed inside of the system.

(1) The composite honeycomb filter was regenerated at 80ºC, and the volumetric heat storage density showed no apparent difference between that obtained by regenerating a filter at 120ºC.

(2) A long duration of 5 hr of supplying high-temperature air (> 40ºC) was observed in the open system for the WSS + 13.0 wt% $CaCl_2$ filter if the air flow rate was less than 2.0 m^3/h. For the WSS + 22.4 wt% $CaCl_2$ filter, a duration of almost 8 hr was achieved by supplying humid air at a flow rate of 3.0 m^3/h, and the outlet air temperature reached 51ºC.

(3) The released sorption heat by the WSS + 22.4 wt% $CaCl_2$ filter in the heat discharging process within 600 min was about 841 kJ, and the coefficient of the heat extraction performance reached 65%.

(4) For the WSS + 22.4 wt% $CaCl_2$ filter, the volumetric heat transfer rate was maintained at an average value of 10.5 kW/m^3 for 432 min when the outlet air temperature was greater than 40ºC.

Thus, the composite mesoporous material supported with $CaCl_2$ showed potential for the storing low-temperature industrial waste heat with a high volumetric heat storage density. Moreover, the composite mesoporous material has the advantage of a long duration time for supplying stable heat with a low heat loss.

2.6 REFERENCE

[1] H. Kameyama, Y. Kato, Honebuto energy road map, Kagaku Kogyo Sya, Japan, 2005.

[2] C.Y. Liu, K. Morofuji, K.Tamura, K. Aika, Water sorption of $CaCl_2$ containing materials as heat storage media, Chemistry Letters, 33(3) (2004) 292-293

[3] E.A. Levitskij, Y.I. Aristov, M.M. Tokarev, V.N. Parmon, "Chemical heat accumulators": A new approach to accumulating low potential heat, Solar Energy Materials and Solar Cells, 44 (1996) 219-235.

[4] W. Wongsuwan, S. Kumar, P. Neveu, F. Meunier, A review of chemical heat pump technology and applications, Applied Thermal Engineering, 21 (2001) 1489-1519.

[5] M.A. Tahat, Heat-pump/energy-store using silica gel and water as a working pair, Applied Energy, 69 (2001) 19-27.

[6] B.B. Saha, S. Koyama, J.B. Lee, K. Kuwahara, K.C.A. Alam, Y. Hamamoto, A. Akisawa, T. Kashiwagi, Performance evaluation ofa low-temperature waste heat driven multi-bed adsorption chiller, International Journal of Multiphase Flow, 29 (2003) 1249-1263.

[7] R.d. Boer, W.G. Haije, J.B.J. Veldhuis, S.F. Smeding, Solid-sorption cooling with integrated thermal storage: the SWEAT prototype, in, The International Conference on Heat Powered Cycles, HPC, Larnaca, Cyprus, 2004.

[8] R.d. Boer, W.G. Haije, J.B.J. Veldhuis, Determination of structural, thermodynamic and phase properties in the Na_2S-H_2O system for application in a chemical heat pump, Thermochimica Acta, 395 (2003) 3-19.

[9] V.M.v. Essen, H.A. Zondag, J.C. Gores, L.P.J. Bleijendaal, M. Bakker, R. Schuitema, W.G.J.v. Helden, Z. He, C.C.M.Rindt, Characterization of $MaSO_4$ hydrate for thermochemical seasonal heat storage, Journal of Solar Energy Engineering, 131 (2009) 041014-041011-041017.

[10] C. Ferchaud, H. Zondag, R.d. Boer, C. Rindt, Characterization of the sorption process in thermochemical material for seasonal solar heat storage application, in: The 12th International Conference on Energy Storage, 2012, pp. 1-10.

[11] H. Ogura, M. Kubota, H. Suzuki, T. Yamakawa, Fundamental Experimental Study on Chemical Heat Pump for Storing Low-Temperature Waste Heat and Releasing Cold-Heat, KAGAKU KOGAKU RONBUNSHU, 35(5) (2009) 506-510.

[12] H. Mikami, M. Kubota, H. Ogura, H. Suzuki, Studies on cold-heat production of chemical heat pump for refrigeration truck driven by waste heat, in: Conference of Refrigeration and Air-conditioning in Japan, Kanazawa, 2010, pp. 607-610.

[13] Y.I. Aristov, G. Restuccia, G.Cacciola, V.N. Parmon, A family of new working materials for solid sorption air conditioning systems, Applied Thermal Engineering, 22 (2002) 191-204.

[14] B. Dawoud, Y.I. Aristov, Experimental study on the kinetics of water vapor sorption on selective water sorbents, silica gel and aluminia under typical operating conditions of sorption heat pumps, International Journal of Heat and Mass Transfer, 46 (2003) 273-281.

[15] J. Jänchen, D. Ackermann, H. Stach, W. Brösicke, Studies of the water adsorption on zeolites and modified mesoporous materials for seasonal storage of solar heat, Solar Energy, 76 (2004) 339-344.

[16] D. Zhu, H. Wu, S. Wang, Experimental study on composite silica gel supported $CaCl_2$ sorbent for low grade heat storage, International Journal of Thermal Sciences, 45 (2006) 804-813.

[17] Y.I. Aristov, M.M. Tokarev, L.G. Gordeeva, V.N. Snytnikov, V.N. Parmon, New composite sorbent for solar-driven technology of fresh water production from the atmosphere, Solar Energy, 66(2) (1999) 165-168.

[18] H. Wu, S. Wang, D. Zhu, Effects of impregnating variables on dynamic sorption characteristics and storage properties of composite sorbent for solar heat storage, Solar Energy, (2007) 864-871.

[19] S. Nakabayashi, K. Nagano, M. Nakamura, J. Togawa, A. Kurokawa, Improvement of water adsorption ability of natural mesoporous material by impregnating with chloride salts for development of a new desiccant filter, Adsorption, 17 (2011) 675-686.

[20] I.V. Ponomarenko, I.S. Glaznev, A.V. Gubar, Y.I. Aristov, S.D. Kirik, Synthesis and water sorption properties of a new composite "$CaCl_2$ confined into SBA-15 pores", Microporous and Mesoporous Materials, 129 (2010) 243-250.

[21] A. Kurokawa, J. Togawa, Y. Nabeshima, K. Nagano, The evaluation of the moisture sorption mechanism of chloride-impregnated Wakkanai Siliceous Shale, KAGAKU KOGAKU RONBUNSHU, 37(5) (2011) 394-399.

[22] Y.I. Aristov, New family of solid sorbents for adsorptive cooling: material scientist approach, Journal of Engineering Thermophysics, 16(2) (2007) 63-72.

[23] Y.I. Aristov, M.M.Tokarev, G.Cacciola, G. Restuccia, Selective water sorbents for multiple applications, 1. $CaCl_2$ confined in mesopores of silica gel: sorption properties, Reaction Kinetics and Catalysis Letters, 59(2) (1996) 325-333.

[24] Y.I. Aristov, G. Restuccia, M.M. Tokarev, H.-D. Buerger, A. Freni, Selective water sorbents for multiple applications. 11. $CaCl_2$ confined to expanded vermiculite, Reaction Kinetics and Catalysis Letters, 71(2) (2000) 377-384.

[25] Y. Kato, K. Kobayashi, Y. Yoshizawa, Durability to repetitive reaction of magnesium oxide/water reaction system for a heat pump, Applied Thermal Engineering, 18(3-4) (1998) 85-92.

[26] A. Ristić, D. Maučec, S.K. Henninger, V. Kaučič, New two-component water sorbent $CaCl_2$-FeKIL2 for solar thermal energy stoage, Microporous and Mesoporous Materials, 164 (2012) 266-272.

3 NUMERICAL SIMULATION OF AN OPEN SORPTION THERMAL ENERGY STORAGE SYSTEM USING COMPOSITE SORBENTS BUILT INTO A HONEYCOMB STRUCTURE

Hokkaido University

3.1 INTRODUCTION

Thermal energy storage technology has the potential to meet society's need for more efficient, environmentally friendly energy use in a variety of sectors, and it appears to be the only viable solution to overcome the mismatch between the supply and demand of thermal energy [1]. Effective storage of thermal energy could reduce both fossil energy demand and carbon dioxide emissions. A composite thermal energy storage material with low heat loss and high heat storage density for the storage of low-temperature industrial waste heat (80°C) was developed in our previous work [2]. The composite material based on a natural mesoporous stone (Wakkanai siliceous shale (WSS)), whose main composition is SiO_2, was built into a honeycomb shape, and it was installed in an open sorption thermal energy storage system, with which it can be regenerated by hot air at 80-120°C. Compared to the traditional sensible heat storage and latent heat storage materials, the developed composite material exhibits low heat loss as it can be stored at ambient temperatures as long as it is separated with the functional gas (water vapor) [3]. Another advantage of this material would be the low cost, due to the low price of natural mudstone WSS and cheap $CaCl_2$. Furthermore, from the viewpoint of thermal energy storage density, this material can compete with the traditional sensible heat storage and phase change materials from Fig.16 in [2].

So far, there are few research studies about open sorption thermal energy storage system. Wu and Zhu and Wu et al. [4, 5] developed an open-type thermal energy storage setup with 40 kg composite sorbent pellets (silica gel filled with $CaCl_2$). Moreover, they also reported a three-dimensional numerical model [6] to determine the dynamic characteristics of composite sorbents and to calculate the specific capacity and coefficient of performance (COP) of the open system. According to their results, the developed system showed high thermal energy storage density and can be regenerated at low temperature (<100ºC). Ostrovskii et al. [7, 8] have proposed a non-stationary model to describe water sorption in a flow adsorber with a fixed bed of selective water sorbents (SWSs) (calcium chloride in a porous matrix) at pressures of 7 atm and 1 atm, respectively. An analytical expression for the sorption rate constant as a function of the moisture content of the sorbent is proposed that takes into account the monotonic decrease in this constant with an increase in the amount of water sorbed. Unfortunately,

both of the two open systems described above keep the functional fluid flow through the inter particles of their composite materials without an individual flow passage for fluid, which would cause a high pressure drop. Moreover, a heat exchanger is needed to improve the heat exchange between the air and the composite material [4].

In fact, the heat and mass transfer between the flowing air and the composite material occurring in this open system is very similar with the heat and mass transport which happens in solid desiccant systems. Many researchers have simulated heat and moisture transfer in solid desiccant systems, in which the coupled heat and moisture transfer is of great importance to the system performance [9]. Among these models, Charoensupaya et al. [10] proposed a one-dimensional heat and mass transfer model to analyze an open-cycle desiccant cooling system based on a hypothetical isotherm equation. Then a one-dimensional transient model has been established by Zheng et al. [11, 12], with which the optimum rotational speed for air dehumidification was determined. Zhang et al. [13] also proposed a one-dimensional theoretical model based on the size and structure of the channel in their desiccant wheel for wheel design optimization. However, the actual transfer process occurring in the desiccant wheel cannot be reflected by these models, as the solid side resistance (heat conduction and mass diffusion within solid side) were ignored. Realizing the above problem, many researchers have developed models by taking both gas and solid side resistances into account, including Majumdar [14], Ge et.al [15], Gao et al. [16], Zhang and Niu [9, 17], Yamaguchi et al. [18] etc. By considering both the gas and solid side resistance, the precisions of simulation models can be greatly improved [15].

Compared to the common solid desiccant system, the operating relative humidity range of our system is much larger (2%-95%) during the sorption process. In this case, the formation of crystalline hydrate needs to be considered. Compared to the traditional solid desiccant materials, the presence of hydrates or salt solution in the matrix's pores, however, can significantly change the sorbent capacity and also induce qualitatively new phenomena [8], which increases the difficulty of simulating the sorption and desorption processes of composite materials. In order to increase the precision of simulation results, Ge et al. [15] used a one-dimensional model to predict the performance of silica gel haloid compound desiccant wheel by considering both the gas

and solid side resistances. For the solid side resistance, both pore diffusion and surface diffusion have been considered.

The objective of our current research is to simulate the processes of sorption (heat release) and desorption (heat storage) within this thermal energy storage unit quickly and accurately by numerical simulation. Such a simulation can be used to predict the temperature distribution of the thermal energy storage unit and the flowing air, quickly evaluate the performance of the thermal energy storage system, and optimize the air conditions for practical applications. Moreover, the air condition and the necessary volume of this composite thermal energy storage unit are expected to be designed and calculated by this model according to the requirement of a certain application.

3.2 MATHEMATICAL MODEL

For a thermal energy storage system, heat storage process and heat release process are included. An open sorption thermal energy storage experimental setup was built as described in our previous study [2]. In the heat storage (heat charging or endothermic) process, hot air is used to regenerate the material, during which the water vapor bonded to the material is discharged to the ambient environment and the heat is stored. In the heat release (heat discharging or exothermic) mode, high-humidity air flows through the system to recover the exothermic heat due to the sorption of the water vapor. A composite mesoporous honeycomb thermal energy storage unit was the key component in that open sorption thermal energy storage system operated under atmospheric pressure of 1 atm. The honeycomb structure can assure high heat and mass transfer contact area with a low pressure drop. The pressure drop is less than 15 Pa at a flow rate of 10 m^3/h when the dimension of the unit is 10 cm × 10 cm × 10 cm. The thermal energy storage unit was made by impregnating calcium chloride ($CaCl_2$) into the mesopores of WSS honeycomb unit. The schematic of the honeycomb structure and a cross section of one channel used in the model are shown in Fig. 3-1 (a), in which the length is illustrated as L and size of each channel can also be checked. Three samples with different $CaCl_2$ contents were made, and were short for WSS + 2.2 wt % $CaCl_2$, WSS + 13.0 wt% $CaCl_2$, WSS + 22.4 wt% $CaCl_2$, respectively. The physical properties of these composite mesoporous materials including pore volume distributions, porosity and true density.etc can be checked in Fig. 2 and Table 1 in reference [2].

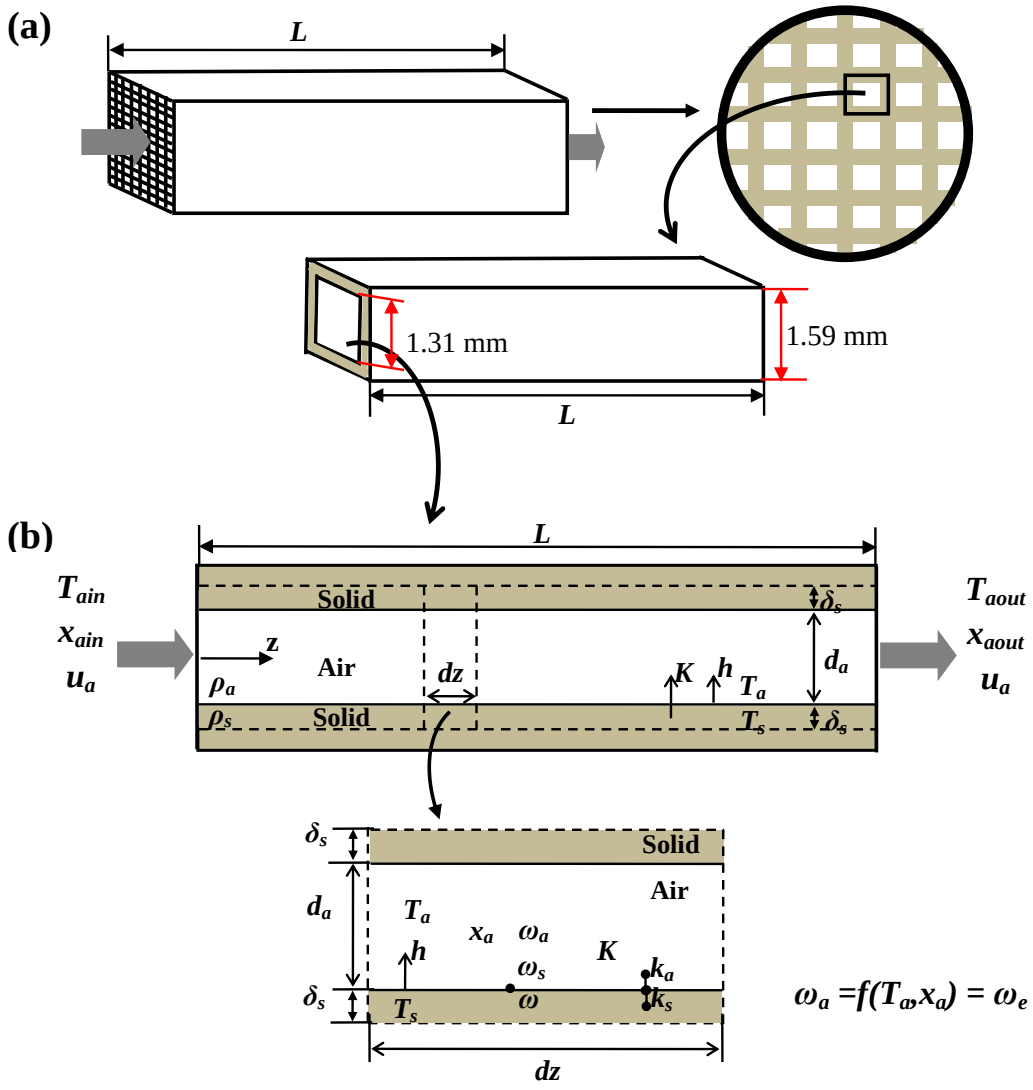

Fig. 3-1 The one-dimensional transient model illustration

The performance of the thermal energy storage unit is modeled by just tracking the air and solid condition in one single channel. A one-dimensional transient model, illustrated in Fig. 3-1 (b), was proposed to predict the temperature of the composite material and the temperature and humidity of the flowing moist/hot air and to evaluate the performance of the thermal energy storage medium.

3.2.1 Heat and mass transfer analysis

As humid/hot air enters the channel of the honeycomb unit, a fraction of the water vapor is sorbed/desorbed by the composite material. The sorption/desorption process is accompanied by a release/absorption of heat, creating a strong coupling between heat and mass transfer [19]. Generally, the water vapor transfers from the air to the pores of the composite material mainly in two steps. First, water molecules are transported from the air to the surface of the composite material due to convective mass transfer, which is called gas side mass transfer. In the next step, the water vapor transfers from the surface of the composite material to the inter particle pores and then to the intra particle pores. Mass diffusion inside the solid involves multiple mechanisms – molecular diffusion, Knudsen diffusion, and surface diffusion [20] – occur in the porous material. Water molecules in the vapor phase diffuse from the surface of the composite solid layer to the surface of the particles through molecular and Knudsen diffusion in the inter-particle pores. The sorbed water molecules then diffuse from the surface of the particles into the intra-particle pores through surface diffusion, and water vapor molecules in the intra-particle pores diffuse through molecular and Knudsen diffusion [21]. The mass transfer is also accompanied by heat transfer. Heat transfer between the flowing air and the channel of the composite material occurs primarily due to the convective heat transfer along the surface of each channel. The heat transfer inside the solid layer would be the heat conduction between the solid particles.

3.2.1.1 Heat transfer Biot number

The heat transfer Biot number B_{ih} is calculated to determine whether thermal conduction on the solid side is relevant, which is defined as follows:

$$B_{ih} = \frac{h\delta_s}{\lambda_s} \qquad 3\text{-}1$$

The convective heat transfer coefficient h is estimated from the Nusselt number Nu for developed laminar flow in a square channel, considering constant and uniform temperature at the interface as 2.89.

$$h = Nu\frac{\lambda_a}{d_a} \tag{3-2}$$

The effective thermal conductivity λ_s is considered to be related to the amount of water sorbed.

$$\lambda_s = \lambda_{s,dry} + \lambda_{H_2O}\omega \tag{3-3}$$

Thickness of the solid layer δ_s of 0.14 mm and thermal conductivity of the dry material $\lambda_{s,dry}$ of 0.2 W/(m·K) were used for the Biot number B_{ih} calculation. The calculated maximum heat transfer Biot number B_{ih} for our system is 0.035; therefore, the solid inside heat conduction resistance can be ignored due to the small heat transfer Biot number (B_{ih} < 0.1).

3.2.1.2 Mass transfer Biot number

Similar to the heat transfer Biot number B_{ih}, the mass transfer Biot number B_{im} is introduced to determine the dominant mass transfer resistance [22]. B_{im} represents the relative importance of the intraparticle diffusion resistance and fluid to particle mass transfer resistance, which is defined as follows [20]:

$$B_{im} = \frac{h_m\delta_s}{D_{eff}} \tag{3-4}$$

The solid inside mass transfer resistance can be ignored if the mass transfer Biot number is small (B_{im} <0.1), similar to the requirement for ignoring heat conduction for small heat transfer Biot numbers [21].

The gas side mass transfer coefficient h_m is estimated after the calculation of the convective heat transfer coefficient. When both heat and mass transfer occur simultaneously, the mass and heat transfer coefficients are related by the Lewis equation [23]:

$$h_m = \frac{h}{\rho_a C_{p,a} Le} \tag{3-5}$$

The molecular diffusion coefficient D_m is calculated based on the kinetic theory of gases, and for a water vapor-air mixture, it is given by [14, 17]:

$$D_m = 1.758 \times 10^{-4} \frac{(T_s + 273.15)^{1.685}}{P_v} \quad 3\text{-}6$$

In the above equation, P_v is the pressure in atmospheres (Pa). The calculated molecular diffusion coefficient is on an order of 1.0×10^{-5} m^2/s.

Knudsen diffusion D_K is significant at low pressure and small pore diameter, and it depends on the radius of the pore r_p and the material's temperature T_s [24]:

$$D_K = 97 r_p ((T_s + 273.15) / M)^{1/2} \quad 3\text{-}7$$

The average pore diameter of WSS + 22.4 wt% $CaCl_2$ is about 6 nm. When temperature is 25ºC, the calculated Knudsen diffusion coefficient D_K is 1.18×10^{-6} m^2/s.

The overall pore diffusivity D_P inside the solid pores can be obtained from Bosanquit's equation [20]:

$$1/D_P = 1/D_m + 1/D_K \quad 3\text{-}8$$

Surface diffusion D_s, the transport of sorbed molecules on the pore surface, can be expressed as a function of temperature [25]:

$$D_s = D_{s,0} \exp(-0.974 \times 10^{-3} \frac{\Delta H}{T_s + 273.15}) \quad 3\text{-}9$$

$D_{s,0}$ is a constant for surface diffusion calculation, which has a constant value of 1.6×10^{-6} m^2/s. The calculated surface diffusion coefficient is in the order of 1.0×10^{-10} m^2/s.

The pore diffusion and the surface diffusion are considered to occur in parallel [18]. The apparent pore diffusion coefficient D_{eff} was defined by taking the water vapor content gradient as the driving force of diffusion [20].

$$D_{eff} = \frac{\varepsilon_s}{\tau_p} D_p + \frac{\rho_s}{\rho_a} \frac{D_s}{\tau_s} \alpha \qquad 3\text{-}10$$

In the above equation, α reflects the local slope of the equilibrium sorption amount to the absolute humidity, and it can be represented as: $d\omega_e / dx_a$. τ_p accounts for the increase in diffusional length due to the tortuosity of real pores, which is set as 3 in this study assuming the random pore direction [20]. τ_s is the tortuosity factor for surface diffusion, which accounts for the increase in diffusion resistance in real pores compared with theoretically smooth surface [22], which is set the same as τ_p in this calculation. In this study, the overall pore diffusivity D_P is in the order of 1.0×10^{-7} m^2/s, whiles the effective surface diffusion coefficient, the latter term of Eq. 3-10, based on the pore diffusion is in the order of 1.0×10^{-5} m^2/s. Therefore, the surface diffusion is dominant compared to the pore diffusion in the composite material, and the apparent pore diffusion coefficient can be changed to the following equation:

$$D_{eff} = \frac{\rho_s}{\rho_a} \frac{D_s}{\tau_s} \alpha \qquad 3\text{-}11$$

The calculated B_{im} is about 0.3 when the calculating temperature is 25°C, indicating that neither the gas side mass transfer resistance nor the mass diffusion inside the composite material can be ignored.

3.2.2 Governing equations

3.2.2.1 Assumptions

The governing equations describing the mass and energy balances are developed based on the following assumptions:

(1) The structure and composition of the honeycomb unit are assumed homogeneous.

(2) All the channels are considered identical in the calculations.

(3) The pressure and temperature of the air are assumed to be constant in the direction perpendicular to air flow, and the air's velocity is assumed to be constant along the

thickness of the air layer and throughout the sorption/desorption process. Pressure, temperature, and the amount of sorbed water vapor are assumed to be constant along the thickness of the composite material.

(4) The flowing air is incompressible and laminar because the hydraulic diameter of each cell is 1.31 mm, and a typical Reynolds number is in the order of 100.

(5) The heat conduction and water vapor diffusion in the air along the length of the material is negligible.

(6) Convective heat transfer is used to describe the interfacial heat transfer between the solid composite material and the airflow.

(7) The specific heat and density of the dry composite material are constant.

(8) The impregnation of hydroscopic salt is assumed not to affect the sorption process such as the diffusion of water vapor into solid salt or through the liquid film of $CaCl_2 \cdot nH_2O$.

(9) The LDF model is adopted to predict the sorption rate by considering both the gas side and the solid side mass transfer resistances.

3.2.2.2 Conservation equations

The mass conservation equation for water vapor in the air can be written as follows:

$$\rho_a \frac{\partial x_a}{\partial t} + \rho_a u_a \frac{\partial x_a}{\partial z} = -\rho_s \frac{\partial \omega}{\partial t} \frac{\delta_s}{\delta_a} \qquad 3\text{-}12$$

The moisture balance of the composite material can be written using the Linear driving force (LDF) model:

$$\frac{\partial \omega}{\partial t} = \frac{K}{\delta_s}(\omega_e - \omega) \qquad 3\text{-}13$$

The energy conservation equation for the air is as follows:

$$\rho_a C_{p,a} \frac{\partial T_a}{\partial t} + \rho_a u_a C_{p,a} \frac{\partial T_a}{\partial z} = \frac{h}{\delta_a}(T_s - T_a) \qquad 3\text{-}14$$

The energy conservation equation for the composite solid is as follows:

$$\frac{\partial(\rho_s C_{p,s} T_s)}{\partial t} = \frac{h}{\delta_s}(T_a - T_s) + \frac{\partial(\rho_s \omega)}{\partial t}(\Delta H) \qquad 3\text{-}15$$

The specific heat of the composite material is considered to be related to the amount of water vapor sorbed according to Eq. 3-16:

$$C_{p,s} = C_{p,s,dry} + C_{p,H_2O}\omega \qquad 3\text{-}16$$

3.2.3 Boundary and initial conditions

(1) Boundary conditions

Inlet condition: Uniform distributions of T_a and x_a are assumed as the inlet air condition.

$$x_a = x_{a,in},\ T_a = T_{a,in} \qquad \text{at z = 0} \qquad 3\text{-}17\ (a)$$

Outlet condition: The adiabatic and impermeable condition of the outlet of the thermal energy storage unit was set. It is assumed that the absolute humidity gradient and temperature gradient of the air vanished at the outlet of the channel.

$$\frac{\partial x_a}{\partial z} = 0,\ \frac{\partial T_a}{\partial z} = 0 \qquad \text{at z = L} \qquad 3\text{-}17\ (b)$$

(2) Initial condition

The initial sorption amount of the composite material of one process is equal to the final sorption amount of the reverse process. The temperature distribution along the length of the heat storage unit is constant, as are the temperature and moisture of the air. Therefore, the initial conditions for the air and the composite material are set as follows:

$$x_a = x_{a,0},\ T_a = T_{a,0},\ T_s = T_{s,0},\ \omega_0 = \omega_{sor/desor} \qquad \text{at } t = 0 \qquad 3\text{-}18$$

3.2.4 Parameter settings

3.2.4.1 Determination of the equilibrium sorption amount

Two phases of H_2O co-exist, namely, gas and sorbed water inside the pores of the composite medium. The water vapor sorption isotherms of the composite material were tested by the water vapor sorption analyzer Hydrosorb HS-1 (Quantachrome Instruments). At the four measured temperatures (25, 30, 35, 40°C), the equilibrium sorption amount is essentially independent of temperature and only related to the relative humidity, as shown in Fig. 3-2 (a). Therefore, the equilibrium sorption amount ω_e is assumed to be independent of temperature, and is only a function of relative humidity in the calculation.

$$\omega_e = f(RH) \tag{3-19}$$

The water vapor sorption isotherms shown in Fig. 3-2 (a) was tested by heating the material at 150ºC under the vacuum condition for 4 hours to make sure that the material had been dried completely. However, for WSS + 22.4 wt% $CaCl_2$, the equilibrium sorption amount tends to be nonzero when the relative humidity is small if it is regenerated at 80ºC. This condition is due to the formation of calcium chloride dihydrate, which is verified by Fig. 4 in [2].

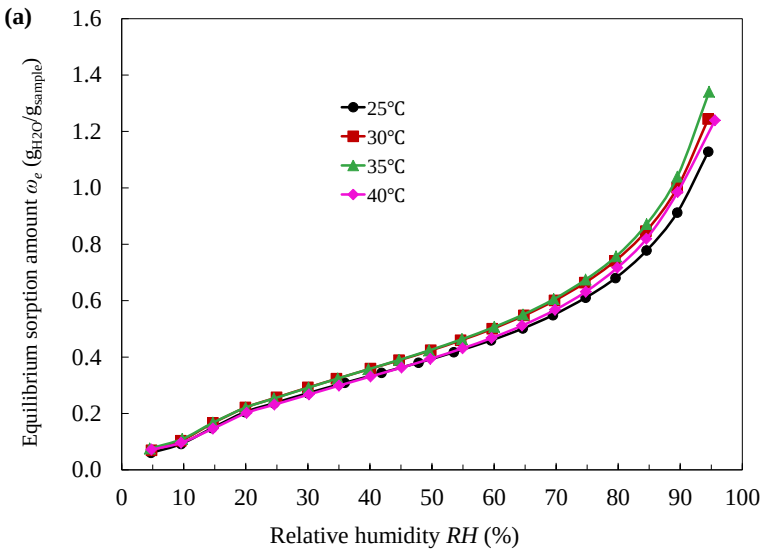

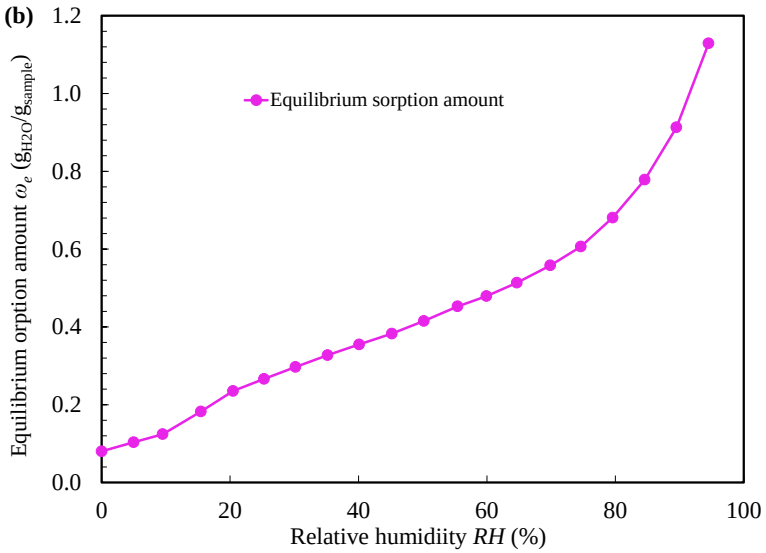

Fig. 3-2 (a) Equilibrium sorption amount at different temperatures for the WSS +22.4 $CaCl_2$; (b) equilibrium sorption fitting lines used in simulation for the WSS +22.4 $CaCl_2$

Therefore, in order to get a clear idea about the effect of crystalline dehydrate on the equilibrium sorption amount at each relative humidity, the water vapor sorption isotherm was tested again by heating the same material at 80ºC for 4 hours, and the initial sorption amount is nonzero when the relative humidity is small, which can be seen in Fig. 3-2 (b). The equilibrium sorption amount used in the simulation was obtained by the cubic spline interpolating method based on several measured sorption amount values.

3.2.4.2 Determination of the sorption heat

The sorption/desorption heat for the composite material can be obtained from its sorption characteristics, which is related to the water sorption amount [26]. The sorption heat is high when the sorbed water is smaller than 2 moles per mole of $CaCl_2$ (corresponds to $CaCl_2 \cdot 2H_2O$) then it remains at a constant value [26]. In this simulation, the sorption heat is assumed to be constant and equal to the latent heat of water during the sorption amount range, within which the calcium chloride dihydrate was considered stable during both the sorption process and desorption process.

3.2.4.3 Overall mass transfer coefficient

The total mass transfer resistance $\frac{1}{K}$ is calculated by adding both resistances in series according to [27]:

$$\frac{1}{K} = \frac{1}{k_a} + \frac{1}{k_s} \qquad 3\text{-}20$$

The air side mass transfer coefficient k_a can be calculated based on the solid side.

$$k_a = \frac{\rho_a h_m}{\rho_s \alpha} \qquad 3\text{-}21$$

The solid side mass transfer coefficient k_s is defined by the following equation according to [20, 28]:

$$k_s = \frac{15 D_s}{\delta_s} \qquad 3\text{-}22$$

3.2.5 Numerical solution and experimental validation

The governing equations were discretized using the explicit finite difference (FDM) method. The discrete equations were derived over each length interval and time interval and numerically solved by Fortran code.

Table 3-1 Air states and initial conditions of both air and composite material in sorption/desorption process

Process		Sorption	Desorption
Inlet air condition	Inlet air flow rate f_a (m^3/h)	3.0	3.8
	Inlet air temperature T_a (°C)	25	80
	Inlet air relative humidity *RH* (%)	95	3
Initial condition	Air temperature T_a (°C)	25	25 (lnlet) 35 (outlet)
	Air relative humidity *RH* (%)	3.0	95.4 (lnlet) 36.6 (outlet)
	Composite material's temperature T_d (°C)	25	30
Repetition test	Inlet air flow rate f_a (m^3/h)	2.0	2.8
	Inlet air temperature T_a (°C)	25	80
	Inlet air relative humidity *RH* (%)	95	3

In this study, experimental results from tests of the open sorption thermal energy storage setup were used to validate the simulation results. The dimensions of the thermal energy storage unit were 20 cm (length) × 10 cm (width) ×10 cm (height). The WSS + 22.4 wt% $CaCl_2$ was chosen for the validation of this program due to its excellent performance in previous experiments, and the simulation conditions are shown in Table 3-1. The calculated outlet air absolute humidity, change of the sorption amount, outlet air temperature, and the composite material's temperature and corresponding instantaneous sorption amount, as well as the relevant experimental values, are illustrated in Fig. 3-3 (a), (b) and Fig. 3-4 for the sorption process and in Fig. 3-5 (a), (b) and Fig. 3-6 for the desorption process, respectively.

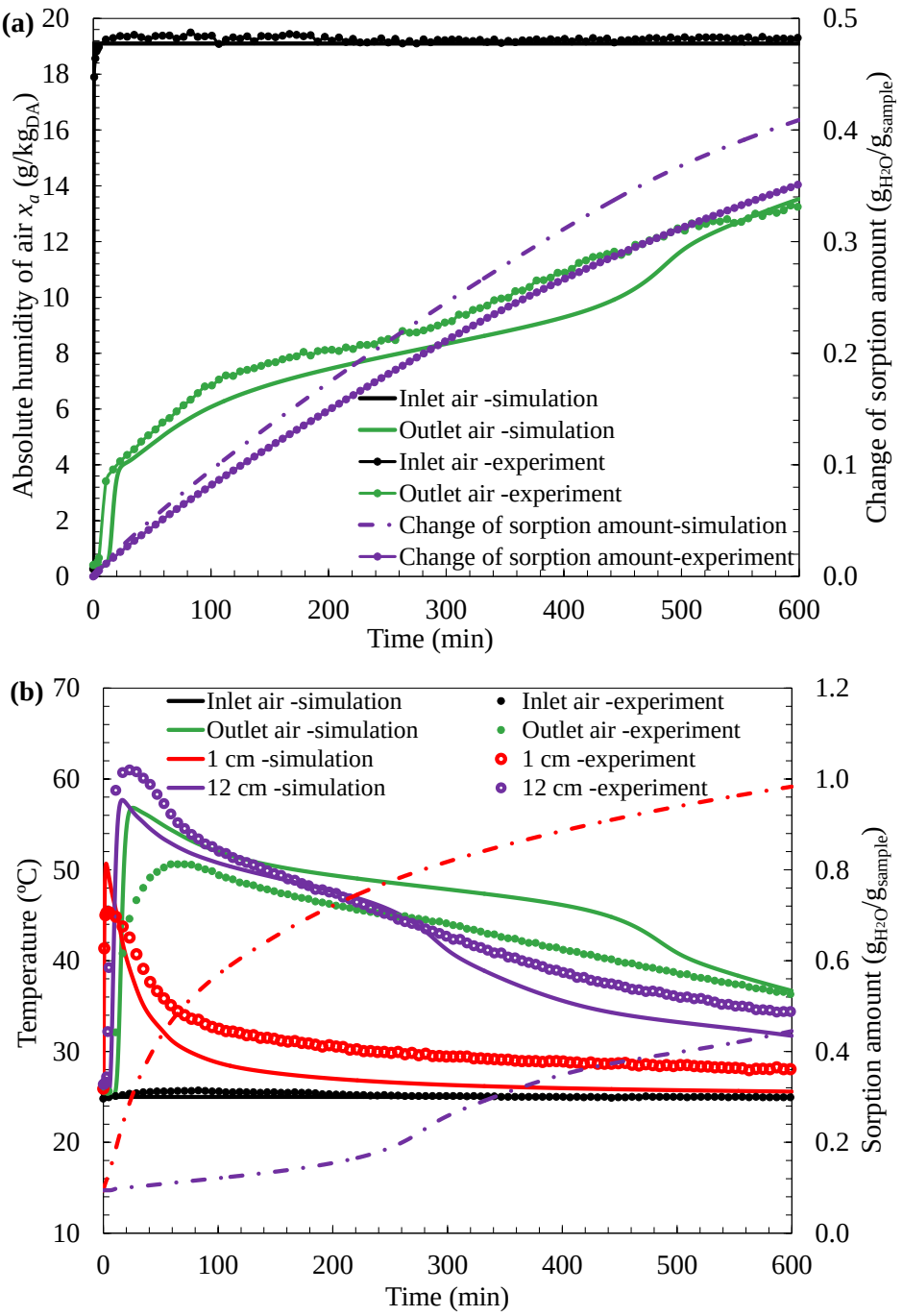

Fig. 3-3 (a) Comparison of inlet/ outlet air absolute humidity and change of the sorption amount during sorption process; (b) comparison of inlet/outlet air temperature and temperature of the WSS + 22.4 wt% $CaCl_2$ in heat release process (humid air flow rate: 3.0 m3/h; regeneration temperature: 80°C)

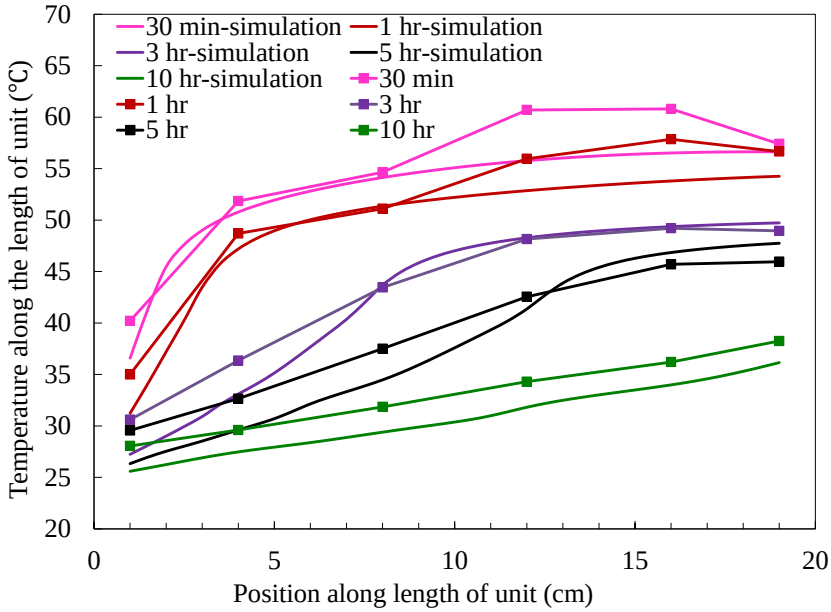

Fig. 3-4 Temperature profile of the WSS + 22.4 wt% $CaCl_2$ in heat release process (humid air flow rate: 3.0 m3/h; regeneration temperature: 80°C)

Fig. 3-3 (b) and Fig. 3-4 demonstrate that the simulated composite material's temperatures match the experimental values well both in terms of time and of the position along the length of the WSS + 22.4 wt% $CaCl_2$. The simulation results for the general trend in the outlet air temperature with time are also similar to the experimental results, although the simulated outlet air temperature differs by approximately 3 to 4°C from the measured values (cf. Fig. 3-3 (b)).

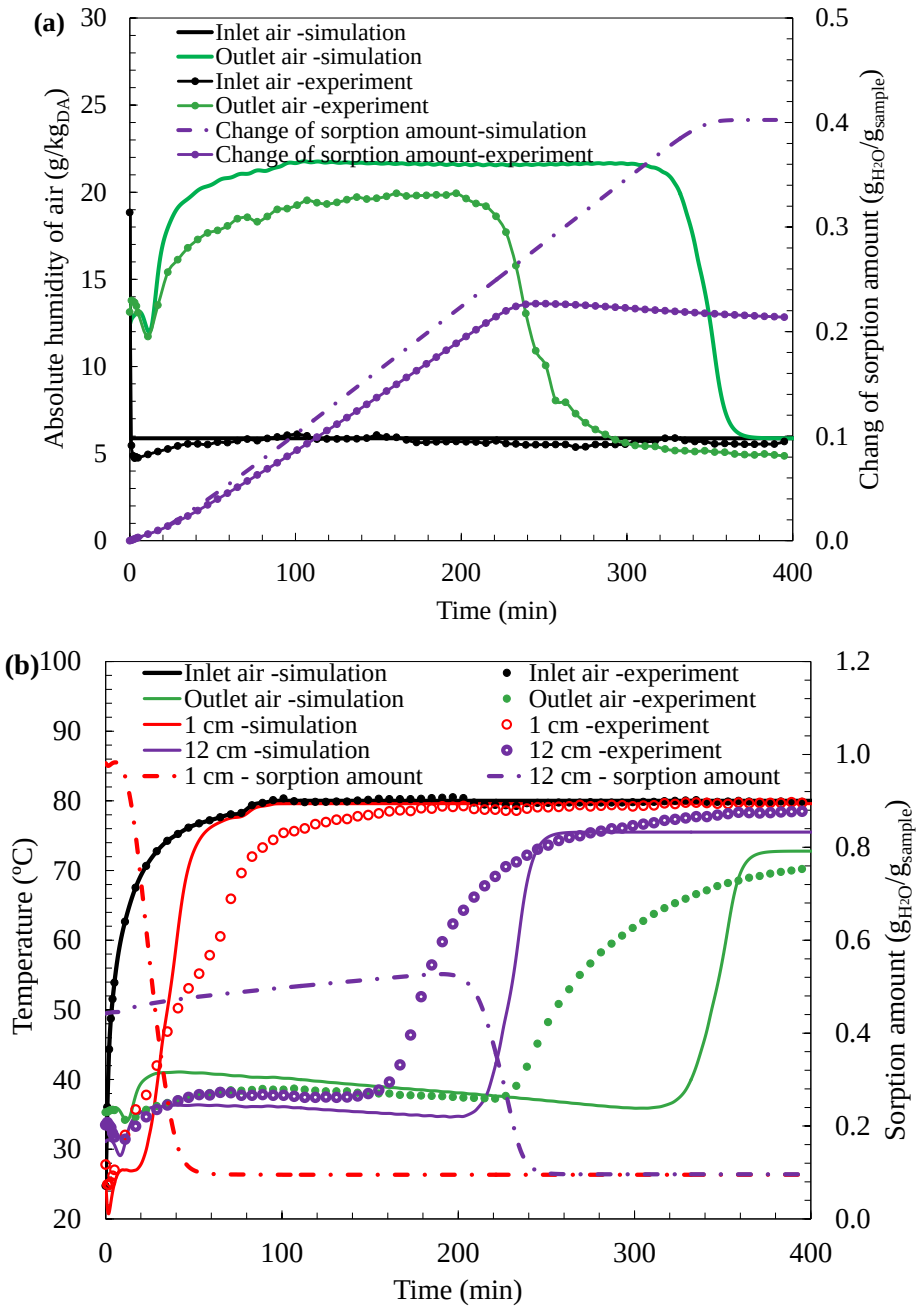

Fig. 3-5 (a) Comparison of inlet/ outlet air absolute humidity and change of the sorption amount during desorption process; (b) comparison of inlet/outlet air temperature and temperature of the WSS + 22.4 wt% $CaCl_2$ in heat desorption process (hot air flow rate: 3.8 m^3/h; regeneration temperature: 80°C)

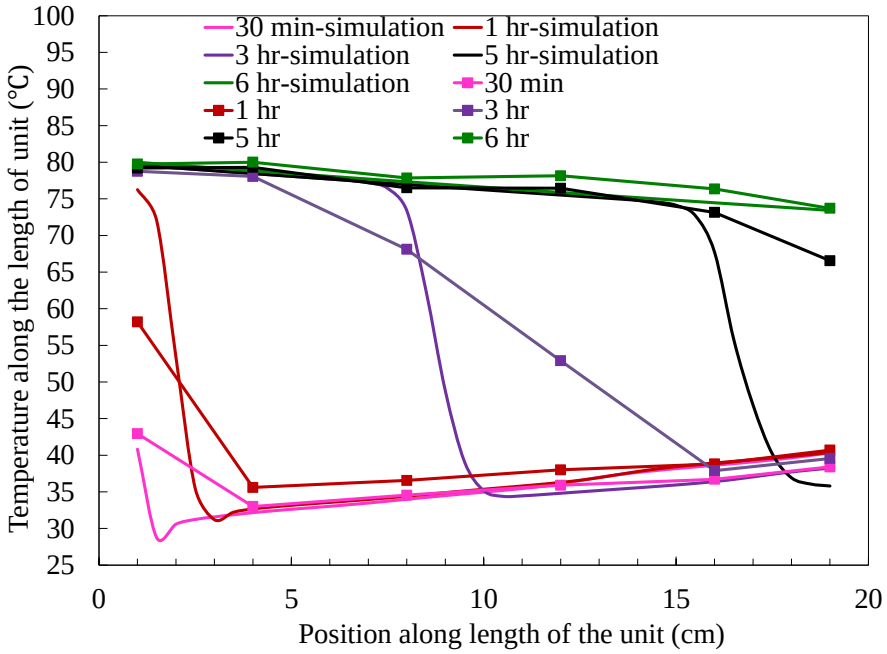

Fig. 3-6 Temperature profile of the WSS + 22.4 wt% $CaCl_2$ in heat storage process (hot air flow rate: 3.8 m^3/h; regeneration temperature: 80°C)

The simulated outlet air absolute humidity result shows that more water vapor is sorbed in the simulation than in the experiment, which indicates that more heat was released in the simulation, causing higher outlet air temperatures. This discrepancy is likely due to two major sources. First, the uneven velocity distribution over the cross section of the inlet has an impact on the water vapor sorption amount during the experiment. We measured the temperature and relative humidity at the center of the cross section of the inlet and outlet of the heat storage unit. The highest sorption behavior (high relative humidity can produce a high sorption amount according to Fig. 3-2 (b)) was calculated according to the measured inlet air relative humidity. Second, according to Fig. 3-5 (b), the measured final temperature (< 80°C) of the latter part of the heat storage unit affects the equilibrium sorption amount in the desorption process. In the simulation, the initial sorption amount in the sorption process is defined as the sorption amount under the local air's relative humidity, which is higher than the actual value for the latter part of the heat storage unit.

Comparison of the regeneration process results are illustrated in Fig. 3-5 (a), (b) and Fig. 3-6. The calculated material's temperature, as well as the outlet air temperature and absolute humidity, approximately fit the measured values during the beginning of the

desorption process. However, the calculated material's temperature, outlet air temperature, and outlet absolute humidity lag behind the measured values as the desorption process progresses. This discrepancy is mainly caused by (a) the higher calculated sorption amount in the sorption process and (b) the difference in the change of sorption amount between the sorption process (cf. Fig. 3-3 (a)) and the desorption process (cf. Fig. 3-5 (a)) in the experiment. The uneven distribution of velocity over the cross section of the heat storage unit also contributes to this difference. For the sorption process, the velocity of the humid air is lower than that of the hot air in the desorption process. Therefore, the uneven distribution in the relative humidity of the inlet air is more pronounced in the sorption process than in the desorption process.

Regeneration/sorption processes were simulated 20 times using a humid air flow rate of 2.0 m^3/h, an air temperature of 25°C, a hot air flow rate of 2.8 m^3/h, and a regeneration temperature of 80°C by inputting the initial conditions repeatedly according to the experimental measurements. The comparison of the simulated outlet air temperature and the experimental results is illustrated in Fig. 3-7 (a) and (b). The simulated outlet air temperature differs only slightly from the measured values in the sorption process in contrast to the larger discrepancy observed for the desorption process. The likely reasons for the discrepancy observed in the desorption process have been explained above. The results of the repeated simulations allow us to ensure that this program can provide a stable performance over many operation times.

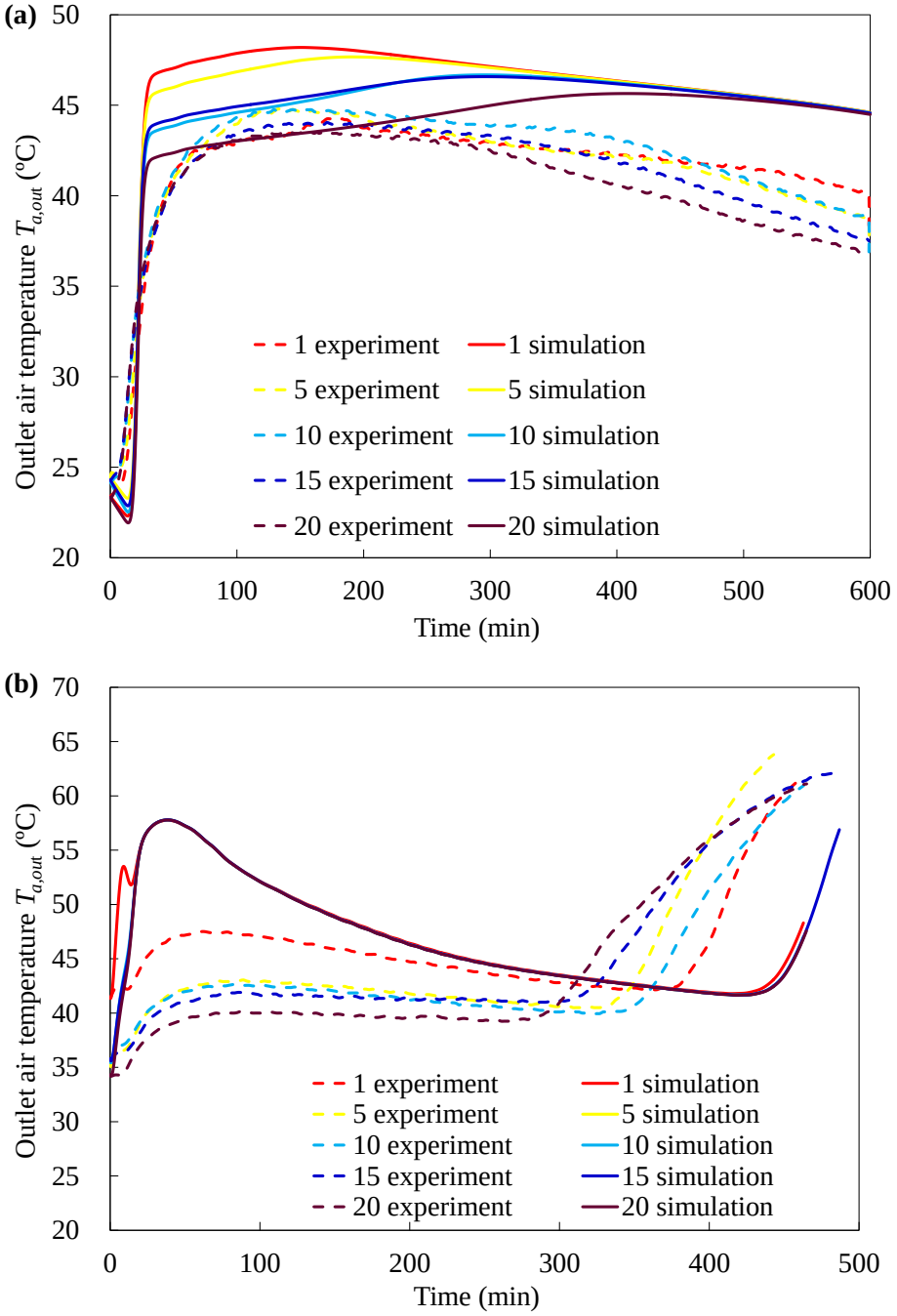

Fig. 3-7 (a) Comparison of the outlet air temperature during the heat release process; (b) comparison of the outlet temperature during the regeneration process of the WSS + 22.4 wt% $CaCl_2$ (humid air flow rate: 2.0 m^3/h; hot air flow rate: 2.8 m^3/h; regeneration temperature: 80°C)

3.3 DEFINITIONS OF PERFORMANCE EVALUATION INDICES

Numerical tests of the WSS + 22.4 wt% $CaCl_2$ under various thermal energy storage conditions were performed to test the effect of each key parameter, determine the best practical operating conditions, and evaluate the performance of the open sorption thermal energy storage system.

To evaluate the performance of the thermal energy storage system, we used multiple performance indices. The volumetric heat storage density Q_V (available heat output in the sorption proScess per m^3), the actual total heat output Q_{sor}, the maximum potential stored heat Q_{max}, and the coefficient and effective coefficient of heat extraction performance ε and ε_{eff} in the heat release process were defined as follows:

$$Q_V = C_{p,a}\rho_a f / V \int_{\Delta t}(T_{a,out} - T_{a,in})dt \qquad 3\text{-}23$$

In the above equation, during the time interval Δt, the temperature difference of outlet air and inlet air ΔT is no lower than 15ºC.

$$Q_{sor} = (\Delta\omega)(\Delta H)m_{s,dry} \qquad 3\text{-}24$$

$$Q_{\max} = (\Delta\omega)_{\max}(\Delta H)m_{s,dry} \qquad 3\text{-}25$$

$$\varepsilon = (Q_V V)/Q_{\max} \qquad 3\text{-}26$$

$$\varepsilon_{eff} = (Q_V V)/Q_{sor} \qquad 3\text{-}27$$

The heat recovery rate η of this thermal energy storage system must also be evaluated by incorporating the performance of the regeneration process, which is important when the exhaust heat or renewable energy is limited. The total heat consumed to regenerate the composite material can be calculated from the difference in the inlet and outlet air temperature:

$$Q_{desor} = C_{p,a}\rho_a f \int_0^t (T_{a,in} - T_{a,out})dt \qquad 3\text{-}28$$

η is evaluated as the ratio of the heat released in the sorption process and the heat stored in the desorption process:

$$\eta = Q_{sor} / Q_{desor} \tag{3-29}$$

The effective heat recovery rate η_{eff} is related to the ratio between the effective heat absorbed by the flowing air in the sorption process and the total heat input in the desorption process.

$$\eta_{\text{eff}} = (Q_V V) / Q_{desor} \tag{3-30}$$

3.4 RESULTS AND DISCUSSION

Because we examined the influence of the filling amount of $CaCl_2$ during the sorption process in our previous work, we focused on the other important parameters in the present study. The input parameters for each section are listed in Table 3-2.

Table 3-2 Calculation conditions

Key parameters	Inlet air temperature (°C)	Inlet air relative humidity (%)	Humid air flow rate (m^3/h)	Length of filter (cm)
Section 3.4.1	15 20 25 30	95	3.0	20
Section 3.4.2	25	65 75 85 95	3.0	20
Section 3.4.3	25	95	3.0 4.0 5.0 6.0	20
Section 3.4.4	25	95	3.0	10 15 20 25

3.4.1 Influence of the inlet air temperature

The dynamic variations of the relative humidity and temperature of the outlet air and the temperature difference between the inlet and outlet air are shown in Fig. 3-8. Here, the material's initial temperature is the same as the given inlet air temperature in the sorption process. The relative humidity of the inlet air was kept at 95% for all four inlet

air temperatures. Because the composite material was very dry at the initiation of the sorption process, the outlet air was dehumidified in this process. Fig. 8 also illustrates that the outlet air's relative humidity rises when the inlet air temperature is high. This process is thought to occur because high temperature causes high water vapor content (high absolute humidity) in the flowing air. The system cannot discharge heated air with a high outlet and inlet temperature difference for long when the inlet air temperature is high during the heat discharging process.

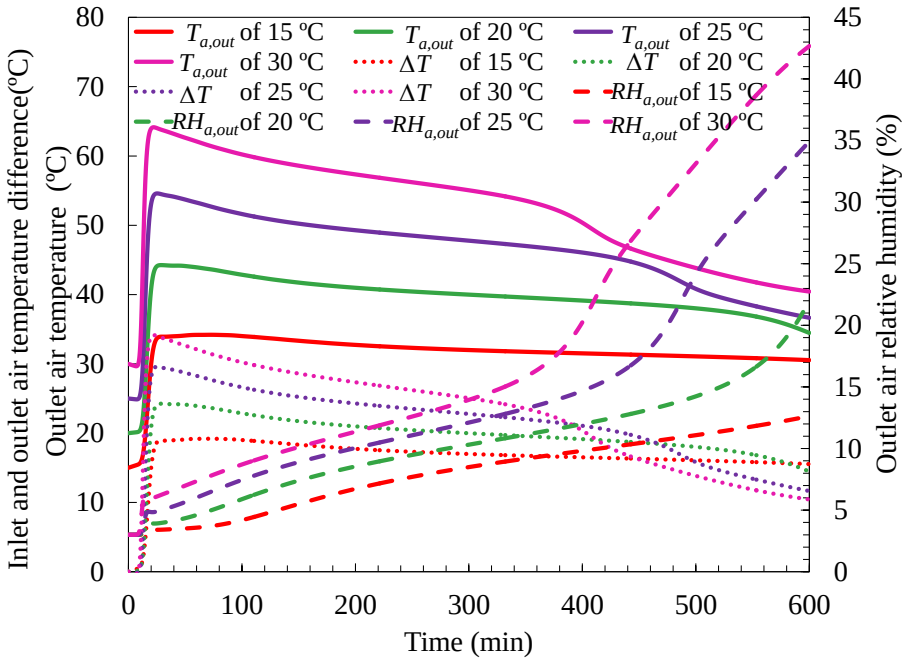

Fig. 3-8 Outlet air relative humidity, outlet air temperature and outlet and inlet air temperature difference change with time of different inlet air temperatures

3.4.2 Effect of the inlet air relative humidity

As shown in Fig. 3-9, the duration of the discharge of high-temperature outlet air is prolonged when the relative humidity increases. Indeed, the equilibrium sorption amount also increases with higher relative humidity according to the isothermal equilibrium sorption amount line shown in Fig. 3-2 (b). It is notable that the water vapor content of the inlet air has an important impact on the outlet air temperature during the heat release process due to the high sorption amount at high relative

humidity. The relative humidity of the inlet air is an important parameter for the optimal performance of the thermal energy storage unit.

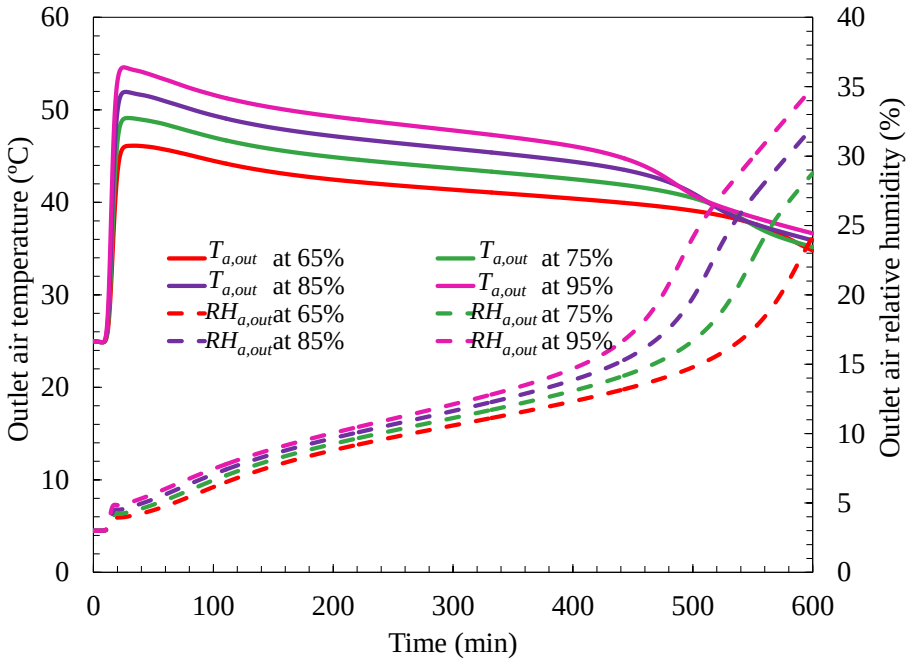

Fig. 3-9 Outlet air relative humidity and outlet air temperature change with time of different inlet air relative humidies

3.4.3 Influence of the humid air flow rate

Fig. 3-10 shows that the outlet air's relative humidity increases with the humid air's flow rate, an effect caused by the relationship between the sorption rate and the supplied mass flow of water vapor. The discharge duration of the high-temperature outlet air decreases when the air flow rate is high, as more heat is released per time with a faster flow. Additionally, the rate of outlet air temperature increase grows greater with increasing air flow rate. The same phenomenon was found in our previous experiment [2], and we believe this effect is due to thinning of the air film near each channel's surface, which causes the water vapor diffusion rate to increase due to lower gas film resistance. More water vapor could thus diffuse to the composite material and be sorbed while simultaneously generating more heat.

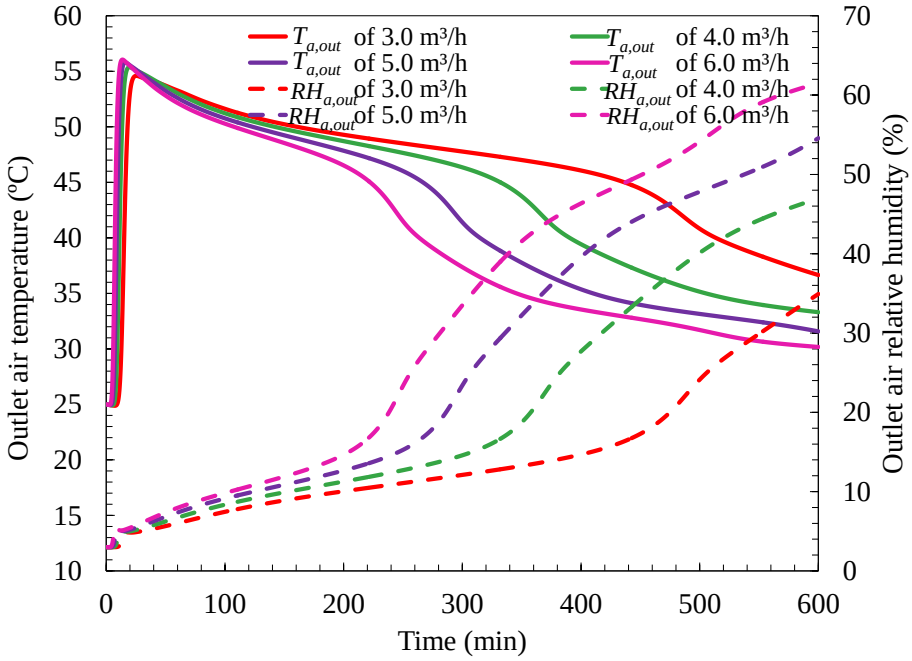

Fig. 3-10 Outlet air relative humidity and outlet air temperature change with time of different humid air flow rates

3.4.4 Influence of the length of the thermal energy storage unit

The performance of the WSS + 22.4 wt% $CaCl_2$ with a length of 10 cm is compared with the experimental results illustrated in Fig. 3-11 (a) and (b). The simulated outlet air absolute humidity and the temperature of the material approximately fit the measured values, indicating that our simulation can be applied to predict the behavior of thermal energy storage units with different lengths. The results for various lengths are shown in Fig. 3-11. Increasing the length of the heat storage unit increases the contact time between the flowing air and each channel. A longer one thus leads to a longer-duration discharge of high-temperature outlet air. However, the maximum outlet temperature of the longer one is not significantly higher than that of the shorter one.

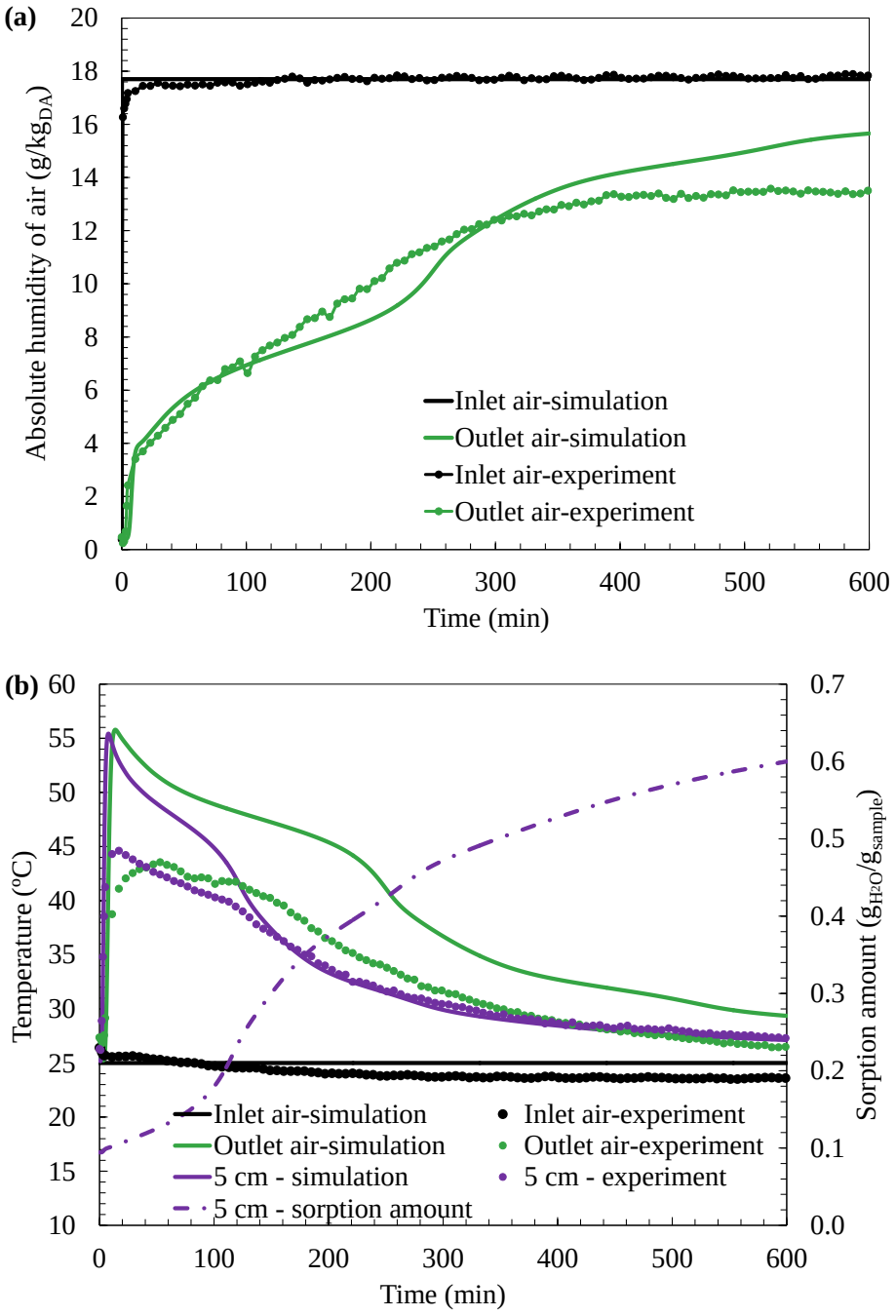

Fig. 3-11 (a) Comparison of inlet and outlet air absolute humidity; (b) comparison of inlet/outlet air temperature and temperature of the WSS + 22.4 wt% $CaCl_2$ with a length of 10 cm in heat release process (humid air flow rate: 3.0 m^3/h; regeneration temperature: 80°C)

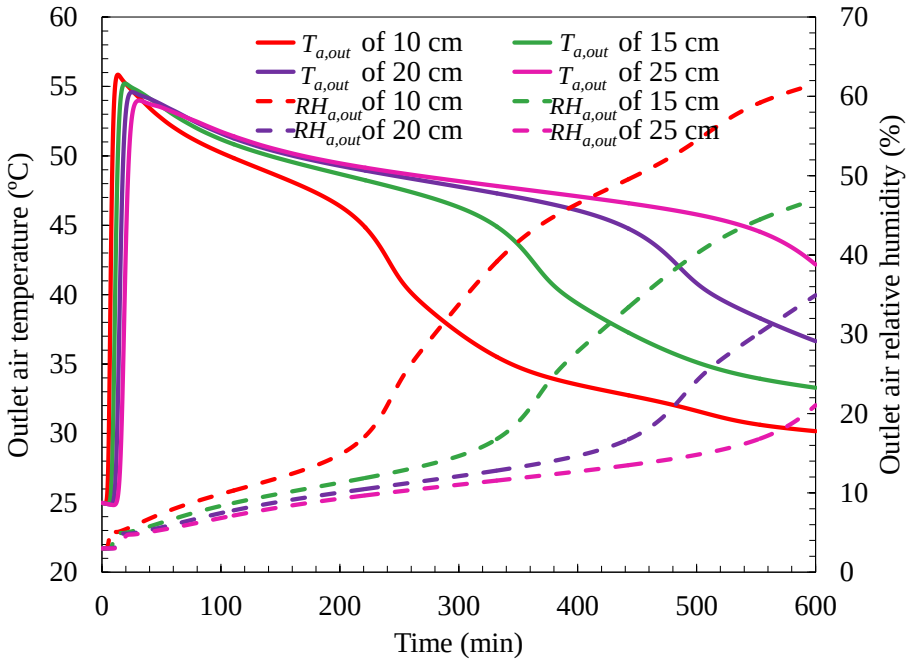

Fig. 3-12 Outlet air relative humidity and outlet air temperature change with time of different length of the thermal energy storage units

3.4.5 Comprehensive evaluation of the mass flow of water vapor in the humid air

Inlet air temperature, relative humidity, and flow rate all influence the same parameter, mass flow of water vapor X_a, defined by the equation $X_a = \rho_a f x_{a,in}$. The effect of the mass flow of water vapor can be seen in Fig. 3-13 (a) and (b). When more water vapor is supplied, more water vapor can be sorbed, releasing more heat (cf. Fig. 3-13 (a)). Moreover, with higher amounts of supplied water vapor, the effective heat that can be utilized per unit volume will be higher. For a given humid air flow rate, the higher the mass flow of water vapor, the better the performance, with heat released and volumetric heat storage density both increasing with the mass flow of water vapor.

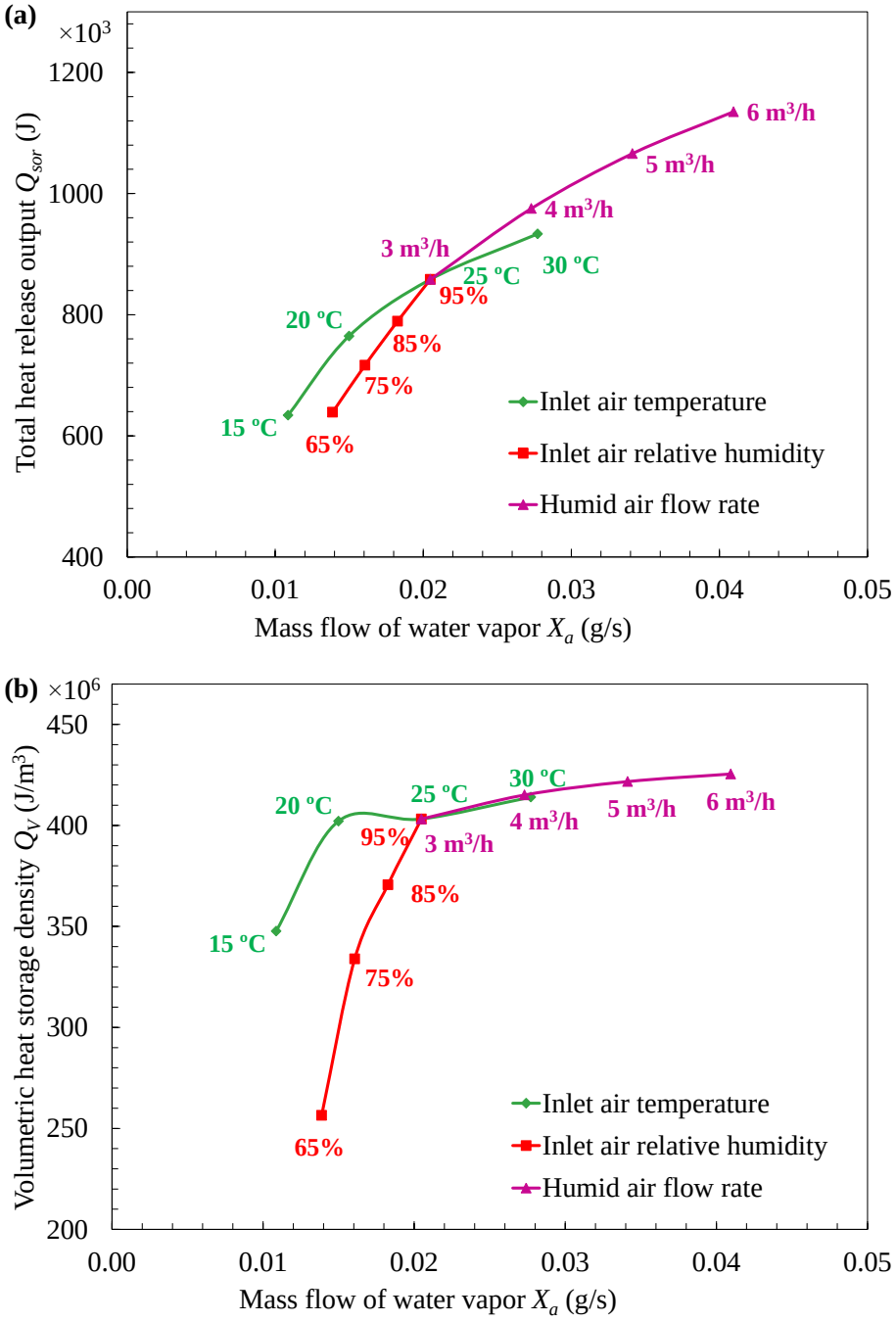

Fig. 3-13 (a) Effect of absolute water vapor content on total heat release amount; (b) effect of absolute water vapor content on volumetric heat storage density

3.4.6 Evaluation of each key parameter of the thermal energy storage system

The effects of each parameter have been evaluated by calculating the effective coefficient of heat extraction ε_{eff} and the volumetric heat storage density Q_V (shown in

Fig. 3-14 (a), (b), and (c)), the total heat release amount Q_{sor} and the coefficient of heat extraction ε (shown in Fig. 3-15 (a) and (b)), and η and η_{eff} (shown in Fig. 3-16 (a) and (b)). In the simulation, the hot air's temperature is 80°C, with a flow rate of 3.8 m^3/h during the regeneration process. When calculating all the evaluation indices, the simulation time of the sorption process was kept constant at ten hours, but for some cases, the simulation was repeated with a different operating time to further explore certain phenomena.

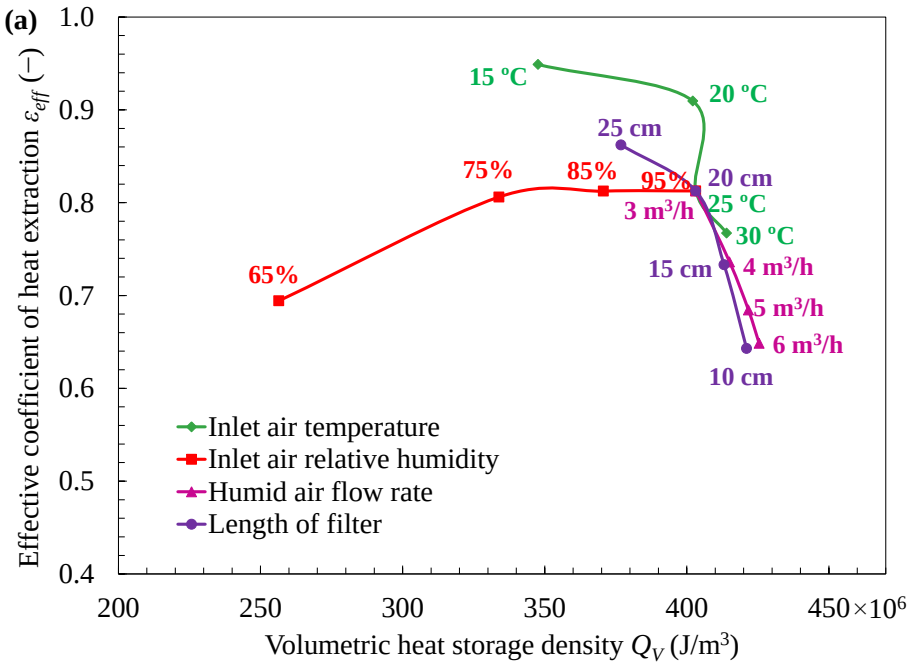

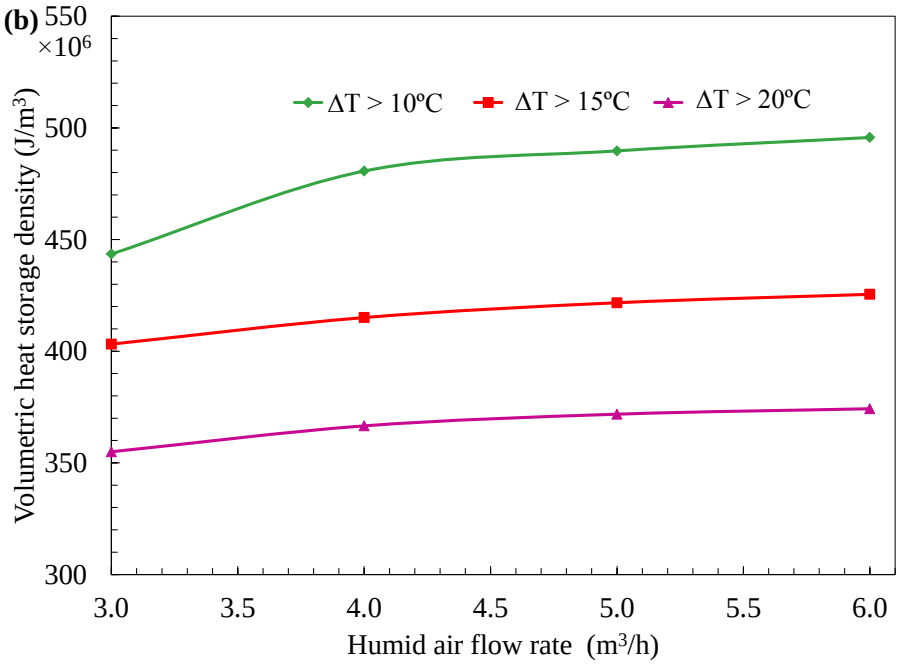

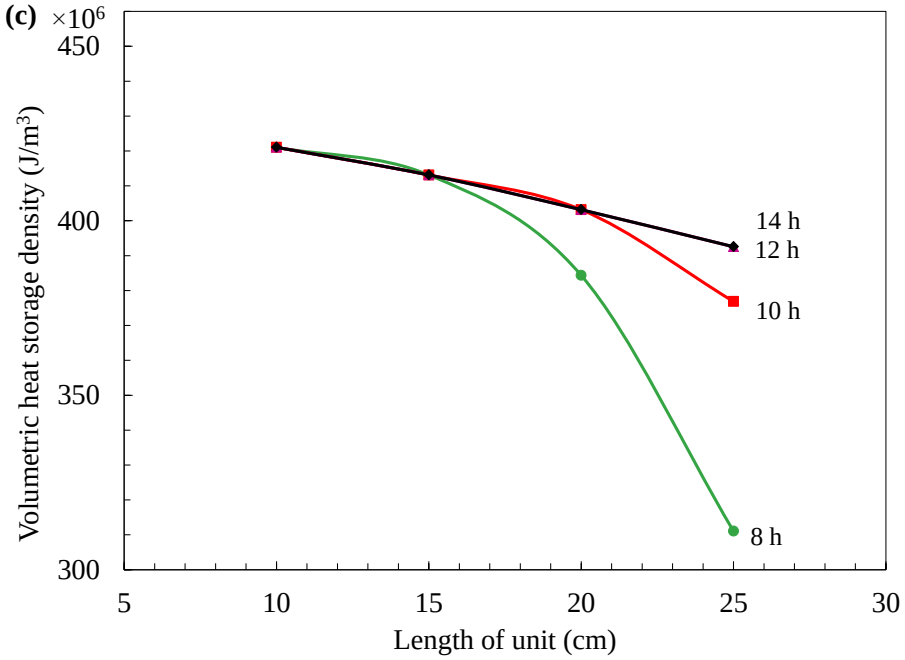

Fig. 3-14 (a) Effect of each parameter on volumetric heat storage density and effective coefficient of heat extraction during heat release process; (b) effect of inlet and outlet air temperature difference on volumetric heat storage density; (c) effect of heat release duration on volumetric heat storage density

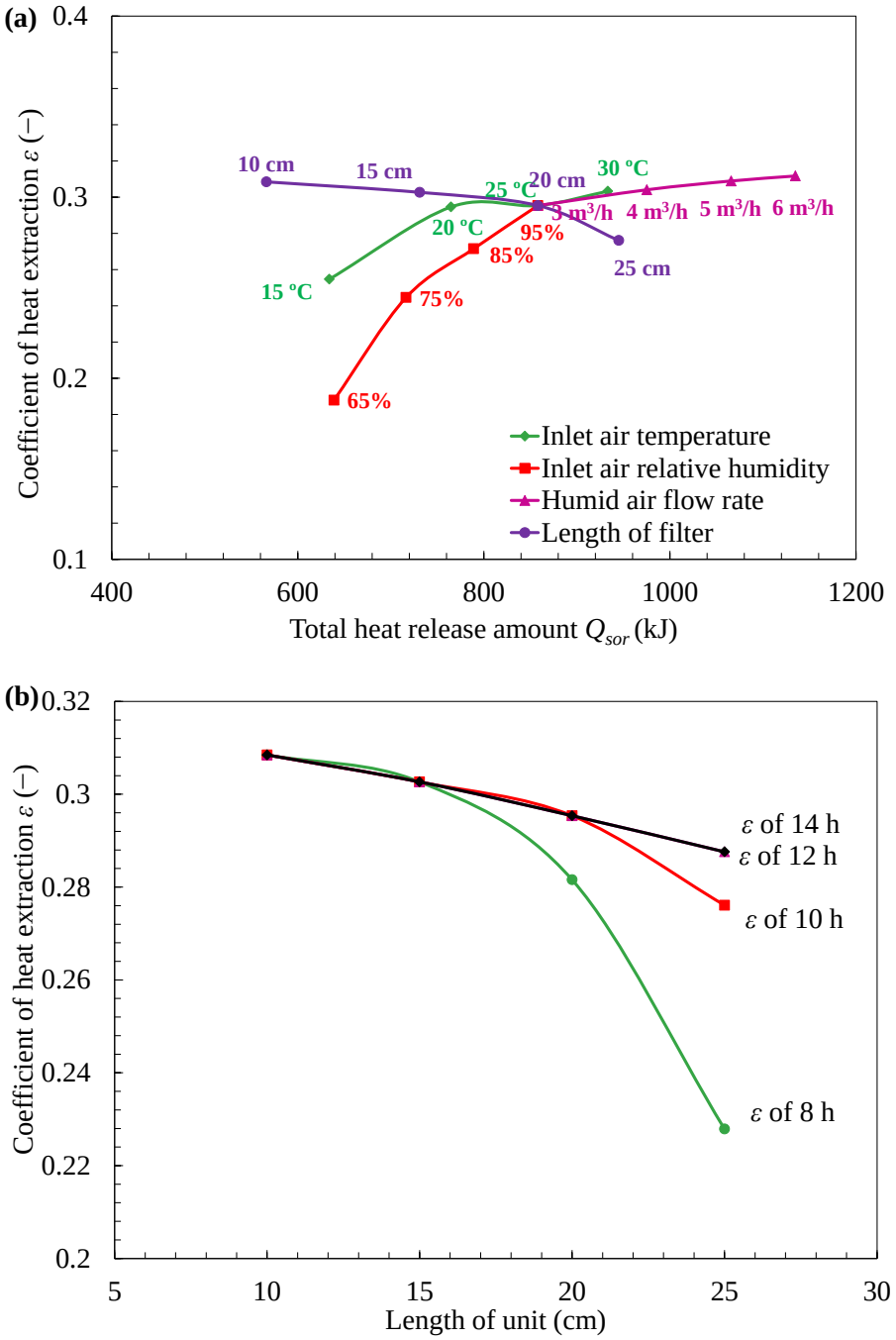

Fig. 3-15 (a) Effect of each parameter on total heat release amount and coefficient of heat extraction during heat release process; (b) effect of heat release duration on coefficient of heat extraction

Fig. 3-14 (a) demonstrates that because of the high mass flow of water vapor in the air, high inlet air relative humidity, and high inlet air temperature, our system could exhibit a high volumetric heat storage density. For different operating requirements for air temperature, the humid air flow rate shows an important effect on the volumetric heat

storage density. If the required temperature is lower than 35°C, the lowest volumetric heat storage density occurs when the flow rate is 3.0 m^3/h, as shown in Fig. 3-14 (b). However, under other requirements, the flow rate does not affect the volumetric heat storage density.

Within ten hours, the shortest thermal energy storage unit shows the highest volumetric heat storage density; however, for a different desired operating time, another length may be better (cf. Fig. 3-14 (c)). A longer honeycomb thermal energy storage unit can supply almost the same amount of effective heat per volume.

The effective coefficient of heat extraction increases when the inlet air relative humidity or the length of the heat storage unit rises or when the humid air flow rate decreases. When the relative humidity is maximized, the humid air flow rate is 3 m^3/h and the inlet air temperature is kept at 20 to 30ºC, the system achieves a high volumetric heat storage density, as well as a high ε_{eff}, as illustrated in Fig. 3-14 (a).

When high mass flow of water vapor is supplied (cf. Fig. 3-13 (a)), the resulting inlet air relative humidity, inlet air temperature, and speed of the humid air can produce a high total heat release amount. According to Fig. 3-15 (a), if the heat release time is within ten hours, the heat storage unit's length is shorter than 25 cm and shows almost the same coefficient of heat extraction. However, if hot air is needed for duration longer than ten hours, a longer one provides a better performance compared to cases where hot air is provided for a shorter time due to its higher sorption ability, as illustrated in Fig. 3-15(b).

When the exhaust heat or renewable heat to be stored is limited, the heat recovery rate η and effective heat recovery rate η_{eff} must be considered to evaluate the whole cycle's performance. Fig. 3-16 indicates that, due to the effect of the mass flow of water vapor, high inlet air temperature, high relative humidity, and a large air low rate produce a high heat recovery rate, while a shorter one can achieve a high η due to the high sorption amount of the whole thermal energy storage unit. However, a longer one can provide a better η_{eff} for a release duration of ten hours due to its high ε_{eff}.

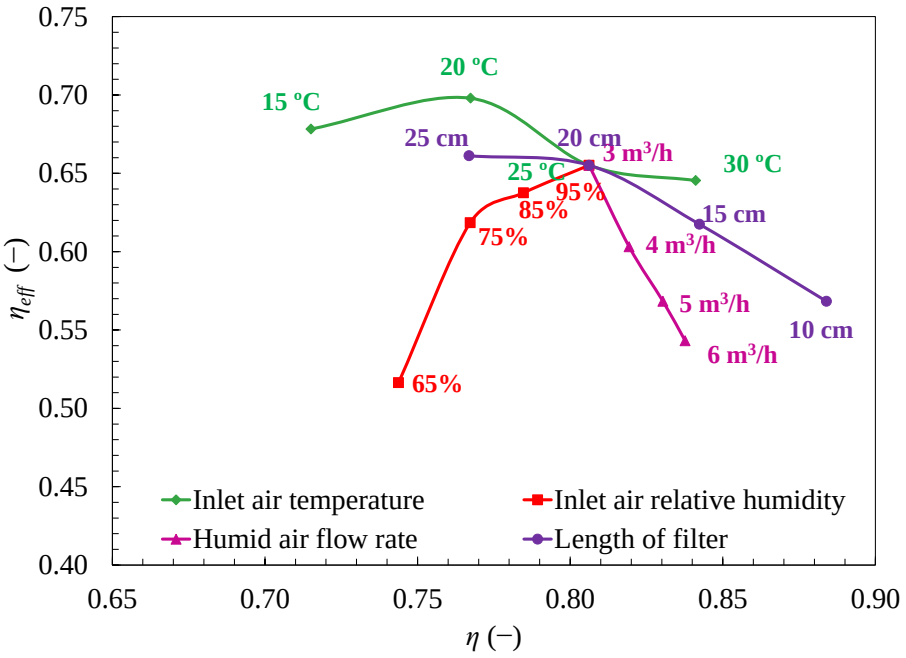

Fig. 3-16 Effect of each parameter on η and η_{eff} of the open sorption thermal energy storage system

Based on the above analysis, the optimal operating conditions for ten hours of heat release are as follows: $T_{a,in}$ = 25°C or 30°C, $RH_{a,in}$ = 95%, f_a = 3.0 m^3/h, L = 20 cm or 25 cm to get a high volumetric heat storage density Q_V, a high effective coefficient of heat extraction ε_{eff} and a high effective heat recovery rate η_{eff}. If a longer-duration heat release is required, a longer thermal energy storage unit is necessary.

3.4.7 Simulation of an application of the open thermal heat storage system

In this section, the thermal energy storage system is applied to a paint-drying system. When thick coats of paint are needed for large pumps, the hot ventilated air required for paint drying is usually supplied by a kerosene-fueled blower during the daytime. Ventilation with natural outdoor air is generally used during the nighttime (cf. Fig. 3-17 (a)). Speeding up the drying process while minimizing the cost is an important challenge. One solution is to run the kerosene-fueled blowers in the nighttime as well as during the day, but doing so requires watchmen and is thus costly. Therefore, we propose the incorporation of our open sorption thermal energy storage unit into this

system. The exhaust heat from the kerosene-fueled blowers employed during the daytime can be stored using the thermal energy storage unit. The stored heat can be utilized to heat up ventilated air, which can be employed in the drying booth during the nighttime as shown in Fig. 3-17 (b). Another advantage of this system is the low relative humidity of the supply air from the thermal energy storage unit. Our system can simultaneously shorten the drying process and save energy.

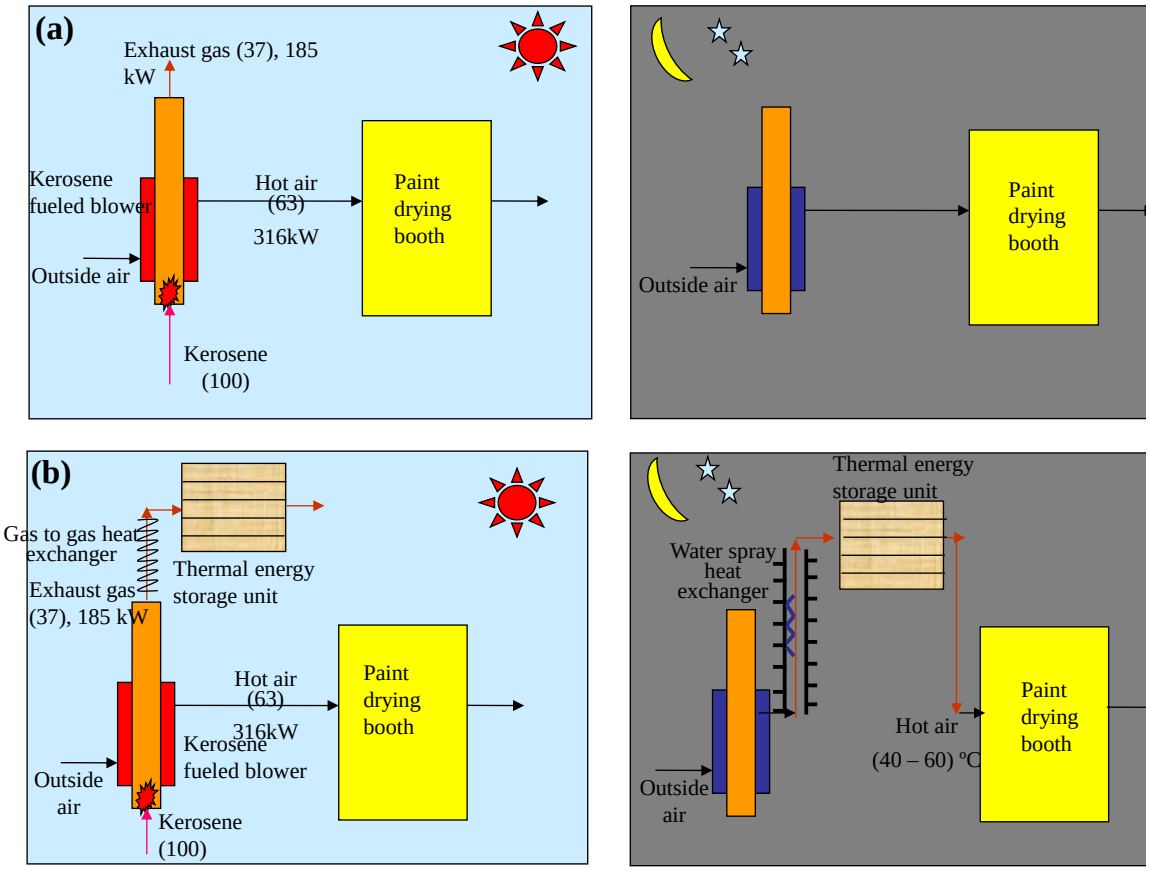

Fig. 3-17 (a) Previous paint drying system; (b) improved system incorporated with the developed sorption thermal energy storage unit

In our proposed application, the hot air needed for regenerating the composite material is supplied by the heated exhaust from the blower. The operating conditions of the thermal energy storage system are shown in Table 3-3. During the daytime, the kerosene fuel blower with efficiency of 63% is used to dry the paint drying booth. While an air to gas heat exchanger is assumed to exchange heat with the exhaust gas from the kerosene boiler to regenerate the thermal energy storage unit. For the nighttime operation, a spray heat exchanger with fins outside is assumed to be used to

increase the relative humidity of the flowing air, which is necessary for the thermal energy storage unit to supply high temperature air in the nighttime. In fact, the spray heat exchanger is a humidifier with high heat exchanger rate to increase the inlet air temperature by absorbing heat from the indoor air at the same time.

Table 3-3 Application condition for designing the thermal energy storage unit

	Parameters	Value
Kerosene boiler	Heat output	500 kW
	Combustion gas temperature	200°C
	Operation time duration	8:00-18:00
Kerosene fuel blower	Efficiency	63%
	Exchanged gas's temperature	>100°C
Gas to gas heat exchanger	Efficiency	80%
	Air's temperature	(80-85)°C

The proposed system was designed to be able to supply hot air in the nighttime for at least 14 hours. Wet air with a relative humidity of 95% was selected because of its effectiveness in all evaluation indices. Because of the natural outdoor air temperature and the indoor air temperature, an inlet humid air temperature of 25°C was selected. A humid air flow rate of 3.0 m^3/h was chosen to ensure a sufficient duration of hot air release, as illustrated in Fig. 3-10, and high ε_{eff} and η_{eff}, as shown in Fig. 3-14 (a) and Fig. 3-16, respectively. According to Fig. 3-14 (c), when the air flow rate is 3 m^3/h, the 25 cm thermal energy storage unit achieves the same available heat for operating times of 12 hours and 14 hours, indicating that the maximum available heat can be reached within 12 hours for this thermal energy storage unit length. For the proposed application, a longer one of at least 33 cm was used to supply air at temperatures greater than 40°C for 14 hours.

For the heat storage process, hot air from the gas-to-gas heat exchanger flows through the heat storage unit for ten hours to regenerate it. The flow rate of the hot air through each thermal energy storage unit was set to at least 3.8 m^3/h in order to be regenerated completely within ten hours. If the simulated results fulfilled the requirements of the

drying system, the size of the heat storage unit was then decided according to the exhaust heat supply side and the performance of the storage unit.

Fig. 3-18 shows the outlet air temperature and relative humidity trends during the sorption and desorption processes. According to our simulation, the hot air (temperature greater than 40°C) generated by the thermal energy storage unit can dry the painting booth for 14 hours with low relative humidity in nighttime. The exhaust heat produced during the daytime operation of the blowers can also regenerate the heat storage unit successfully.

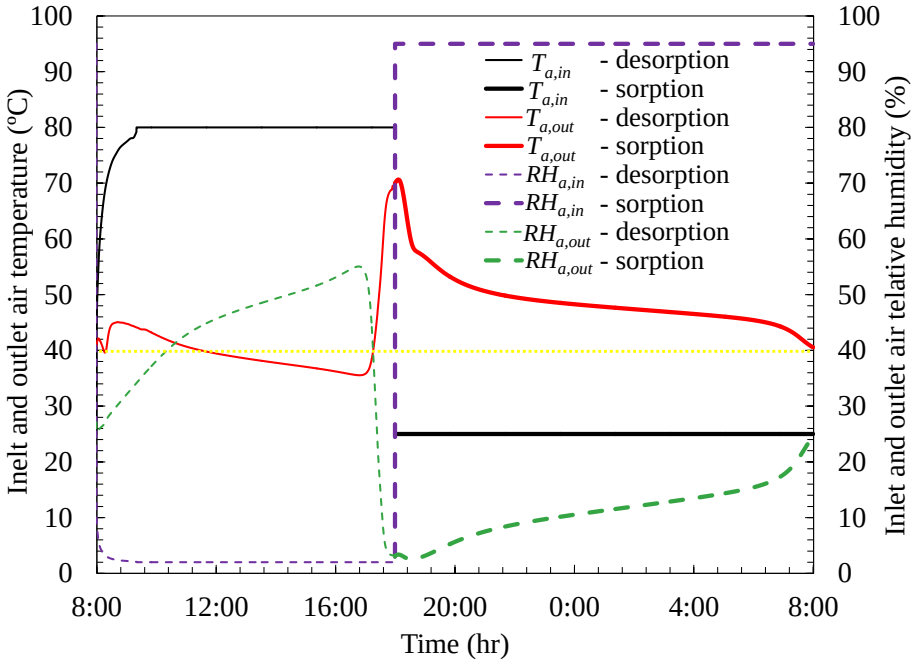

Fig. 3-18 Simulated outlet air relative humidity and outlet air temperature during the sorption and desorption processes, respectively

The volumetric heat transfer rate, a key parameter defined in Eq. 3-31, effectively determines the size of the thermal energy storage system, as is shown in Fig. 3-19.

$$W_V = C_{p,a}\rho_a f \left|T_{a,out} - T_{a,in}\right| / V \qquad 3\text{-}31$$

From the value of the desorption volumetric heat transfer rate and the exhaust heat amount, the necessary volume of the thermal energy storage unit was determined to be 7.0 m^3, which means that at least 2300 thermal energy storage unit with dimensions: 10 cm (width) ×10 cm (height) ×33 cm (length) are necessary.

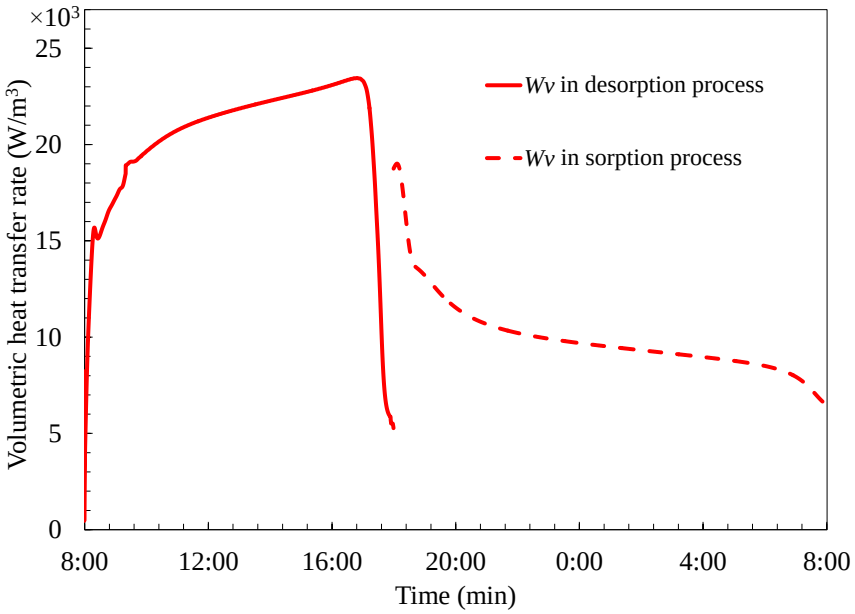

Fig. 3-19 Volumetric heat transfer rate of the open thermal energy storage unit

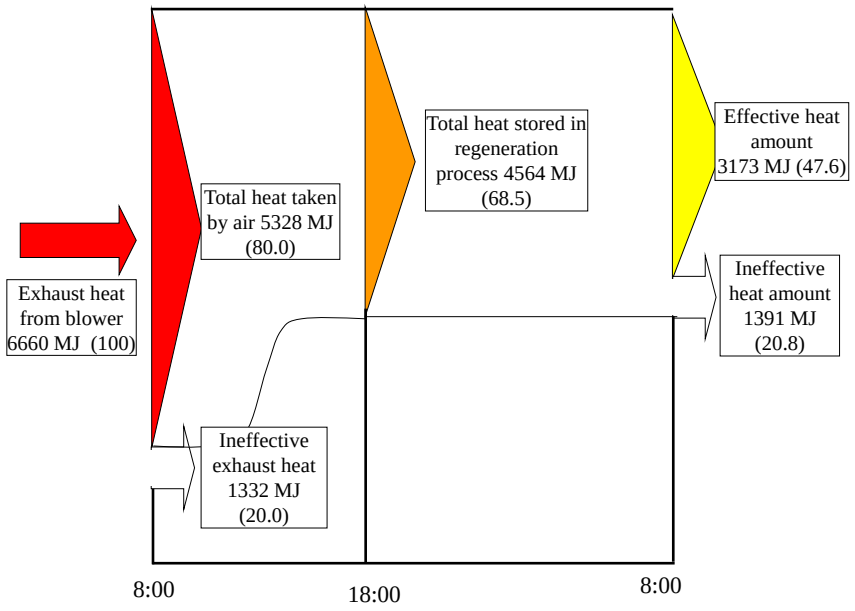

Fig. 3-20 Energy flow chart of the improved paint drying system incorporated with the open thermal energy storage unit

The energy flow chart for this application shown in Fig. 3-20 was studied to investigate the efficiency of the thermal energy storage system in the drying process. The total exhaust heat generated by the blower is 6660 MJ within its operation time, and a fraction of this heat (4564 MJ) must be utilized to regenerate the thermal energy

storage unit in the daytime. The effective heat needed to dry the paint-film is approximately 3173 MJ at nighttime, which is approximately 48% of the total exhaust heat. Thus, the thermal energy storage unit can recover half of the exhaust heat and improve the dryness quality (keeping proper temperature and low relative humidity of supplied air) of the paint-film.

3.5 SUMMARY

A numerical simulation model was created to investigate the capability of a composite mesoporous thermal energy storage unit to store thermochemical energy. This program, based on the effect of coupled heat and mass transfer, effectively simulates our open sorption thermal energy storage system. From the numerical results, we obtained the following conclusions:

1. The simulation results can approximately predict the experimental values. The discrepancies observed between simulation and experiment in the desorption process have been explained above.

2. Using our simulation program, we analyzed the effects of the inlet air temperature and relative humidity, humid air flow rate, and thermal energy storage unit length on the system's performance. Optimal operating conditions were thus selected as follows: $T_{a,in}$ = 25°C or 30°C, $RH_{a,in}$ = 95%, f_a = 3.0 m^3/h, L = 20 or 25 cm for a heat release duration of ten hours.

3. A realistic application was proposed and simulated. Based on the simulation results, the thermal energy storage unit can supply air with a temperature greater than 40°C for 14 hours, and the unit can be regenerated within ten hours during the daytime. Finally, 47.6% of the exhaust heat generated by a kerosene-fueled blower can be recovered using the thermal energy storage unit, and the dryness quality level of the paint-film can be improved.

3.6 REFERENCE

[1] I. Dincer, Thermal energy storage systems as a key technology in energy conservation, International Journal of Energy Research, 26 (2002) 567-588.

[2] H. Liu, K. Nagano, D. Sugiyama, J. Togawa, M. Nakamura, Honeycomb filters made from mesoporous composite material for an open sorption thermal energy storage system to store low-temperature industrial waste heat, International Journal of Heat and Mass Transfer, 65 (2013) 471-480.

[3] G. Balasubramanian, M. Ghommem, M.R. Hajj, W.P. Wong, J.A. Tomlin, I.K. Puri, Modeling of thermochemical energy storage by salt hydrates, International Journal of Heat and Mass Transfer, 53 (2010) 5700-5706.

[4] D. Zhu, H. Wu, S. Wang, Experimental study on composite silica gel supported $CaCl_2$ sorbent for low grade heat storage, International Journal of Thermal Sciences, 45 (2006) 804-813.

[5] H. Wu, S. Wang, D. Zhu, Effects of impregnating variables on dynamic sorption characteristics and storage properties of composite sorbent for solar heat storage, Solar Energy, (2007) 864-871.

[6] H. Wu, S. Wang, D. Zhu, Y. Ding, Numerical analysis and evaluation of an open-type thermal storage system using composite sorbents, International Journal of Heat and Mass Transfer, 52 (2009) 5262-5265.

[7] N.M. Ostrovskii, N.A. Chumakova, N.M. Bukhavtsova, N.V. Vernikovskaya, Y.I. Aristov, Effect of capillary condensation on water sorption by composite calcium chloride in a porous matrix sorbents, Theoretical Foundations of Chemical Engineering, 41(2) (2007) 200-204.

[8] N.M. Ostrovskii, N.A. Chumakova, N.M. Bukhavtsova, N.V. Vernikovskaya, Y.I. Aristov., Modeling of the limiting step of Water Sorption by Composite Sorbents of the "Calcium Chloride in Porous Matrix" Type, Theoretical Foundations of Chemical Engineering, 41(1) (2007) 83-90.

[9] J.L. Niu, L.Z. Zhang, Effects of wall thickness on the heat and moisture transfers in desiccant wheels for air dehumidification and enthalpy recovery, International Communications in Heat and Mass Transfer, 29(2) (2002) 255-268.

[10] D. Charoensuphya, W.M. Worek, Parametric study of an open-cycle adiabatic, solid, desiccant cooling system, Energy, 13(9) (1988) 739-747.

[11] W. Zheng, W.M. Worek, Numerical simulation of combined heat and mass transfer processes in a rotary dehumifier, Numerical Heat Transfer, Part A: Applications, 23(2) (1993) 211-232.

[12] W. Zheng, W.M. Worek, D. Novosel, Performance optimization of rotary dehumidifiers, Journal of Solar Energy Engineering, 117 (1995) 40-44.

[13] X.J. Zhang, Y.J. Dai, R.Z. Wang, A simulation study of heat and mass transfer in a honeycombed rotary desiccant dehumidifer, Applied Thermal Engineering, 23 (2003) 989-1003.

[14] P. Majumdar, Heat an mass transfer in composite desiccant pore structure for dehumidification, Solar Energy, 97(1) (1998) 1-10.

[15] T.S. Ge, F. Ziegler, R.Z. Wang, A mathematical model for predicting the performance of a compound desiccant wheel (A model ofcompound desiccant model), Applied Thermal Engineering, 30 (2010) 1005-1015.

[16] Z. Gao, V.C. Mei, J.J. Tomlinson, Theoretical analysis of dehumidification process in a desiccant wheel, Heat Mass Transfer, 41 (2005) 1033-1042.

[17] L.Z. Zhang, J.L. Niu, Performance comparisons of desiccant wheels for air dehumidification and enthalpy recovery, Applied Thermal Engineering, 22 (2002) 1347-1367.

[18] S. Yamaguchi, K. Saito, Numerical and experimental performance analysis of rotary desiccant wheels, International Journal of Heat and Mass Transfer, 60 (2013) 51-60.

[19] A.G. Fedorov, R. Viskanta, Analysis of transient heat/mass transfer and adsorption/desorption internations, International Journal of Heat and Mass Transfer, 42 (1999) 803-819.

[20] M. Suzuki, Adsorption engineering, Kodansya Ltd., Tokyo and Elsevier Science Publishers B. V., Amsterdam, Japan, 1990.

[21] C.Q. Zhai, Performance modeling of desiccant wheel design and operation, Carnegie Mellon University, Carnegie mellon University, 2008.

[22] H.H. Xing, Desiccant Dehumidification Analysis, Master Thesis, Massachusetts Institute of Technology, Massachusetts Institute of Technology, 2000.

[23] Y.A. Cengel, Heat Transfer: A Practical Approach, second ed., McGraw-Hill, 2003.

[24] J. Karger, D. M.Ruthven, D. N.Theodorou, Diffusion in Nanoporous Materials, 2 Volume Set, 2012.

[25] K.J. Sladek, E.R. Gilliland, R.F. Baddour, Diffusion on surface. 2. Correlation of diffusivities of physically and chemically adsorbed species, Industrial and Engineering Chemistry Fundamentals, 13(2) (1974) 100-105.

[26] Y.I. Aristov, M.M.Tokarev, G.Cacciola, G. Restuccia, Selective water sorbents for multiple applications, 1. $CaCl_2$ confined in mesopores of silica gel: sorption properties, Reaction Kinetics and Catalysis Letters, 59(2) (1996) 325-333.

[27] T. Tsujiguchi, A. Kodama, Optimum operating/design concept for adsorbent desiccant wheel, in: Japan Society of Refregerating and Air Conditioning Engineers, Sapporo, Japan, 2012, pp. 107-118.

[28] A. Sakoda, M. Suzuki, Fundamental study on solar powered adsorption cooling system, Journal of Chemical Engineering of Japan, 17(1) (1984) 52-57.

4 A COMPOSITE MATERIAL MADE FROM MESOPOROUS SILICEOUS SHALE IMPREGNATED WITH LiCl FOR AN OPEN SORPTION THERMAL ENERGY STORAGE SYSTEM

Hokkaido University

4.1 INTRODUCTION

From the viewpoint of sustainable society development, the use of solar energy is highly encouraged because it contributes to the reduction of fossil fuel consumption and greenhouse gases emission. The problem of discontinuity utilization of solar energy must be solved for supplying heat when the solar energy is not possible to be obtained or not enough during rainy days or in night. In recent years, the subject of thermal energy storage has caused intense research interests, as a means of better use of a preferred energy source [1], which has the potential to meet society's need for more efficient, environmentally friendly energy use in a variety of sectors, and it appears to be the only viable solution to overcome the mismatch between the supply and demand of thermal energy [2]. A thermal energy storage system with low heat loss and high heat storage density was suggested to be incorporated into the solar energy utilization system to improve the solar energy utilization efficiency.

Abhat [3] classified the substances used for thermal energy storage into three main types: (1) sensible heat through material's temperature change, (2) latent heat through the phase change of a material, or (3) chemical heat (Sorption and Thermochemical) [4] by thermally inducing changes in a material's chemical or physical structure. Sensible heat storage materials typically require large volumes to store sufficient amount of heat with large thermal losses. Phase change materials (PCMs) rely mostly on reversible solid-liquid phase transformation, such as paraffin and fatty acids [5-7]. They showed stabilities to store thermal energy over a large temperature range with relatively high heat storage density. However, these materials appropriate only for short duration heat storage and are expensive [8].

The chemical thermal energy storage has a higher storage density than the other types of thermal energy storage with low heat loss, which is particularly appropriate for short and long term storage applications. Heat is stored through chemical and physical adsorption in material [9] for a chemical energy storage method. In view of the environmental impact and low-temperature heat sources (< 100ºC), water vapor sorption on solid materials is promising as a kind of thermal energy storage method [10, 11], by which heat is stored by a reversible desorption/sorption process. Silica gel is a common sorption heat pump material, and its potential as a thermal energy material for

storing low-temperature heat was also examined by Tahat [12], Saha et al. [13, 14], etc.. However, the specific heat storage capacity is not so high because of low adsorption amount and low adsorption heat [10], consequently incurring large and heavy thermal energy storage apparatus. Besides adsorption materials, some pure chemical substances are being researched as potential low-temperature energy storage materials. Boer et al. [15] developed a sodium sulfide (Na_2S) cooling system with a copper wire-fin heat exchanger, and showed that the storage capacity of Na_2S in the form of $Na_2S \cdot 5H_2O$ is approximately 3.84 MJ/kg for heat and 2.54 MJ/kg for cooling respectively. However, Na_2S is very corrosive and must be used in a vacuum system to prevent contact with metals. Several potential materials for seasonal storage of solar energy have been tested by Energy research Centre of the Netherlands (ECN) [16-18]. The magnesium sulphate heptahydrate ($MgSO_4 \cdot 7H_2O$) was concluded to be promising for the development of an autonomous thermochemical storage system [17]. However, it cannot release all the stored heat under practical conditions [19, 20]. Indeed, a pure salt can hardly be directly used, because of corrosive properties, strong swelling and expansion when reacting with water, very slow kinetics and hysteresis of the reaction with water [21].

Composite materials have been developed recently as novel thermal energy storage materials by impregnating hygroscopic salt inside the matrix of a porous adsorbent for multiple applications. Aristov et al. [10, 22, 23] presented sorption properties and kinetics of the selective water sorbents (SWSs), and calculated their thermodynamic performance in heat pump and refrigeration systems. Moreover, the composite materials for utilization in adsorption chillers driven by low-temperature heat were also tested [24, 25]. Jänchen et al. [26] tested the storage density of granulated and impregnated mesoporous material in a lab-scaled closed storage system. The developed composite materials exhibit high potential to be used in closed system with lower regeneration temperature compared to their matrices. For the other type of thermochemical energy storage method: open-type thermal energy storage, Zhu and Wu et al. [27-29] developed an open-type thermal energy storage setup with 40 kg composite sorbent pellets (silica gel filled with $CaCl_2$), which showed high thermal energy storage density and can be regenerated at low temperature (<100ºC). Unfortunately, the open systems described above keep the functional fluid flowing through the inter particles of the composite materials, which would cause high pressure

drop. Moreover, a heat exchanger is needed to improve the heat exchange between the air and the composite material [27].

However, for chemical thermal energy storage system, the simultaneous heat and mass transfer enhancement [30] is very important to be done not just from the aspect of heat exchanger, but also from improvement of materials and from the choice of the best system for specific application. In this study, we developed a new composite material by filling lithium chloride (LiCl) into the mesopores of Wakkanai siliceous shale (WSS), which is possible to be used to store heat at about 60°C. Its performance as a sorption thermal energy storage material was evaluated experimentally, and its performance has been compared with the previous composite material impregnated with calcium chloride ($CaCl_2$).

4.2 MATERIAL

Wakkanai siliceous shale (WSS) is a type of siliceous mudstone that is widely distributed in Wakkanai, the north part of Hokkaido in Japan, which is a natural mesoporous material of silicon dioxide (SiO_2) [31]. The picture of WSS mudstone is shown in Fig. 4-1 as well as an electronic microscopic image. The material exhibits a relatively high sorption property with main mesopore diameters of 4 to 20 nm. Before the composite material was made, WSS was sintered in an oven at 800ºC for two hours to ensure the existence of mesopores and a certain degree of strength. The sintered WSS with an addition of binder (clay) was made into a honeycomb ceramic unit (10 cm (width) × 10 cm (length) × 20 cm (height)) to solve the problem of low heat and mass transfer of thermochemical energy storage material. The structure of the honeycomb unit is presented in Fig. 4-2 with 36 cells/cm^2 and each cell's wall thickness is 0.28 mm.

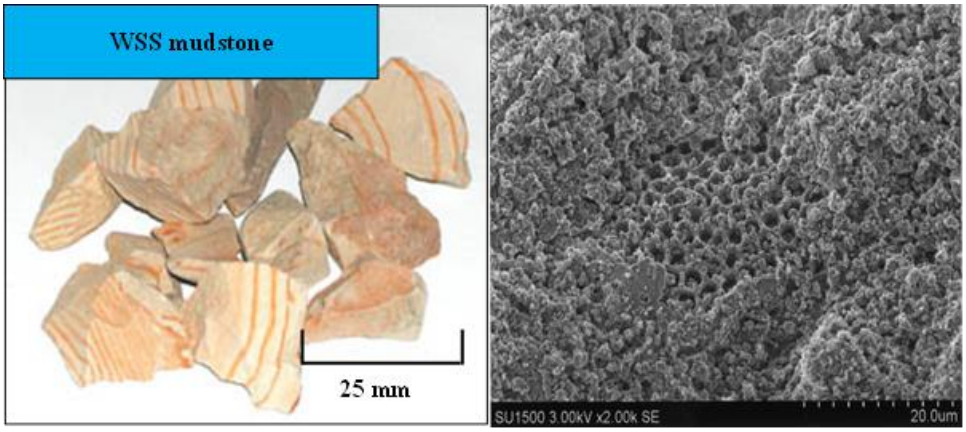

Fig. 4-1 Picture of the appearance and microscopic structure of WSS mudstone

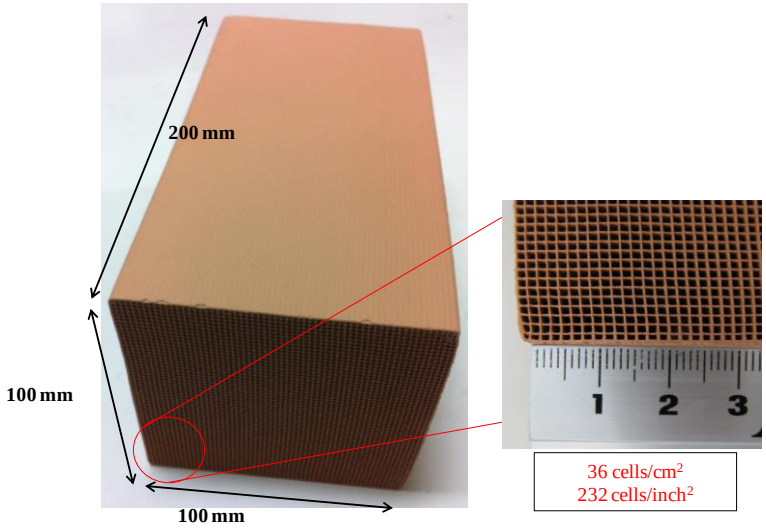

Fig. 4-2 Picture of WSS honeycomb unit

4.2.1 The manufacture of the composite material

The manufacturing procedure of this composite material is shown schematically in Fig. 4-3. First, the original WSS honeycomb unit was dried at 150ºC in an oven for 4 hr to obtain its dry weight. Then, the unit was cooled to room temperature and immersed in an aqueous solution of LiCl with concentration of 20.0 wt%. The WSS honeycomb unit immersed in the solution of LiCl was vacuumed in a glass vacuum container to 3.14×10^3 Pa (the saturated water vapor pressure at 25ºC) for 15 min. Then it was dried at ambient air for several hours before being put into the oven at 150ºC. Finally, weight percentage of 9.6 wt% LiCl supported composite mesoporous ceramic honeycomb unit was obtained. The original ceramic honeycomb unit is denoted as WSS, and the composite ceramic sample impregnated with LiCl is denoted as WSS + 9.6 wt% LiCl. This composite material will be compared with the other developed composite material in our previous research [32], WSS impregnated with 22.4 wt% $CaCl_2$, which will be denoted as WSS + 22.4 wt% $CaCl_2$.

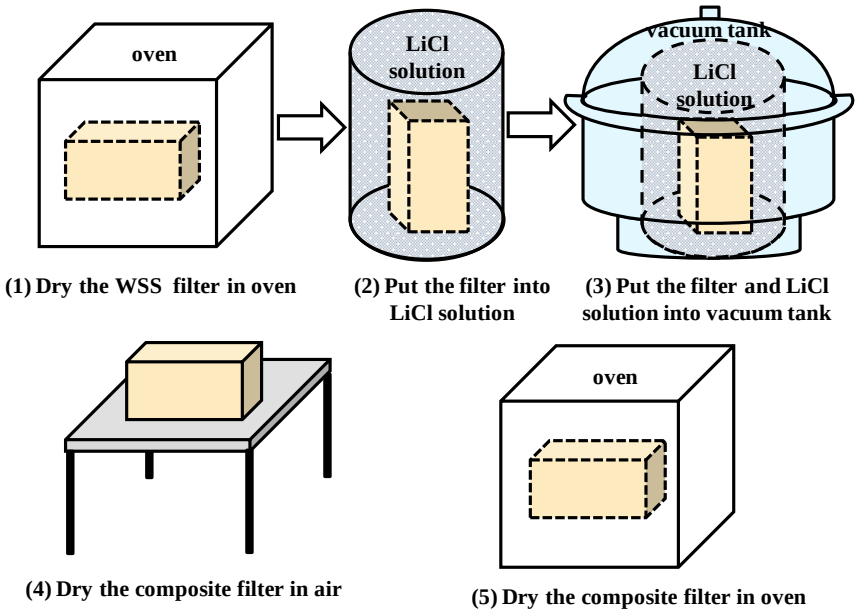

Fig. 4-3 The manufacturing procedure of the composite honeycomb unit

4.2.2 Physical properties of the WSS + 9.6 wt% LiCl

The physical properties including the pore volume and specific surface area of the mesoporous composite material were measured by standard nitrogen gas sorption/desorption measurements. The material was degassed at 150ºC in vacuum and then the sorption measurements of nitrogen were carried out at 77 K. The composite material's specific surface area was calculated by the Brunauer-Emmett-Teller (BET) equation, and the fine pore volume was calculated by Barrett, Joyner, and Halenda (BJH) equation.

Table 4-1 Physical properties of the composite material

Properties	WSS	WSS +22.4 wt% $CaCl_2$	WSS +9.6 wt% LiCl
Specific surface area (m^2/g)	111.7	38.4	58.3
Pore volume (cm^3/g)	0.309	0.152	0.237
True density (kg/m^3)	2150	2150	2142
Porosity (%)	60	49	55

The pore volume distributions of the original ceramic material and WSS + 9.6 wt% LiCl are presented in Fig. 4-4, as well as WSS + 22.4 wt% $CaCl_2$ as a comparison. It can be observed that the pores of the original ceramic material were filled by the two kinds of hygroscopic salts, and the pore volume decreased with supporting content of salt, no matter the species of salt. The fine pore volume, along with the true density and porosity is presented in Table 4-1.

From both Fig. 4-4 and Table 4-1, it can be seen clearly that fewer pores were filled by LiCl due to the low impregnated mass of LiCl. It is considered that the composite material would be affected by the impregnated species of hygroscopic salt, and the performance of these two different composite materials to store thermal energy will be investigated in later sections.

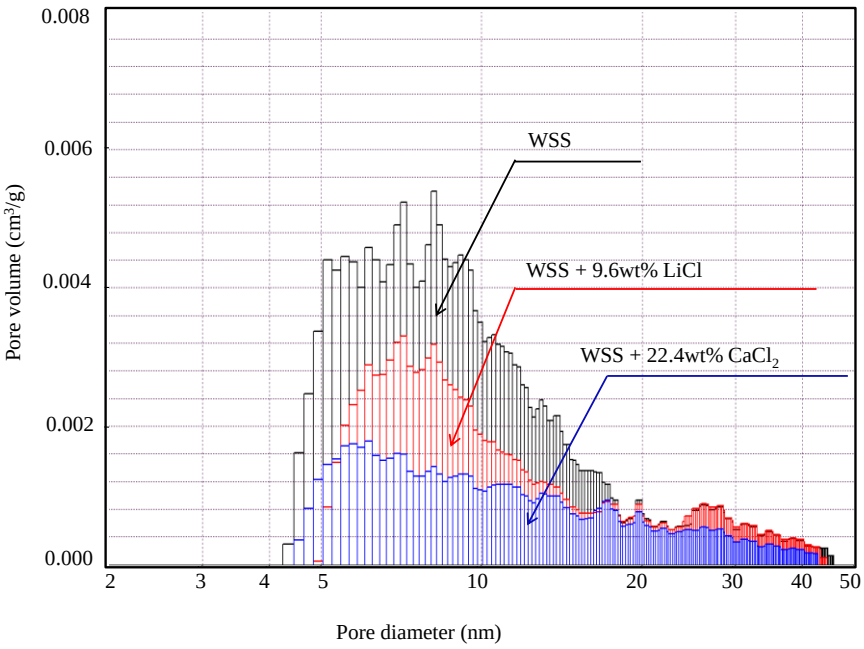

Fig. 4-4 Pore volume distributions of WSS + 9.6 wt% LiCl

4.2.3 The sorption performance of the composite mateiral

The water vapor sorption isotherms of the composite material were tested under closed condition by the water vapor sorption analyzer Hydrosorb HS-1 (Quantachrome Instruments) at 25ºC. The composite material was degassed at 150ºC under the vacuum condition for 4 hours to make sure that the material had been dried completely. Then it

would be degassed again at 25ºC under vacuum condition for another 2 hours before starting to sorb water vapor. As a comparison, the sorption amount of the composite material was also tested in open condition by putting the material into a constant temperature & humidity chamber at a certain temperature (25ºC) and relative humidity (5-95%) until reaching the equilibrium state at each tested relative humidity condition.

The comparison of the sorption amount of the two composite materials for both closed and open systems was shown in Fig. 4-5, from which it can be easily found that the two composite materials show remarkable increase of sorption capacity in a wide range of relative humidity. For two composite materials, big differences between the sorbed water amount under vacuum condition (closed system) and sorption amount under atmospheric pressure (open system) are not found. The little difference is probably because that the water vapor reacts with the impregnated salt effectively in the open system when the relative humidity is low (< 15%) or extremely high (> 70%). Based on the same matrix of WSS the isothermal sorption amount of the WSS + 9.6 wt% LiCl almost keeps same with that of WSS + 22.4 wt% $CaCl_2$ at the same relative humidity for both closed system and open system due to almost same moles of impregnated salts per mass of matrix. The composite material interacts with water vapor based on the following mechanisms [33]: a) Heterogeneous adsorption on the pore surface of ceramic material; b) Chemical reaction (chemical adsorption) between vapor and the salt; c) Liquid absorption by the salt hydrate salt·$n$$H_2O$. According to the three mechanisms explained above, the two different composite materials exhibiting almost the same sorption amount indicates that the last two mechanisms: chemical reaction (chemical adsorption) between vapor and the salt and liquid absorption by the salt hydrate are the two main sorption behaviors of the composite material. Due to the nearly same sorption amount of the WSS + 9.6 wt% LiCl and WSS + 22.4 wt% $CaCl_2$, the comparison of the two materials will be conducted in this research.

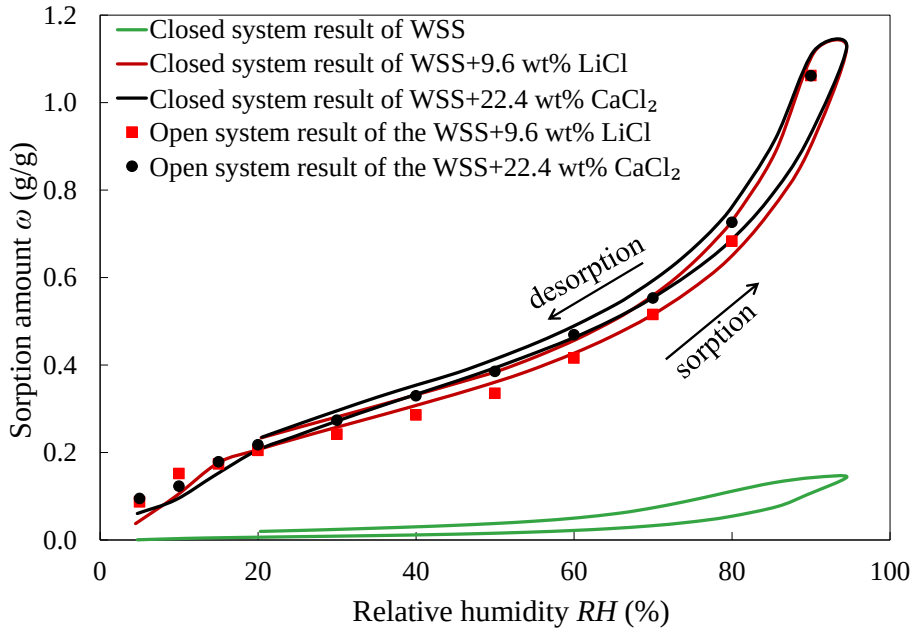

Fig. 4-5 Comparison between the sorption amount of WSS + 9.6wt% LiCl and that of WSS + 22.4 wt% $CaCl_2$ for both closed system and open system

4.2.4 Regeneration temperature of the WSS + 9.6 wt% LiCl

The sorption isobar of the WSS + 9.6 wt% LiCl was measured in a temperature range of 25ºC to 150ºC at a partial water vapor pressure of 22.18 hPa by thermogravimetric (TG)/differential thermal analysis (DTA). The water vapor content was calculated as $\omega = m_{H_2O}(T)/m_{dry}$. The desorption isobar is considered to be able to determine the regeneration temperature range of the tested composite material.

The desorption isobars of the WSS + 9.6 wt% LiCl and the WSS + 22.4 wt% $CaCl_2$ measured at a partial water vapor pressure of 22.18 hPa were presented in Fig. 4-6.

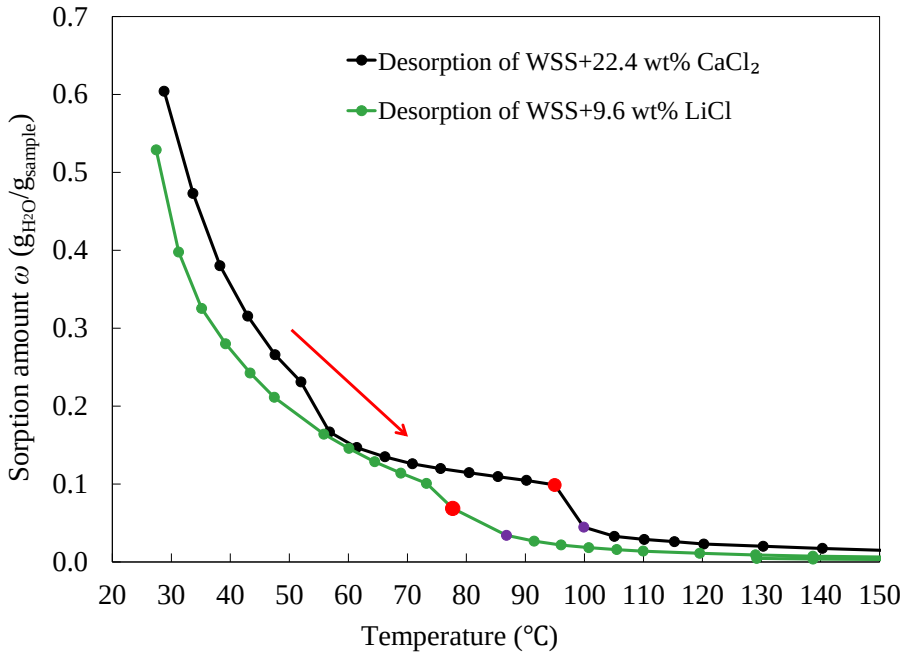

Fig. 4-6 Isobars of the water vapor sorption of the WSS + 9.6 wt% LiCl and the WSS + 22.4 wt% $CaCl_2$ at a partial water vapor pressure of 22.18 hPa

The water content can also be presented as a number of water molecules with respect to one molecule of hygroscopic salt, which is calculated as the following equation:

$$n=[\omega-(1-m_{salt}/m_{dry})\omega_{WSS}(T)][(M_{salt}/M_{H_2O})/(m_{salt}/m_{dry})] \qquad 4\text{-}1$$

Two clear sorption water vapor plateaus indicating the formation of the $CaCl_2 \cdot H_2O$ and $CaCl_2 \cdot 2H_2O$ can be detected in the isobar of the WSS + 22.4 wt% $CaCl_2$ in Fig. 4-6 as $n \approx 1$ and $n \approx 2$. It can be seen that $CaCl_2 \cdot H_2O$ was obtained at 99.8ºC for WSS + 22.4 wt% $CaCl_2$ [32]. While for the WSS + 9.6 wt% LiCl, the crystalline hydrates $LiCl \cdot H_2O$ and $LiCl \cdot 2H_2O$ were also detected in the isobar, however, the transition temperature from $LiCl \cdot 2H_2O$ to $LiCl \cdot H_2O$ is in the range of 77 to 87ºC. This transition temperature is about 15ºC lower than the temperature changing from $CaCl_2 \cdot 2H_2O$ to $CaCl_2 \cdot H_2O$ in the case of the WSS + 22.4 wt% $CaCl_2$. It is can be explained by the lower desorption activation energy of the composite WSS + 9.6 wt% LiCl compared to that of the WSS + 22.4 wt% $CaCl_2$ [34]. In fact, not only the mesopores, but also different type of hygroscopic salt will affect the formation of crystalline hydroscopic hydrate. Therefore, the WSS + 9.6 wt% LiCl is superior to be regenerated with at low temperature and with small energy.

4.2.5 Sorption kinetics of water vapor on the composite material

Sorption kinetics measurements were conducted at atmospheric pressure at 25ºC with a relative humidity of 70% in a constant temperature & humidity chamber. First, the two kinds of composite materials (WSS + 9.6 wt% LiCl and WSS + 22.4 wt% $CaCl_2$) were regenerated at desired temperature 150ºC for 4 hours. Then they were placed on the electronic balance located in the constant temperature & humidity chamber at the same time, which was set at the desired temperature and relative humidity. The weights of the composite materials would be periodically recorded by a computer connected with the two balances, and the measurement can be ended until the weight of the materials does not change.

The sorption dynamics of each material were got by regenerating the material at 150ºC, and then putting into the constant temperature & relative humidity chamber at 25ºC, *RH* 70%. The sorption kinetic curves of the two materials showing the sorbed water vapor amount as a function of time were shown in Fig. 4-7, as well as the sorption rate. The sorption capacity of the WSS + 22.4 wt% $CaCl_2$ is higher than that of the WSS + 9.6 wt% LiCl at a relative humidity of 70%.

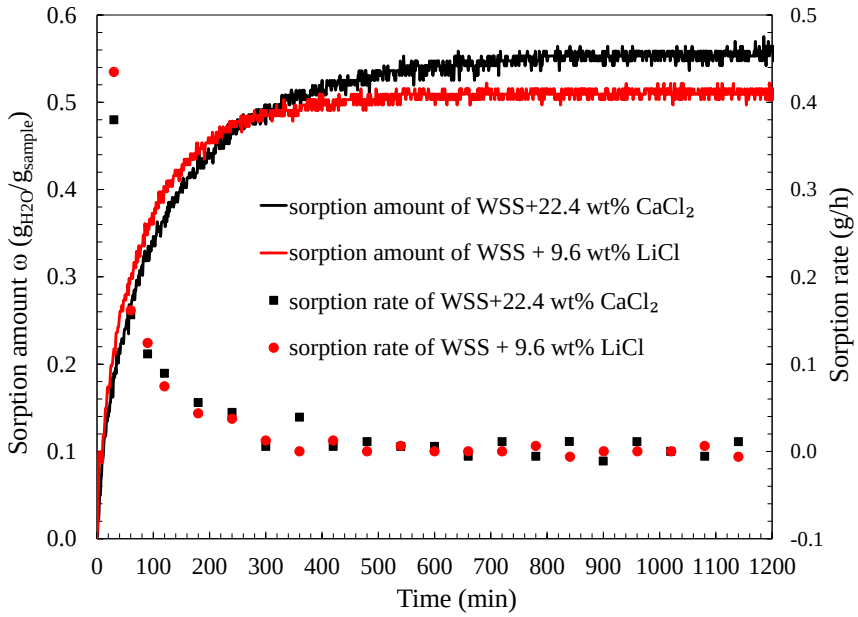

Fig. 4-7 The sorption kinetics of water vapor on the WSS + 9.6 wt% LiCl and the WSS + 22.4 wt% $CaCl_2$ (regeneration temperature 150ºC) at a temperature of 25ºC and *RH* 70%

It is easily can be seen that the WSS + 9.6 wt% LiCl shows higher sorption rate when the sorption amount is lower than 0.35 g/g during the first 100 minutes. There are three possible reasons can be responsible for this rate difference. (1) For the mesoporous material with main pore distribution from 4 to 20 nm, the Knudsen diffusion is the dominant pore diffusion mechanism, because of which more collisions between a water molecule and the pore wall happen. After collision with the wall, the molecule remains on the surface for some time *t* that is related with the activation energy of desorption $t \propto \exp(E/RT)$. The low desorption activation energy of the WSS + 9.6 wt% LiCl is possible to be the reason to increase the mass transfer rate of the water diffusion due to the short time *t* [23]. (2) The mean pore size of the WSS + 9.6 wt% LiCl is larger than the average size of the WSS + 22.4 wt% $CaCl_2$ (cf. Fig. 4-4), which means that the Knudsen coefficient is larger because of its relation with the pore diameter $D_K = \frac{d_P}{3}\sqrt{8RT/\pi M}$ [35]. (3) The formation of the solution film of the hygroscopic salt near the surface of the channel would be the limiting factor for the water vapor sorption afterwards [36]. In this case, the sorption rate is mostly affected by the solution film properties. Dawoud and Aristov [23] also pointed out that in smaller pores the diffusion coefficient in the confined salt solution is expected to be smaller in respect to that in the larger pores. It is partly explained why the WSS + 9.6 wt% LiCl with larger pores showed higher sorption rate in a certain sorption range. While when the volume of the total mesopores cannot hold all the sorbed water, the sorbed water will be mainly located into the macropores of the WSS. In this case the sorption does not occur in a confined state but a bulk state, which may explain why the sorption rate of the WSS + 22.4 wt% $CaCl_2$ is larger than that of the WSS + 9.6 wt% LiCl when the sorption amount exceeds 0.35 g/g.

4.2.6 Activation energy

The activation energy of water desorption was investigated by TG/DTA with inside water vapor condition maintained at a constant absolute pressure 17 hP. The dry weight of the testing material was 6-10 mg. At first, the sample was heated up to 150ºC for 30 minutes under continuous pumping during which the absolute pressure is about 500 Pa.

Then the measuring cell was disconnected from the vacuum pump and connected to an evaporator maintained at 15ºC (17 hPa), and then the material was started to be cooled down to T_0 (T_0=35ºC), at which time the material can sorb water until reaching a constant weight. The desorption activation energy was tested by heating the material sorbed a certain amount of water at a constant heating rate while keeping connecting with the water evaporator, which making sure the water vapor pressure is 17 hPa during. As the temperature becomes high enough, the material will desorb gradually. In the measurement, the material weight change, material temperature and weight change rate was recorded.

The transformation rate can be expressed by a single step kinetic equation with one function depending solely on the temperature, and the other one depending solely on the extent of conversion, a [37]:

$$a = \frac{m_{H_2O}(T)}{m_{s,dry}} / \frac{m_{H_2O}(T_0)}{m_{s,dry}} \tag{4-2}$$

$$\frac{da}{dt} = k(\boldsymbol{T})\, f(a) \tag{4-3}$$

where, the rate constant $K(\boldsymbol{T})$ is generally assumed to follow Arrhenium equation yielding

$$\frac{da}{dt} = k_0 \exp(-\frac{E}{R\boldsymbol{T}})\, f(a) \tag{4-4}$$

In the calculation of activation energy, the peak method (maximum rate method) [38] is adopted. Take the time differential of the Eq. 4-4 at the maximum desorption rate point, the following equation can be obtained.

$$\left(\frac{d^2a}{dt^2}\right)_P = 0 \tag{4-5}$$

$$\ln(\frac{\beta}{\boldsymbol{T}_p^{\,2}}) = \ln\left[(-\frac{df(a)}{a})_P \cdot \frac{AR}{E}\right] - \frac{E}{R\boldsymbol{T}_P} \tag{4-6}$$

Where $\boldsymbol{T_P}$ is the peak desorption temperature and β is the heating rate. By taking the linear dependencies of $\ln(\beta/\boldsymbol{T_P}^2)$ versus $1/\boldsymbol{T_P}$ at different heating rate, the activation energy for desorption can be obtained.

$$E = R \cdot \frac{d \ln(\frac{\beta}{\boldsymbol{T}_p^{\,2}})}{d \frac{1}{\boldsymbol{T}_p}} \qquad 4\text{-}7$$

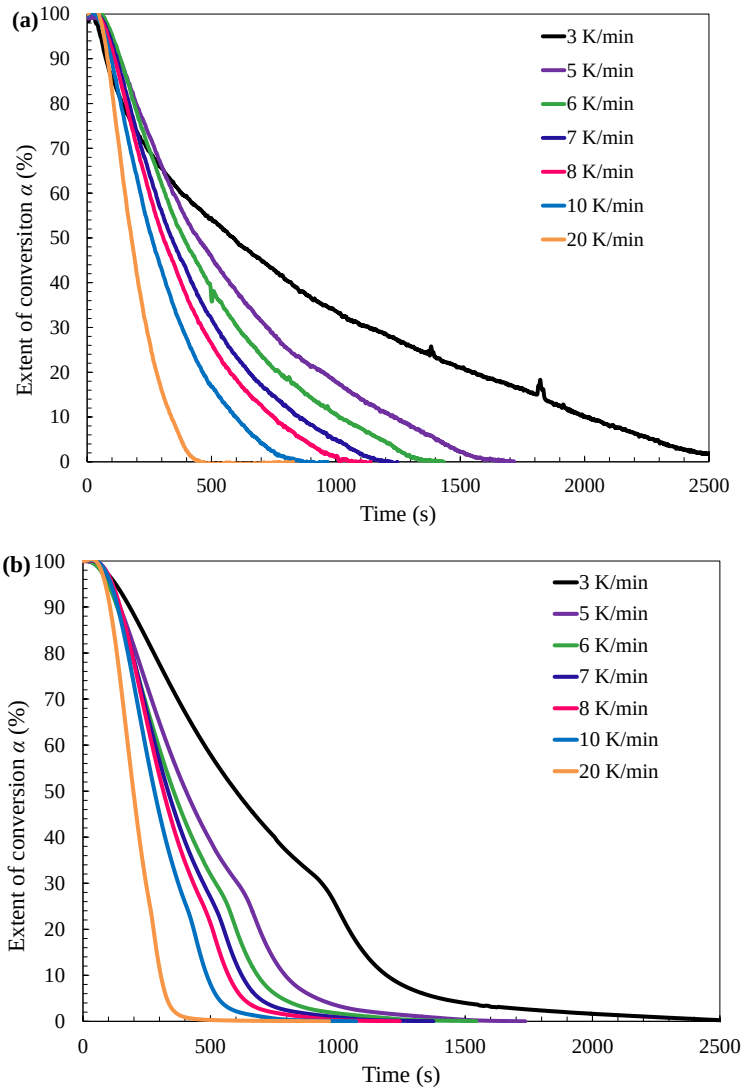

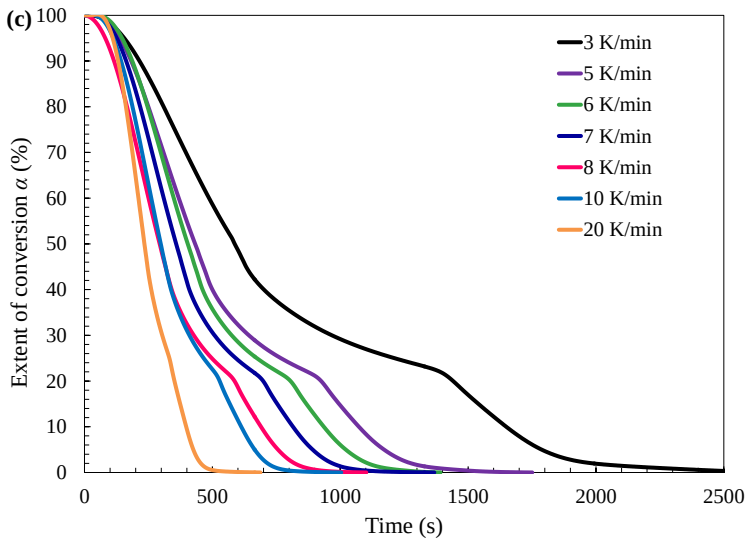

Fig. 4-8 Kinetic desorption curves of the (a) WSS (b) WSS + 9.6 wt% LiCl and (c) WSS + 22.4 wt% $CaCl_2$

Kinetic curves of water desorption from the WSS and the two composite materials are presented in Fig. 4-8 (a), (b) and (c). From Fig. 4-8 (a) it can be seen that the first several minutes of the curves demonstrate faster water desorption. The desorption rate continues decreasing with the desorption process. While it is so obvious to see that the two composite materials: WSS + 9.6 wt% LiCl and WSS + 22.4 wt% $CaCl_2$ desorb fast again after the first stage of quick desorption (cf. Fig. 4-8 (b) and (c)). This can be even clearly illustrated by Fig. 4-9 (a), (b) and (c), from which the maximum temperature for desorption can also be determined. It is considered that for the hygroscopic salt impregnated composite material, the first portions of water evaporate from less concentrated solutions, and this desorption process is similar with the water evaporation process. With the temperature increases, more concentrated solutions or crystalline hydrates are going to be dehydrated, which needs a higher temperature.

The activation energy calculated from the slope of the kinetic curve in the $\ln(\beta/T_P^2)$ versus $1/T_P$ coordinates in Fig. 4-10. The slope of the linear relation between $\ln(\beta/T_P^2)$ and $1/T_P$ and the calculated activation energy by Eq. 4-7 are given in Table 4-2. The activation energies of water desorbed from WSS + 9.6 wt% LiCl and WSS + 22.4 wt% $CaCl_2$ were 87.7 and 126.1 kJ/mol, respectively. Fig. 4-10 also indicates that desorption activation on WSS + 9.6 wt% LiCl and WSS + 22.4 wt% $CaCl_2$ is more than that on the supportive matrix WSS, which is a physical desorption process. This is probably

because the acting force between water molecules and the salt became stronger than the surface of the WSS. The key point is the desorption activation energy of the WSS + 9.6 wt% LiCl is lower than that of the WSS + 22.4 wt% $CaCl_2$, which is because the Ca^{2+} is higher than that of Li+ [34]. Because of lower desorption activation energy, it would be easier for WSS + 9.6 wt% LiCl to be desorbed at lower temperature compared to the WSS + 22.4 wt% $CaCl_2$.

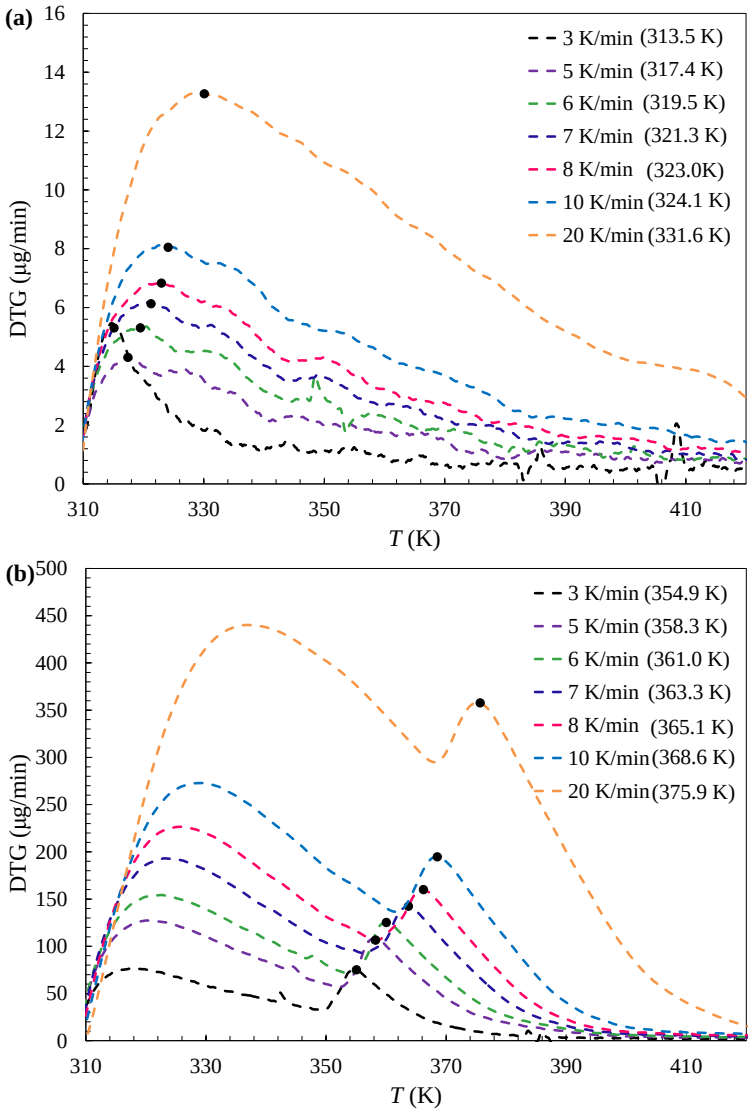

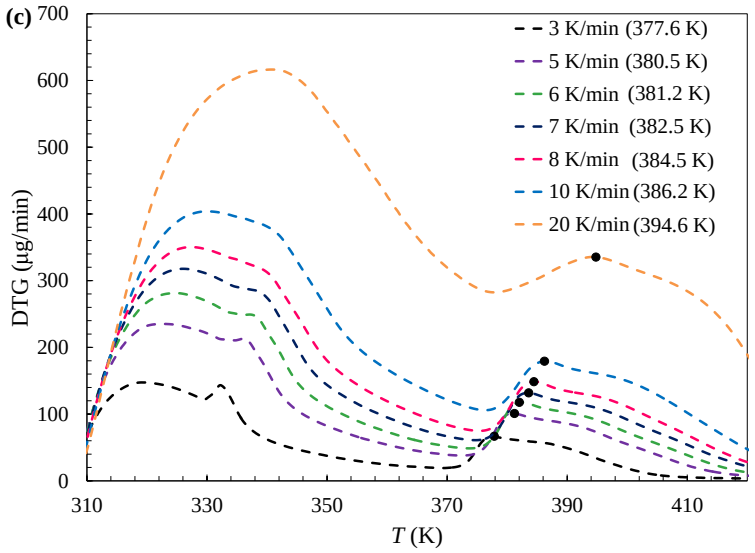

Fig. 4-9 Weight change rate DTG changes with temperature of the (a) WSS and (b) WSS + 9.6 wt% LiCl and (c) WSS + 22.4 wt% $CaCl_2$

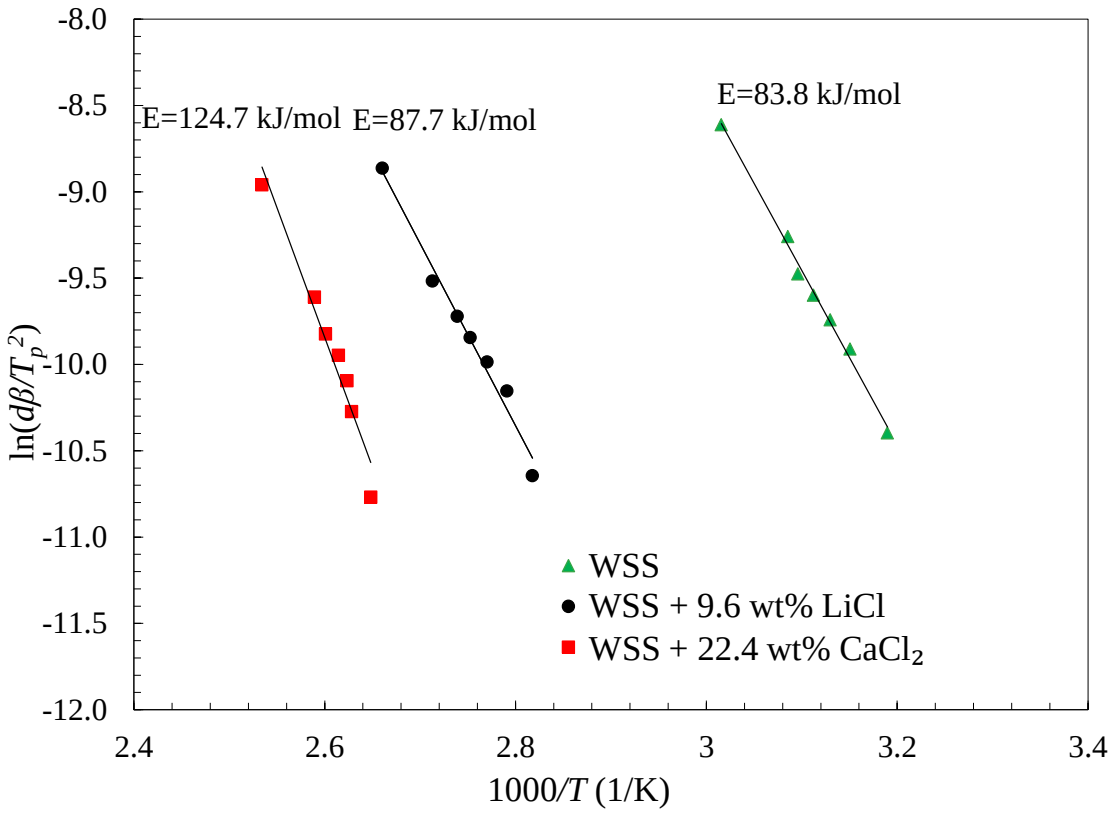

Fig. 4-10 Linear dependence between $\ln(\beta/T_P^2)$ versus $1/T_P$ of water desorbed from the three tested materials7

Table 4-2 Activation energies of water desorption from the tested three samples

	WSS	WSS +22.4 wt% $CaCl_2$	WSS +9.6 wt% LiCl
$d(\ln(\beta/T_P^2))/d(1/T_P)$	10.089	15.002	10.556
Degree of fitting R^2	0.994	0.9582	0.9827
E (kJ/mol)	83.8	124.7	87.7

4.3 OPEN SORPTION THERMAL ENERGY STORAGE EXPERIMENTS

4.3.1 Open sorption thermal energy storage experimental setup

A direct open sorption thermal energy storage experimental setup was constructed in our previous study [32], and it is used in this study to examine the performance of the WSS + 9.6 wt% LiCl as a thermal energy storage unit in the shape of a honeycomb. An open sorption thermal energy storage system is operated at atmospheric pressure, which can use endothermic and exothermic processes to store and recover heat respectively.

The schematic diagram of the experimental setup is provided in Fig. 4-11. The tested unit WSS + 9.6 wt% LiCl was placed inside the test section with six T-type Φ1.0 mm sheathed thermocouples inserted at different positions. In the heat storage (heat charging or endothermic) process, hot air is used to regenerate the material. In the heat supply (heat discharging or exothermic) process, high-humidity air flows through the system to recover the exothermic heat due to the sorption of the water vapor.

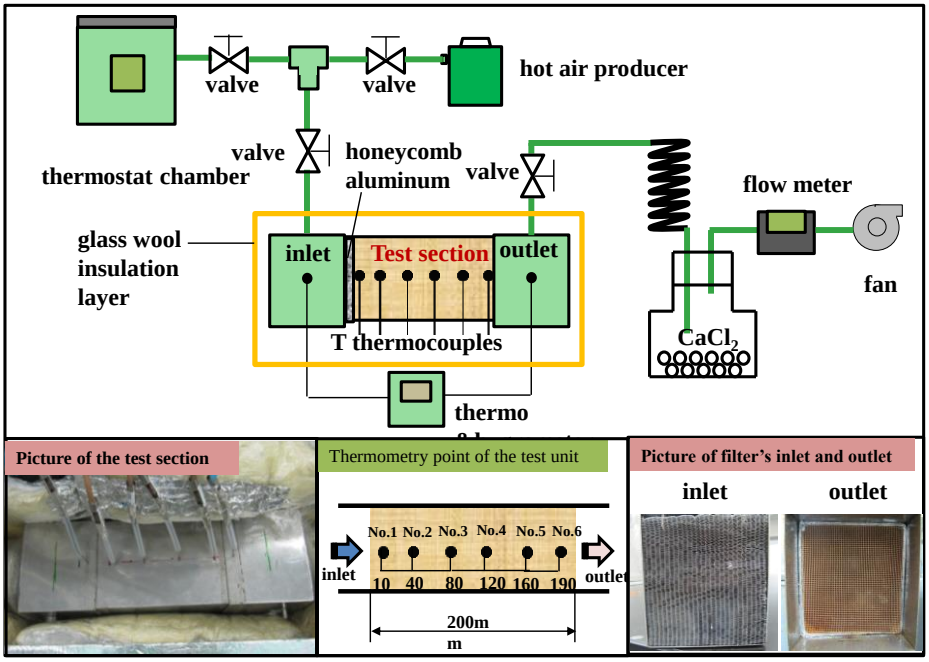

Fig. 4-11 Schematic diagram of the direct open sorption thermal energy storage system

Hot air in the heat storage process was created by a hot-air producer. Humid air in the heat release process was supplied by a highly stable constant temperature & humidity chamber. The relative humidity and temperature of the inlet and outlet air were measured and recorded by two thermo hygrometers (Rotronic Instrument Corp., Hauppauge, NY, USA). After the regeneration process, the material was cooled to the initial temperature of the thermal energy storage unit during the heat release process. Humid air (25ºC, *RH* 93% ± 3%) then flowed through, which resulted in water vapor being sorbed while sorption heat being released and removed by the flowing air. In this research, the regeneration temperature and humid air flow rate during sorption process were investigated.

4.3.2 Stability of the WSS + 9.6 wt% LiCl

One of the possible operating heat storage conditions was chosen to conduct the repetition test in order to examine the stability of the WSS + 9.6 wt% LiCl. The repetition measurement was conducted by using a Dual Chamber Sample Moving System, which mainly includes two constant temperature & humidity chambers and an automatic moving system. The picture of the Dual Chamber Sample Moving System can be checked in Fig. 4-12. The sample in one chamber can be moved quickly to the other chamber automatically without changing the other chamber's air condition. The sorption and desorption processes of the WSS + 9.6 wt% LiCl were done respectively in these two chambers, in which different air conditions were set.

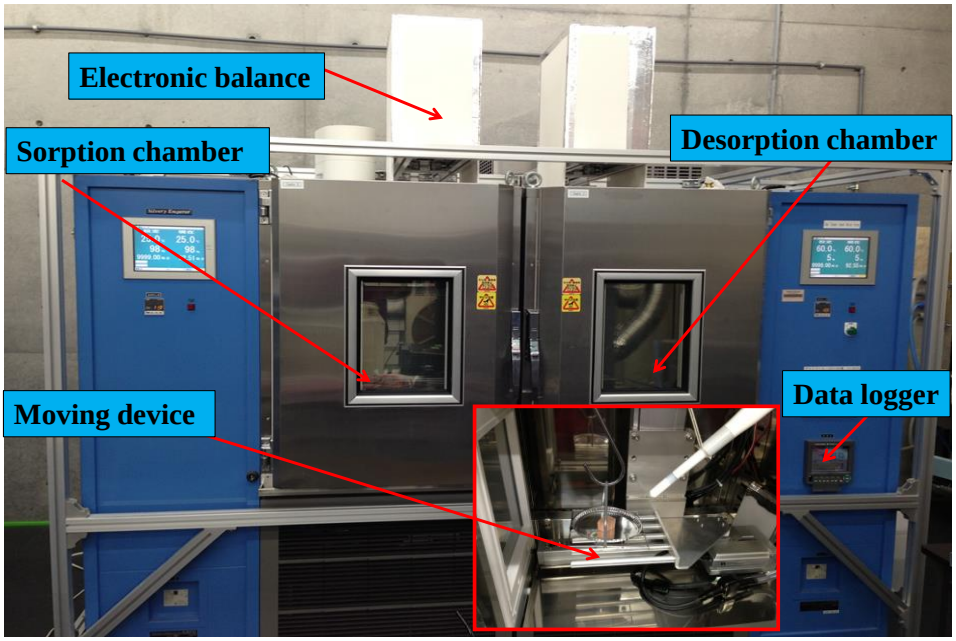

Fig. 4-12 Picture of the Dual Chamber Sample Moving System

4.4 RESULTS AND DISCUSSION

4.4.1 Effect of regeneration temperature on the heat recovery air in heat release process

Regeneration temperatures of 60ºC, 80ºC, 100ºC, and 120ºC were measured, and a humid air flow rate of 2.0 m^3/h was set the same in the heat release process (25ºC, *RH* 93% ± 3%). The results of this investigation are provided in Fig. 4-13 (a) and (b).

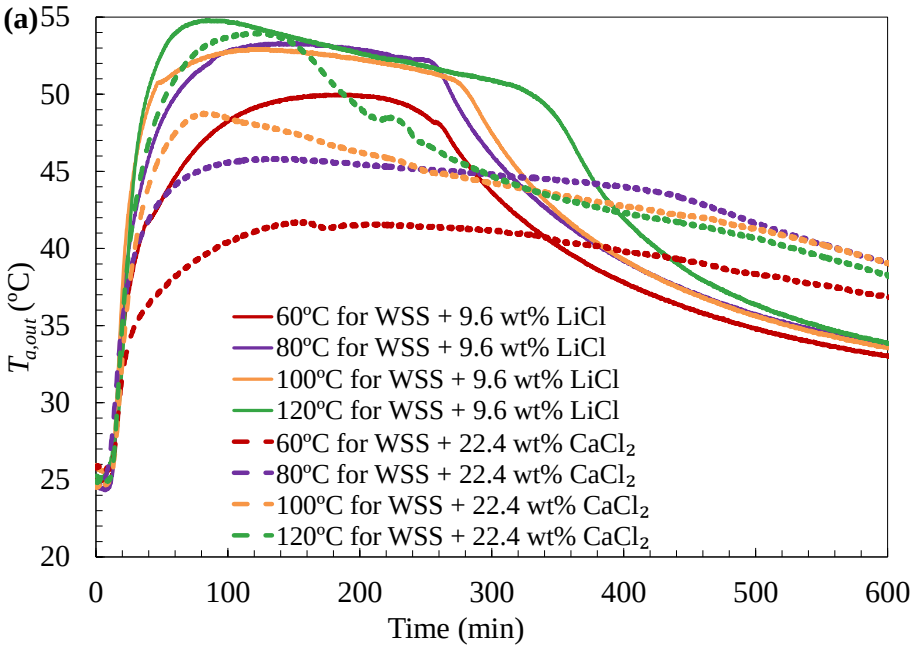

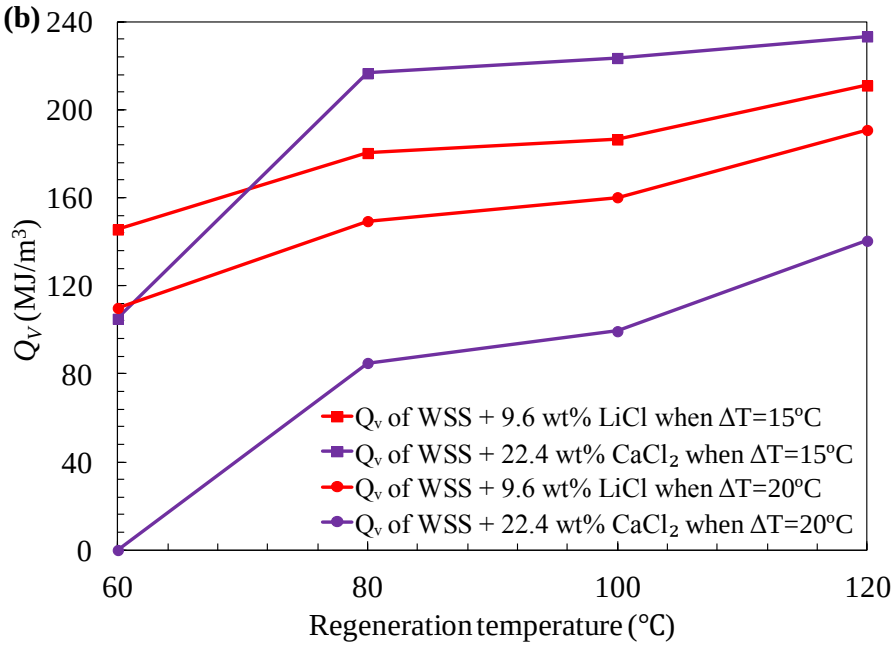

Fig. 4-13 (a) Time variation of the outlet air temperature and (b) variation of the volumetric heat storage density corresponding to different regeneration temperatures

From Fig. 4-13 (a), we can see that for WSS + 22.4 wt% $CaCl_2$ the maximum outlet air temperature increases greatly with the high regeneration temperature, while in the case of the WSS + 9.6 wt% LiCl, the regeneration temperature affects little to the maximum outlet air temperature. It could be understood that for the WSS + 9.6 wt% LiCl, when the sorption amount of material is low, the sorption rate is higher than that of the WSS + 22.4 wt% $CaCl_2$ even it is regenerated at a lower temperature (cf. Fig. 4-7). The high sorption rate may positively affect the maximum air temperature in heat release process by sorbing more water in a certain time. The sorbed water amounts of the two units are calculated according to air flow rate and absolute humidity difference of the inlet and outlet air (cf. Fig. 4-14):

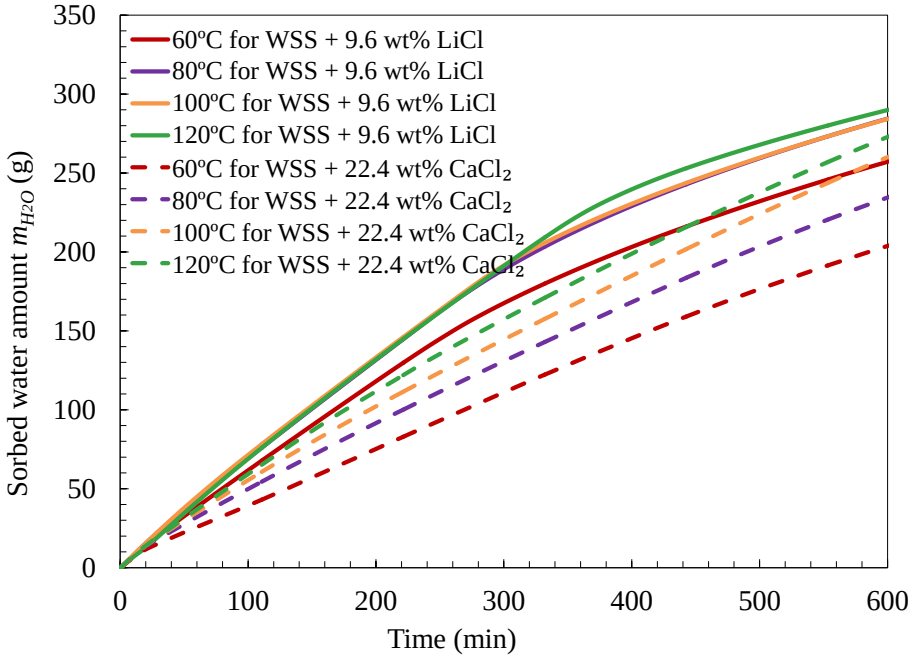

Fig. 4-14 Time variation of the sorbed water amount of the WSS + 9.6 wt% LiCl and the WSS + 22.4 wt% $CaCl_2$ corresponding to different regeneration temperatures

$$m_{H_2O} = \int_0^t \rho_a Q_a (x_{a,in} - x_{a,out}) dt \qquad 4\text{-}8$$

It can be seen clearly from Fig. 4-14 that the slope of the sorbed water amount curve of the WSS + 9.6 wt% LiCl is larger than that of the WSS + 22.4 wt% $CaCl_2$ during the first 300 minutes, and it assures a high outlet air temperature as 50 to 55ºC for these four regeneration temperatures. While after that the slope turns to be lower, which causes the outlet air temperature decreases and hot air supply duration shortens. For the WSS + 22.4 wt% $CaCl_2$, the slope is increasing with the increasing of the regeneration temperature, that is why the maximum outlet air temperature relies so much on the regeneration temperature for this material.

The average sorption amount change of the thermal energy storage unit was determined by Eq. 4-9, which will explain why the WSS + 9.6 wt% LiCl sorbs water fast.

$$\Delta\omega = \left\{ \int_0^t \rho_a Q_a (x_{a,in} - x_{a,out}) dt \right\} / m \qquad 4\text{-}9$$

Time variation of the inlet and outlet absolute humidity and the average sorption amount changes of the WSS + 9.6 wt% LiCl and the WSS + 22.4 wt% $CaCl_2$ regenerated at 60ºC was shown in Fig. 4-15. Due to the high sorption rate during the initial time, the outlet air absolute humidity of the WSS + 9.6 wt% LiCl is so low making sure a large amount of water vapor has been sorbed. The sorption amount changes for the two materials are in the low sorption amount range (< 0.35 g_{H2O}/g_{sample}), that is why the sorbed water amount of the WSS + 9.6 wt% LiCl is high (cf. Fig. 4-14).

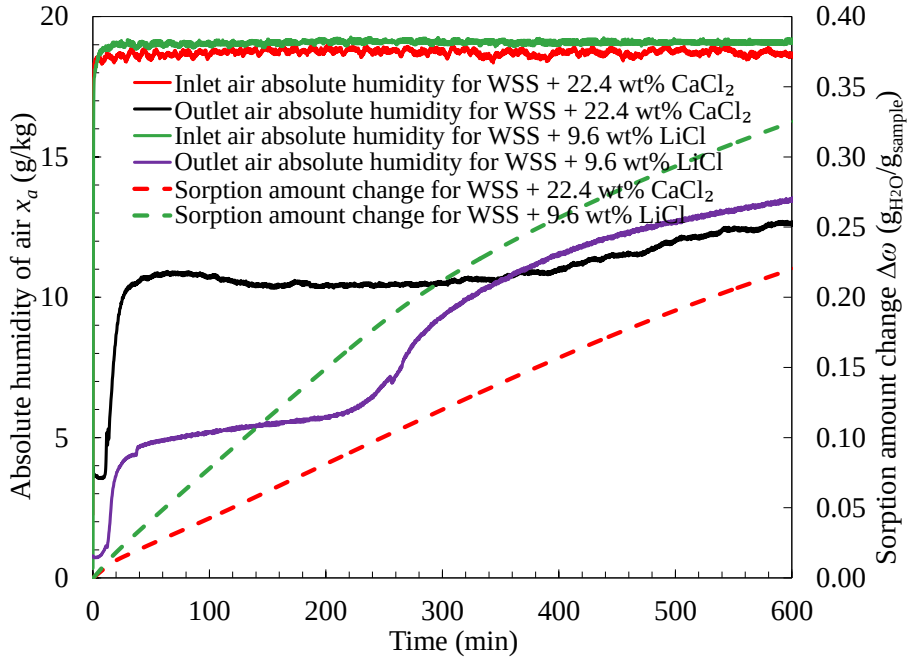

Fig. 4-15 Time variation of the inlet and outlet absolute humidity and the average sorption amount changes of the WSS + 9.6 wt% LiCl and the WSS + 22.4 wt% $CaCl_2$ regenerated at 60ºC

In our previous study, we assumed that for an actual system, an air temperature difference of greater than 15ºC is required with a long temperature duration of 5-8 hr for different applications. If the same assumption adopted, from Fig. 4-13 (a) we can see that the WSS + 9.6 wt% LiCl can be even regenerated at 60°C by supplying hot air greater than 40°C for longer than 5 hours. But outlet air temperature and high temperature air supply duration are not the only criterion to decide the regeneration temperature. In addition, the volumetric heat storage density is introduced to decide a proper regeneration temperature, which is defined as follows:

$$Q_V = C_{p,a}\rho_a Q_a / V \int_{\Delta t} (T_{a,out} - T_{a,in}) dt \quad \text{4-10}$$

In the above equation, during the time interval Δt, the temperature difference of outlet air and inlet air ΔT is no lower than the setting value.

The temperature difference of the outlet and inlet air are set as 15ºC and 20ºC to compare the performance of the composite thermal energy storage unit under different regeneration temperatures. In this case, the volumetric heat storage density is calculated only when the outlet air temperature is greater than 40ºC ($\Delta T \geq$ 15ºC) or 45ºC ($\Delta T \geq$ 20ºC). The volumetric heat storage densities at different regeneration temperatures of WSS + 9.6 wt% LiCl and WSS + 22.4 wt% $CaCl_2$ were compared (see Fig. 4-13 (b)). For WSS + 9.6 wt% LiCl, when the temperature difference is as high as 20ºC, the volumetric heat storage density is 40 MJ/m^3 smaller than the heat storage density calculated when the temperature difference is 15ºC at each measured regeneration temperature. However, the WSS + 22.4 wt% $CaCl_2$ does not exhibit so high volumetric heat storage density when the temperature difference is 20ºC though it shows higher heat storage density with outlet air temperature greater than 40ºC when the regeneration temperature is greater than 80ºC. In a word, compared to the performance of the WSS + 22.4 wt% $CaCl_2$, the WSS + 9.6 wt% LiCl can be regenerated at lower regeneration temperature but supply high temperature air in heat release process.

Therefore, if only low-temperature heat (about 60ºC), no matter for the temperature difference is 15ºC or 20ºC, the WSS + 9.6 wt% LiCl can be possible to supply hot air greater than 40ºC or 45ºC with high thermal energy storage density and low heat loss.

4.4.2 Influence of humid air flow rate on heat recovery air during the heat release process

Time changes in the outlet air temperature after flowing through WSS + 9.6 wt% LiCl at different air flow rates (1.0-3.0 m^3/h) were measured and shown in Fig. 4-16 (a). Before the humid air flowed in, the heat storage unit was regenerated at 80ºC. Fig. 4-16 (a) illustrates very clearly that for WSS + 9.6 wt% LiCl, the duration of high-temperature air (> 40ºC) decreased with increasing air flow rate. The rising rate of

outlet air temperature increased with the increasing of air flow rate due to the high mass flow of water vapor in the humid air.

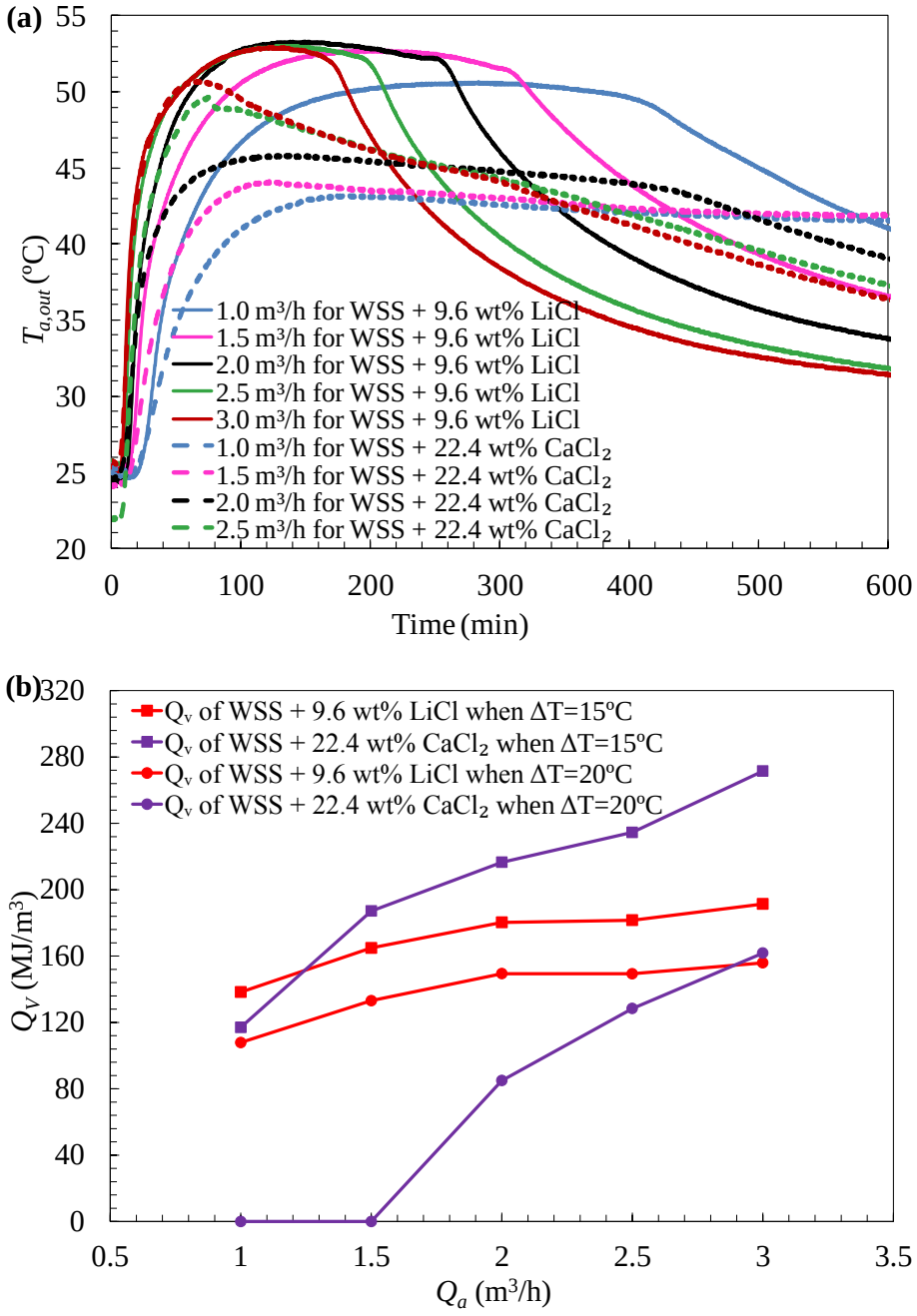

Fig. 4-16 (a) Time variation of the outlet air temperature and (b) variation of the volumetric heat storage density corresponding to different air flow rates

Speaking to the maximum outlet air temperature, it is interesting to see that when the flow rate is larger than 1.5 m^3/h, the maximum outlet air temperature keeps as 52 to 53°C. However, for WSS + 22.4 wt% $CaCl_2$ the maximum temperature is very sensitive

with the humid air flow rate, and during the tested 5 different flow rates, the maximum outlet air temperature increased with the increasing flow rate. The outlet air temperature resulted from the balance between the heat exchanges with the material (heat transfer rate, temperature of the composite material), the mass flow amount of the air taking away heat (flow rate) and the released sorption heat by the composite material eventually. The generated sorption heat is limited by two factors: convective mass transfer rate of the water vapor transferred to the surface of the composite material and the other one is the solid side mass transfer rate. When the air flow rate was increased, the thickness of the air film near each channel's surface thinned, so the water vapor diffusion rate would be increased due to lower gas film resistance. More water vapor could diffuse to the composite material and be sorbed by generating more heat at the same time. On the other hand, when the air flow rate was increased, the heat transfer rate could be increased. Fig. 4-17 (a) and (b) shows the temperature distribution one hour and two hours after the sorption process starts along the length of the WSS + 9.6 wt% LiCl (Fig. 4-17 (a)) and the WSS + 22.4 wt% $CaCl_2$ (Fig. 4-17 (b)), respectively. The first point of each temperature distribution line in Fig. 4-17 (a) and (b) is the inlet air temperature, and the last point is the outlet air temperature due to efficient heat exchange. It is so clear that the temperature of the position next to the outlet affects the outlet air temperature much, which means that the maximum outlet air temperature is mostly decided by the heat exchange with the material near the outlet. Therefore, with air flow rate increases, the maximum outlet air temperature of the WSS + 9.6 wt% LiCl can almost keep constant due to the compensation of heat transferred from the solid side (with improved heat transfer rate) for the heat taken away by more flowing air when the air flow rate is greater than 1.5 m^3/h. When the air flow rate is 1.0 m^3/h, the maximum outlet air temperature is lower than that of other flow rates because the material's temperature near outlet is a litter bit lower at 2 hours (Fig. 4-17 (a)). While for the WSS + 22.4 wt% $CaCl_2$, the increase of the material temperature near the outlet of the unit and the improved convective heat transfer rate contributes to the increasing of the outlet maximum air temperature with flow rate, especially the contribution of the increased composite material temperature.

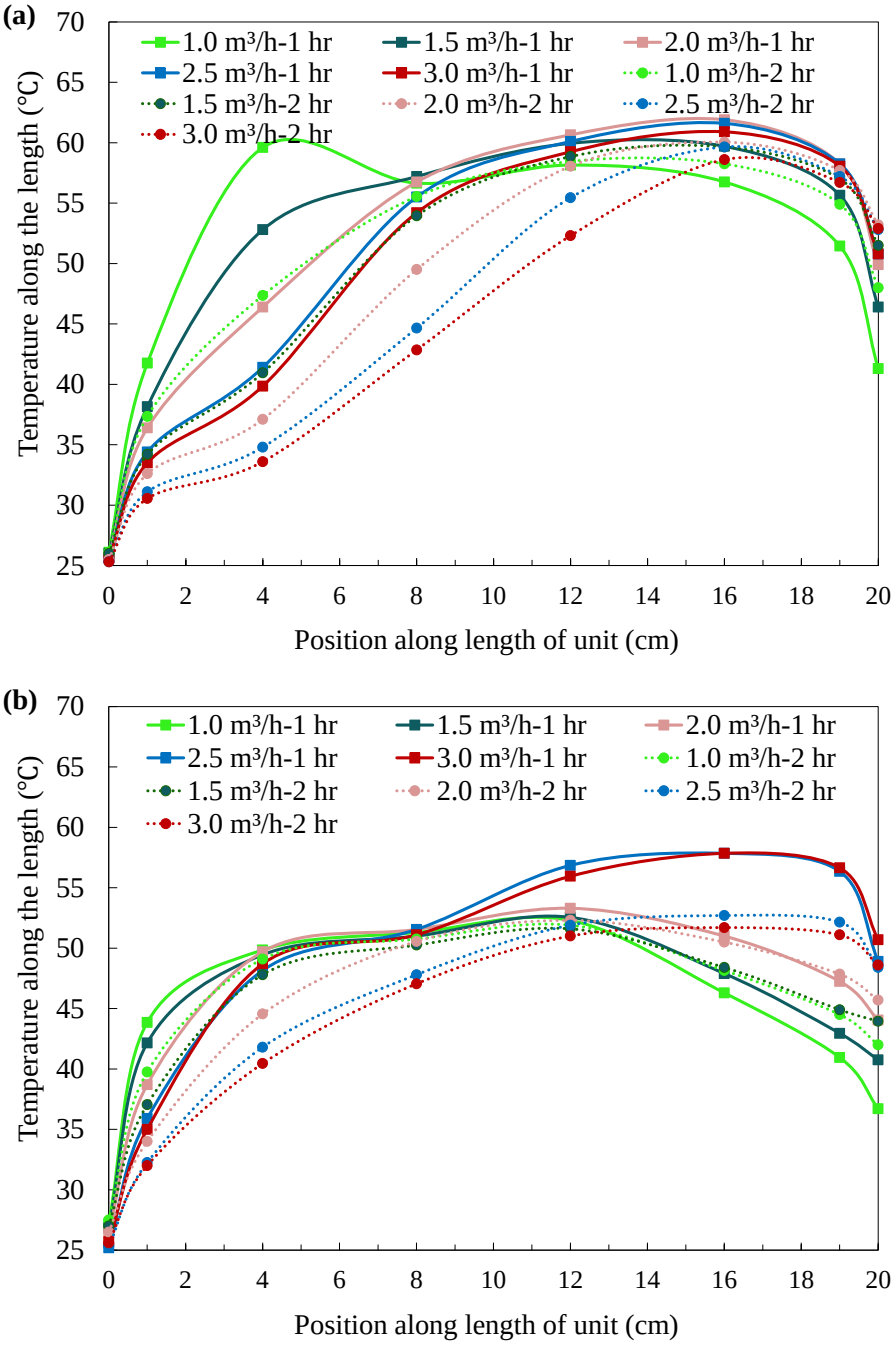

Fig. 4-17 (a) Temperature distribution of the WSS + 9.6 wt% LiCl at one hour and two hours and (b) Temperature distribution of the WSS + 22.4 wt% $CaCl_2$ at one hour and two hours corresponding to different air flow rates

The temperature of the material at position near the outlet increases with flow rate for WSS + 22.4 wt% $CaCl_2$ and it can be understood as follows. For the WSS + 22.4 wt% $CaCl_2$, the sorption rate is not only limited by the air side but also by the solid side. When the air flow rate increases, the air side mass transfer resistance decreases, but the

solid side sorption rate also increases due to the increased moisture concentration difference at the position near outlet. The mass transfer improvement both from air side and solid side is considered to be the reason for the increasing temperature of the WSS + 22.4 wt% $CaCl_2$ near outlet when the air flow rate is high. In the case of the WSS + 9.6 wt% LiCl with high solid side sorption rate, the total sorption rate is considered to be limited mainly by the air side mass transfer resistance. When the humid air flow rate is high, the sorption rate of the composite material near the outlet increases, and the generated heat can compensate the heat transferred to the flowing air to keep a relative constant composite material's temperature corresponding to different air flow rate.

So the presence of hydrates or salt solution in the matrix's pores can significantly change the sorbent capacity and also induce qualitatively new phenomena [36]. The sorption rate can be affected by the nature of the salt. The Fig. 4-16 (a) also shows that the maximum outlet air temperature of the WSS + 22.4 wt% $CaCl_2$ is lower than that of the WSS + 9.6 wt% LiCl at the same flow rate. It could be explained that the WSS + 9.6 wt% LiCl can sorb much more water vapor within a certain time though supplied with the same mass flow of water vapor as the WSS + 22.4 wt% $CaCl_2$ (cf. Fig. 4-18). The constant maximum temperature means that the WSS + 9.6 wt% LiCl can supply hot air with a relatively high constant temperature even the flow rate changes at a certain range.

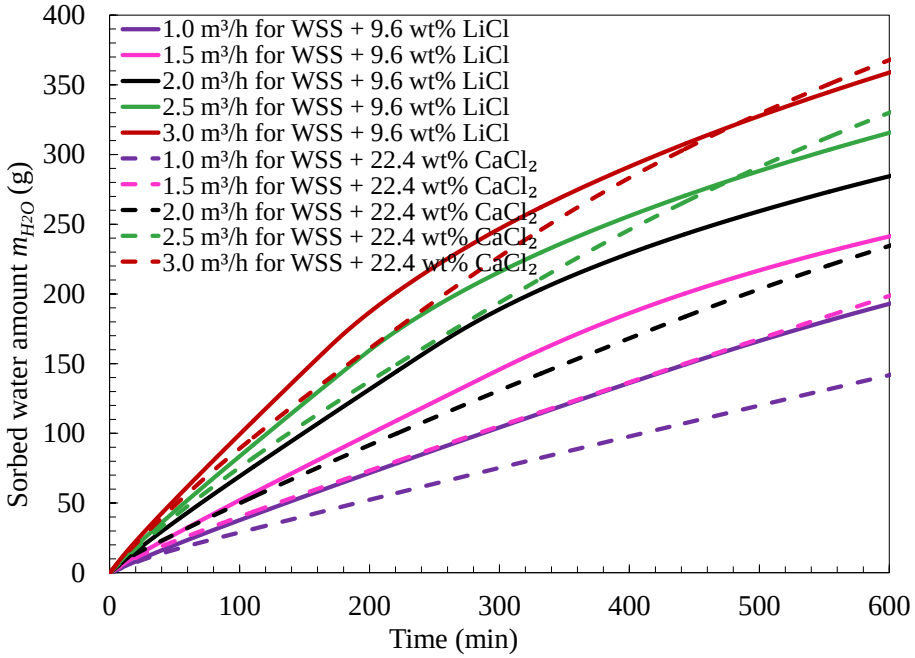

Fig. 4-18 Time variation of the sorbed water amount of the WSS + 9.6 wt% LiCl and the WSS + 22.4 wt% $CaCl_2$ corresponding to humid air flow rates

It can be clearly seen from Fig. 4-16 (b) that for WSS + 9.6 wt% LiCl, it presents an almost constant volumetric heat storage density when the humid air flow rate is greater than 1.5 m^3/h, though lower than that of WSS + 22.4 wt% $CaCl_2$ due to shorter duration of high temperature air supply when the temperature difference is 15ºC. However, as the WSS + 9.6 wt% LiCl can assure a high constant outlet air temperature, it exhibits a higher volumetric heat storage density compared to the WSS + 22.4 wt% $CaCl_2$ when the outlet and inlet air temperature difference is 20ºC.

In a word, compared to the performance of the WSS + 22.4 wt% $CaCl_2$, the WSS + 9.6 wt% LiCl can supply stable hot air with a certain temperature though the supply humid air's flow rate is adjusted during the heat release process.

4.4.3 Stability of the WSS + 9.6 wt% LiCl

According to the above results of the open sorption thermal energy storage experiment, the desorption temperature 60ºC is effective to be able to regenerate the developed composite material. Therefore, the desorption chamber was set at 60ºC, *RH* 5% for 3 hours to regenerate the sample of WSS + 9.6 wt% LiCl, while the sorption chamber was

set as 25ºC, *RH* 95% for 5 hours to examine the stability of the WSS + 9.6 wt% LiCl. The stability result of the composite material is illustrated in Fig. 4-19. It can be observed that for the WSS + 9.6 wt% LiCl during the tested 250 times, the sorption amount in both sorption and desorption processes remained unchanged indicating that the composite material is stable, though the sorption amount oscillation exists, which was hypothesized caused by the swelling in the composite material. However, the stability of this material under real operation condition has to be verified after a large number cycles, which will be the next effort in our experimental activity.

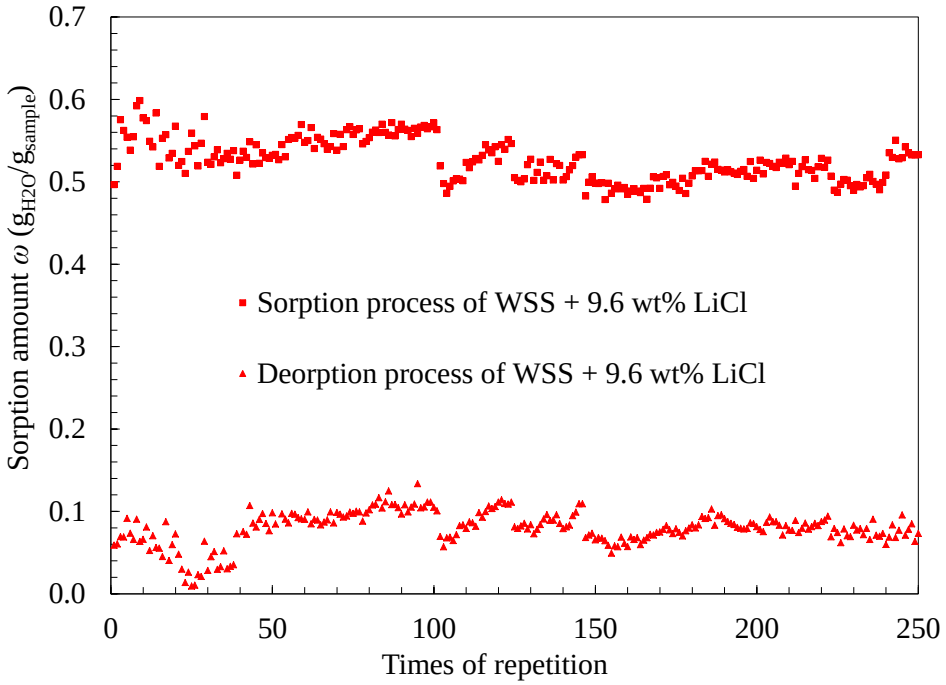

Fig. 4-19 Stability of WSS + 9.6 wt% LiCl (Desorption process: 60ºC, RH 5%; sorption process: 25ºC, RH 95%)

4.5 SUMMARY

A composite mesoporous honeycomb thermal energy storage unit was formed by filling LiCl into pores of WSS for a direct open sorption thermal energy storage system. The properties of the developed WSS + 9.6 wt% LiCl were measured. Next, the WSS + 9.6 wt% LiCl was examined by the developed open sorption thermal energy storage experimental setup, and its performance was compared with the WSS + 22.4 wt% $CaCl_2$.

(1) This material has almost the same sorption amount at each relative humidity as the material filled with 22.4 wt% $CaCl_2$.

(2) When the sorption amount is small, the sorption rate of the WSS + 9.6 wt% LiCl is higher compared to the WSS + 22.4 wt% $CaCl_2$.

(3) The WSS + 9.6 wt% LiCl can be regenerated at 60ºC, and it shows higher volumetric heat storage density than the WSS + 22.4 wt% $CaCl_2$ when the outlet and inlet air temperature difference is 20ºC at the same regeneration temperature.

(4) Compared to the performance of the WSS + 22.4 wt% $CaCl_2$ at the same regeneration temperature, the humid air flow rate affects little on the maximum outlet air temperature for WSS + 9.6 wt% LiCl in heat release process.

(5) The WSS + 9.6 wt% LiCl is stable when it is regenerated at 60ºC during the tested 100 sorption/desorption cycles, which indicates that this material can be used for a rather long time.

Thus, the composite mesoporous honeycomb thermal energy storage unit WSS + 9.6 wt% LiCl showed potential for storing solar energy with a higher volumetric heat storage density compared to some PCM materials in practical use.

4.6 REFERENCE

[1] G. Ervin, Solar heat storage using chemical reactions, Journal of Solid State Chemistry, 22 (1977) 51-61.

[2] I. Dincer, Thermal energy storage systems as a key technology in energy conservation, International Journal of Energy Research, 26 (2002) 567-588.

[3] A. Abhat, Low temperature latent heat thermal energy storage: heat storage materials, Solar Energy, 30 (1983) 313-332.

[4] IEA, Compact thermal energy storage: Material development and system integration., Solar Heating and Cooling Programme, 2008.

[5] J.M. Marı´n, B. Zalba, L.F. Cabeza, H. Mehling, Improvement of a thermal energy storage using plates with paraffin-graphit composite, International Journal of Heat and Mass Transfer, 48 (2005) 2561-2570.

[6] K. Nagano, S. Takeda, T. Mochida, K. Shimakura, T. Nakamura, Study of a floor supply air conditioning system using granular phase change material to augment building mass thermal storage-Heat response in small scale experiments, Energy and Buildings, 38 (2006) 436-446.

[7] C. Alkan, A. Sari, Fatty acid/poly (methyl methacrylate) (PMMA) blends as form-stable phase change materials for latent heat thermal energy storage, Solar Energy, 82 (2008) 118-124.

[8] G. Balasubramanian, M. Ghommem, M.R. Hajj, W.P. Wong, J.A. Tomlin, I.K. Puri, Modeling of thermochemical energy storage by salt hydrates, International Journal of Heat and Mass Transfer, 53 (2010) 5700-5706.

[9] S. Pal, M.R. Hajj, W.P. Wong, I.K. Puri, Thermal energy storage in porous materials with adsorption and desorption of moisture, International Journal of Heat and Mass Transfer, 69 (2014) 285-292.

[10] E.A. Levitskij, Y.I. Aristov, M.M. Tokarev, V.N. Parmon, "Chemical heat accumulators": A new approach to accumulating low potential heat, Solar Energy Materials and Solar Cells, 44 (1996) 219-235.

[11] W. Wongsuwan, S. Kumar, P. Neveu, F. Meunier, A review of chemical heat pump technology and applications, Applied Thermal Engineering, 21 (2001) 1489-1519.

[12] M.A. Tahat, Heat-pump/energy-store using silica gel and water as a working pair, Applied Energy, 69 (2001) 19-27.

[13] B.B. Saha, S. Koyama, J.B. Lee, K. Kuwahara, K.C.A. Alam, Y. Hamamoto, A. Akisawa, T. Kashiwagi, Performance evaluation ofa low-temperature waste heat driven multi-bed adsorption chiller, International Journal of Multiphase Flow, 29 (2003) 1249-1263.

[14] B.B. Saha, S. Koyama, T. Kashiwagi, A. Akisawa, K.C. Ng, H.T. Chua, Waste heat driven dual-mode, multi-stage, multi-bed regenerative adsorption system, International Journal of Refrigeration, 26 (2003) 749-757.

[15] R.d. Boer, W.G. Haije, J.B.J. Veldhuis, Determination of structural, thermodynamic and phase properties in the Na_2S-H_2O system for application in a chemical heat pump, Thermochimica Acta, 395 (2003) 3-19.

[16] V.M.v. Essen, J.C. Gores, L.P.J. Bleijendaal, H.A. Zondag, R. Schuitema, M. Bakker, W.G.J.v. Helden, Characterization of salt hydrates for compact seasonal thermochemical storage, in: The 3rd International Conference of Energy Sustainability ES 2009, San Francisco, California, USA, 2009.

[17] K. Visscher, J.B.J. Veldhuis, Comparison of candidate materials for seasonal storage of solar heat through danamic simulation of building and renewable energy system, in: The 9th International Building Performance Simulation Association, Montreal, Canada, 2005.

[18] K. Visscher, Simulation of thermo chemial seasonal storage of solar heat-material selection and optimum performance simulation, in: 2nd workshop Matlab/Simulink for building simulation, Paris, France, 2004.

[19] V.M.v. Essen, H.A. Zondag, J.C. Gores, L.P.J. Bleijendaal, M. Bakker, R. Schuitema, W.G.J.v. Helden, Z. He, C.C.M.Rindt, Characterization of $MaSO_4$ hydrate for thermochemical seasonal heat storage, Journal of Solar Energy Engineering, 131 (2009) 041014-041011-041017.

[20] C. Ferchaud, H. Zondag, R.d. Boer, C. Rindt, Characterization of the sorption process in thermochemical material for seasonal solar heat storage application, in: The 12th International Conference on Energy Storage, 2012, pp. 1-10.

[21] Y.I. Aristov, New composite adsorbents for conversion and storage of low temperature heat: Activity in the Boreskov Institute of Catalysis, Journal of Heat Transfer Society of Japan, 45(192) (2006) 12-19.

[22] Y.I. Aristov, G. Restuccia, G.Cacciola, V.N. Parmon, A family of new working materials for solid sorption air conditioning systems, Applied Thermal Engineering, 22 (2002) 191-204.

[23] B. Dawoud, Y.I. Aristov, Experimental study on the kinetics of water vapor sorption on selective water sorbents, silica gel and aluminia under typical operating conditions of sorption heat pumps, International Journal of Heat and Mass Transfer, 46 (2003) 273-281.

[24] A. Freni, A. Sapienza, I.S. Glaznev, Y.I. Aristov, Experimental testing of a lab-scale adsorption chiller using a novel selective water sorbent "silica modified by calcium nitrate", International Journal of Refrigeration, 35 (2012) 518-524.

[25] B.B. Saha, A. Chakraborty, S. Koyama, Y.I. Aristov, A new generation cooling device employing $CaCl_2$-in-silica gel-water system, International Journal of Heat and Mass Transfer, 52 (2009) 516-524.

[26] J. Jänchen, D. Achermann, H. Stach, W. Brösicke, Studies of the water adsorption on zeolites and modified mesoporous materials for seasonal storage of solar heat, Solar Energy, 76 (2004) 339-344.

[27] D. Zhu, H. Wu, S. Wang, Experimental study on composite silica gel supported $CaCl_2$ sorbent for low grade heat storage, International Journal of Thermal Sciences, 45 (2006) 804-813.

[28] H. Wu, S. Wang, D. Zhu, Effects of impregnating variables on dynamic sorption characteristics and storage properties of composite sorbent for solar heat storage, Solar Energy, (2007) 864-871.

[29] H. Wu, S. Wang, D. Zhu, Y. Ding, Numerical analysis and evaluation of an open-type thermal storage system using composite sorbents, International Journal of Heat and Mass Transfer, 52 (2009) 5262-5265.

[30] Y.I. Aristov, Challenging offers of material science for adsorption heat transformation: A review, Applied Thermal Engineering, 50 (2013) 1610-1618.

[31] S. Nakabayashi, K. Nagano, M. Nakamura, J. Togawa, A. Kurokawa, Improvement of water adsorption ability of natural mesoporous material by

impregnating with chloride salts for development of a new desiccant filter, Adsorption, 17 (2011) 675-686.

[32] H. Liu, K. Nagano, D. Sugiyama, J. Togawa, M. Nakamura, Honeycomb filters made from mesoporous composite material for an open sorption thermal energy storage system to store low-temperature industrial waste heat, International Journal of Heat and Mass Transfer, 65 (2013) 471-480.

[33] Y.I. Aristov, New family of solid sorbents for adsorptive cooling: material scientist approach, Journal of Engineering Thermophysics, 16(2) (2007) 63-72.

[34] X. Li, H. Li, S. Huo, Z. Li, Dynamics and isotherms of water vapor sorption on mesopourous silica gels modified by different salts, Kinetics and Catalysis, 51(5) (2010) 754-761.

[35] M. Suzuki, Adsorption engineering, Kodansya Ltd., Tokyo and Elsevier Science Publishers B. V., Amsterdam, Japan, 1990.

[36] N.M. Ostrovskii, N.A. Chumakova, N.M. Bukhavtsova, N.V. Vernikovskaya, Y.I. Aristov., Modeling of the limiting step of Water Sorption by Composite Sorbents of the "Calcium Chloride in Porous Matrix" Type, Theoretical Foundations of Chemical Engineering, 41(1) (2007) 83-90.

[37] S. Vyazovkin, Computational aspects of kinetic analysis.: Part C. The ICTAC Kinetics Project — the light at the end of the tunnel?, Thermochimica Acta, 355(1–2) (2000) 155-163.

[38] M.J. Starink, The determination of activation energy from linear heating rate experiments: a comparison of the accuracy of isoconversion methods, Thermochimica Acta, 404(1–2) (2003) 163-176.

5 COMPOSITE MATERIAL MADE FROM LiCl FOR LOW-REGENERATION CHLSOED SORPTION AIR COOLER SYSTEM

Hokkaido University

5.1 INTRODUCTION

The technology of solid-gas chemical heat pump (CHP) has been attracted intense interests due to its effectiveness to utilize renewable energy and store industrial waste heat. Solid-gas CHP is ecological friendly, as the included materials don't utilize Chlorofluorocarbons (CFCs) and Hydrocllorofluorocarbons (HCFCs) as refrigerants [1]. Water has been focused as the refrigerant because of its typical environmentally safety. It is envisaged that a solid-gas CHP system would be very cost effective and would involve minimal maintenance in a long term operation, as it would have very few moving parts. The possibility to use heat sources from 50 to 150°C may be useful in energy saving applications, such as those employing solar energy or waste heat [1].

Recently, the pure chemicals are being researched as reactants to react with water. The SWEAT (Salt Water Energy Accumulation and Transformation) developed by Boer et al. [2, 3] using the sodium sulphide (Na_2S)-water as the working pair have been developed to store 5kWh of heat, and 3kWh of cold which can be combined in various capacities [2]. A fibrous cellulose material was selected to support Na_2S to assure open porosity, mechanical stability, and occasional melting of the salt. Unfortunately, besides their toxicity for environment, salt $Na_2S{\cdot}5H_2O$ and $Na_2S{\cdot}2H_2O$ cannot be dehydrated in summer with an outside temperature of 35°C and a heat source below 80°C.

A first theoretical study at ECN (Energy Research Centre of the Netherlands) on which material is the most suitable for compact seasonable heat storage identified magnesium sulfate ($MgSO_4$) as the most promising material [4] because of low cost, non-toxicity, non-corrosivity and high theoretical energy density. However, it was found that the material was difficult to take up water under practical conditions because of the low reaction rate and the low delivered power. The magnesium chloride ($MgCl_2$) was also confirmed as the most promising material for compact seasonal heat storage. $MgCl_2$ has high practical storage density, fast heat release rate, but it will release hydrochloric acid (HCl) when the regeneration temperature is higher than 140°C, and it is very hygroscopic [5, 6].

Mauran et al. [7] developed a cooling and heating system using water and strontium bromide ($SrBr_2$) impregnated into expanded natural graphite. It is able to store 60 kWh or 40 kWh for the heating or cooling respectively with reactor's total volume of 1 m^3. However, the low heat transfer at interface between the reactive layer and the heat exchanger limits the heating and cooling powers.

Heat pump using reversible $CaCl_2$/water system has been proposed for easy obtainment and low price. Sasaki et al. [8] tested the performance of the reversible $CaCl_2/CaCl_2 \cdot 2H_2O$ reaction to store waste heat. However, the operation condition has to be chosen to avoid the deliquescence temperature and pressure range. The low thermal conductivity in the range of 0.1-0.2 W/(m·K) and agglomeration of the salt resulting low performance is also responsible for its development [9].

Hence, various methods have been developed to solve the low heat and mass transfer problems of pure chemical materials. One method is to prepare composite material with heat transfer promoter [10], such as expanded graphite (EG) [11]. The thermophysical properties and reaction characteristics of composite reactants of $CaCl_2$ and EG have been tested experimentally by Fujioka [12]. The results showed that 10 times of the thermal conductivity and high permeability and reaction rate can be achieved by introducing EG.

Another method to improve the heat and mass transfer by integrating reactant with heat exchanger [10]. Freni et al. [13, 14] tested an advanced solid sorption chiller based on a heat exchanger coated with a compact layer of selective water sorbent: SWS-1L ($CaCl_2$ in mesoporous silica gel). Their results showed a specific power of 150-200 W/kg of adsorbent and a cycle time of only 10-20 min with a cooling coefficient of performance (COP) ranged between 0.15-0.3. Aristov et al. [11, 15, 16] developed an adsorptive cooling system with packed SWS-1L inside a high efficient heat exchanger, with which the cooling COP can achieve 0.6 at regeneration temperature as low as 85-95ºC. Freni et al. [17] utilized a novel composite water sorbent "silica modified by calcium nitrate" (SWS-8L) regenerated lower than 90ºC. With grains of this composite material embedded inside a high thermal efficient aluminum heat exchanger, cooling COP and specific cooling power are 0.51-0.71 and 190-389 W/kg, respectively.

Composite material $LiCl/SiO_2$ has recently been synthesized and studied for water sorption and found promising for various applications [18]. Though $CaCl_2$ is the most ordinary desiccant, LiCl is also well known for its particular hydrophilic property and has been widely used in the dehumidifier and in desiccant cooling systems [19].

The final goal of our research is to develop a sorption cooler with heat source's temperature lower than 80ºC. In this study, in order to achieve a high performance, the composite material with high sorption amount was developed by combining LiCl with (Wakkanai Siliceous Shale) WSS. Next, a lab-scale unit including a reactor packed with this composite material was constructed and tested to evaluate the performance of the composite material working in a sorption cooler. The heating and cooling COP and specific cooling power are focused on to assess whether the developed system using the composite material could potentially contribute to utilize solar energy or low temperature industrial waste heat by producing cold heat without consumption any fossil fuel.

5.2 MATERIAL

For development of the composite material, the lithium chloride (Purity >98.0%, Wako Pure Chemical Industries, Ltd.) was used as the chemical material. Wakkanai siliceous shale (WSS), a kind of mesoporous material was used as the matrix of the composite material. WSS is a type of siliceous mudstone that is widely distributed in the northern part of Hokkaido in Japan, whose main composition is silicon dioxide (SiO_2) [20]. Micro powders of WSS were adopted as one of the component of the composite material, and the picture of WSS mudstone and micro powders is shown in Fig. 5-1. The particle size distribution of WSS micro powders can be checked in Fig. 5-2, from which it can be known that the particle size is mainly distributed in the range of 1 to 20 μm. The WSS was adopted because of its porous property, and its main pores distributed from 4 to 20 nm [21].

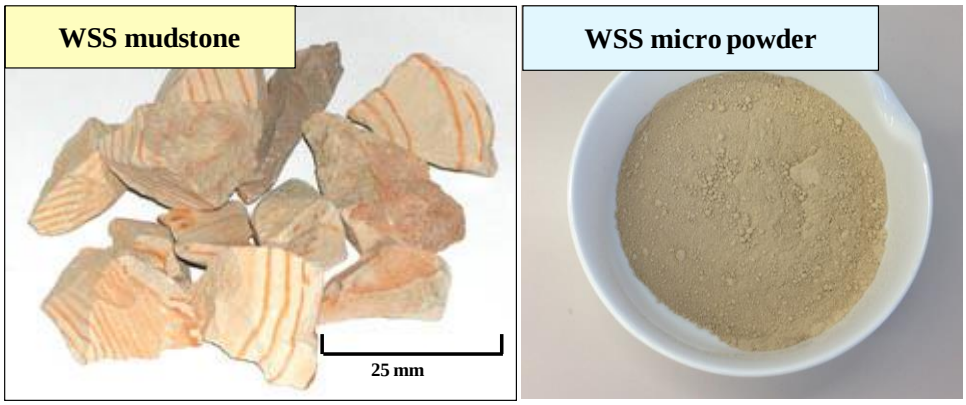

Fig. 5-1 Picture of WSS mudstone (left) and micro powder (right)

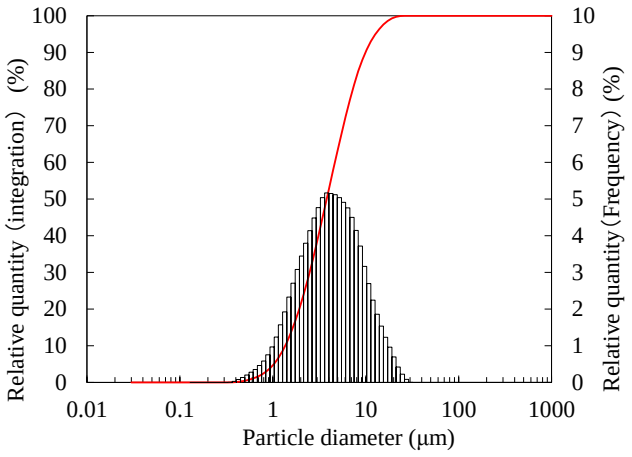

Fig. 5-2 Particle distribution of WSS micro powders [22]

5.2.1 Manufacturing procedure of the composite material

The mixing weight ratio *x* of LiCl and WSS is defined as Eq. 5-1.

$$x = \frac{m_{LiCl}}{m_{LiCl} + m_{WSS}} \tag{5-1}$$

The common preparation procedure is to impregnate an aqueous solution of inorganic salt into porous matrices, dry and calcine them to deposit the salt inside the pores of porous matrices. In this research, micro powders of the WSS were used as the matrices, and the manufacturing procedures are shown in Fig. 5-3:

(1) The micro powders of WSS were dried at 150ºC in an oven for 24 hours.

(2) The dry LiCl weight was calculated according to Eq. 5-1 by setting *x* as 10, 20, 30, and 40%. The LiCl solution was prepared at room temperature then.

(3) The dry WSS powders were immersed into the solution of LiCl prepared in step (2), and LiCl + WSS slurry was made.

(4) The LiCl + WSS slurry was vacuumed in a vacuum container to 3.14×10^3 Pa (the saturated water vapor pressure at 25ºC) for 20 minutes.

(5) The LiCl + WSS slurry was dried in the oven again at 150ºC for almost 24 hours until the dry composite material obtained.

The original ceramic material is denoted as WSS, and the other four LiCl-supported composite ceramic samples are denoted as WSS + 10 wt% LiCl, WSS + 20 wt% LiCl, WSS + 30 wt% LiCl, and WSS + 40 wt% LiCl, respectively.

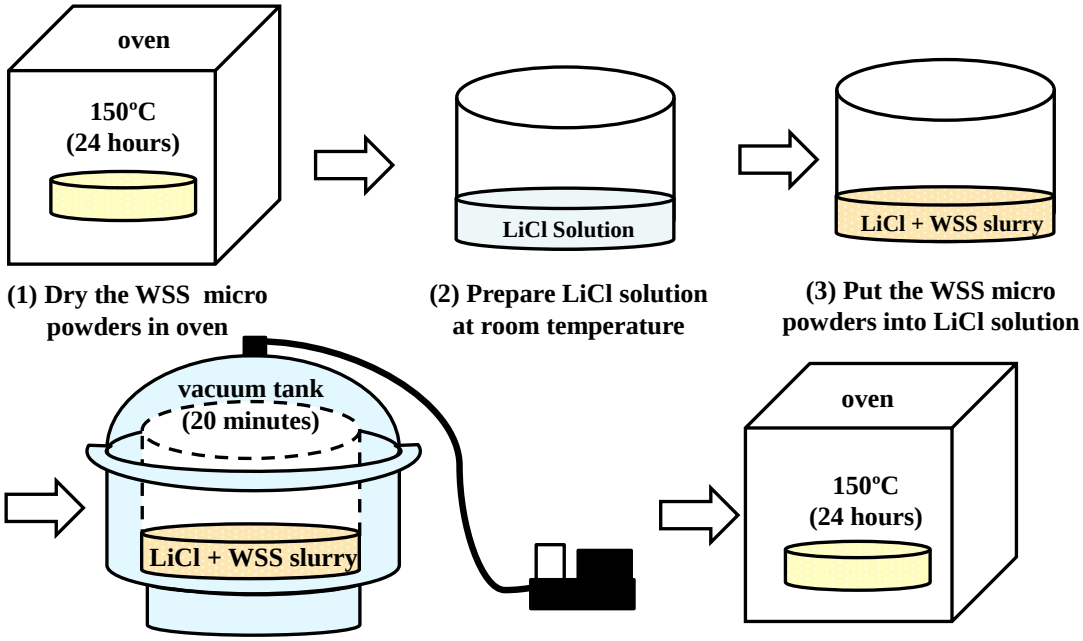

Fig. 5-3 Manufacturing procedure of the composite material

5.2.2 Physical properties of the developed composite material

The pore volume and specific surface area of the mesoporous material were measured by the standard nitrogen gas sorption/desorption measurement. The pore volume distributions of the original WSS micro powders and the other four composite samples with different impregnated amount of LiCl are presented in Fig. 5-4. It can be observed that parts of the pores of the original ceramic material were filled by LiCl, and the pore volume decreased with the increasing supporting amount of LiCl.

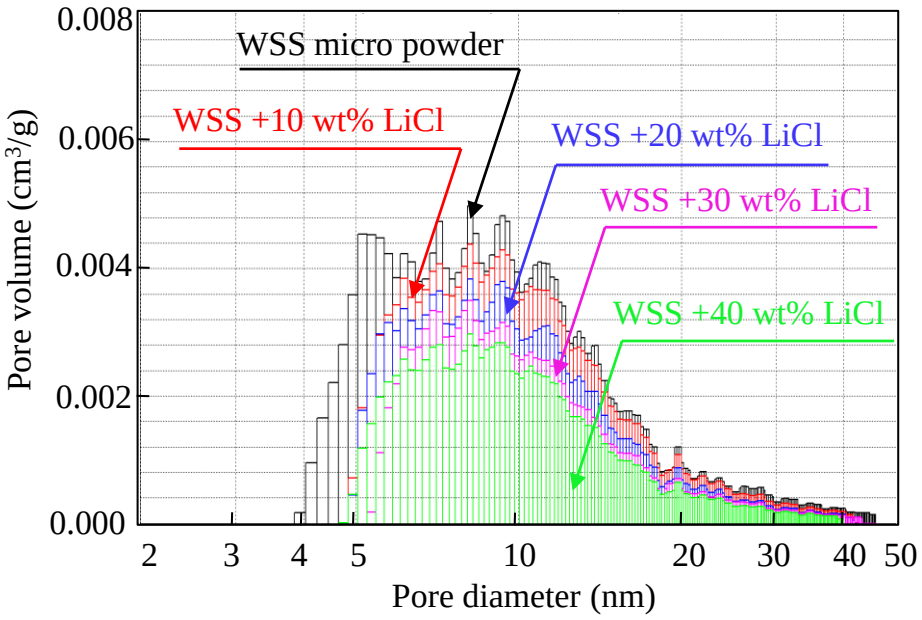

Fig. 5-4 Pore distribution of WSS micro powders and other four composite materials

Table 5-1 Physical properties of the WSS micro powders and the other four composite materials

Properties \ Samples	WSS	WSS+10wt% LiCl	WSS+20wt% LiCl	WSS+30wt% LiCl	WSS+40wt% LiCl
Salt content (%)	0	10	20	30	40
Specific surface area (m^2/g)	126.2	91.2	77.03	63.26	58.2
Pore volume (cm^3/g)	0.34	0.293	0.24	0.213	0.186
True density (kg/m^3)	2150	2142	2133	2125	2117

The composite material's specific surface area was calculated by the Brunauer-Emmett-Teller (BET) equation. The fine pore volume calculated by Barrett, Joyner, and Halenda (BJH) is presented in Table 5-1 along with the true density. The specific surface area of the WSS decreased from 126.2 m^2/g to 58.2 m^2/g after being

impregnated with 40 wt% LiCl, and the pore volume decreased from 0.34 to 0.186 cm^3/g. From the physical characteristics (cf. Table 5-1 and Fig. 5-4) of the WSS and the other four composite samples, it is readily understood that the LiCl was generally located inside the pores, which mainly caused the decrease of the specific surface area, pore volume and porosity.

5.2.3 Isobaric chart of the composite material/water working pair

5.2.3.1 Testing apparatus

The isobaric sorption diagram apparatus is shown in Fig. 5-5. A Thermogravimetry/Differential Thermal Analyzer (EXSTAR TG-DTA6200, SEIKO SII) is connected with a water container working as an evaporator/condenser controlled by a temperature control bath. The TG/DTA and the water container are connected in a vacuumed and closed condition.

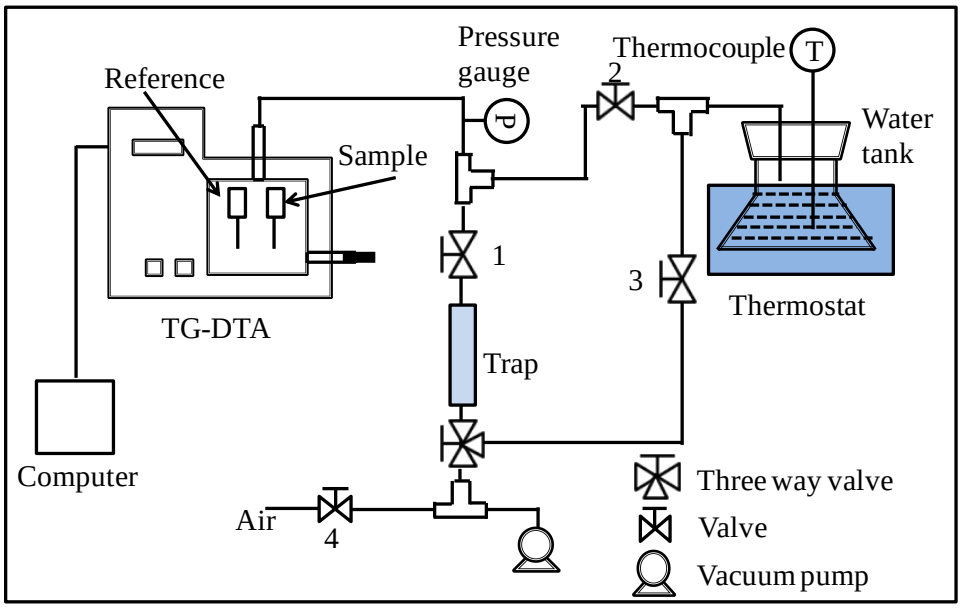

Fig. 5-5 Schematic drawing of the experimental apparatus employed

The tested material was placed in a platinum cell, which was put next to the reference cell in the device. The platinum cell was heated by an electric furnace, whose temperature was directly measured by a thermocouple installed inside the TG/DTA. Water vapor is introduced to the TG/DTA via the valve 2. Purified water was kept in a

vacuum glass container, whose temperature was controlled by a water circuit connected to the circulating thermal bath.

5.2.3.2 Experimental procedure

About 10 mg composite material is installed in the platinum cell of the TG/DTA. The temperature of the water vapor vessel is adjusted to the required testing temperature (corresponding to a certain saturation pressure) for sorption process. The temperatures of the connecting piping and valves have to be adjusted and controlled to the required temperature. The testing cell and the evaporator/condenser are vacuumed to the appropriate pressures by the connected vacuum pump. The material is heated up at a heating rate of 5 K/min and kept at a constant temperature at 150ºC for 10 min to get the dry condition of the material. The joint valve 2 connecting the TG/DTA and the water container is open. After that, the water vapor sorption occurs with the material temperature cooled down gradually to each setting temperature. The equilibrium sorption amount will be reached at each setting temperature. This sorption process at each setting temperature finished until reaching a certain low temperature. The obtained weight and temperature data are to be recorded every second during the testing period by a computer.

5.2.3.3 Isobaric chart of water sorption on the composite material

The water sorbed amount of each tested material was recorded in the temperature range of 25-150ºC at different partial pressure ranging from 1 kPa to 6 kPa. The water content was calculated as $\omega = m(P_{H_2O}, T) / m_0$.

Fig. 5-6 (a) (b) (c) and (d) shows the water vapor sorption isobars on the tested four composite materials: WSS + 10 wt% LiCl, WSS + 20 wt% LiCl, WSS + 30 wt% LiCl and WSS + 40 wt% LiCl at different partial water vapor pressures measured by the above revised TG/DTA. All the curves were found to be similar but shifted and partially extended along the temperature axis [23]. However, unlike the composite material impregnated with calcium chloride, there is no apparent plateau found in each curve no matter the water vapor pressure changes. It indicates that the formation of a solid crystalline hydrate may not happen in the testing temperature and pressure range

in the sorption process. This is probably due to the strong deliquescence of LiCl and the narrow temperature and pressure range tested in this section. It can be understood from Fig. 5-6 that water sorption on the developed composite materials depends on both temperature and partial vapor pressure, so the equilibrium is bivariant.

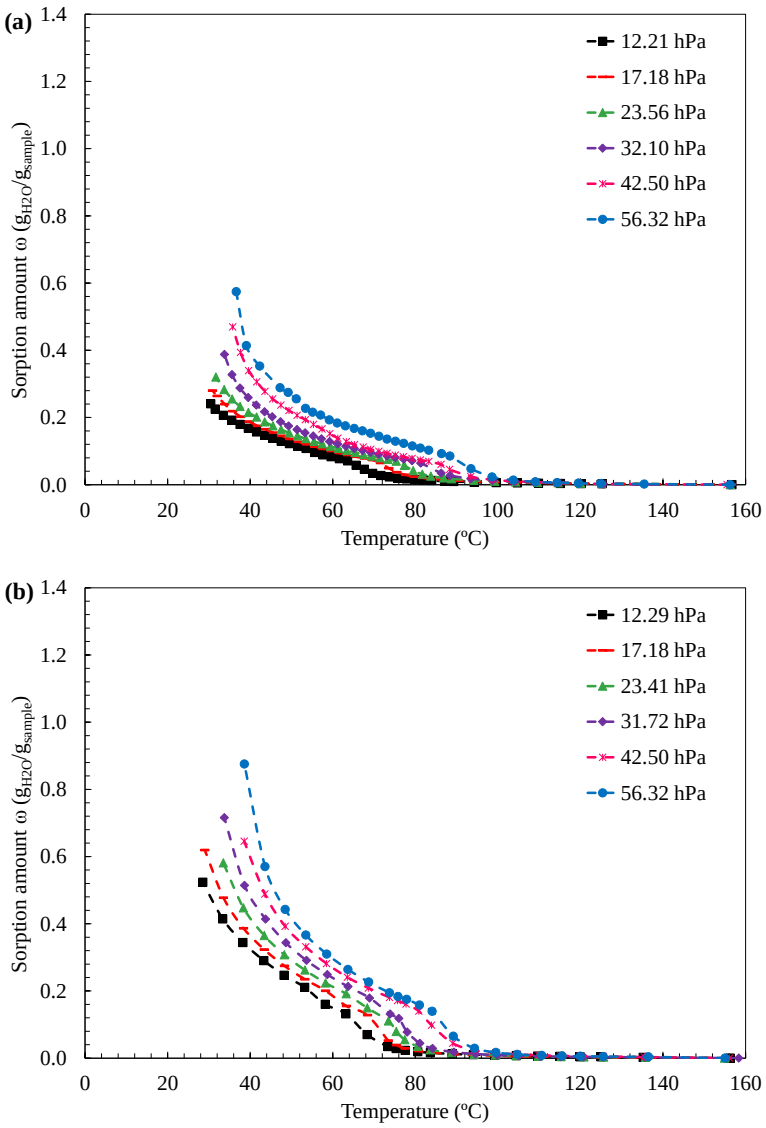

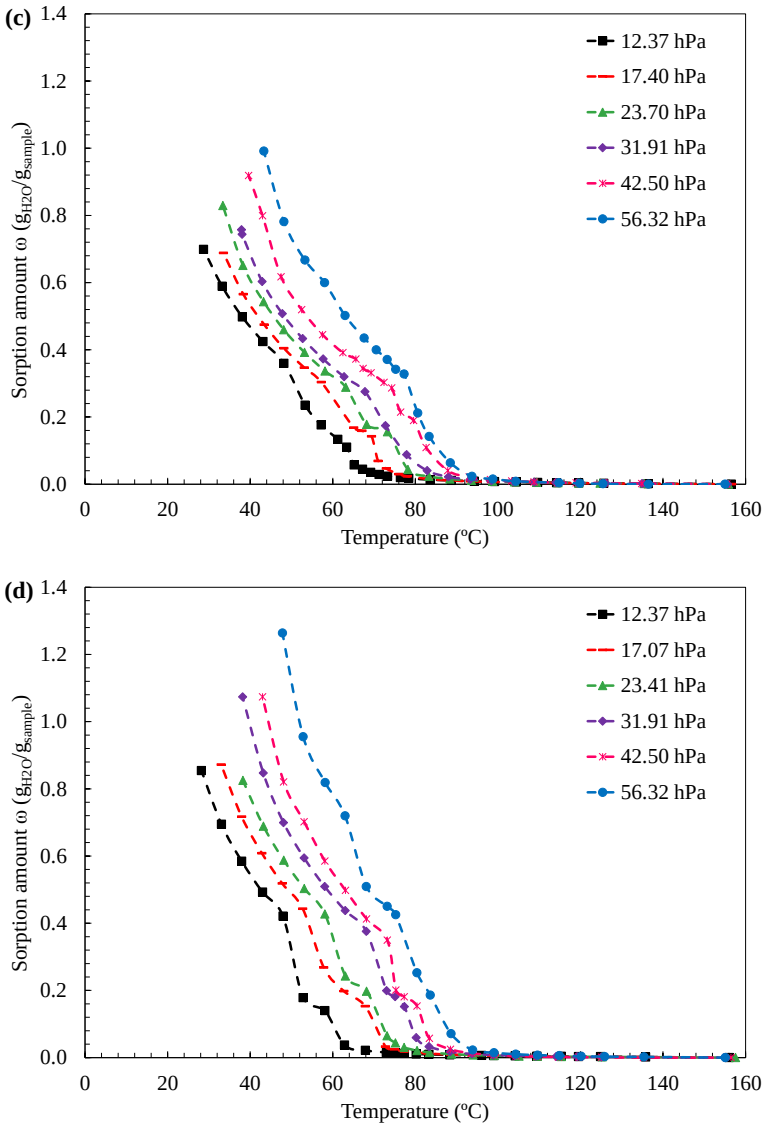

Fig. 5-6 Isobaric diagrams of the composite material (a) WSS + 10wt% LiCl, (b) WSS + 20wt% LiCl, (c) WSS + 30wt% LiCl and (d) WSS + 40wt% LiCl

Water sorption isosters on the tested four composite materials are shown in Fig. 5-7, which are straight lines in the $\ln(P_{H2O})$ vs. $1/\boldsymbol{T}$ presentation as follows [23]:

$$\ln(P_{H_2O}) = A(\omega) + B(\omega)/\boldsymbol{T} \qquad 5\text{-}2$$

$$\Delta H = B(\omega)R \qquad 5\text{-}3$$

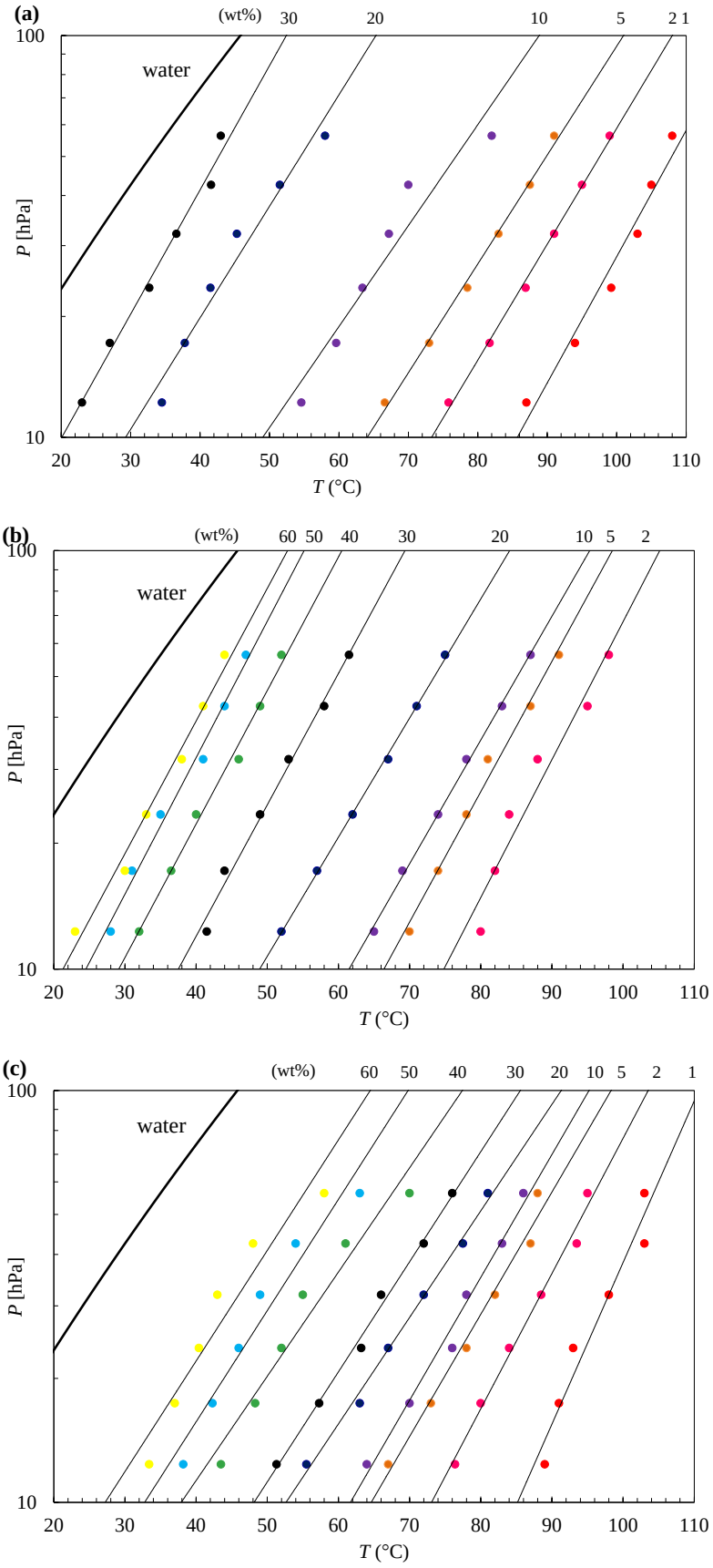
(a)
(wt%) 30 20 10 5 2 1
water
100
10
P [hPa]
20 30 40 50 60 70 80 90 100 110
T (°C)
(b)
(wt%) 60 50 40 30 20 10 5 2
water
100
10
P [hPa]
20 30 40 50 60 70 80 90 100 110
T (°C)
(c)
(wt%) 60 50 40 30 20 10 5 2 1
water
100
10
P [hPa]
20 30 40 50 60 70 80 90 100 110
T (°C)

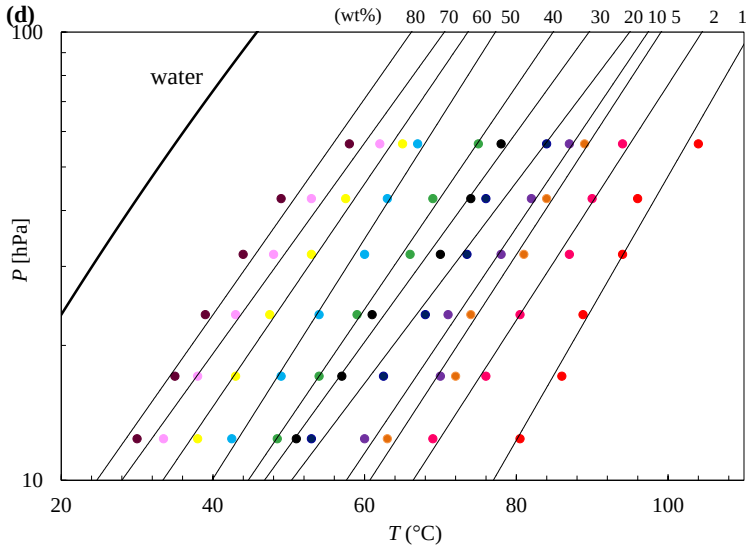

Fig. 5-7 Water sorption isosters on the composite material (a) WSS + 10wt% LiCl, (b) WSS + 20wt% LiCl, (c) WSS + 30wt% LiCl and (d) WSS + 40wt% LiCl

Table 5-2 Isosteric sorption heat (kJ/mol) of the four composite materials with different sorption amount

ω / Material	5%	10%	20%	30%	40%	50%	60%	70%	80%
WSS + 10 wt% LiCl	64.09	56.42	54.33	55.47	–	–	–	–	–
WSS + 20 wt% LiCl	74.66	68.17	61.52	63.19	59.86	60.11	56.54	–	–
WSS + 30 wt% LiCl	69.75	69.01	57.63	57.95	52.97	54.44	52.59	–	–
WSS + 40 wt% LiCl	63.06	60.58	57.65	49.83	50.96	53.30	54.91	50.18	46.42

The slope depends on the water content ω and the isosteric water sorption heat can be calculated by Eq. 5-3, in which R is the universal gas constant. The calculated isosteric sorption heat is presented in Table 5-2. For ω > 10% the sorption heat appears to be close to 50 kJ/mol, though there are some discrepancies for WSS + 20 wt % LiCl due to some inevitable measuring errors. While, a significant increase in isosteric sorption heat at ω < 10% is caused by the formation of solid hydrates, in which water molecules

are bound stronger. The sorption heat of the composite material related to the amount of salt remained constant in the range $\omega > 0.2$ indicating that water was mainly sorbed by the impregnated salt rather than by the porous supporting material.

5.2.4 Isothermal sorption properties of the developed composite material

The water vapor sorption isotherms of the WSS and pure LiCl were tested at 25ºC at each relative humidity condition (see Fig. 5-8) by the water vapor sorption analyzer Hydrosorb HS-1 (Quantachrome Instruments).

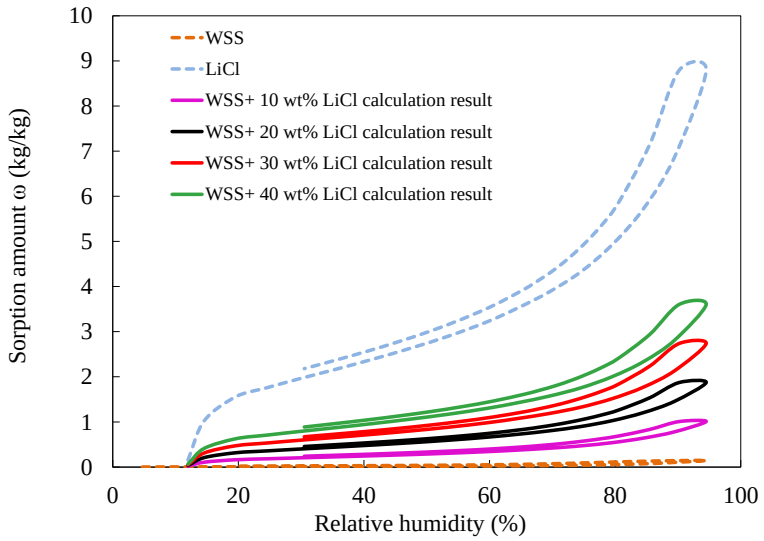

Fig. 5-8 Isothermal sorption amount of the composite materials

The isotherm sorption amounts of the other four composite materials were calculated according to the impregnated salt amount and the sorption properties of the WSS and LiCl following Eq.5-4.

$$\omega = \omega_{WSS} \cdot (1-x) + \omega_{LiCl} \cdot x \qquad 5\text{-}4$$

The calculated isotherm sorption amount of the composite material is illustrated in Fig. 5-8, from which it can be clearly seen that the material with higher salt content exhibits high sorption amount. According to our previous research result, when the temperature

is lower than 100ºC, the equilibrium sorption amount is essentially independent of temperature and only related to the relative humidity, as shown in Eq. 5-5.

$$\omega = f(RH) \qquad 5\text{-}5$$

The composite material developed in this research interacts with water vapor based on the following mechanisms [11]: a) Heterogeneous adsorption on the pore surface of ceramic material; b) Chemical reaction (chemical adsorption) between vapor and the salt; c) Liquid absorption by the hydrate $LiCl{\cdot}nH_2O$. The latter two mechanisms were the main sorption behavior of the composite material [11]. The isotherm sorption line of WSS + *x* wt% LiCl indicates that crystalline hydrates were formed at low relative humidity, and then salt solution was formed particularly at a high relative humidity, which filled the pores either completely or partially. It is this volume filling that leads to the high sorption capacity of composite materials [11]. By adding LiCl, the driving force of the sorption becomes the interaction of the water vapor with the hygroscopic LiCl.

5.2.5 Specific heat of the composite material with different sorption amount

The specific heat is a fundamental property of thermal energy storage material. In this research, the measurement of specific heat of the composite material was conducted in a wide temperature range (5-90ºC) to evaluate the thermodynamic performance of the studied composite material. The measurement was performed by a differential scanning calorimetry (DSC) over the composite material with different water sorption amount. The pre-preparation of the composite material with a certain amount of water sorbed was conducted in a constant temperature & humidity chamber. First the testing material was dried at 150ºC for 1 day to get its dry weight. The dry material would be put into the constant temperature & humidity chamber for one day to get its equilibrium sorption amount at the setting temperature and humidity condition before being sealed. The high sorption amount can be obtained by setting high relative humidity according to Fig. 5-8.

The specific heat for the dry composite material with different LiCl content is same according to our experimental result, therefore, only the effect of water content on the

specific heat is investigated. The obtained results are presented in Fig. 5-9, which shows a linear behavior of the specific heat as a function of the temperature for a specific sorption amount. When the sorption amount reaches to a certain value (>0.8 kg/kg), the specific heat seems no big change.

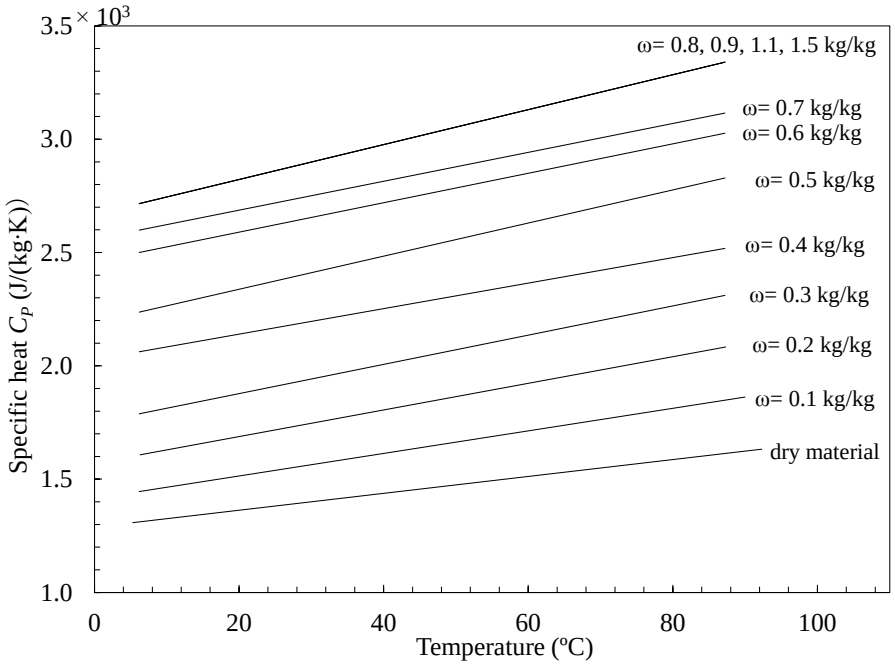

Fig. 5-9 Specific heat of the composite material at different water contents

Activation energy

5.2.6 Activation energy

The activation energy of water desorption was investigated by TG/DTA with inside water vapor condition maintained at a constant absolute pressure 17 hP. The dry weight of the testing material was 6-10 mg. At first, the sample was heated up to 150ºC for 30 minutes under continuous pumping during which the absolute pressure is about 500 Pa. Then the measuring cell was disconnected from the vacuum pump and connected to an evaporator maintained at 15ºC (17 hPa), and then the material was started to be cooled down to T_0 (T_0 = 35ºC (WSS + 10 wt% LiCl), T_0 = 35ºC (WSS + 20 wt% LiCl), T_0 = 50ºC (WSS + 30 wt% LiCl), T_0 = 57ºC (WSS + 40 wt% LiCl)), at which time the material can sorb water until reaching a constant weight. The desorption activation energy was tested by heating the material sorbed a certain amount of water at a constant

heating rate while keeping connecting with the water evaporator, which making sure the water vapor pressure is 17 hPa during. As the temperature becomes high enough, the material will desorb gradually. In the measurement, the material weight change, material temperature and weight change rate was recorded.

The transformation rate can be expressed by a single step kinetic equation with one function depending solely on the temperature, and the other one depending solely on the extent of conversion rate, *a* [24]:

$$a = \frac{m_{H_2O}(\boldsymbol{T})}{m_{s,dry}} / \frac{m_{H_2O}(\boldsymbol{T_0})}{m_{s,dry}} \tag{5-6}$$

$$\frac{da}{dt} = k(\boldsymbol{T})\, f(a) \tag{5-7}$$

where, the rate constant $k(\boldsymbol{T})$ is generally assumed to follow Arrhenium equation yielding

$$\frac{da}{dt} = A\exp(-\frac{E}{R\boldsymbol{T}})\, f(a) \tag{5-8}$$

In the calculation of activation energy, the peak method (maximum rate method) [25] is adopted. Take the time differential of the Eq. 5-8 at the maximum desorption rate point, the following equation can be obtained.

$$\left(\frac{d^2a}{dt^2}\right)_P = 0 \tag{5-9}$$

$$\ln(\frac{\beta}{\boldsymbol{T}_p^{\,2}}) = \ln\left[(-\frac{df(a)}{a})_P \cdot \frac{AR}{E}\right] - \frac{E}{R\boldsymbol{T_P}} \tag{5-10}$$

Where T_P is the peak desorption temperature and β is the heating rate. By taking the linear dependencies of $\ln(\beta/\boldsymbol{T_P}^2)$ versus $1/\boldsymbol{T_P}$ at different heating rate, the activation energy for desorption can be obtained.

$$E = R \cdot \frac{d\ln(\frac{\beta}{\boldsymbol{T}_p^{\,2}})}{d\frac{1}{\boldsymbol{T_P}}} \tag{5-11}$$

The weight change rate DTG measured by TG/DTA for the four samples were illustrated in Fig. 5-10 (a), (b), (c) and (d), from which the maximum temperature for desorption can be determined. It is obviously to see that for all the four tested samples there are apparently two desorption rate peaks. It is considered that for the hygroscopic salt impregnated composite material, the first portions of water evaporate from less concentrated solutions, and this desorption process is similar with water evaporation. With temperature increases, more concentrated solutions or crystalline hydrates are going to be dehydrated, which need a higher temperature.

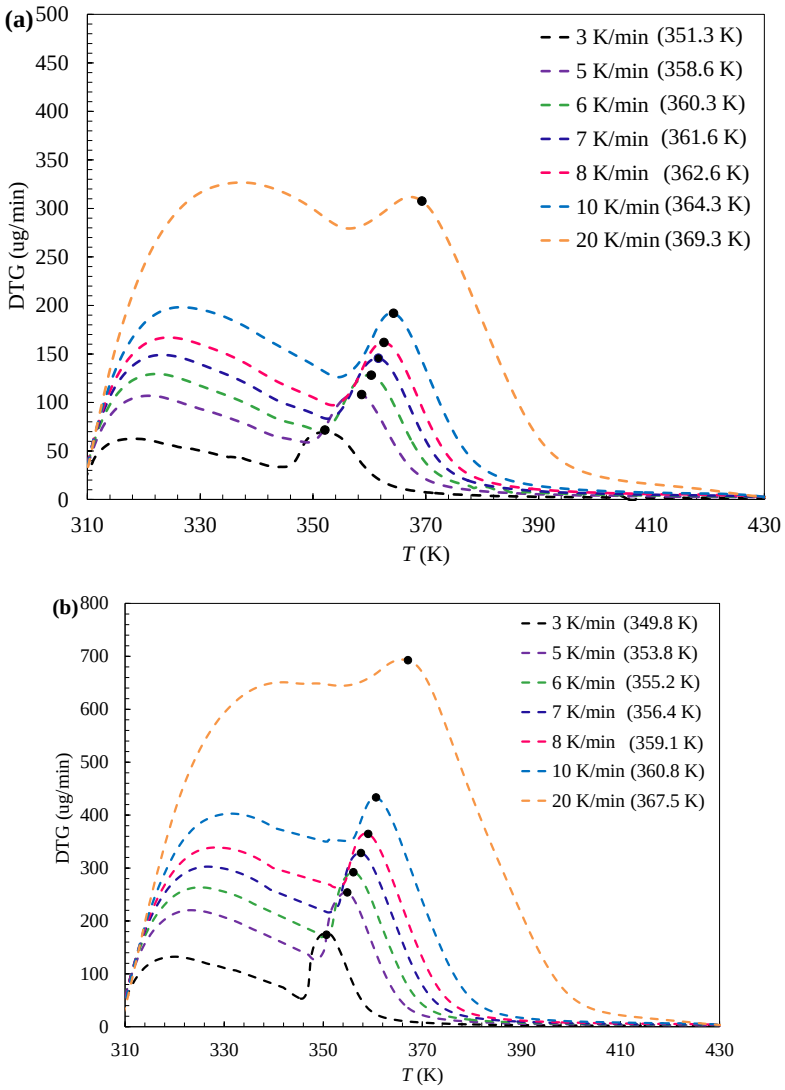

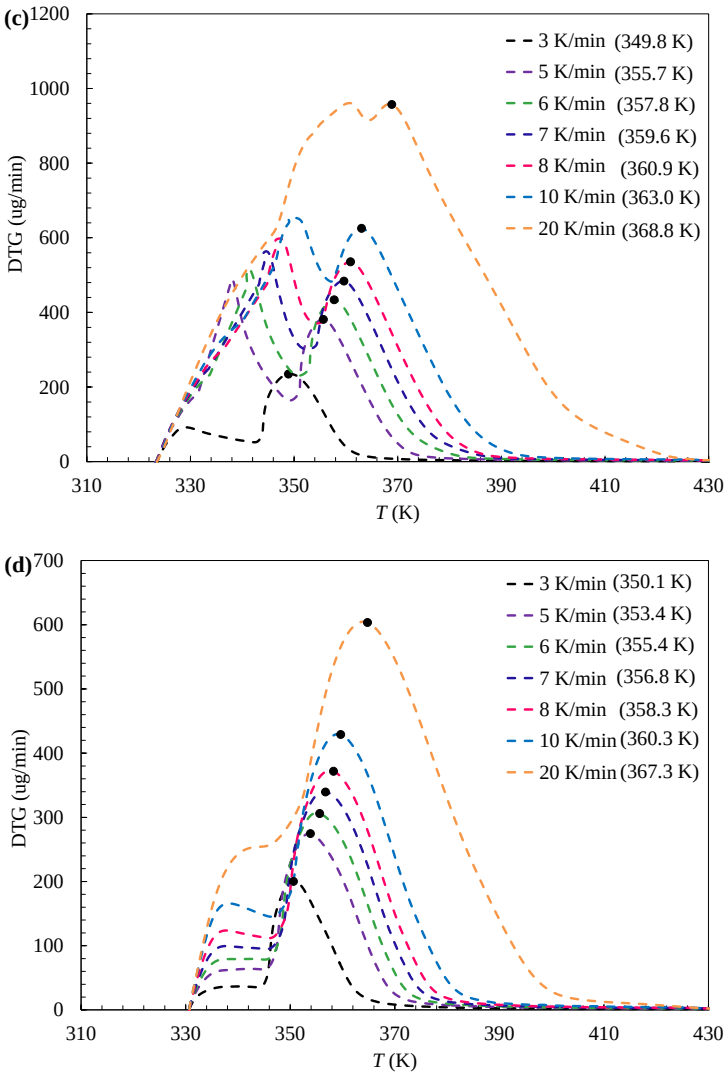

Fig. 5-10 Weight change rate DTG changes with temperature of the (a) WSS + 10 wt% LiCl and (b) WSS + 20 wt% LiCl and (c) WSS + 30 wt% LiCl and (d) WSS + 40 wt% LiCl

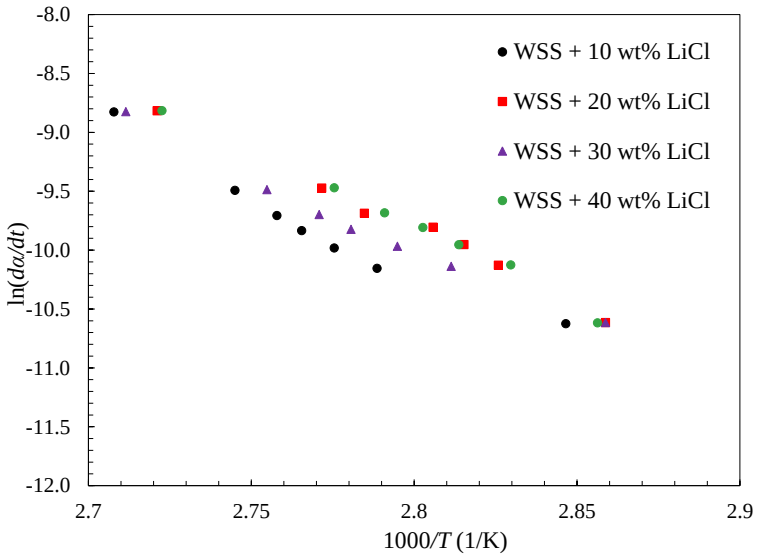

Fig. 5-11 Linear dependence between $\ln(\beta/T_P^2)$ versus $1/T_P$ of water desorbed from the four tested materials

Table 5-3 Activation energies of water desorption from the tested four samples

Samples / Properties	WSS	WSS +10 wt% LiCl	WSS +20 wt% LiCl	WSS +30 wt% LiCl	WSS +40 wt% LiCl
$d(\ln(\beta/T_P^2))/d(1/T_P)$	10.089	12.835	12.657	12.02	13.098
Degree of fitting R^2	0.994	0.9504	0.9904	0.9852	0.9933
E (kJ/mol)	83.8	106.7	105.2	99.9	108.9

The linear dependence between $\ln(\beta/T_P^2)$ versus $1/T_P$ of water desorbed from the four tested samples are shown in Fig. 5-11. The slope of the linear relation between $\ln(\beta/T_P^2)$ and $1/T_P$ and the calculated activation energy by Eq. 5-11 are given in Table 5-3. The activation energies of water desorbed from four samples with different LiCl amount are around 105 kJ/mol, which is higher than the activation energy of the pure WSS. This is probably because the acting force between water molecules and the salt became stronger than the surface of the WSS. The key point is that the desorption activation energy of sample with higher salt content is same as that of the one with low salt content when the salt weight content is limited in 40%. This effect is probably due to

the same phenomena either the smaller size of salt nano-crystallites deposited on the matrix surface from less concentrated salt solution or by the salt-matrix interaction for the different salt content.

5.3 EXPERIMENTS OF SMALL SCALE CHEMICAL HEAT PUMP

5.3.1 Operation principle of the sorption cooling system

In a typical gas-solid heat pump configuration, a material is separated into two components by heating (endothermic or heat storage process), due to which the components (dry composite material and water in this research) are stored in separate vessels and are recombined to generate heat (exothermic or heat release process) when it is needed [26].

There are usually two containers: one is reactor, and the other one is evaporator/condenser. In the heat release step, the water vapor evaporated from the evaporator flows to the high temperature reactor side after opening the connecting valve due to the pressure difference between the two containers. The exothermic process of the material at high temperature level with the water vapor takes place in the reactor. The cold heat can be obtained by water evaporation [27]. The heating/cooling isosteric steps were considered completed when the pressure of the reactor reached the condenser/evaporator pressure respectively. In the heat storage step, the regeneration heat is stored by decomposition of the material with a certain amount of water sorbed in the high temperature side reactor. The produced water vapor flows into the low temperature side condenser due to a pressure difference and then condenses by releasing low temperature heat.

5.3.2 Description of the experimental setup

The schematic diagram of the experimental setup is shown in Fig. 5-12. The main components are a reactor (high temperature side) and a condenser/evaporator (low temperature side).

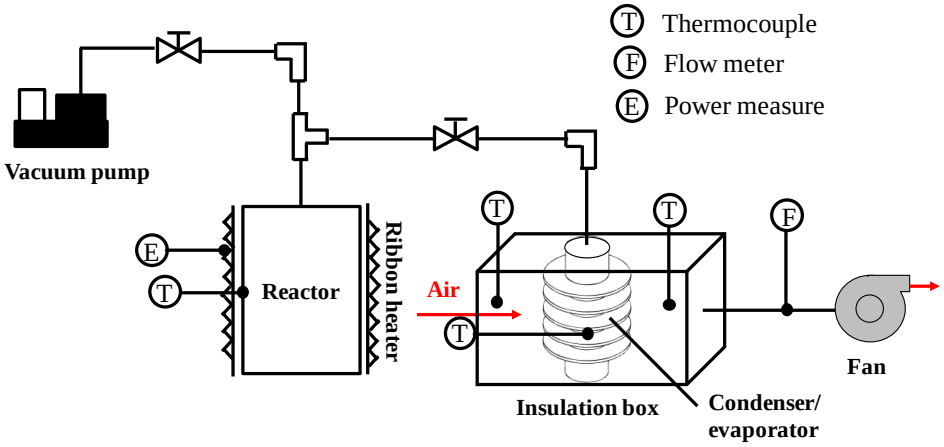

Fig. 5-12 Schematic of the testing sorption cooler

The reactor with a dimension of 50 mm × 50 mm × 20mm (cf. Fig. 5-13) is connected to a vacuum pump and a condenser/evaporator made of fin-tube. The external source of thermal energy for heating of the reactor is a ribbon electric heater, surrounding the reactor to regenerate the material during desorption process. The temperature of the heater is controlled by a temperature controller. The consumed electricity is recorded by a power measure (WT 210, Yokogawa Electric Corporation). The whole device is put into a constant temperature chamber to provide heating/cooling energy to evaporator/condenser of the experimental device. The cooling/heating heat produced in the evaporator/evaporator can be taken away by the flowing air operated by a fan, whose flow rate is measured by a flow meter, and inlet and outlet temperatures are measured by two Pt thermocouples. The temperature of the reactor in sorption process (heat release process) is maintained by a hot air producer, with which the sorption heat can be taken away. The temperature measurements of reactor and condenser/evaporator were performed through two K type thermocouples pasted on the surface of the reactor and condenser/evaporator, respectively. All components are thermally insulated to prevent heat dissipation. A vacuum pump is used for initial out-gassing of the whole system including the reactor and evaporator/condenser. The testing facility is equipped with a data acquisition.

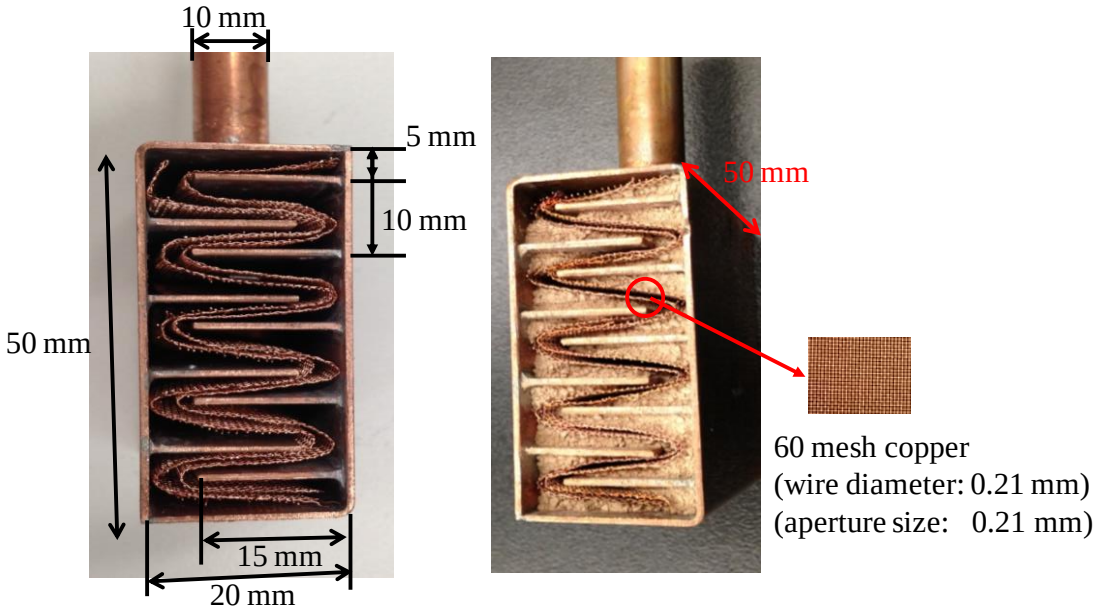

Fig. 5-13 Picture of reactor with inner installed fins and dual layers of meshes before (left) and after (right) filled with material

5.3.3 Experimental procedure

Table 5-4 shows the information about the reactor and packed material during experiments. The reactor shows good heat transfer and mass transfer properties due to the high heat transfer area and installed mass transfer passages, respectively. The testing procedure was the following:

(1) The initial out-gassing of the reactor, condenser/evaporator is done first.

(2) The connection valve between the evaporator and the reactor is open to start the sorption process and the valve is closed after reaching the setting operation time.

(3) The condenser temperature is set as T_{con}. The water sorbed material is heated by the ribbon heater. The connection valve between the condenser and the reactor is open to start the desorption process until the reactor temperature reaching the setting regeneration temperature T_{re}. The valve is closed after the operation time.

(4) The reactor is cooled until reaching the setting temperature of the sorption process T_{con}; and the temperature of the evaporator is set as T_{ev}.

Table 5-4 Information about the reactor and packed material

Terms	WSS +10 wt% LiCl	WSS +20 wt% LiCl	WSS +30 wt% LiCl	WSS +40 wt% LiCl
Inner volume of the reactor (L)	0.05			
Weight of the reactor (g)	177.82	176.37	176.37	176.37
Heat transfer surface area per unit volume (m^2/m^3)	450			
Grain size (μm)	1-20			
Weight of the filled material (g)	15.83	18.44	18.25	16.91
Filled weight of LiCl (g)	1.58	3.69	5.48	6.76
Maximum water sorption amount (g/g) at 12ºC	1	2	3	4

5.3.4 Evaluation parameters

Several tests were carried out considering working conditions typical for cooling machines: (T_{ev} = 12ºC, T_{con} = 30ºC, T_{re} = 80ºC), which was reported in an isosteric chart of water sorption on the composite material WSS + 40 wt % LiCl in Fig. 5-7. Fig. 5-7 shows that the composite material with higher salt content can exchange more water during sorption/desorption processes, even when the regeneration temperature is as low as 80ºC and the condensation temperature is 30ºC.

The testing condition was characterized by a specific cycle time and inlet air temperature, outlet air temperature, temperatures of the reactor and condenser/evaporator. The experimental data measured for each working condition was properly treated in order to calculate the performance of the sorption air cooler under test. In particular, the amount of heating and cooling energy provided or removed from a specific component was calculated considering the energy transfer between the flowing air and the air cooler.

The effective cooling power q_C was calculated by the temperature difference of the inlet and outlet air temperature and mass flow amount of the air according to Eq. 5-12. Then the mass and volumetric specific cooling power q_{SC} and q_{VC} can be obtained by

the ratio between the effective cooling power and the filling amount of the composite material, the volume of the reactor, respectively.

$$q_C = Q_a \rho_a C_p (T_{a,in} - T_{a,out}) \quad 5\text{-}12$$

$$q_{SC} = q_C / m \quad 5\text{-}13$$

$$q_{VC} = q_C / \boldsymbol{V} \quad 5\text{-}14$$

The obtained condensation heating power q_H in desorption process is calculated according to Eq.5-15. The mass specific and volumetric specific heating power q_{SH} and q_{VH} are defined same as specific cooling power as shown in Eq. 5-16 and Eq. 5-17.

$$q_H = Q_a \rho_a C_p (T_{a,out} - T_{a,in}) \quad 5\text{-}15$$

$$q_{SH} = q_H / m \quad 5\text{-}16$$

$$q_{VSH} = q_H / \boldsymbol{V} \quad 5\text{-}17$$

The cooling COP considering total electricity consumption $\mathrm{COP}_{C,total}$ and heating COP considering total electricity consumption $\mathrm{COP}_{H,total}$ as parameters evaluating the performance of the whole operating system were calculated as the ratio between the cooling/heating effect generated in the evaporator/condenser and the average amount of thermal energy supplied in desorption process.

$$\mathrm{COP}_{C,total} = \frac{Q_C}{E_{total}} = \frac{\int_0^t q_C \, dt}{\int_0^t P_e \, dt} \quad 5\text{-}18$$

$$\mathrm{COP}_{H,total} = \frac{Q_H}{E_{total}} = \frac{\int_0^t q_H \, dt}{\int_0^t P_e \, dt} \quad 5\text{-}19$$

The cooling COP only considering necessary regeneration heat $\mathrm{COP}_{C,re}$ and heating COP only considering necessary regeneration heat $\mathrm{COP}_{H,re}$ are calculated by Eq. 5-20 and Eq. 5-21, respectively. The two COPs are thought to be able to improve the built system.

$$\mathrm{COP}_{C,re} = \frac{Q_C}{E_{re}} = \frac{\int_0^t q_C \, dt}{(\Delta H)(\Delta\omega)m / M + C_P m(1+\omega)(T_{re} - T_{con})} \quad 5\text{-}20$$

$$\mathrm{COP}_{H,total} = \frac{Q_H}{E_{re}} = \frac{\int_0^t q_H \, dt}{(\Delta H)(\Delta\omega)m / M + C_P m(1+\omega)(T_{re} - T_{con})} \quad 5\text{-}21$$

5.4 RESULTS AND DISCUSSION

For the testing material, it will undergo the following four steps [13]: (1) the isosteric heating: the material is heated by the heater surrounded the reactor until reaching the pressure of condensation; (2) the desorption phase: condenser and reactor are connected and the material is still heated; (3) the isosteric cooling: the material is cooled until reaching the pressure of evaporation; (4) The sorption process: the connection valve is open and the evaporated water vapor from evaporator will be sorbed by the material in the reactor.

5.4.1 Sorption process results

The sorption process experiments were performed at evaporation temperature of 12°C, regeneration temperature of 80ºC, condensation temperature of 30ºC, and operation time of 60 min. The testing material is WSS + 40wt% LiCl. The temporal changes of water temperature inside the evaporator and temperatures of the inlet and outlet air, which flows past the fin tube evaporator, are shown in Fig. 5-14, as well as the reactor's temperature. It can be observed that the temperature of the water inside evaporator decreases fast when the sorption process starts, and the minimum temperature can even decrease to 7ºC. The temperature difference about 3ºC of the inlet and outlet air temperature is considered as the result of effective heat exchange with the fin-tube type evaporator.

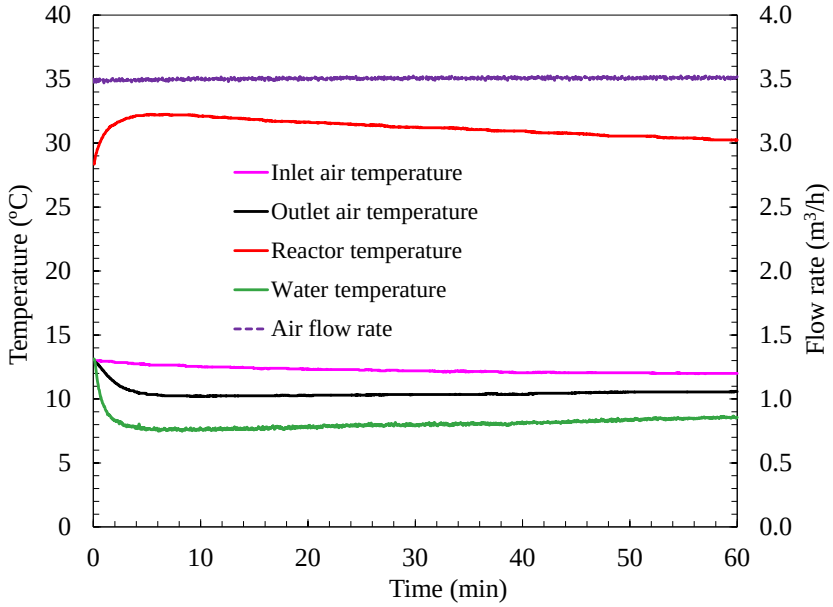

Fig. 5-14 Reactor and water temperature changes with time during heat release process

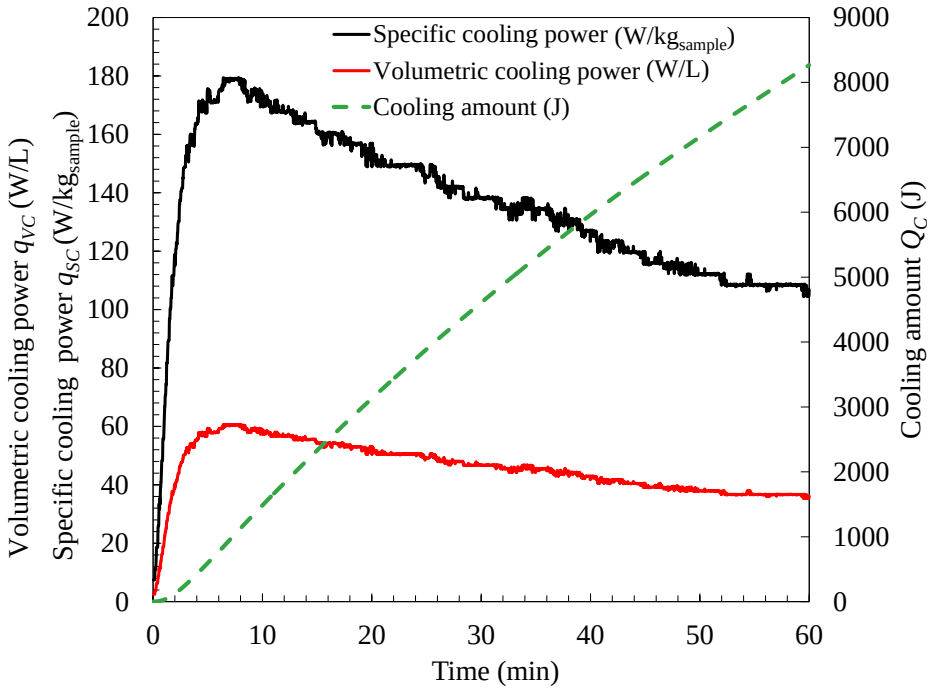

Fig. 5-15 Time variation of mass specific cooling power, volumetric cooling power and cooling amount in sorption process

The instantaneous effective power is delivered by air flowing past the evaporator, and the mass specific, volumetric cooling power q_{SC} and q_{VC} and cooling amount Q_C

obtained during heat discharging of the system is plotted in Fig. 5-15. When the regeneration temperature is 80ºC, the maximum effective specific cooling power is about 180 W/kg, and the volumetric cooling power is 60 W/L. In this research, large inlet and outlet air temperature difference is promising for further development of the sorption air cooler. Increase the sorption speed by decreasing the water vapor transfer resistance to the particle of the sorbent or enlarge the contacting area of the composite material and the sorbate (water vapor) is thought to be able to improve the cold heat generation resulting high specific cooling power. In fact, for the sorption process proceeded at low evaporation pressure, both the improvement of the evaporation and decrease the water vapor transfer resistance to the sorbent particles are necessary to be considered [28]. On the other hand, the heat transfer improvement of the evaporator side is also necessary to obtain large specific cooling power.

5.4.2 Desorption process results

When the material is heated to a certain temperature, the water vapor can be desorbed from the surface of the material, and condenses in the condenser, which is connecting with the reactor. The condensation heat can be taken away by the air flowing past the fin-tube condenser. The temporal changes in the reactor temperature, water temperature and inlet and outlet air temperature in desorption process are shown in Fig. 5-16 when the condensation temperature is 30ºC, and the material was heated to 80ºC. In the regeneration process, the desorbed water vapor can flows to the condenser side due to the pressure difference of the reactor and condenser. Because of the effective heat and mass transfer of the developed system, the water's temperature can increase 6.5ºC, which means that large amount of water vapor has been desorbed from the composite material, and the desorption temperature 80ºC is enough to regenerate the material when the condensation temperature is 30ºC.

The time variation of the mass specific, volumetric heating power and heating amount Q_H in desorption process is shown in Fig. 5-17. The heating power in desorption process is a little bit higher than the cooling power in sorption process due to higher desorption rate under the investigated regeneration condition and the better heat taken performance of the fin-tube of during heat storing process.

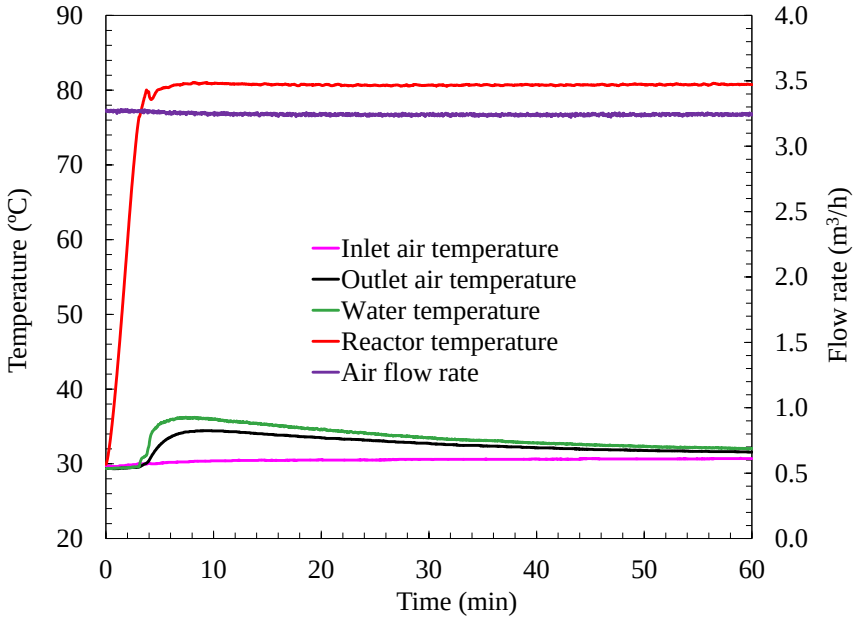

Fig. 5-16 Time variation of reactor and water temperature in desorption process

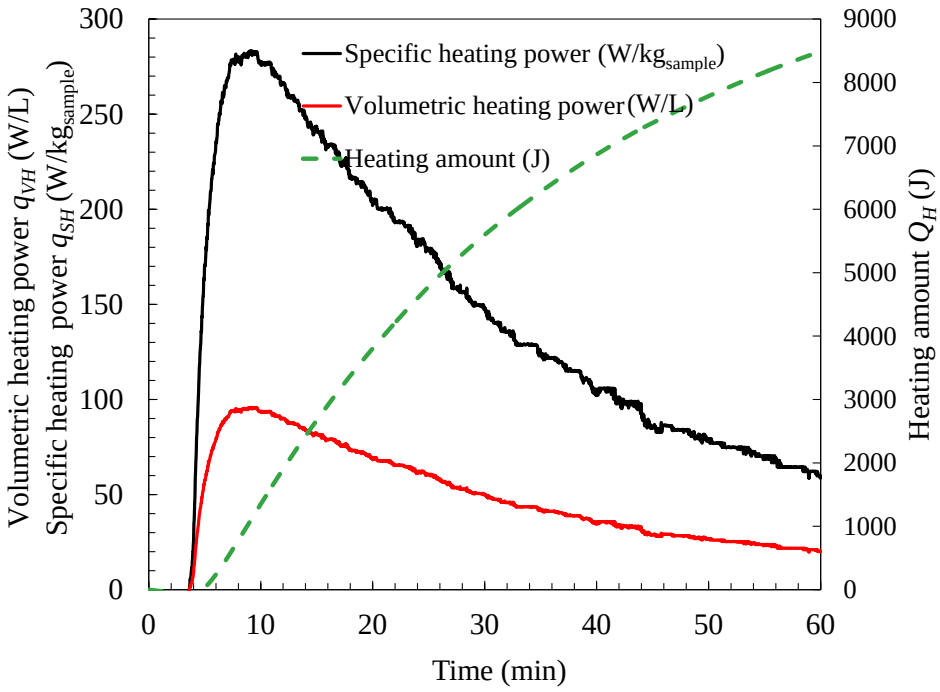

Fig. 5-17 Time variation of the specific heating power, volumetric heating power and heating amount in desorption process

The energy consumption that the reactor heated from the initial temperature to the setting regeneration temperature is considered as the sensible heat. The heat loss during regeneration process can be obtained by calculating the heat transferred to the ambient

air from insulation materal. In this section, the necessary regeneration heat is calculated by substracting sensible heat and heat loss from the total electricity consumption. The sensible heat, regeneration heat and heat loss are listed in Fig. 5-18. Table 5-5 shows the calculated cooling and heating COP. When the sensible heating energy consumption and heat loss are ignored, the cooling $COP_{C,re}$ and heating $COP_{H,re}$ calculated according to Eq. 5-20 and Eq. 5-21 are 0.293 and 0.304, respectively. The COP of this system depends on many factors such as the thermo-physical properties of the composite material, operating temperatures corresponding to operating pressures and heat loss. If the reactor is much lighter with same heat and mass transfer enhancement function and the heat loss is small, the cooling and heating COP could be improved.

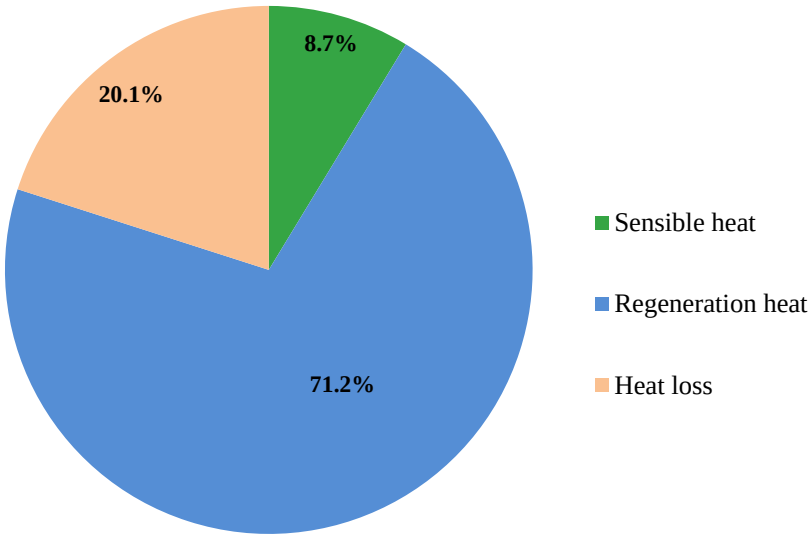

Fig. 5-18 Energy comsumption percentage of total electricity consumption

Table 5-5 Cooling and heating COP calculation

Parameter	Q_C (J)	Q_H (J)	E_{total} (J)	E_{re} (J)	$COP_{C,total}$ (–)	$COP_{H,total}$ (–)	$COP_{C,re}$ (–)	$COP_{H,re}$ (–)
Value	8265.6	8490.7	39550	28178	0.21	0.21	0.29	0.30

5.4.3 Effect of operation duration in both heat charge and heat discharge process

The influence of the operation time during both heat release and heat storage processes on the performance of the composite material filled sorption air cooler were studied. The tests were carried out according to the operation condition listed in Table 5-6. Equal durations of heat storage (desorption) and heat release (sorption) processes were settled.

Table 5-6 Experimental conditions for different operation times

Material	WSS + 40 wt% LiCl			
Initial vacuum condition (kPa)	< 0.3			
Air flow rate in sorption process (m^3/h)	3.5			
Air flow rate in desorption process (m^3/h)	3.25			
Desorption temperature (ºC)	80			
Condensation temperature (ºC)	30			
Operation time (min)	30	60	90	120
Inlet air temperature (ºC)	12			

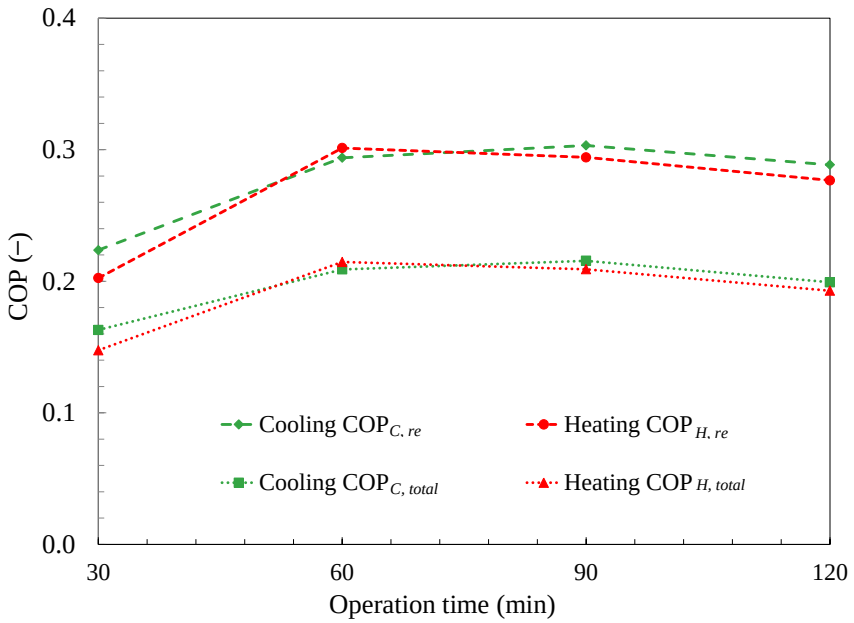

Fig. 5-19 Effect of operation time on cooling and heating COP

Fig. 5-19 shows the obtained cooling COP and heating COP when the evaporation temperature is 12ºC, and regeneration temperature is 80ºC. No matter the sensible heat and heat loss are considered or not, the heating and cooling COPs tend to be large when the operation time is in the range of 60 to 90 min. Since the sensible heating and heat loss consume large electricity in the desorption process, the total cooling and heating COPs is smaller. The results also give us a hint to increase the COP by lightening the weight of the reactor, increase the amount of the composite material and improve the insulation property of the device as much as possible within the heat and mass transfer limitation ranges.

The time variation of specific cooling power and heating power is given in Fig. 5-20 (a) and (b). The mass specific cooling power and volumetric cooling power shows no difference for different operation times during sorption process. The maximum value of 180W/kg was detected. It can be easily understood that the initial dry state of the material before starting the sorption process is same for all the tested four operation times. Cycle times as short as 30 min resulted in lower performance with low specific heating power (cf. Fig. 5-20 (b)), as the amount of water for desorption is small due to short time sorption. Another factor would be the different sorption kinetics of the composite material during different operation times. When the operation time is too short, it was probably not sufficient for complete hydration of the WSS + *x* wt% LiCl. The obtained results indicate that the operation time of 60 or 90 min gives a reasonable compromise between cooling COP and mass specific cooling and heating power.

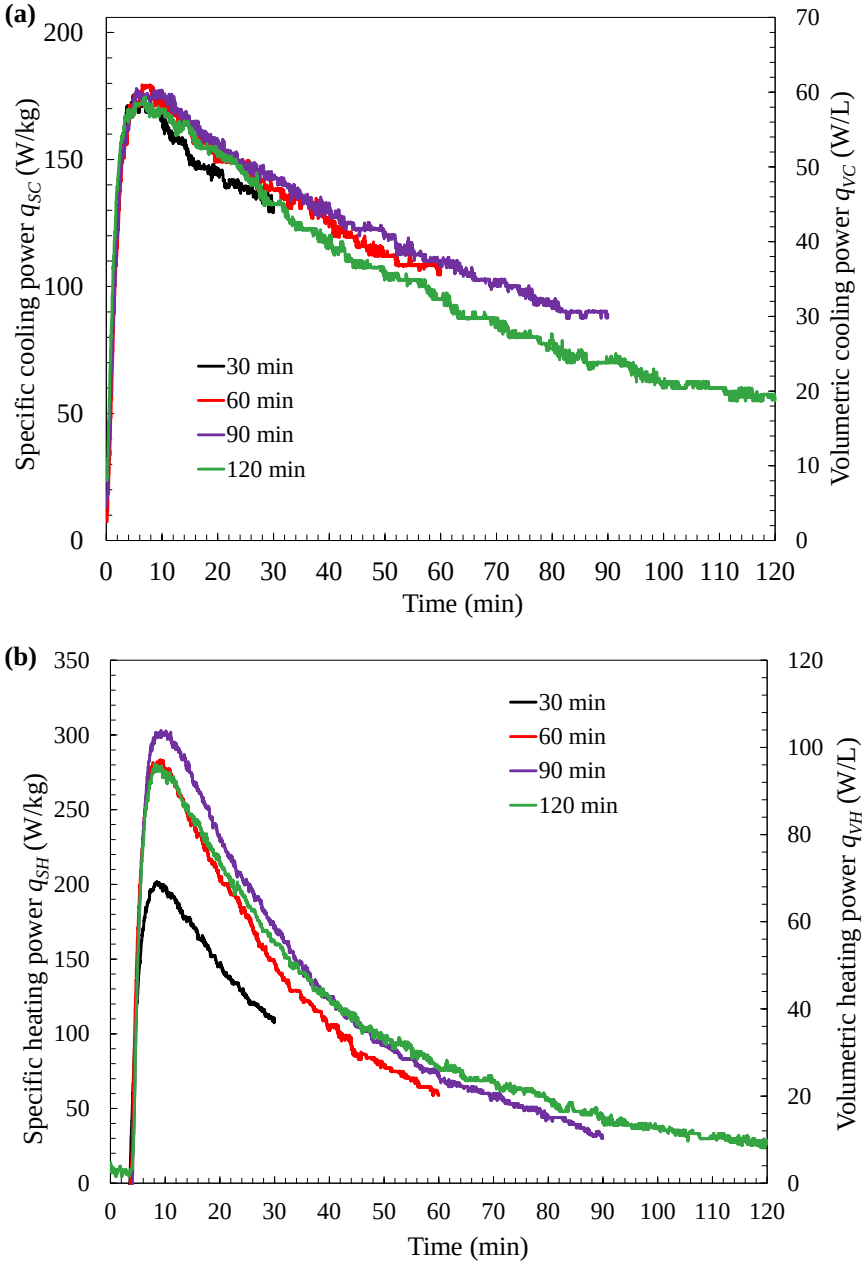

Fig. 5-20 Effect of operation time on (a) specific cooling power and (b) specific heating power

5.4.4 Effect of regeneration temperature

The tests were carried out according to the operation condition listed in

Table 5-7. Fig. 5-21 shows the cooling and heating COPs as a function of the regeneration temperature, when the condensation temperature is 30ºC, the evaporation

temperature is 12ºC and the operation time is 60min. It can be easily seen that the desorption temperature has a strong influence on the air cooler performance. It can be observed that the good performance can be achieved when the regeneration temperature is 80ºC, whose heating and cooling COP is almost same with that regenerated at 85 or 90ºC. It demonstrates that the sorption air cooler can be driven by low-temperature heat source.

Table 5-7 Experimental conditions for different regeneration temperatures

Material	WSS + 40 wt% LiCl				
Initial vacuum condition (kPa)	< 0.3				
Air flow rate in sorption process (m^3/h)	3.5				
Air flow rate in desorption process (m^3/h)	3.25				
Condensation temperature (ºC)	30				
Desorption temperature (ºC)	70	75	80	85	90
Operation time (min)	60				
Inlet air temperature (ºC)	12				

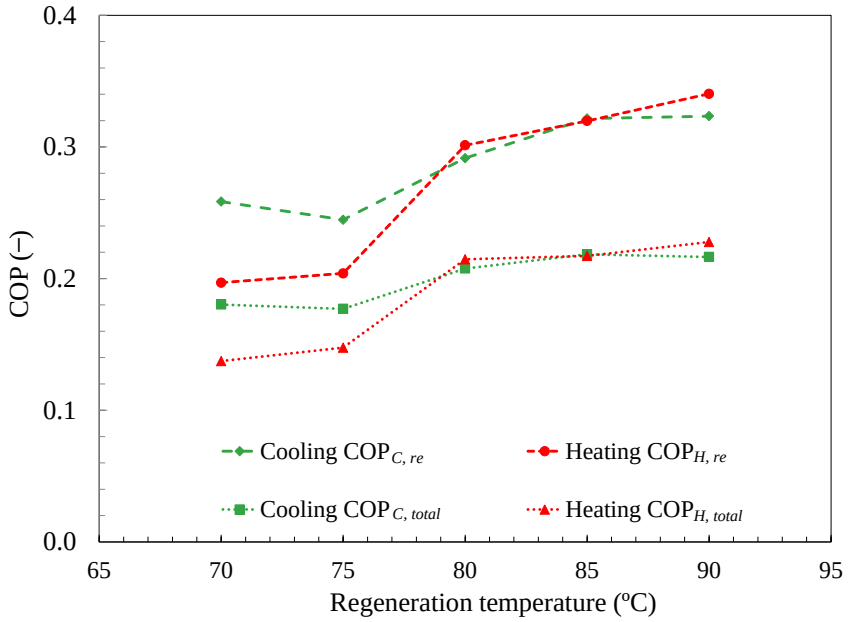

Fig. 5-21 Effect of regeneration temperature on cooling and heating COP

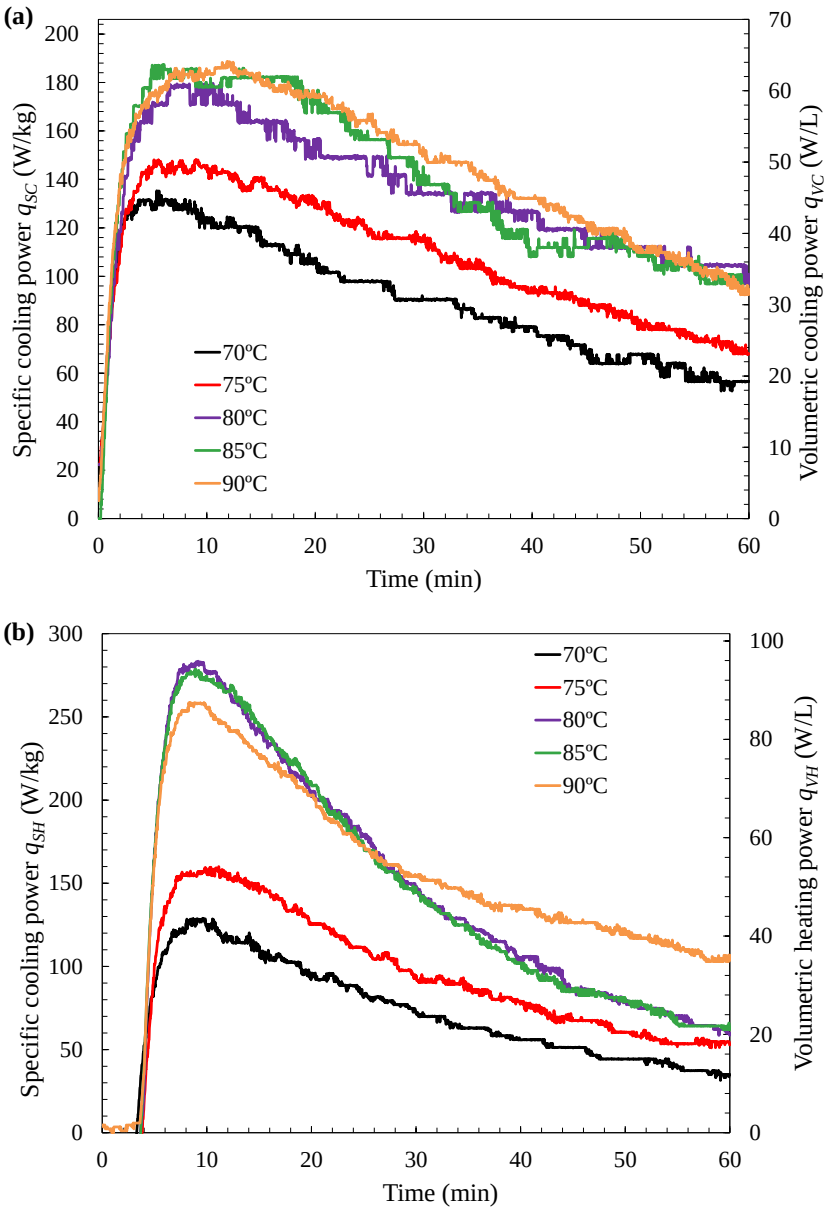

Fig. 5-22 Effect of regeneration temperature on (a) specific cooling power and (b) specific heating power

According to the calculated specific cooling power and heating power shown inFig. 5-22 (a) and (b), high regeneration temperature is likely easy to obtain a high cooling or heating power by inputting large heat in desorption process. In fact, due to the limitation of heat transfer of the evaporator side, when the desorption temperature is higher than 80ºC, the heat transfer of the air flowing over evaporator/condenser is the limited factor to get higher power. Based on the current design of the sorption air cooler,

80ºC seems an optimized regeneration temperature to get a high COP and specific heating/cooling power.

5.4.5 Effect of condensation temperature on performance of the air cooler

The tests to evaluate the influence of condensation temperature were carried out according to the operation condition listed in Table 5-8. The cooling and heating COP as functions of the condensation temperature is shown in Fig. 5-23 when the evaporation temperature is 12ºC, regeneration temperature is 80ºC (Fig. 5-23 (a)) and 90ºC (Fig. 5-23 (b)), and the operation time is 60 min. A performance drop is obvious to see when the condensation temperature is high as 40ºC. Of course, by increasing the regeneration temperature from 80ºC to 90ºC, the performance can be improved, but in this way the energy consumption would be high.

Table 5-8 Experimental conditions for different condensation temperatures

Material	WSS + 40 wt% LiCl					
Initial vacuum condition (kPa)	< 0.3					
Air flow rate in sorption process (m^3/h)	3.5					
Air flow rate in desorption process (m^3/h)	3.25					
Desorption temperature (ºC)	80			90		
Condensation temperature (ºC)	30	35	40	30	35	40
Operation time (min)	60					
Inlet air temperature (ºC)	12					

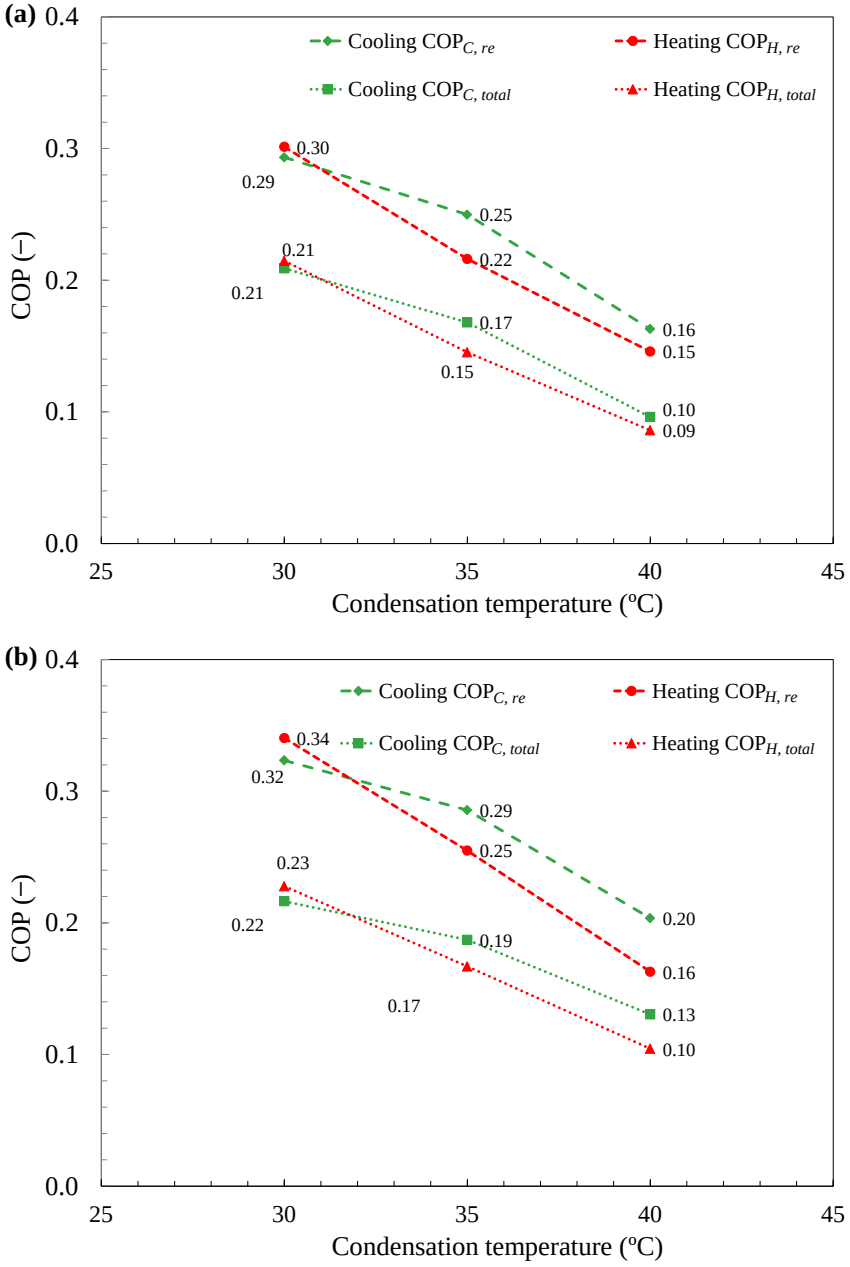

Fig. 5-23 Effect of condensation temperature on cooling and heating COP (a) regeneration temperature of 80ºC and (b) regeneration temperature of 90ºC

For the water inside the evaporator/condenser, high temperature means high saturation pressure. Lowering the condensation temperature can increase the pressure difference in the reactor and evaporator and thus increases the cooling power, which can be proved by Fig. 5-24 (a). Increase the condensation temperature in regeneration process will cause the pressure difference of the reactor and condenser decreases, and small

amount of water condenses in the condenser, resulting in lower specific heating power (cf. Fig. 5-24 (b)).

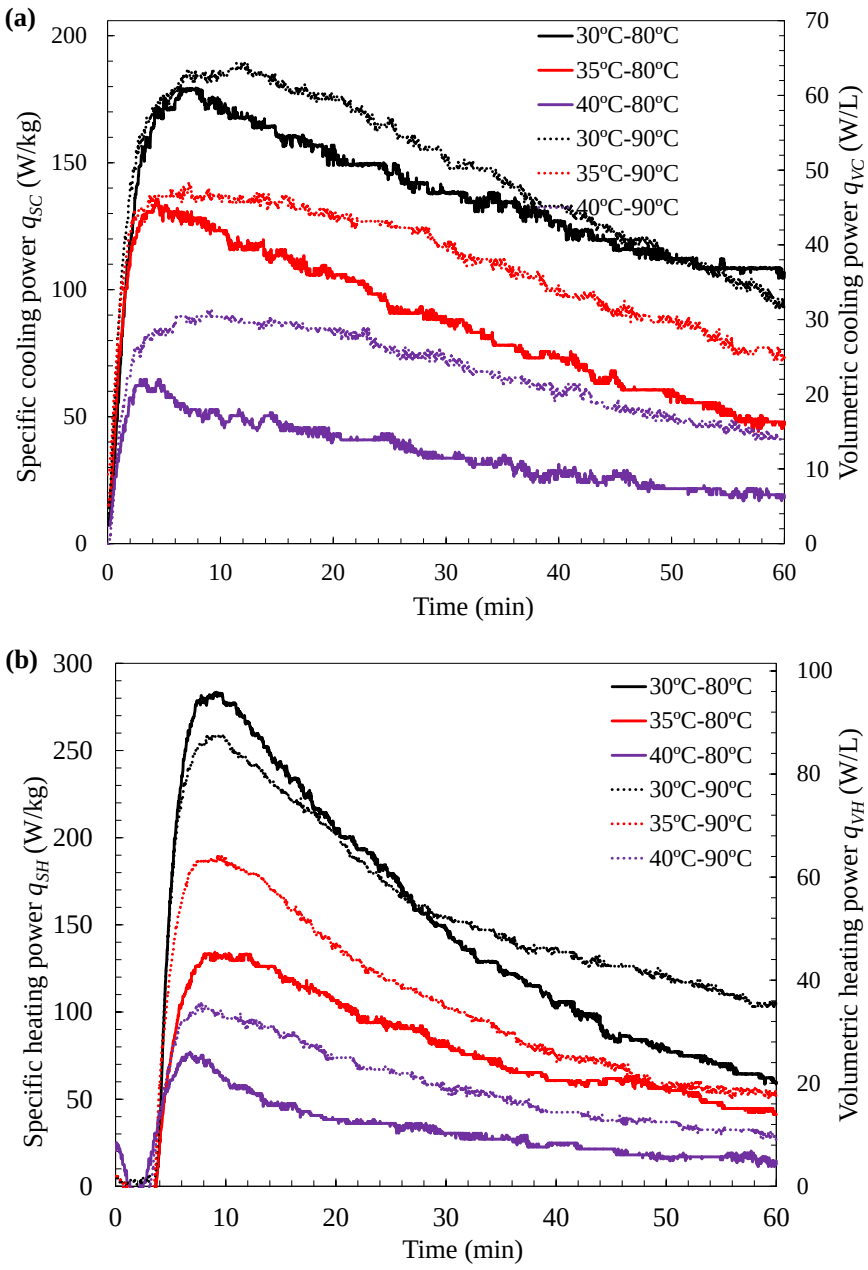

Fig. 5-24 Effect of condensation temperature on (a) specific cooling power and (b) specific heating power

5.4.6 Effect of salt content in the composite material

The tests to evaluate the influence of the LiCl content were carried out according to the operation conditions listed in Table 5-9. The heating COP and cooling COP changing with different salt content is illustrated in Fig. 5-25. It so obvious to see that large percentage of LiCl in composite material can contribute high heating and cooling COP. It was observed that the salt content can affect both the final water uptake and the reaction temperature (cf. Fig. 5-7 and Fig. 5-8). For composite material with high LiCl content, the sorption and desorption cycle is conducted under the condition with more water content, which means that the sorption amount change during one cycle is larger than that of the composite material with small LiCl content. This is probably the reason why WSS + 40 wt% LiCl shows high heating and cooling COP. Same conclusion can be given for the specific cooling and heating power (cf.Fig. 5-26). However, for higher content of LiCl, the properties are similar with that of the pure LiCl, which is easy to get agglomeration after one time use. Moreover, the mass transfer resistance is considered to tend to be high after increasing LiCl content. In the range of this research, WSS + 40 wt% LiCl exhibits the best performance during the four samples.

Table 5-9 Experimental conditions for different LiCl content in the composite material

Terms	WSS + 10 wt% LiCl	WSS + 20 wt% LiCl	WSS + 30 wt% LiCl	WSS + 40 wt% LiCl
Initial vacuum condition (kPa)	< 0.3			
Air flow rate in sorption process (m^3/h)	3.5			
Air flow rate in desorption process (m^3/h)	3.25			
Desorption temperature (°C)	80			
Desorption time (min)	60			
Condensation temperature (°C)	30			
Inlet air temperature (°C)	12			

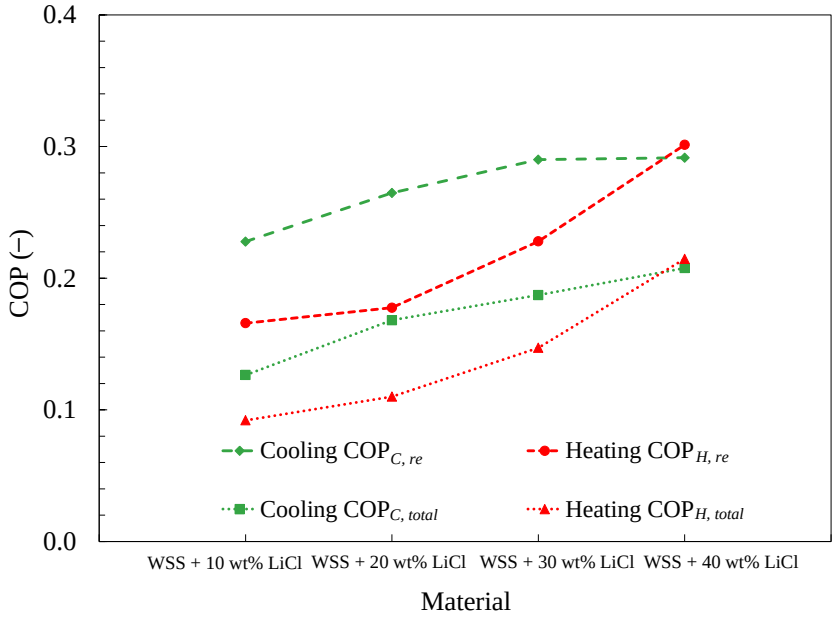

Fig. 5-25 Effect of LiCl content on cooling and heating COP

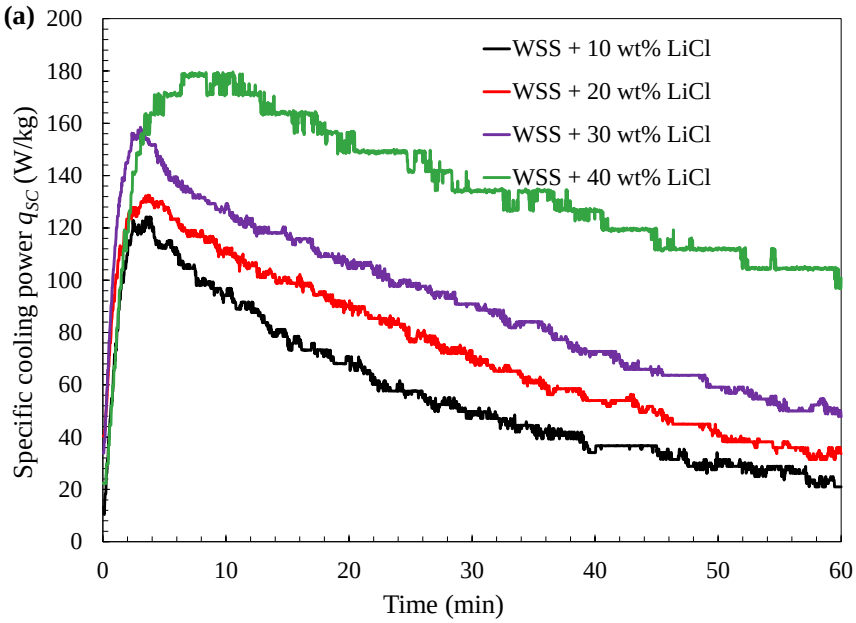

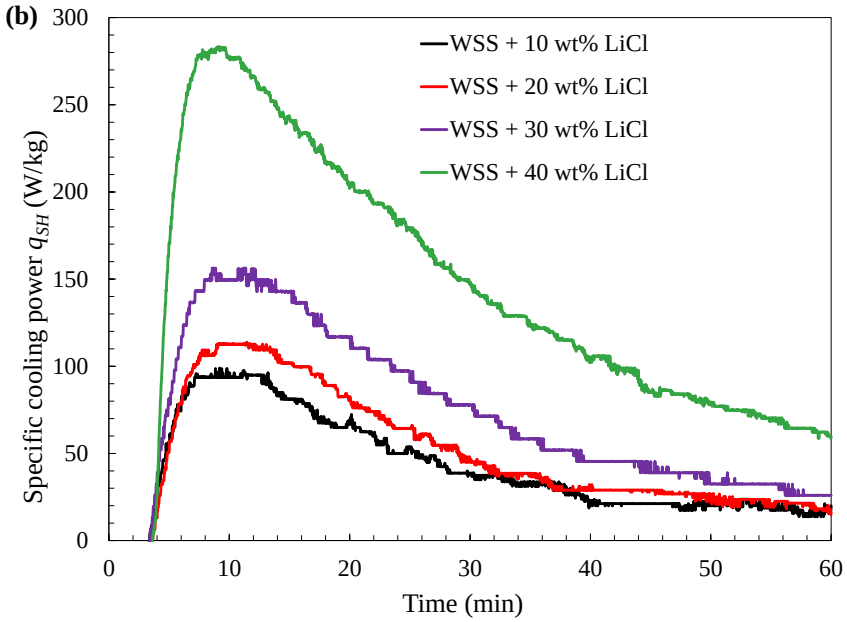

Fig. 5-26 Effect of LiCl content on (a) specific cooling power and (b) specific heating power

5.4.7 Performance comparison

Table 5-10 illustrates the typical performance evaluated for this developed sorption air cooler using composite material, which is also compared with other advanced sorption heat pump prototype Freni et al. [13]. It is evident that the coated heat exchanger developed by Freni et al. surely presents better heat transfer properties than the pelletized bed they developed previously [13]. It is confirmed that the coated heat exchanger exhibits a high global heat transfer coefficient. The cycle time is much shorter and consequently, the specific power is one order of magnitude higher than the pelletized bed type. As a comparison, it is obvious that the developed sorption air cooler shows a higher specific cooling power than the pelletized bed, and a higher COP than the coated type heat exchanger system. In fact, for the developed sorption air cooler the COP considering total electricity consumption is a little bit lower due to heavy reactor and large heat loss, and low sorption rate in heat release process lengthens the cycle time.

Table 5-10 Performance comparison between the developed composite material and other composite materials developed by Freni et al. [13]

	SWS-1L coated HEX	SWS-1L pelletized bed	WSS +40 wt% LiCl
Salt content α (%)	33.7 wt% $CaCl_2$	33.7 wt% $CaCl_2$	40 wt% LiCl
q_{SC} (W/kg)	150-200	20-40	180
τ_{cycle} (min)	10-20	90-150	120
COP_C	0.15-0.3	0.4-0.6	0.3
T_{des} (ºC)	90-100	90-100	80

A better performance of the air cooler can be obtained by using a multi-bed configuration with several reactors connected, by reducing the thickness of the wall of reactor and condenser and by improving insulation properties. Optimization of design of the condenser/evaporator to improve the heat transfer properties of heat transfer fluid could also further enhance the performance of the system. The next efforts in our experimental activity will be addressed in these directions.

5.5 SUMMARY

In this research, composite material for closed thermal energy storage system was developed by impregnating LiCl into mesopores of WSS. The properties of the composite material were investigated. A sorption air cooler was built and tested using our developed composite material.

(1) The sorption capacity of the composite mateiral was increased dramatically after impregnated with LiCl.

(2) The sorption time and desorption time of 60 or 90 min gives a reasonable compromise between cooling COP and mass specific cooling and heating power.

(3) 80ºC seems an optimized regeneration temperature to get a high COP and specific heating/cooling power.

(4) A lower condensation temperature can increase the pressure difference in the reactor and evaporator and thus increases the cooling power.

(5) For the four tested samples, WSS + 40 wt% LiCl exhibits the best performance.

The effective heat exchange and mass transfer properties of the sorbent reactor, led to a high inlet and outlet air temperature difference due to the rapid evaporation of the water inside the evaporator.

The obtained result shows a good perspective to improve the performance of this developed sorption cooler.

5.6 REFERENCE

[1] R.G. Oliveira, R.Z. Wang, A consolidated calcium chloride-expanded graphite compound for use in sorption refrigeration systems, Carbon, 45 (2007) 390-396.

[2] R.d. Boer, W.G. Haije, J.B.J. Veldhuis, S.F. Smeding, Solid-sorption cooling with integrated thermal storage: the SWEAT prototype, in, The International Conference on Heat Powered Cycles, HPC, Larnaca, Cyprus, 2004.

[3] R.d. Boer, W.G. Haije, J.B.J. Veldhuis, Determination of structural, thermodynamic and phase properties in the Na_2S-H_2O system for application in a chemical heat pump, Thermochimica Acta, 395 (2003) 3-19.

[4] V.M.v. Essen, J.C. Gores, L.P.J. Bleijendaal, H.A. Zondag, R. Schuitema, M. Bakker, W.G.J.v. Helden, Characterization of salt hydrates for compact seasonal thermochemical storage, in: The 3rd International Conference of Energy Sustainability ES 2009, San Francisco, California, USA, 2009.

[5] W.v. Helden, Materials for compact seasonal heat storage, 2010.

[6] H.A. Zondag, V.M.v. Essen, L.P.J. Bleijendaal, B.W.J. Kikkert, M. Bakker, Application of $MgCl_2 \cdot 6H_2O$ for thermochemical seasonal solar heat storage, in: the 5th International Renewable Storage Conference IRES 2010, Berlin, Germany, 2010.

[7] S. Mauran, H. Lahmidi, V. Goetz, Solar heating and cooling by a thermochemical process. First experiments of a prototype storing 60 kWh by a solid/gas reaction, Solar Energy, 82 (2008) 623-636.

[8] M. Sasaki, S. Uemura, H. Ogura, Heat storage characteristics of chemical heat storage tank using $CaCl_2/CaCl_2 \cdot 2H_2O$ for heat transport system by vehicle, in: Conference of Heating, Air-Conditioning and Sanitary Engineers of Japan, Sapporo, Japan, 2012, pp. 2645-2648.

[9] S.T. Kim, J. Ryu, Y. Kato, Reactivity enhance of packed bed chemical material using expanded graphite for chemical heat pump, in: The 12th International Conference on Energy Storage, 2012.

[10] K. Fujioka, K. Hatanaka, Y. Hirata, Composite reactants of calcium chloride combined with functional carbon materials for chemical heat pumps, Applied Thermal Engineering, 28 (2008) 304-310.

[11] Y.I. Aristov, New family of solid sorbents for adsorptive cooling: material scientist approach, Journal of Engineering Thermophysics, 16(2) (2007) 63-72.

[12] K. Fujioka, H. Suzuki, Thermophysical properties and reaction rate of composite reactant of calcium chloride and expanded graphite, Applied Thermal Engineering, 50 (2013) 1627-1632.

[13] A. Freni, F. Russo, S. Vasta, M. Tokarev, Y.I. Aristov, G. Restuccia, An advanced solid sorption chiller using SWS-1L, Applied Thermal Engineering, 27 (2007) 2200-2204.

[14] A. Freni, M.M. Tokarev, G. Restuccia, A.G. Okunev, Y.I. Aristov, Thermal conductivity of selective water sorbents under the working conditions of a sorption chiller, Applied Thermal Engineering, 22 (2002) 1631-1642.

[15] G. Restuccia, A. Freni, S. Vasta, Y.I. Aristov, Selective water sorbent for solid sorption chiller: experimental results and modelling, International Journal of Refrigeration, 27 (2004) 284-293.

[16] L.G. Gordeeva, A. Freni, G. Restuccia, Y.I. Aristov, Adsorptive air conditioning systems driven by low temperature energy sources: choice of the working pairs, Journal of Chemical Engineering of Japan, 40(13) (2007) 1287-1291.

[17] A. Freni, A. Sapienza, I.S. Glaznev, Y.I. Aristov, Experimental testing of a lab-scale adsorption chiller using a novel selective water sorbent "silica modified by calcium nitrate", International Journal of Refrigeration, 35 (2012) 518-524.

[18] L.G. Gordeeva, A.D. Grekova, T.A. Krieger, Y.I. Aristov, Adsorption properties of composite materials (LiCl + LiBr)/silica, Microporous and Mesoporous Materials, 126 (2009) 262-267.

[19] H.J. Chen, Q. Cui, Y. Tang, X.J. Chen, H.Q. Yao, Attapulgite based LiCl composite adsorbents for cooling and air conditioning applications, Applied Thermal Engineering, 28 (2008) 2187-2193.

[20] S. Nakabayashi, K. Nagano, M. Nakamura, J. Togawa, A. Kurokawa, Improvement of water adsorption ability of natural mesoporous material by impregnating with chloride salts for development of a new desiccant filter, Adsorption, 17 (2011) 675-686.

[21] H. Liu, K. Nagano, D. Sugiyama, J. Togawa, M. Nakamura, Honeycomb filters made from mesoporous composite material for an open sorption thermal energy storage system to store low-temperature industrial waste heat, International Journal of Heat and Mass Transfer, 65 (2013) 471-480.

[22] J. Togawa, K. Nagano, Feasibility study on the desiccant air conditioning system used Wakkanai Siliceous Shale 11th Report: Development of micronized technique for Wakkanai Siliceous Shale in: Society of Heating, Air-Conditioning and Sanitary Engineers of Japan, Sapporo, Japan, 2013, pp. 53-56.

[23] Y.I. Aristov, M.M.Tokarev, G.Cacciola, G. Restuccia, Selective water sorbents for multiple applications, 1. $CaCl_2$ confined in mesopores of silica gel: sorption properties, Reaction Kinetics and Catalysis Letters, 59(2) (1996) 325-333.

[24] S. Vyazovkin, Computational aspects of kinetic analysis.: Part C. The ICTAC Kinetics Project — the light at the end of the tunnel?, Thermochimica Acta, 355(1–2) (2000) 155-163.

[25] M.J. Starink, The determination of activation energy from linear heating rate experiments: a comparison of the accuracy of isoconversion methods, Thermochimica Acta, 404(1–2) (2003) 163-176.

[26] H. Kameyama, Y. Kato, Honebuto energy road map, Kagaku Kogyo Sya, Japan, 2005.

[27] H. Ogura, M. Haguro, Y. Shibata, Y. Otsubo, Reaction characteristics of $CaSO_4/CaSO_4 \cdot 1/2H_2O$ reversible reaction for chemical heat pump, Journal of Chemical Engineering of Japan, 40(13) (2007) 1252-1256.

[28] H. Ogura, M. Kanamori, H. Matsuda, M. Hasatani, Generation of low-temperature heat by use of $CaO/H_2O/Ca(OH)_2$ reaction, KAGAKU KOGAKU RONBUNSHU, 19(6) (1993) 941-946.

6 DEVELOPMENT OF COATED TYPE REACTOR FOR A CLOSED CHEMICAL HEAT PUMP SYSTEM

Hokkaido University

6.1 INTRODUCTION

For lower-regeneration temperature (lower-temperature heat source), there are many materials have been investigated for chemical heat pumps. The final choice depends on criteria as toxicity of products, power, thermal energy storage density, complexity and cost and so on [1]. Water was selected as the refrigerant because of its environmentally safety.

Aristov developed [2, 3] an adsorptive cooling system with one of the selective water sorbents (SWSs) - SWS-1L (Calcium chloride in silica gel KSK) driven by low-temperature heat. The test showed that the cooling coefficient of performance (COP) can achieve 0.6 at regeneration temperature as low as 85-95ºC. However, the low specific power of the device is not promising due to the design of the reactor and shape of the material.

Greiner [4] described a system, in which the preferred reaction is: $MgCl_2 \cdot 4H_2O \leftrightarrow MgCl_2 \cdot 2H_2O + 2H_2O$. A kind of throwaway portable cooling devices was introduced, in which a container of water in the box to be cooled was evaporated from a wick and absorbed by $MgCl_2 \bullet 2H_2O$ in a connected container outside of the box. By suitable modifications, $MgCl_2 \bullet 4H_2O$ was regenerated at 107°C, and the cycle could be used for storage of heat or cold. Metal hydrides do have the advantage of high thermal conductivity. A disadvantage is high chemical cost. The ECN results [5] showed $MgCl_2$ has high practical storage density, fast heat release forms, but it will release HCl when the regeneration temperature higher than 140°C, and is very hygroscopic [6, 7].

The SWEAT [8, 9] (Salt Water Energy Accumulation and Transformation) project is focused on the development of a prototype of a modular solid-sorption cooling system for residential and industrial applications. The sodium sulphide (Na_2S) - water works as the working pair. Na_2S-H_2O has a eutectic melting point of 83ºC [9], which imposes the upper limits for the regeneration temperature in its system. The conclusion that the monohydrate or pentahydrate of sodium sulphide gives a high thermal energy storage density and a high thermal power density was also given by Iammak et al. [10]. However, Boer et al. [8] revealed that it is very corrosive and has to be operated under high vacuum condition.

A first theoretical study at ECN on which material is most suitable for compact seasonable heat storage identified magnesium sulfate ($MgSO_4$) as most promising material [5] because of low costs, non-toxicity, non-corrosivity and high theoretical energy density. However, it was found that the material was difficult to take up water under practical conditions.

Mauran et al. [1] developed a cooling and heat system using strontium bromide $SrBr_2$ as reactant and H_2O as refrigerant fluid. The $SrBr_2$ is implemented with an expanded natural graphite to increase the thermal conductivity and permeability in low pressure. It is able to store 60 kWh or 40 kWh for the heating or cooling function respectively with reactor's total volume of 1 m^3. The low heat transfer at interface between the reactive layer and the exchanger limits the heating and cooling powers.

Chemical heat pump using reversible $CaCl_2$/water system has been proposed for easy obtainment and low price. Fujii et al. [11] developed a chemical heat pump using $CaCl_2$ to store solar energy. Sasaki et al. [12] also tested $CaCl_2$ as a thermal energy storage material to recover waste heat. The developed system cannot run within a large temperature and pressure range In order to avoid the deliquescence of $CaCl_2$. However, $CaCl_2$ has not been widely used because of low performance and complexity compared to conventional compression heat pumps. The low thermal conductivity in the range of 0.1-0.2 W/(m·K) and agglomeration of the salt can be responsible for its development.

Due to the limitation of low heat and mass transfer of the chemical thermal energy storage materials, various methods have been developed to solve the heat transfer and mass transfer problems.

One method is to prepare composite material with heat transfer promoter [13]. Expanded graphite (EG) is often used to improve the kinetics of the reversible gas/solid reaction, with which an increase of the thermal conductivity of the composite up to 20-30 W/(m·K) can be achieved [2]. Fujioka et al. [14] tested the thermophysical properties and reaction characteristics of composite reactants of $CaCl_2$ and EG experimentally. The results showed that 10 times of the thermal conductivity can be achieved by introducing EG by increasing permeability and reaction rate at the same time.

For improving the heat transfer of the material, there is another method [13] by integrating of reactant into a heat exchanger. Freni et al. [15] tested an advanced solid sorption chiller based on a heat exchanger coated with a compact layer of selective water sorbent: SWS-1L ($CaCl_2$ in mesoporous silica gel). Their result showed a specific power of 150-200 W/kg of adsorbent and a cycle time of only 10-20 min. Moreover, the cooling COP ranged between 0.15-0.3.

The final goal of our research is to develop a low-regeneration chemical heat pump. The high mass transfer resistance of pure material will be solved by developing composite material by impregnating LiCl into WSS micro powders. The low heat transfer is expected to be improved by coating the composite material on the surface of corrugated heat exchanger. The performance of the new type reactor will be evaluated by a lab-scale prototype.

6.2 EXPERIMENTS OF COATED TYPE CHEMICAL HEAT PUMP

WSS is a kind of mesoporous material, which is located in the north part of Hokkaido, Japan. The pore distribution and sorption properties have been investigated in our previous study[16]. The composite material of WSS impregnated with 40% LiCl was used as the sorbent in this study, due to its excellent sorption properties studied previously, which is going to be short for WSS + 40 wt% LiCl. The physical properties, sorption properties, and thermal properties have been studied in previous study.

6.2.1 The composite material coated heat exchanger

The corrugated heat exchanger before and after being coated with WSS + 40 wt% LiCl is shown in Fig. 6-1. The main features of the bed are listed in Table 1. The heat exchanger is made of aluminum to make sure a light inert weight. The coating procedure is listed as follows:

1) The heat exchanger was treated with acid, and then put into oven at 120ºC waiting to be used.

2) The micro powders of WSS (< 20μm) were dried at 120ºC for 24 hours.

3) The slurry to WSS and LiCl was prepared in a vacuum tank.

4) The corrugated aluminum heat exchanger was coated by the slurry made in step 3.

5) The coated heat exchanger was put in the atmosphere for 24 hours before being heated at 120ºC for 24 hours to get the dry weight.

Fig. 6-1 Corrugated heat exchanger before being coated (left); being coated with slurry of WSS + 40 wt% LiCl (middle) and after coated (right)

Table 6-1 Main features of the lab-scale CHP experimental setup

Parameters	Value
Total metal mass of one heat exchanger (kg)	0.454
Total volume of one heat exchanger (m^3)	0.5625×10^{-3}
Heat exchanging area of one heat exchanger (m^2)	0.0525
Total mass of the coated material on one heat exchanger (kg)	0.143
Number of coatey heat exchangers inside reactor (–)	2
Total mass of the LiCl (kg)	0.1144

6.2.2 Experimental setup

The schematic diagram of the experimental setup was shown in Fig. 6-2. It consists of a vacuum reactor connected to an evaporator/condenser with corrugated heat exchanger inside. The composite material coated heat exchanger is placed in the cylindrical reactor. Four T-type thermocouples are inserted inside the composite material coated heat exchanger at different positions, whose mean temperature is considered as the material temperature during experiments.

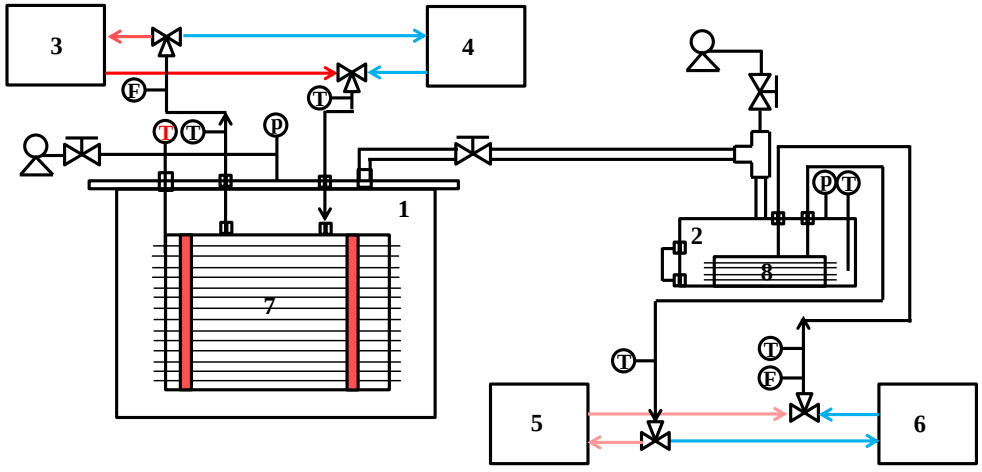

1. reactor
2. condenser/evaporator
3. circulating thermostatic bath
4. circulating thermostatic bath
5. circulating thermostatic bath
6. circulating thermostatic bath
7. corrugated type heat exchanger coated with reactant
8. corrugated tube heat exchanger

Thermocouple
Vacuum gauge
Flow meter
Solenoid valve
Three way valve
Vacuum pump

Fig. 6-2 Schematic diagram of experimental setup

Four thermo cryostats allow the heating/cooling of the closed system. The temperature controllers of circulating thermal baths have an accuracy of ± 0.2°C. Water was used as external heat transfer fluid inside of the thermo cryostats. There are two Pt thermocouples set at the inlet/outlet of each heat transfer circuit. Moreover, the flow rates of the thermal fluids are measured by two flow meters.

The water temperature inside the condenser/evaporator was measured by one Pt thermocouple. The reacted water amount can be measured by the level gauge set on the condenser/evaporator. Two digital vacuum gauges are connected to the reactor and the condenser/evaporator. The accuracy of the pressure measuring system is ±15 Pa. The testing facility is equipped with a data acquisition.

The picture of the experimental setup is shown in Fig. 6-3, with reactor on the left side and condenser/evaporator on the right side.

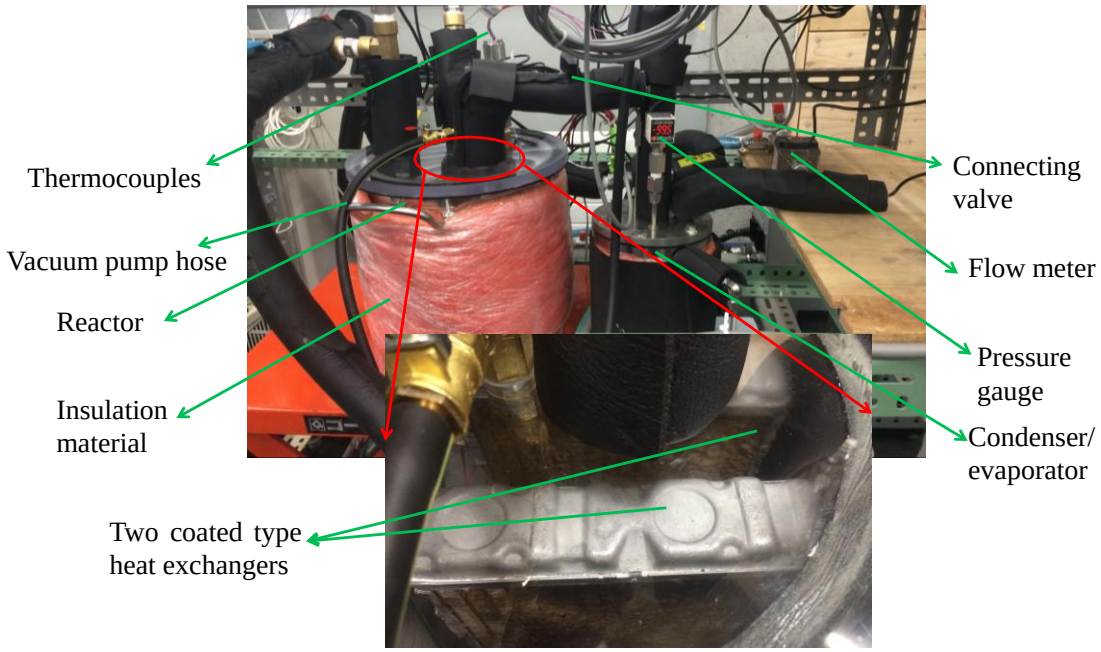

Fig. 6-3 The testing experimental setup for procucing cooling heat

6.2.3 Experimental procedure

A cooling experimental cycle (T_{inev}= 12°C, T_{inre}= 30°C, T_{incon}= 30°C, T_{inre}= 80°C) is presented in Fig. 6-4 in the Clapeyron diagram of WSS + 40 wt % LiCl tested in our previous study, which relates the equilibrium pressure and temperature at fixed water

vapor content. The experimental cycle is plotted on the isosteric chart of WSS + 40 wt% LiCl measured by a thermogravimetry.

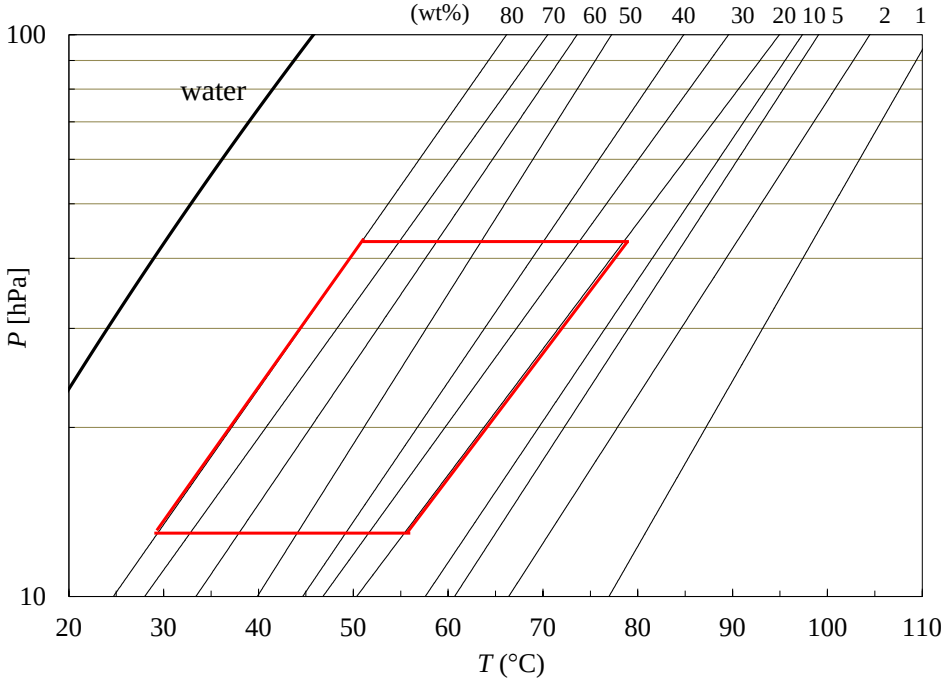

Fig. 6-4 Cooling cycle on the Clapeyron diagram of WSS + 40 wt % LiCl

First, the reactor and evaporator/condenser are vacuumed to the appropriate pressures by the connected vacuum pump. The cooling cycle will be conducted by the following procedures:

(1) The composite material is heated by the fluid from the high temperature circulating thermostatic bath until the pressure of the reactor reaching condensation pressure (T_{inre} = 80°C);

(2) Open the valve connecting the reactor and condenser to start the heat release process. The condenser and reactor keep being connected and the composite material is still heated until the condensation temperature is almost same with initilal value;

(3) The coated heat exchanger is cooled until the equilibrium pressure reaching the pressure of evaporation (inlet temperature of the external fluid T_{inev}= 12°C, T_{inso}= 30°C);

(4) The connection between evaporator and reactor is open to start the heat release process until the evaporation temperature is same with T_{inev}= 12°C.

6.2.4 Evaluation indices

The performance of the heat pump system can be evaluated by specific cooling power q_{SC} specific heating power q_{SH} and the coefficient of performance (COP), which was calculated as the following equations:

$$q_{SC} = \frac{\rho_{\mathrm{H_2O},evap} Q_{\mathrm{H_2O},evap} C_{P,\mathrm{H_2O}} (T_{in,evap} - T_{out,evap})}{m_{s,dry}} \quad 6\text{-}1$$

Where, the $T_{in,evap} - T_{out,evap}$ refers to the temperature difference between the inlet and outlet of the external heat transfer water of the evaporator.

When the water vapor evaporated from the evaporator, it will flow to the reactor and be sorbed by the composite material inside, and sorption heat can be released and taken away by the fluid inside the heat exchanger. In this case, the specific heating power q_{SH} can be obtained by the following equation:

$$q_{SH} = \frac{\rho_{\mathrm{H_2O},reac} Q_{\mathrm{H_2O},reac} C_{P,\mathrm{H_2O}} (T_{in,reac} - T_{out,reac})}{m_{s,dry}} \quad 6\text{-}2$$

Where, the $T_{in,reac} - T_{out,reac}$ refers to the temperature difference between the inlet and outlet of the external heat transfer water of the reactor.

While in the regeneration process, the composite material with a certain amount of water will be decomposed into relative dry material and water vapor, which is going to condense inside the condenser then. The condensation heat in this case can be taken away by the water inside the heat exchanger. The specific condensation power $q_{S,con}$ can be defided as:

$$q_{S,con} = \frac{\rho_{\mathrm{H_2O},con} Q_{\mathrm{H_2O},con} C_{P,\mathrm{H_2O}} (T_{in,con} - T_{out,con})}{m_{s,dry}} \quad 6\text{-}3$$

The COP can be calculated following Eq. 6-4.

$$\mathrm{COP} = \frac{\sum_{t_3}^{t_4} \rho_{\mathrm{H_2O},evap} Q_{\mathrm{H_2O},evap} C_{P,\mathrm{H_2O}} (T_{in,evap} - T_{out,evap}) \Delta t}{\sum_{t_0}^{t_2} \rho_{\mathrm{H_2O},reac} Q_{\mathrm{H_2O},reac} C_P (T_{in,reac} - T_{out,reac}) \Delta t} \quad 6\text{-}4$$

Where, 0: start of cycle; 1: end of isosteric heating; 2: end of desorption phase; 3: end of isosteric cooling; 4: end of cycle; the $T_{in,reac} - T_{out,reac}$ refers to the temperature difference between the inlet and outlet of the external heat transfer water of the reactor. Therefore, the obtained specific cooling power q_{SC}, specific heating power q_{SH}, specific condensation power $q_{S,con}$ and COP are effective performance indices of the heat pump, which are influence by the properties of the material, heat transfer of the heat exchanger, the mass transfer of the water vapor through composite material, as well as the sensible heat due to the inert of the device, and heat loss.

6.3 RESULTS AND DISCUSSION

The tests were carried out according to the experimental condition described in section of experimental procedure. Fig. 6-5 shows the behavior of the average temperature of composite material and inlet and outlet of the heat exchanger on the reactor side during 100 minutes of testing. The first cycle is good heat transfer can be indicated by the small difference of the composite temperature and the external heat transer fluid. The pressure change inside the rector is shown in Fig. 6-6, from which it can be seen that for the two cycles with different cycle time, the isosteric heaing/cooling is less than one minute.

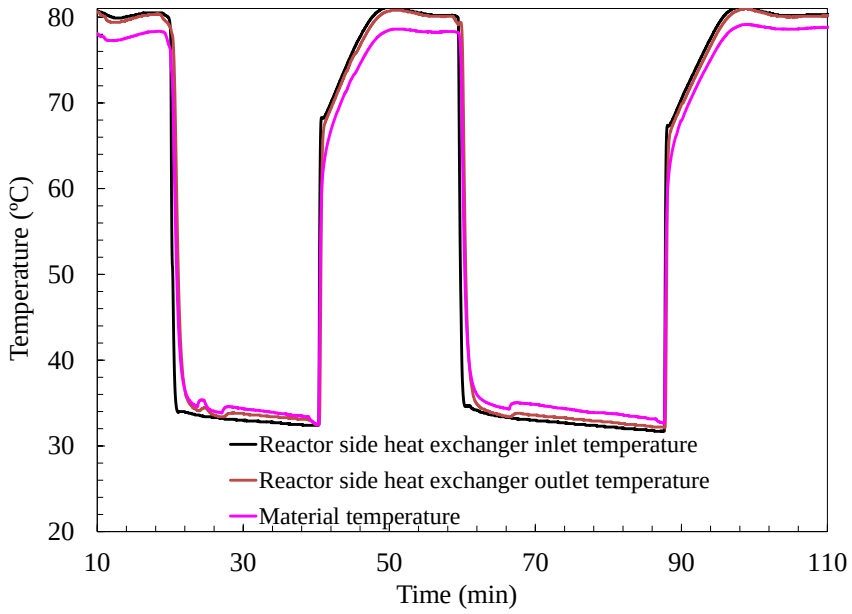

Fig. 6-5 Temperature of the composite material, and inlet and outlet temperatures of the heat exchanger on reactor side changes with time

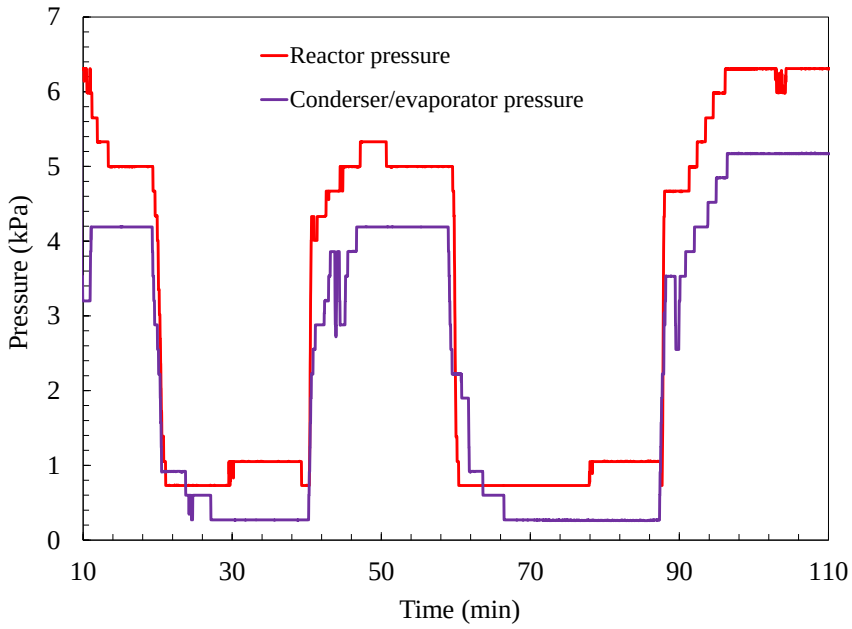

Fig. 6-6 Reactor pressure and condenser/evaporature change with time

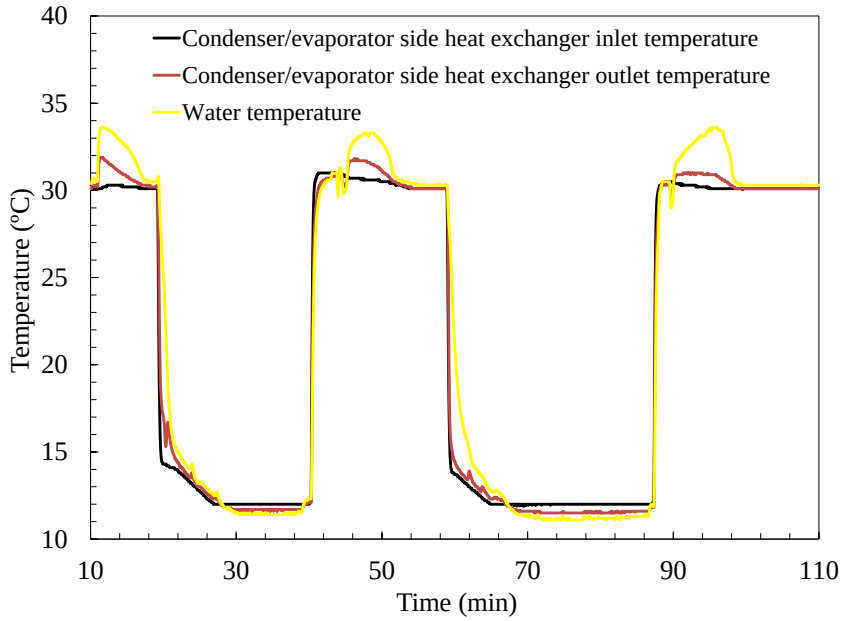

Fig. 6-7 Temperature of the water inside condenser/evaporator, and inlet and outlet temperatures of the heat exchanger on condenser/evaporator side changes with time

The water temperature insider the condenser/evaporator and inlet and outlet of the heat exchanger on the condenser/evaporator side during 100 minutes of testing are shown in Fig. 6-7. The obvious temperature increase of the water in regeneration

process due to water vapor condensation can be observed. At the same time, a long duration of water temperature decrease during the sorption process can also be detected.

The specific cooling power, heating power, condensation power calculated according the corresponding equations in section 6.2.4 are illustracted in Fig. 6-8 as well as the input and extracted power from the heat exchanger fluid. The specific cooling heat is about 200 W/kg, which is equivalent to that of the small sorption air cooler. While a higher specific condensation power is displayed as more than 300 W/kg. More efforts should be don to improve the performance of this system by improve the size matching of the condenser/evaporator and reactor, and reduce inertia gases as small as possible, which is an obstacle for the development of chemical heat pump system operated under negative pressure. The calculated cooling COP according to Eq. 6-4 is 0.1.

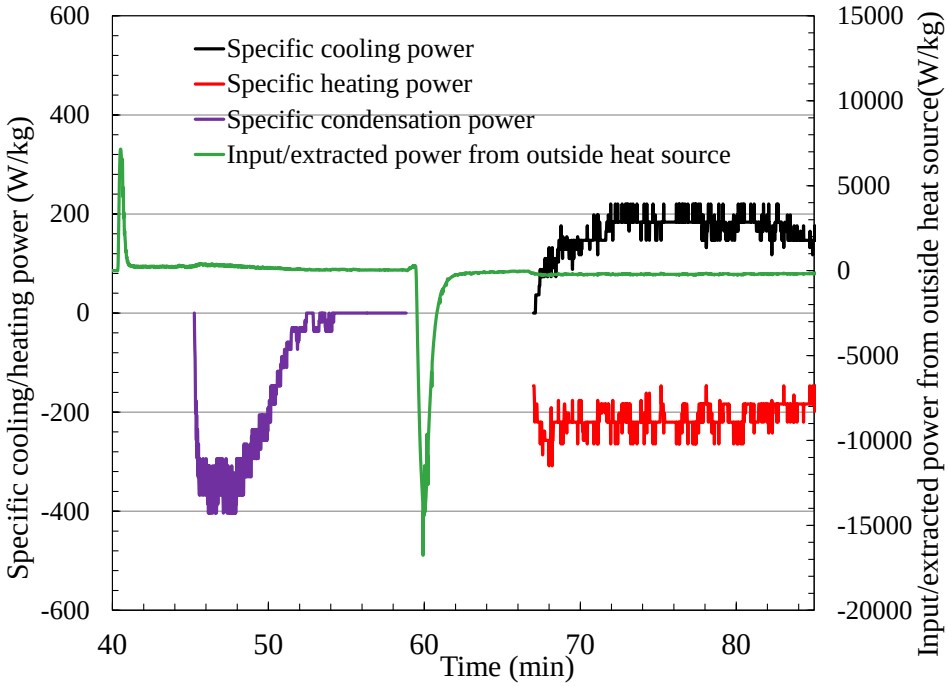

Fig. 6-8 Instantaneous specific cooling and heating power as a function of time

6.4 SUMMARY

The experimental testing on the composite material WSS + 40 wt% LiCl coated type chemical heat pump system was presented. The experimental resuls showed a specific cooling power of 200 W/kg of the compsite material with cycle time of 30-40 min. The effective cooling COP is about 0.08. Consequently, further efforts must be done in order to improve the performance of the closed system.

6.5 REFERENCE

[1] S. Mauran, H. Lahmidi, V. Goetz, Solar heating and cooling by a thermochemical process. First experiments of a prototype storing 60 kWh by a solid/gas reaction, Solar Energy, 82 (2008) 623-636.

[2] Y.I. Aristov, New family of solid sorbents for adsorptive cooling: material scientist approach, Journal of Engineering Thermophysics, 16(2) (2007) 63-72.

[3] G. Restuccia, A. Freni, S. Vasta, Y.I. Aristov, Selective water sorbent for solid sorption chiller: experimental results and modelling, International Journal of Refrigeration, 27 (2004) 284-293.

[4] L. Greiner, Chemical heat pump, in, 1981.

[5] V.M.v. Essen, J.C. Gores, L.P.J. Bleijendaal, H.A. Zondag, R. Schuitema, M. Bakker, W.G.J.v. Helden, Characterization of salt hydrates for compact seasonal thermochemical storage, in: The 3rd International Conference of Energy Sustainability ES 2009, San Francisco, California, USA, 2009.

[6] W.v. Helden, Materials for compact seasonal heat storage, 2010.

[7] H.A. Zondag, V.M.v. Essen, L.P.J. Bleijendaal, B.W.J. Kikkert, M. Bakker, Application of $MgCl_2 \cdot 6H_2O$ for thermochemical seasonal solar heat storage, in: the 5th International Renewable Storage Conference IRES 2010, Berlin, Germany, 2010.

[8] R.d. Boer, W.G. Haije, J.B.J. Veldhuis, S.F. Smeding, Solid-sorption cooling with integrated thermal storage: the SWEAT prototype, in, The International Conference on Heat Powered Cycles, HPC, Larnaca, Cyprus, 2004.

[9] R.d. Boer, W.G. Haije, J.B.J. Veldhuis, Determination of structural, thermodynamic and phase properties in the Na_2S-H_2O system for application in a chemical heat pump, Thermochimica Acta, 395 (2003) 3-19.

[10] K. Lammak, W. Wongsuwan, T. Kiatsiriroj, Investigation of modular chemcial energy storage performance, in: The Joint Conference on Sustainable Energy and Environment (SEE), Hua Hin, Thailand, 2004, pp. 504-507.

[11] I. Fujii, T. Arai, Y. Saitoh, Investigation on chemical heat pump using calcium chloride, in: Proceedings of Japan Solar Energy Society/Japan Wind Energy Association Joint Conference, 1997, pp. 289-292.

[12] M. Sasaki, S. Uemura, H. Ogura, Heat storage characteristics of chemical heat storage tank using $CaCl_2/CaCl_2 \cdot 2H_2O$ for heat transport system by vehicle, in:

Conference of Heating, Air-Conditioning and Sanitary Engineers of Japan, Sapporo, Japan, 2012, pp. 2645-2648.

[13] K. Fujioka, K. Hatanaka, Y. Hirata, Composite reactants of calcium chloride combined with functional carbon materials for chemical heat pumps, Applied Thermal Engineering, 28 (2008) 304-310.

[14] K. Fujioka, H. Suzuki, Thermophysical properties and reaction rate of composite reactant of calcium chloride and expanded graphite, Applied Thermal Engineering, 50 (2013) 1627-1632.

[15] A. Freni, F. Russo, S. Vasta, M. Tokarev, Y.I. Aristov, G. Restuccia, An advanced solid sorption chiller using SWS-1L, Applied Thermal Engineering, 27 (2007) 2200-2204.

[16] H. Liu, K. Nagano, D. Sugiyama, J. Togawa, M. Nakamura, Honeycomb filters made from mesoporous composite material for an open sorption thermal energy storage system to store low-temperature industrial waste heat, International Journal of Heat and Mass Transfer, 65 (2013) 471-480.

7 APPLICATION PROPOSAL FOR THE DEVELOPED OPEN AND CLOSED THERMAL ENERGY STORAGE SYTEM

7.1 OPEN SYSTEM PROPOSAL

Due to the high thermal energy storage density, low-regeneration temperature and rather simple structure of open thermal energy storage system, it can be used for stroge of solar energy or waste heat from industrial sector.

An example of application of our developed open sorption thermal energy storage system is explained in Chapter 3. Another potential application is to save industrial waste heat at waste heat discharge site. The collected waste heat can be transported and integrated into various processes such as drying at another different place considering the produced dry and hot air by the open heat storage system. The application proposal can be seen in Fig. 7-1. For example, the heat source side can be the garbage incineration plant with plenty of unused exhausted heat.

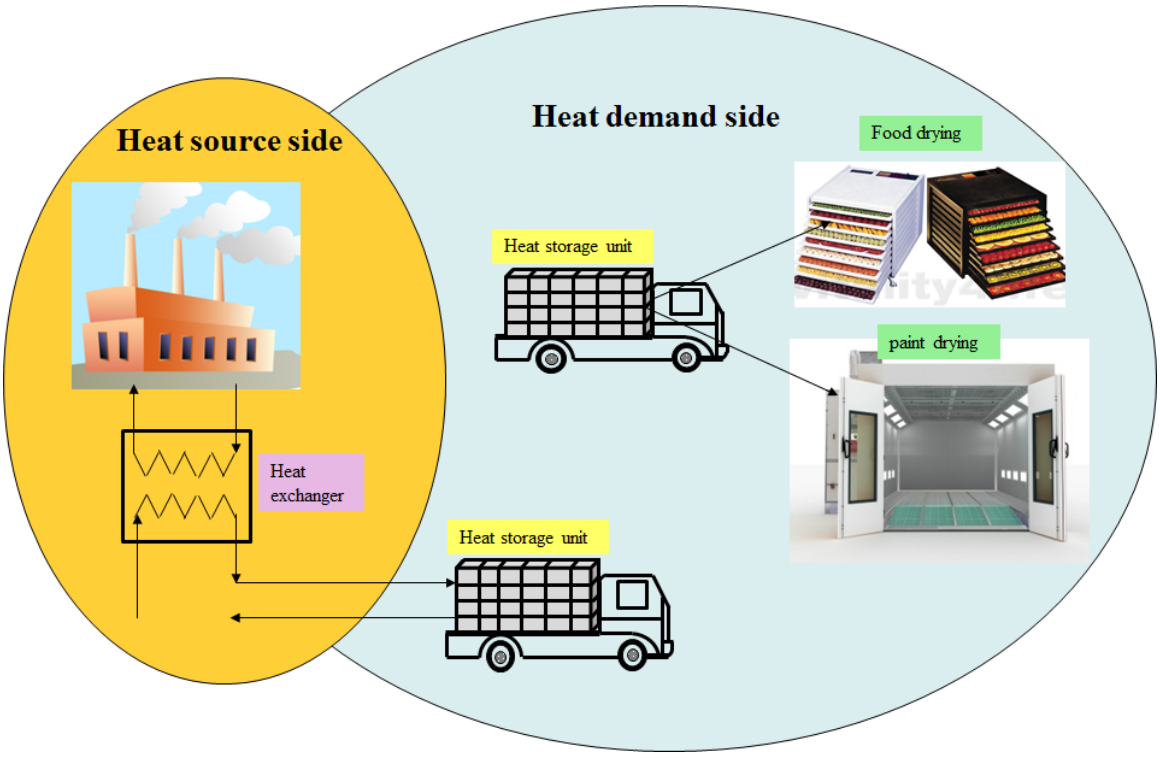

Fig. 7-1 Urban waste heat storage system

The use of industrial waste heat for energy supply in a remote location is considered to be an excellent way to reach better energy efficiency for energy utilization [1]. Mobile energy storage systems transported by truck may bridge the gap between heat

source and demand site in cases where a pipeline-bound connection cannot be realized cost effectively.

7.2 CLOSED SYSTEM PROPOSAL

Closed chemical thermal energy storage system (chemical heat pump) can be an competitive option to existing space heating and domestive hot water systems [2]. It is considered to be a compact way to store heat for a longer time without typical heat losses compared to traditional sensible and latent heat storage technologies. Taking the high solar irradiation in the daytime in summer as input makes it possible to release heat and produce cold heat at nigh time to supply hot water and cooling. The concept of application proposal to supply hot water and cooling integrated solar collector is shown in Fig. 7-2.

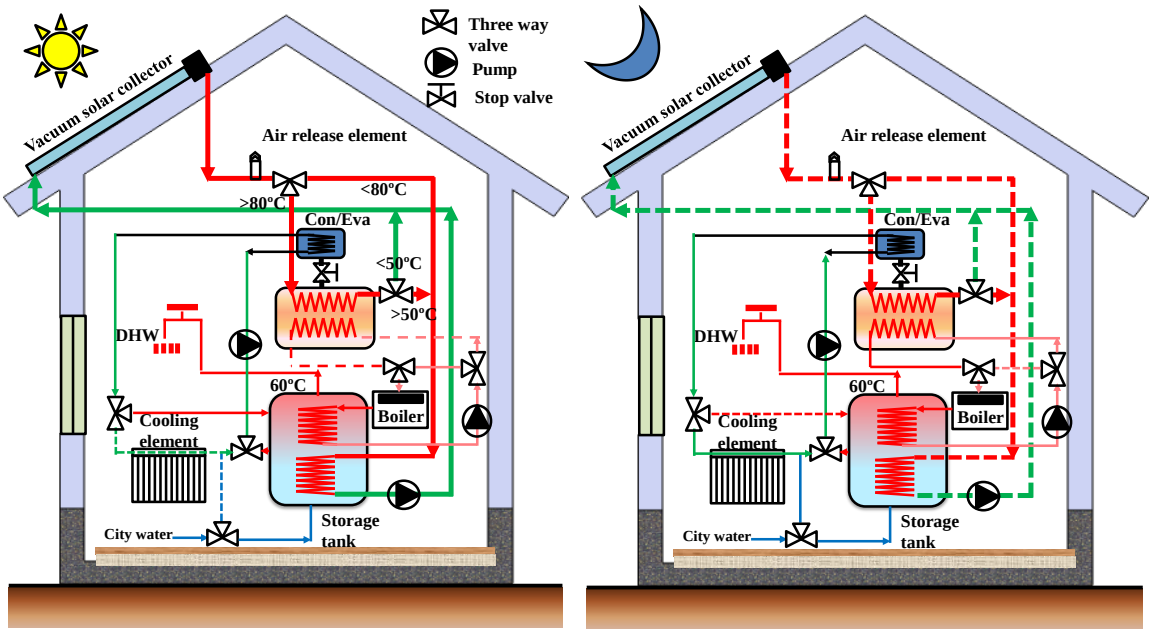

Fig. 7-2 Concept of application proposal integrated solar collector

The system needs a pump to circulate heat transfer fluid from solar collector. In a sunny day, large amount of solar energy can be collected by a vacuum solar collector. The heat can be stored by a water tank for domestic hot water use. When the collected fluid temperature exceeds 70 or 80ºC, it can be used to regenerated the reactor of the chemical heat storage system. The condensed water produced by the condenser is supposed to be stored by the water tank too. In the night time, the reverse process (heat release process) will occur in the reacor. Water will be evaporated from evaporator accomping with cooling effect, which can be used for space cooling. The reaction heat is designed to input into water tank for hot water use.

In fact, the research of chemical thermal energy storage technology is still at an experimental stage, and it is far away being put into practical condition. More development and large-scale demonstraction projectes are needed to validate the performance of a chemicaml thermal energy storage system.

7.3 REFERENCE

[1] A. Krönauer, E. Lävemann, A. Hauer, Mobile sorption heat storage in industrial waste heat recovery, in: The 12th International Conference on Energy Storage, 2012.

[2] C. Finck, H.v.t. Spijker, A.-J.d. Jong, E. Henquet, H. Oversloot, R. Cuypers, Design of a modular 3 kWh thermochemical heat storage system for space heating application, in: 2rd International Conference on Sustainable Energy Storage, Trinity College Dublin, Ireland, 2013.

8 GENERAL CONCLUSION

Thermal energy storage is one of the key technologies for energy conservation, which caused increasing attention to study this essential technique. Among kinds of therml energy storage methods, chemical thermal energy storage technology is one of the most important technologies to save fossil fuel, encourage using renewable energies and reduce the emission of greenhouse gases to achieve a clean and sustainable energy society profitable for humankind due to plenty of advantages. However, there are some problems described in the first charpter as follows:

(1) The low heat and mass transfer problems of the chemical materials should be improved.

(2) Complexity of the closed system;

(3) High price of the material;

(4) Relatively high regeneration temperature is required;

(5) Degradation of the material (after a certain cycles use).

Therefore, the purpose of this thesis was to solve the above mentioned problems of chemical thermal energy storage technology and to develop a suitable material and systems with low-regeneartion temperature for high density of thermal energy storage. The main achievements of each chapter are organized as follows:

In Chapter 1, a general introduction about thermal energy storage technology especially the chemical thermal energy storage was described. Firstly, necessarities of thermal energy storage was introduced. After that sensible heat storage, latent heat storage and chemical heat storage technologies were described. Thirdly, a detail description of the current research situation related with chemical thermal energy storage technologies was reviewed, and problems of chemical thermal energy storage were pointed out. Finally, the purpose and contents of this thesis were described.

In Chapter 2, a new composite mesoporous material impregnated with $CaCl_2$ was developed. Before filling the mesopores with $CaCl_2$, the WSS was constructed into a honeycomb shape to ensure a large contact area and low pressure loss. With $CaCl_2$ impregnated in, the sorption capacity was increased significantly, and the composite

material can be regenerated below 100ºC. Moreover, good stability was observed after 25 repetitions.

An open sorption thermal energy storage experimental setup was constructed to examine the developed composite material. A 2-L composite honeycomb filter was placed inside of the system. The composite honeycomb filter was regenerated at 80ºC, and the volumetric heat storage density showed no apparent difference between that obtained by regenerating a filter at 120ºC. A long duration of supplying high-temperature air (> 40ºC) was observed in the open system for the WSS + 13.0 wt% $CaCl_2$ and the WSS + 22.4 wt% $CaCl_2$ filter.

The composite mesoporous material supported with $CaCl_2$ showed potential for the storing low-temperature industrial waste heat with a high volumetric heat storage density. Moreover, the composite mesoporous material has the advantage of a long duration time for supplying stable heat with a low heat loss.

In Chapter 3, a numerical model was created to investigate the capability of an open chemical thermal energy storage system by using a composite mesoporous material impregnated with $CaCl_2$, which is based on the effect of coupled heat and mass transfer.

The simulation results can approximately predict the experimental values. The discrepancies observed between simulation and experiment in the desorption process have been explained above. Using the simulation program, optimal operating conditions were selected as follows: $T_{a,in}$ = 25°C or 30°C, $RH_{a,in}$ = 95%, f_a = 3.0 m^3/h, L = 20 or 25 cm for a heat release duration of ten hours.

A realistic application was proposed and simulated. Based on the simulation results, the thermal energy storage unit can supply air with a temperature greater than 40°C for 14 hours, and the unit can be regenerated within ten hours during the daytime. Using the thermal energy storage system, 47.6% of the exhaust heat generated by a kerosene-fueled blower can be recovered.

In Chapter 4, a new composite material by impregnating 9.6 wt% LiCl was developed, and the performance in open sorption thermal energy storage system of this composite material was compared with the composite material impregnated with $CaCl_2$ with the same sorption amount.

The WSS + 9.6 wt% LiCl can be regenerated at 60ºC, and it shows higher volumetric heat storage density than the WSS + 22.4 wt% $CaCl_2$ when the outlet and inlet air temperature difference is 20ºC at the same regeneration temperature. This is due to lower desorption activation energy of the WSS + 9.6 wt% LiCl.

Compared to the performance of the WSS + 22.4 wt% $CaCl_2$ at the same regeneration temperature, the humid air flow rate affects little on the maximum outlet air temperature for WSS + 9.6 wt% LiCl in heat release process. This can be understood from the sorption dynamics of the two materials: when the sorption amount is small, the sorption rate of the WSS + 9.6 wt% LiCl is higher compared to the WSS + 22.4 wt% $CaCl_2$.

At last, the WSS + 9.6 wt% LiCl is stable when it is regenerated at 60ºC during the tested 250 sorption/desorption cycles, which indicates that this material can be used for a rather long time.

In Chapter 5, a basic research of the composite material impregnated with LiCl was done by determining the isobaric and isosteric sorption chart of the composite material/water working pair in a closed thermal energy storage system.

A small scale sorption air cooler by using the developed composite material was built, and the performance of the air cooler was tested. The effective heat exchange and mass transfer properties of the sorbent reactor, led to a high inlet and outlet air temperature difference due to the rapid evaporation of the water inside the evaporator. Because of this, a relatively high value of the specific cooling power and a high cooling COP were observed from the experimental results. The result we got shows a good perspective of improving the performance of this developed sorption cooler.

In Chapter 6, a larger scale closed chemical thermal energy storage lab-scale prototype using the developed composite material in Chapter 5 was developed. The performance of the coated type reactor was evaluated and tested.

In Chapter 7, several application proposals for both the developed open and closed chemical thermal energy storage systems were described. It is believed that both solar energy and industrial waste heat can be stored by the closed and open thermal energy storage system in the future.

In Chapter 8, conclusions are briefly summarized for each chapter.

ACKNOWLEDGEMENTS

I would like to express my sincere gratitude and appreciation to my supervisor, Professor Nagano for providing me the opportunity to work in our lab. During these three years, he provided me very valuable advice on my research work, encouragement for the progresses and also helps for my daily life in Sapporo. The working load in the experimental works is rather heavy and difficult, but with the help and advice of Prof. Nagano, I overcame plenty of difficulties. He provided me so much time even on late night and weedends to discuss with me about my research. Duing discussions with him, he provided me significant instructions and advice on how to better arrange the working schedule, how to better improve the working efficiency, and how to do research systematically. He has taught not only the academic knowledge but also the right attitude to do research.

I would like to thank Prof. Hirofumi Hayama and Prof. Tomohiro Akiyama, Yasuhiro Hamada for their service on my doctoral committee and also for their helps on my study during the past three years.

I am highly indebted to several people for their help given to me during my experimental and simulational works. I am especially grateful to Dr. Togawa, who generously and continuously offered his time and effort to provide me theoretical and technical support. His insightful thoughts and strategic ways to problem solving made it possible for me to finish my experiments quickly. Moreover, it is so kind of him to teach me how to use the instruments used in my thesis. I would also like to thank Dr. Nabeshima for his help for teaching me some skills to built experimental setup and some good advices to do simulation. He is such a good senior student for me to give me plenty of advices for each step during these three years. I am grateful to Mr. Nakamura from Hokkaido University for quick responses to my technical problem encountered in experiments every time. His smile always made me feel the warmth of the world. I also wish to thank Ms. Omoteyama for her generous help to provide advice on my experimental work and her help to get me to get used to the life in Japan. I appreciate Miss. Takeda and Mori for their kind helps for dealing so many paper works related to my research and business trip.

I also would like to thank many students in our lab, especially Dichi Sugiyama, Atsushi Morita, Chunyue Jin, Huai Li, Yuanxiang Lai, Jian Zhai, Shengzhe Jin, Yu Zheng, Xin Yin. Many thanks also go to the e3 staff members, especially Dr. Werawan and Miss Yuki.

Thanks for all the friends I made in Hokkaido University, who helped to have a wonderful life during my stay in Sapporo. Some of them are Wenya chen, Weiwei Lan, Ling Sun, Hu Zhang, Zhiping Gan, Yingrui Ma, Hao Zheng, Jiafan Ma, Harisoa, Desi, and Kira. I wish to acknowledge China Scholarship Council (CSC) for providing me the scholarship for 42 months to pursue my doctoral study in Hokkaido University.

Last but not the least, I would like to express my gratitude to my husband Jiaming Gong. He has been giving me love, patience and encouragement during these years. Thank you for your concerns to support every day. I would also like to thank my parents and my grandparents for their help, support and encouragement all the time. I dedicate this thesis to my dear father, for all the love and support during the past 28 years. I will miss you and love you all the time during my entire life.

Life is difficult, and it is no doubt that these three years is one of the most memorable periods in my whole life. The knowledge and experiences gained from these three years will accompany, guide and provide me more knowledge, and confidence for my future.